Proceedings of the CECE Junior 2013

Hotel Continental, Brno, Czech Republic, November 12-13, 2013

"… bringing people and ideas together …"

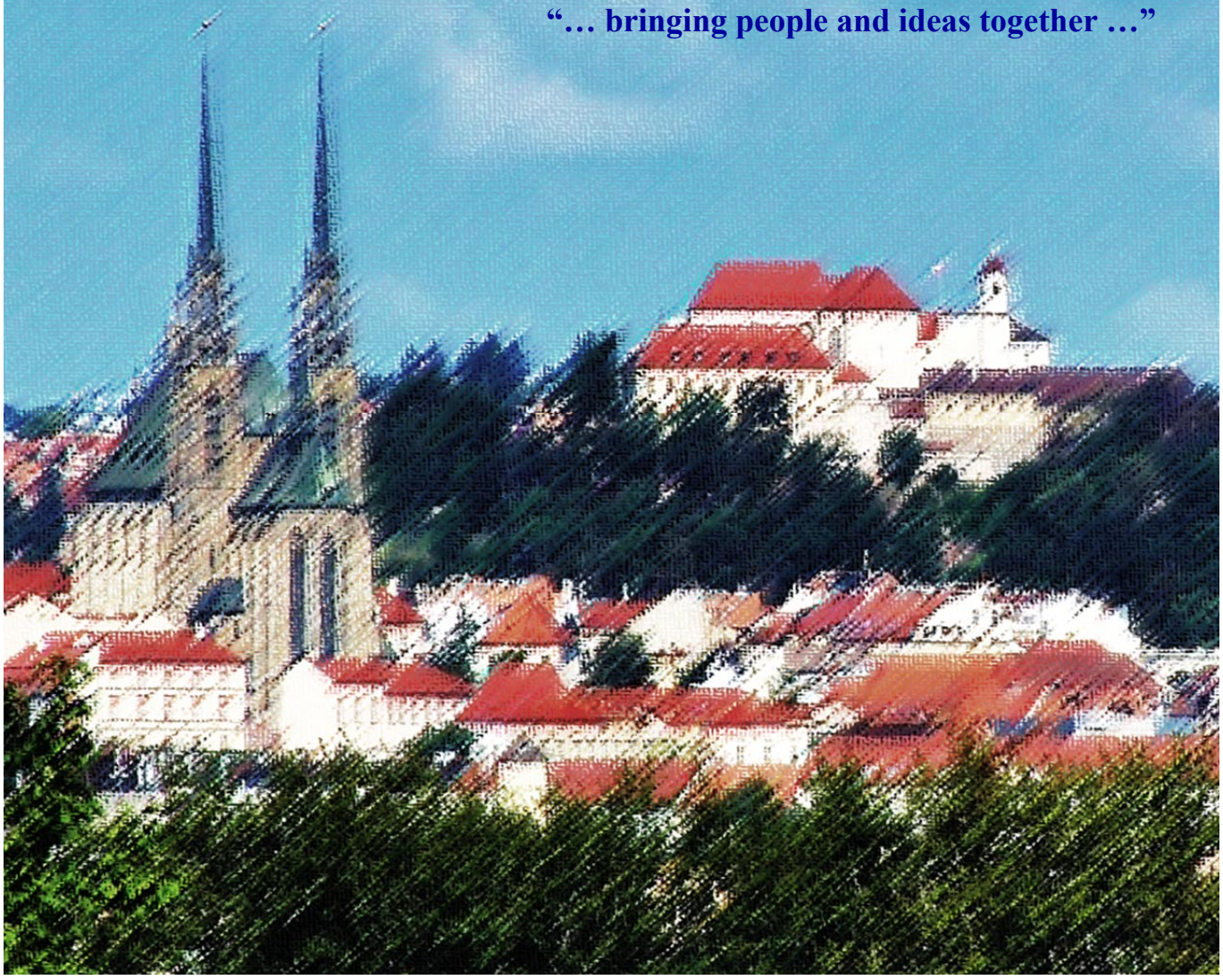

european social fund in the czech republic

EUROPEAN UNION

MINISTRY OF EDUCATION, YOUTH AND SPORTS

OP Education for Competitiveness

INVESTMENTS IN EDUCATION DEVELOPMENT

Organized by:
Institute of Analytical Chemistry AS CR, v. v. i., Veveří 97, 602 00 Brno, Czech Republic

Organizing committee:
František Foret, Jana Křenková, Karel Klepárník, Iveta Drobníková, Monika Staňková. Webmasters: František Matulík, Zbyňek Diviš

Proceedings Editors:
František Foret, Jana Křenková, Andras Guttman***,** Karel Klepárník, Petr Boček
Institute of Analytical Chemistry AS CR, v. v. i., Veveří 97, 602 00 Brno
***** Fulbright Scholar at IACH, Brno – Northeastern University, Boston, MA, USA and University of Pannonia, Veszprem, Hungary

This project is co-financed by the European Social Fund and the state budget of the Czech Republic (CZ.1.07/2.3.00/20.0182).
Tento projekt je spolufinancován z Evropského sociálního fondu a státního rozpočtu České republiky (CZ.1.07/2.3.00/20.0182).

Find the meeting history and more at www.ce-ce.org

Foreword

Since its start in 2004 the CECE has grown from a friendly meeting of collaborating scientists into a recognized international conference. For 2013 the 10th CECE has been split into two parts. The first part was organized by Prof. Ferenc Kilár in Pecs, Hungary, April 25–27, as a tribute to Prof. Stellan Hjertén from Uppsala University and the celebration of his 85th birthday. The second part, CECE Junior, focused on oral presentations of young scientists, has been organized in Brno, Czech Republic, November 12-13, 2013 with over 110 registered participants. Besides two invited plenary lectures (Prof. A. Guttman and Prof. E. Matalová), 23 lectures and 55 posters have been presented. On behalf of the organizers I wish to thank all the participants for their help with the success of the meeting and hope to see all the readers of these proceedings next year in Brno. In the meantime please check the conference web www.ce-ce.org for the latest information.

Franta Foret

Brno, November, 2013

SENSITIVE METHOD OF CASPASE-3 DETECTION IN SINGLE STEM CELL

EVA ADAMOVÁ[a,b,c], KAREL KLEPÁRNÍK[a], and EVA MATALOVÁ[b,c]

[a] *Institute of Analytical Chemistry, v.v.i., Czech Academy of Science, Brno,* [b] *Department of Physiology, University of Veterinary and Pharmaceutical Sciences, Brno,* [c] *Institute of Animal Physiology and Genetics, v.v.i., Czech Academy of Science, Brno, Czech Republic*
adamova@iach.cz

Summary

Caspases are involved in physiological process (e.g. cellular differentiation) but also can cause serious disorders. It is getting necessary to develop sensitive, miniaturized and fast methods amenable to analyze small amounts of samples. Luciferin/luciferase chemi-luminescence reaction is one of the methods of caspase-3 detection. We have developed a miniaturized device enabling detection of caspase-3 and quantitation just in femtogram level (10^{-15} g) in single apoptotic human stem cells (neural crest derived). The technology is based on the specific cleavage of modified luciferin by caspase-3, emissions of photons and their detection by photomultiplier tube working in the photon counting regime.

1. Introduction

Inhibition of apoptosis leads to cancer or autoimmune diseases, induction of apoptosis is responsible for neurodegenerative disorders such as Parkinson's disease Huntington's disease, multiple sclerosis or Alzheimer's disease. Considering this facts make analysis of caspase-3 in single cells essential for further research, clinical practice and also for discovery of new potential drugs. There are various techniques for caspase-3 detection: bioluminescence, fluorimetry (including fluorescence resonance energy transfers or quantum dots), colorimetry, atomic force microscopy, electrochemistry, magnetic resonance imaging and nuclear imaging[1]. Bioluminescence is mostly based on luciferin/luciferase system and detection of emmited photons by a photomultiplier tube. The aim of our study is to improve sensitivy of caspase-3 enabling its detection in individual stem cell.

2. Experimental

Cells (neural crest derived) were treated by camptothecin, a cytostatic alkaloid, for a period of ten hours to induce apoptosis[2]. The portion of 1–5 stem cell was captured and transferred by a micromanipulation system into a detection capillary filled with 2 µl of the reagent (Caspase-Glo™ 3/7 (Promega)) (Fig. 1). The amount of caspase-3 was detected by photomultiplier tube (PMT) working in the photon counting detection regime (Fig. 2).

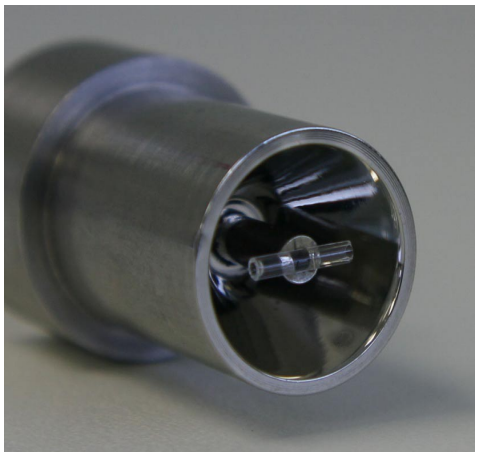

Fig. 1. **Detection capillary filled with 2 µl Caspase-Glo™ 3/7 reagent placed inside reflective chamber**

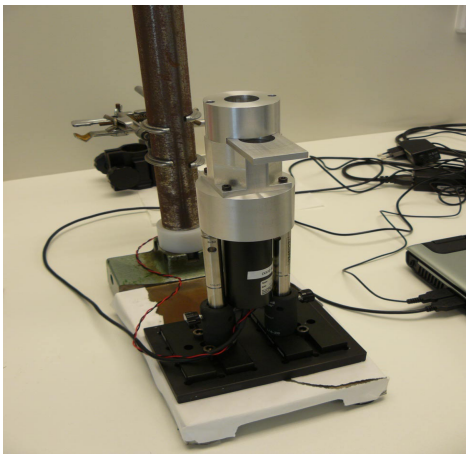

Fig. 2. **Detection chamber above PMT window**

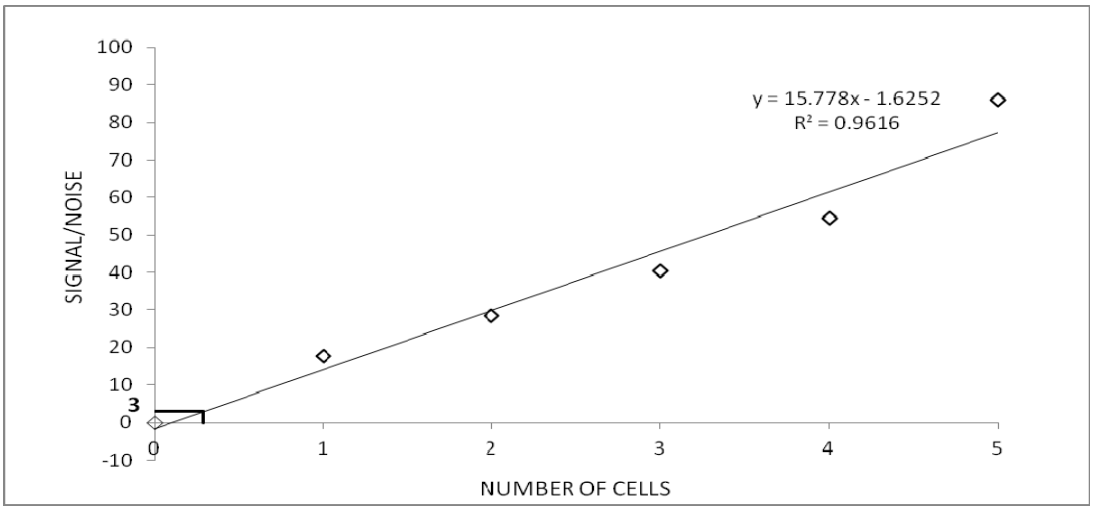

Fig. 3. **Dependence of signal to noise on number of stem cells.** Limit of detection is approximately half of the amount of caspase-3 in a single apoptotic stem cell

3. Results and discussion

The steady signal reached after 50 minutes of cell lysis is proportional to the amount of caspase-3. A decrease of the reagent volume due to evaporation is negligible after one hour of measurement. Considering previous bioluminescence methods there was high signal of background. The prerequisite of a higher sensitivity of our system, when compared with commercial devices, is a low background signal due to the small amount of Caspase -Glo™ 3/7 reagent and implementation of photon counting detection method.

4. Conclusions

The detection limit achieved in the miniaturized device is much lower than the amount of caspase-3 in single apoptotic stem cells. We proved high sensitivity of caspase-3 detection at the level of femtograms.

The research was supported by the Grant Agency of the Czech Republic, projects P206/11/2377 and P304/11/1418. This project is co-financed by the European Social Fund and the state budget of the Czech Republic (CZ.1.07/2.3.00/20.0182).

REFERENCE

1. Huang R., Wang X. J., Wang D. L., Liu F., Mei B., Tang A. M., Jiang J., Liang G. L.: Anal. Chem. *85*, 6203 (2013).
2. Chlastakova I., Liskova M., Kudelova J., Dubska L., Kleparnik K., Matalova E.: In vitro Cell Dev. Biol. Anim. *48*, 545 (2012).

INTEGRATED MICROFLUIDIC DEVICE FOR DROPLET MANIPULATION

EVGENIA BASOVA[a], JAKUB DRS[b], JIRI ZEMANEK[b], ZDENEK HURAK[b], and FRATISEK FORET[a,c]

[a] CEITEC – Central European Institute of Technology, Masaryk University, Brno, [b] Czech Technical University, Prague, [c] Institute of Analytical Chemistry of the Academy of Sciences of the Czech Republic, v. v. i., Brno, Czech Republic
evgenia-basova@rambler.ru

Summary

Droplets based microfluidic systems have a big potential for the miniaturization of processes for bioanalysis. In the form of droplets, reagents are used in discrete volume, enabling high-throughput chemical reactions as well as single-cell encapsulation. Microreactors of this type can be manipulated and applied in bio-testing. In this work we present a platform for droplet generation and manipulation by using dielectrophoresis force. This platform is an integrated microfluidic device with a dielectrophoresis (DEP) chip. The microfluidic device generates microdroplets such as water in oil emulsion.

1. Introduction

Droplets in miniaturized microfluidic systems such as water in oil emulsion are promising for use as well-defined and confined microreactors[1]. The benefits of this system are a large reduction in the volume of reagent in each droplet, the small amount of samples required, and the miniaturization of the equipment itself, reduced cost and reaction time[2]. By reducing the volumes it is possible to enhance the speed of assay. Mixing of reagents in droplet has been proved to be achieved within few minutes and it is much easier in droplets than in continuous microflows. Multiple emulsions or structured drops can offer even more functionalities, such as cell encapsulation for targeted delivery or effective high-throughput screening, which requires a much higher degree of control, with access to individual droplets. Such control can be achieved using microfluidic technology[1], which enables the formation of uniform drops, the drop manipulation[3] and the mixing of small volumes. However, manipulation of drops in the microfluidic device is essential. This work aims at examining the possibility to manipulate the microdroplets by using dielectrophoresis force. Integrated microfluidic device with a DEP chip generates surfactant stabilized droplets using an inert oil as the continuous phase. The control circuit enables us to monitor *in situ* the change of motion direction of a droplet.

2. Experimental

Water in oil emulsion was generated using a T-junction droplet generator chip fabricated as described in the literature. The chip was inserted into the holder and connected to two syringe pumps using bare-fused silica capillaries. Two 250 μL glass syringes were filled with aqueous and continuous phases.

3. Results and discussion

Emulsion formation. We have tested different oil phases such as mineral and silicone oils; decane, dodecane and decalin. In order to stabilize an emulsion, we used a combination of surfactants selected on the basis of hydrophilic lipophilic balance (HLB) values. Hence we have chosen commercially available surfactants Span 80 and Triton X 100. According to the results of the previous studies[5], we investigated three different surfactant mixtures of Span 80 and Triton X 100 in decane. It was demonstrated that the ratio of Span 80 and Triton X 100 98:2 is optimal under the given conditions and these components were added into the emulsion. The studies permitted to determine conditions of emulsion formation. The samples of oil phase such as decane, dodecane, decalin, mineral oil and silicon oil were tested with a more suitable ratio Span 80-Triron X 100 found as mentioned above. The results are presented in the Fig. 1, from which we can derive that the system decalin/Span 80-Tritox X100 has no coalescence. This system is characterized by a stable emulsion for one month. It was chosen for future experiments. The size of water drops was controlled by adjusting flow rates of oil and water with syringe pumps. We have measured the droplet size using an optical microscope. The size of the generated droplets was in the range of 10–50 μm.

Droplet generation. In order to generate emulsion (w/o) we fabricated a microfluidic chip which was connected to microfluidic droplet generation system. Two syringe pumps were filled with continuous and aqueous phases. We conducted the emulsification using a T-junction geometry microfluidic device. The width of the nozzle in the device was 75±1 μm. All dimensions of the microchannels were maintained identical. In the emulsification process, we used the optimized values and ratios of the continuous and aqueous phases. Emulsion was collected by passing the outlet flow from the chipset to the array.

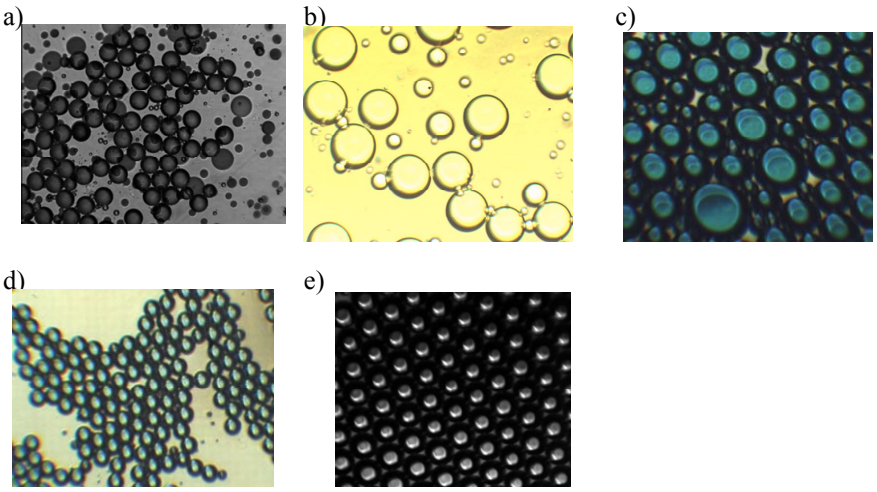

Fig. 1. **Optical micrographs of (a) mineral oil; (b) silicon oil; (c) decan; (d) dodecan; (e) decalin water in oil emulsion in the aqueous phase**

Droplet manipulation. The emulsion was collected onto the array (Fig. 2) and covered with an ITO-glass using parafilm "M" as a spacer. We applied AC voltage 25V at frequency ranging from 50 Hz to 1 MHz across the electrodes. Under these conditions we observed positive dielectrophoresis of water droplets. Droplets were attracted to the edges of electrodes, where the gradient of the electric field is the highest. We have also observed coalescence of droplets induced by AC current. This undesirable phenomenon needs to be avoided. One of possible ways to prevent it is to have sufficient distances between droplets. This could be achieved by using inlet capillary for the emulsion and pulling droplets one by one directly from the capillary. Then the droplets will be manipulated separately.

4. Conclusions

The described platform – a microfluidic device with an integrated dielectrophoresis chip for droplet manipulation – is an essential component for high-throughput bioassay. The generated droplets were placed onto the electrode array where directions of their motion could be influenced through the DEP force. The manipulation flexibility can be further increased by using higher fields, thinner electrodes or different layout of the electrode array. Applying this system for the future work involves single cell encapsulation and detection by optical and mass spectrometric means[4].

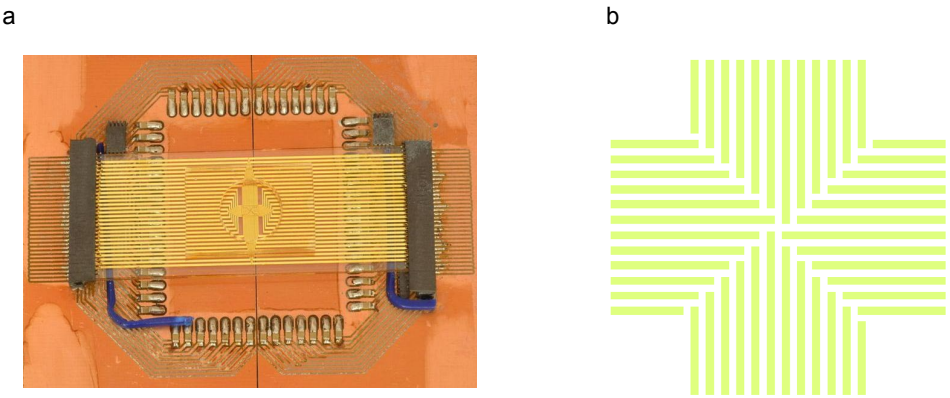

Fig. 2. **a) Schematic top view of the microelectrode array connected to the generator; b) layout of the four-segment microelectrode array which enables inducing motion perpendicular to the electrodes**

This project is co-financed by the European Social Fund and the state budget of the Czech Republic (CZ.1.07/2.3.00/20.0182). The support of the Grant Agency of the Czech Republic (P206/12/G014) and the institutional research plan (RVO 68081715) is also gratefully acknowledged.

REFERENCES

1. Song H., Tice J.: Angew. Chem., Int. Ed. *42*, 768 (2003).
2. Zhang M., Gong X.: Electrophoresis *30*, 3116 (2009).
3. Zemánek J., Hurák Z.: *American Control Conference (ACC) Conference*, 991–996, Montréal, Canada 2012.
4. Lazar I. M., Grym J., et.al.: Mass Spectrom. Rev. *25*, 573 (2006).
5. Porras M., Solans C.: Colloids Surf., A *249*, 115 (2004).

HIGH-THROUGHPUT MALDI TOF MASS SPECTROMETRY IMAGING

ANTONÍN BEDNAŘÍK[a], PAVEL KUBA[b], PAVEL HOUŠKA[b], EUGENE MOSKOVETS[c], IVA TOMALOVÁ[a], PAVEL KRÁSENSKÝ[a], and JAN PREISLER*[a]

[a] Central European Institute of Technology/Department of Chemistry, Masaryk University, Kamenice 5, 625 00 Brno-Bohunice, Czech Republic, [b] Faculty of Mechanical Engineering, Brno University of Technology, Brno, Czech Republic, [c] MassTech, Inc. 6992 Columbia Gateway Drive, Suite #160, Columbia, MD 21046, USA

Summary

Matrix-assisted laser desorption/ionization mass spectrometry (MALDI MS) imaging of biological tissues took an influential place among imaging techniques during the past decade[1–3]. It has been successfully exploited in the field of biomarker discovery, drug and metabolites analysis, brain tissue studies, artwork inspection, and other analytical fields. One of the drawbacks of the technique preventing its spreading to the clinical practice is a difficult imaging automation and a low speed of the MS image acquisition. A novel high-speed MS imaging sampling technique employing scanning of the desorption laser beam introduced earlier[4] is investigated.

1. Introduction

Typical MALDI MS imaging experiment comprises a series of MS signal acquisitions from a surface of matrix-covered tissue, data reading, processing and storage and finally translations between measured points (pixels). Aside from the sample preparation; cryosectioning, washing, drying and matrix application – which can be done parallelly to the image acquisition; the MS imaging time in modern high-repetition laser instruments is limited by the data processing and the target translation between the pixels executed by linear motorized stages. To reduce this bottleneck, we developed a sampling approach utilizing parallel data processing and fast laser beam scanning partially replacing the stages translation.

2. Experimental

2.1. Laboratory-built mass spectrometer

Laboratory-built axial mass spectrometer is equipped with a 355 nm diode-pumped frequency-tripled Nd:YAG laser (DTL-374QT Laser system; Lasers Innovations) efficiently working at frequencies up to 4 kHz. The key instrument feature for the high-throughput MS imaging is a fast precision scanning mirror (6810P; Cambridge Technology) capable of redirecting desorption laser beam on a sub-millisecond time scale. Scanning mirror can move the laser beam few millimeters across the sample, efficiently replacing the translation stage movements.

2.2. Model sample preparation

Model sample for evaluating the performance of laboratory-built instrument; 200 μL of matrix-peptide mixture (20 mg/mL DHB, 10 μM ACTH, 40/60 v/v MeOH/H_2O) was sprayed on the MALDI plate from the distance of 8 cm through a 7-mm circular mask using an airbrush GRAFO T1 (Harder & Steenbeck Airbrush, Norderstedt, Germany).

3. Results and discussion

The MS imaging performance of the laboratory-built instrument with Nd:YAG laser (1–4 kHz) and fast scanning mirror was compared to the performance of the

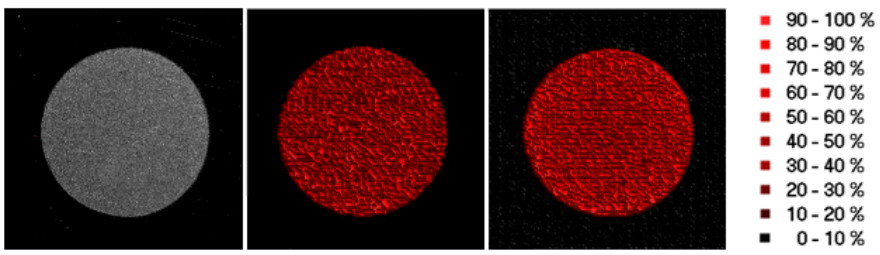

Fig. 1. **(A) Model sample photograph. MS images of the model samples at *m*/*z* = 2466.2±1 recorded in the reflector mode using (B) AutoFlex™ and (C) 4-kHz laboratory-built instrument with 1-mm laser beam scanning**

Table I
Comparison of MS imaging time of 1-cm^2 area (100 μm resolution, 100,000 pixels, 100 laser shots per pixel) with AutoFlex™ Speed and the laboratory-built MS

Device	Sampling mode	f [kHz]	t_{trans} [ms]/ pixel	t_{acq} [ms]	t_{proc} [ms]	t_{cycle} [ms]	t_{total} [min]
AutoFlex™	Stage translation	1	–	–	–	465	77.50
Lab-built MS	Stage translation	1	117	100	17.0	240	39.95
Lab-built MS	1-mm laser scanning	1	22	100	17.0	139	23.16
Lab-built MS	Stage translation	4	117	26	17.0	160	26.70
Lab-built MS	1-mm laser scanning	4	22	26	17.5	66.5	11.08

commercial TOF mass spectrometer (AutoFlex™ Speed) on model sample described above. The 1-cm^2 imaged area consisting of 10,000 measurement points with the spacing 100 μm was recorded with both instruments in traditional rastering mode and in laser beam scanning mode with laboratory-built instrument. The resulting images are showed in Fig. 1. Recorded MS imaging times are summarized in Table I.

4. Conclusions

A new sampling approach, laser beam scanning sampling, was introduced to MALDI MS imaging. In this mode, MS image is acquired with combined laser beam scanning and stage translation reducing the sample translation bottleneck of the MS imaging. The sampling mode utilizing the high-speed motion of the laser beam was shown to significantly outperform translation (rastering) mode, thus decreasing the imaging time. Equipped with the scanning mirror, the laboratory-built axial MALDI TOF MS instrument utilizing 4-kHz UV laser recorded a 100 × 100 pixel MS image in ~11 minutes using 100 laser shots per pixel, improving the speed of the analysis by a factor of ~7 compared to the commercial instrument.

We gratefully acknowledge the financial support of the Czech Science Foundation (Grant No. GCP206/10/J012 and GAP206/12/0538) and the project "CEITEC – Central European Institute of Technology" (CZ.1.05/1.1.00/02.0068) from European Regional Development Fund. We also thank Barry L. Karger and Tomáš Rejtar from Barnett Institute/ Northeastern University for donating the initial instrument to us and consultations. We thank Lukáš Ertl from the Faculty of Mechanical Engineering, Brno University of Technology for early software development.

REFERENCES

1. Caprioli R. M., Farmer T. B., Gile J.: Anal. Chem. *69*, 4751 (1997).
2. van Hove E. R. A., Smith D. F., Heeren R. M. A.: J. Chromatogr., A *1217*, 3946 (2010).
3. Watrous J. D., Alexandrov T., Dorrestein P. C.: J. Mass. Spectrom. *46*, 209 (2011).
4. Bednařík A., Kuba P., Houška P., Tomalová I., Moskovets E., Preisler J.: *9th CE-CE Conference proceedings,* 2012, 24–27.

OPTIMIZATION OF *N*-GLYCOPEPTIDES ANALYSIS METHODS AND THEIR PRELIMINARY APPLICATION TO BARLEY PROTEINS STUDY

DAGMAR BENKOVSKÁ, DANA FLODROVÁ, JANETTE BOBÁLOVÁ, and MARKÉTA LAŠTOVIČKOVÁ

Institute of Analytical Chemistry of the ASCR, v. v. i., Veveří 97, 602 00 Brno, Czech Republic
benkovska@iach.cz

Summary

N-glycosylation is the most frequently studied plant protein post-translational modification. The analysis of *N*-glycopeptides after protein proteolytic digestion offers information about the structure of both oligosaccharide and peptide moiety. However, this method has so far been less commonly used. Since glycopeptides hardly ionize during MS analysis in the presence of non-glycosylated peptides, they need to be separated from the complex peptide mixture. In this study, the glycopeptides enrichment, purification and analysis methods were successfully optimized on two standard *N*-glycoproteins. Concanavalin A (ConA) lectin tips were used for glycopeptide capturing, and obtained fractions were purified on carbon tips and analyzed using MALDI-TOF mass spectrometry. The differences in the CID fragmentation of certain types of glycopeptides were found. This technique was then applied to glycopeptide analysis of barley grain and malt proteins. Several barley glycopeptides were found, however, their identification was very difficult. More proteins separation techniques will be required before this enrichment procedure in further studies.

1. Introduction

Glycosylation, i.e. the covalent linkage of an oligosaccharide side chain to a protein, represents one of the most common protein post-translational modification and the most frequently studied modification in plant proteins. *N*-glycans contain a common trimannosyl-chitobiose core $Man_3GlcNAc_2$ and according to attached saccharide residues, they can be divided in three types: high mannose, complex and hybrid[1,2].

The direct analysis of intact glycopeptides by mass spectrometry offers sequence information on both peptide and glycan moiety. However, this method has so far been less commonly used. The analysis of glycopeptides after proteolytic digest without any pretreatment is difficult because non-glycosylated peptides interfere with ionization of glycopeptides. Therefore, the removing of non-glycosylated peptides from the proteolytic digest is necessary for efficient analysis. Lectin-affinity chromatography is often used to glycopeptides enrichment. Concanavalin A (ConA) is one of the most well characterized and widely used lectins. MALDI-TOF MS/MS analysis of *N*-glycopeptides results in specific fragment ion signals pattern of chibitose core fragmentation that differs in the case of non-core- and core-fucosylated *N*-glycopeptides[3,4].

2. Experimental

Proteins were digested (after reduction and alkylation) overnight at 37 °C using chymotrypsin or trypsin (enzyme-to-protein ratio of 1:50, w:w). Glycopeptides enrichment was performed on ConA lectin TopTips (Glygen Corporation, MD, USA) according to the manufacturer manual. Obtained fractions were purified using carbon Supel Tips and spotted on MALDI target with 2,5-dihydoxybenzoic acid (DHB) or ferulic acid matrix solution. MALDI-TOF MS experiments were performed on AB SCIEX TOF/TOF 5800 System equipped with a 1 kHz Nd:YAG laser (AB SCIEX, Framingham, MA, USA).

3. Results and discussion

3.1. Optimization of *N*-glycopeptide analysis

The analysis of *N*-glycopeptides was optimized using two standard glycopeptides, ribonuclease B (RNase B) and horseradish peroxidase (HRP), after both tryptic and chymotryptic digestion. For glycopeptide enrichment, purification and MALDI-TOF analysis, various methods and their conditions were tested. The best results were obtained by ConA affinity separation and carbon purification.

Glycopeptides were analyzed by MALDI-TOF mass spectrometry and obtained MS/MS spectra were manually interpreted according to the literature[3]. GlcNAc oxonium ions (m/z 204 and 186 and/or 168), typical for CID fragmentation of glycopeptides, and the characteristic fragment patterns for non-core-fucosylated or core-fucosylated *N*-glycopeptides were searched in MS/MS spectra. Thereby, the masses of both peptide and glycan moieties were determined. The structures of glycan and peptide moieties were identified according to fragmentation signals.

Both unbound and bound fractions from ConA standard glycopeptides enrichment were analyzed by MALDI-TOF MS and compared. Significant differences

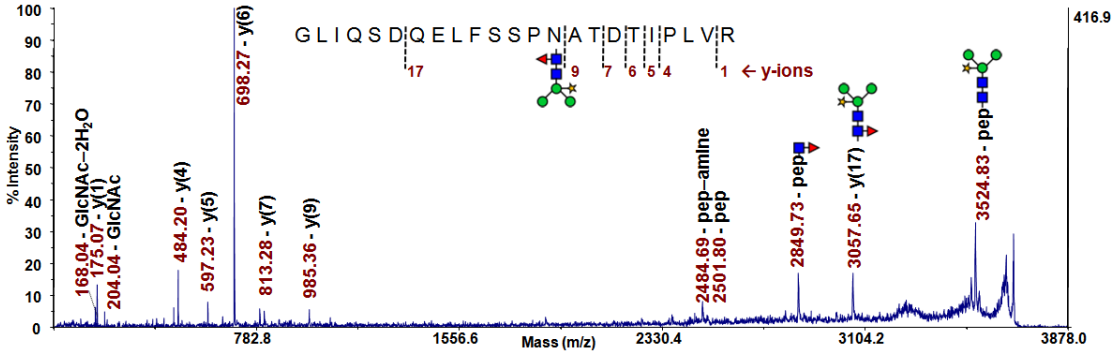

Fig. 1. **MS/MS spectrum of the tryptic glycopeptide G_{272}-R_{294} from horseradish peroxidase containing $GlcNAc_2Fuc_1Man_3Xyl_1$ *N*-glycan (precursor at m/z 3670.9). Ferulic acid was used as a matrix;** ■ GlcNAc ● mannose ★ xylose ▶ fucose

were observed and several glycopeptides were detected in the bound fraction. While RNase B contains high-mannose-type glycans, plant HRP contains various complex-type glycans. The illustrative MS/MS spectrum of one HRP glycopeptide is shown in Fig. 1.

3.2. Analysis of barley *N*-glycopeptides

Optimized methods were applied to the study of barley glycoproteins. The aqueous extracts of grain and malt digested with chymotrypsin were used for enrichment of glycopeptides. Several differences were observed between the MS spectra of the bound and unbound ConA fractions. Six potential glycopeptides were found in the grain sample and nine of them in the malt sample. The illustrative MALDI-TOF fragmentation spectrum of one barley malt glycopeptide is shown in Fig. 2. According to the fragmentation it was deduced that it contains high-mannose glycan $GlcNAc_2Man_6$. However, the fragmentation of all possible glycopeptides was not optimal and their identification was difficult. Obtained glycopeptides originate from a wide range of glycoproteins that are present in the complex grain or malt aqueous extract. Therefore, more protein separation techniques will be required before this enrichment procedure in further studies.

4. Conclusions

In this study, the enrichment of glycopeptides, subsequent glycopeptide purification and mass spectrometric analysis were successfully optimized. The principles of glycopeptides fragmentations and their interpretation were found out. Optimized methods and acquired experiences were utilized in subsequent preliminary investigation of barley grain and malt glycopeptides.

This work was supported by the Czech Science Foundation (grant No. P503/12/P395) and by institutional support RVO:68081715 of Institute of Analytical Chemistry, Academy of Sciences of the Czech Republic, v.v.i. This project is also co-financed by the European Social Fund and the state budget of the Czech Republic (CZ.1.07/2.3.00/20.0182).

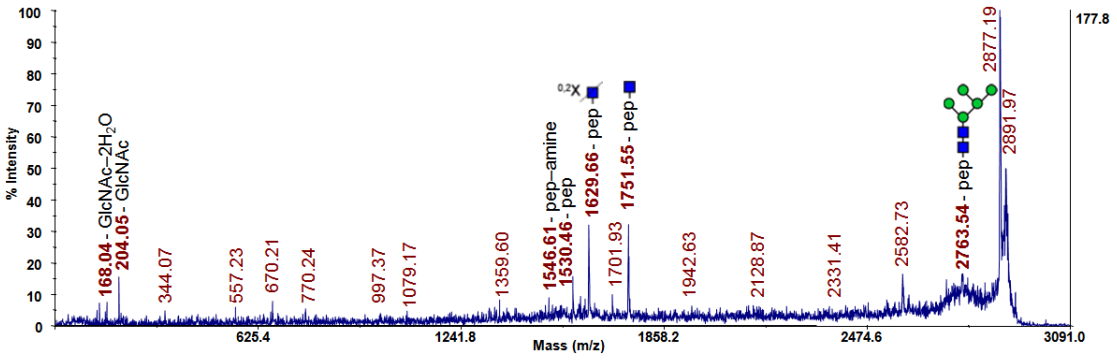

Fig. 2. **MS/MS spectrum of the chymotryptic glycopeptide from barley malt (precursor at m/z 2925). DHB was used as a matrix;**
■ GlcNAc ● mannose

REFERENCES

1. Hillenkamp F., Peter-Katalinič J.: *MALDI MS: A practical guide to instrumentation, methods and applications*, Wiley-VCH, Weinheim 2007.
2. Thiellement H., Zivy M., Damerval C., Méchin V.: *Plant proteomics: methods and protocols*. Humana Press, Totowa 2007.
3. Wuhrer M., Catalina M. I., Deelder A. M., Hokke C. H.: J. Chromatogr., B *849*, 115 (2007).
4. Ito S., Hayama K., Hirabayashi J.: Methods Mol. Biol. *534*, 194 (2009).

NEW APPROACH IN ELECTROCHEMICAL IMMUNOMAGNETIC BIOSENSORS FOR PROTEIN DETECTION

MICHAELA ČADKOVÁ[a,b], VERONIKA DVOŘÁKOVÁ[a,b], LUCIE KORECKÁ[a], RADOVAN METELKA[b], and ZUZANA BÍLKOVÁ[a]

[a] *Department of Biological and Biochemical Sciences, University of Pardubice, Pardubice,* [b] *Department of Analytical Chemistry, University of Pardubice, Pardubice, Czech Republic*
michaela.cadkova@upce.cz

Summary

The simple, sensitive, and selective method for electrochemical detection of ovalbumin is presented. This method is a combination of the selective immunocomplex formation on the surface of magnetic carriers for easy manipulation and preconcentration with a very sensitive electrochemical detection. The evaluation of antigen content is based on electrochemical detection of quantum dots as labels of secondary antibodies, which allows detecting of low amounts of target antigen.

1. Introduction

The detection of low concentrations of target antigen (i.e. proteins) is nowadays of great importance in biosensing area. New trends in this field combine selective immunochemical reaction with the quantum dots (QDs) as a label of secondary antibodies. This approach represents highly selective and sensitive detection method.

QDs are nanoscaled inorganic crystals characterized by very interesting optical and electronic properties[1]. These nanocrystals have a core-shell structure and diameter from 2 to 10 nm. The core is usually composed of elements such as Cd, Pb, or In. The shell usually consists of ZnS (ref.[2]).

Considering the composition, QDs have a great potential for electrochemical detection. Electrochemical techniques are known to have unique advantages in terms of both economic features and high sensitivity, e.g. in the determinations of low levels of heavy metals in different samples[4]. Anodic stripping voltammetry (ASV) in particular utilizes the efficient preconcentration of analyte, which can be combined with sensitive detection step using pulse techniques, like square-wave voltammetry (SWV) or differential pulse voltammetry (DPV). Such techniques effectively discriminate the faradaic current from the background current and they are often used for the identification of the redox processes and the determination of the corresponding current values[1]. Nowadays, the square-wave anodic stripping voltammetry (SWASV) is widely applied in electroanalysis of various species[3].

Additionally, there is a continuous push to use miniaturized electrochemical sensors and integrate as many electrodes as possible on one substrate. Therefore, the use of screen-printed sensors for electrochemical detection of ovalbumin in small sample volumes is presented in this contribution.

2. Experimental

2.1. Voltammetric measurements

All voltammetric measurements were performed with PalmSens interface (PalmSens, Netherlands). With regard to minimization of sample volume the detection of QDs were performed with mercury film screen-printed carbon electrode (ItalSens, Italy). Each screen-printed electrode was pretreated by applying the potential of –1.1 V for 300 s before use. Afterwards, the square wave voltammetric scans were carried out until low and stable background was obtained.

Prior to voltammetric scan, the nanometer-sized quantum dots Qdot®565 ITK Carboxyl Quantum Dots CdSe/ZnS (Life Science) were firstly dissolved with 50 µl HCl. Different concentration of HCl (0.1 M, 1 M, and 3 M) and different time (1, 3, 5, and 10 min) for QDs dissolution were tested. After optimization of QDs detection, the calibration curve of the quantum dots was ascertained using SWASV technique with 2 min of heavy metals accumulation.

2.2. Ovalbumin detection

The immunocomplex for specific immunocapture of ovalbumin was formed onto surface of SiMag-carboxyl magnetic particles (Chemicell, Germany). The anti-ovalbumin antibodies (Tetracore, USA) were covalently immobilized onto surface of magnetic particles. The secondary antibodies were prepared by conjugation of anti-ovalbumin antibodies with Qdot®565 ITK Carboxyl Quantum Dots. The evaluation of ovalbumin concentration was than based on electrochemical detection of QDs presence in analysed sample. Finally, the calibration curve for ovalbumin detection was ascertained.

3. Results and discussion

In this contribution, the electrochemical immunomagnetic assay of ovalbumin with subsequent

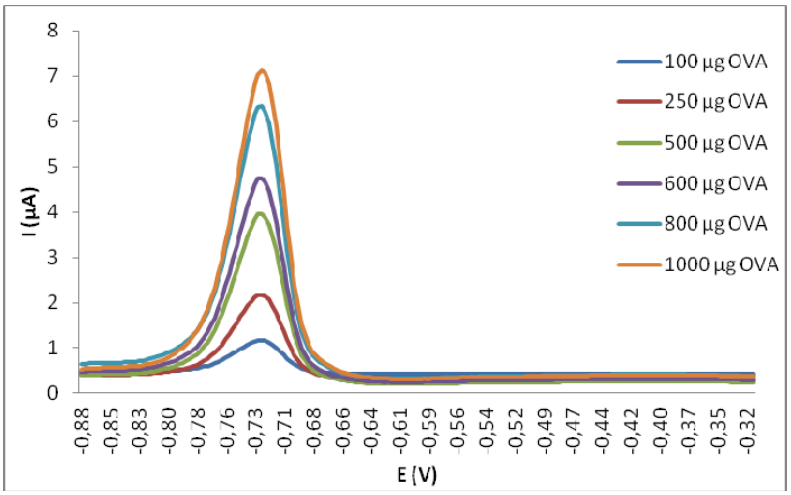

Fig. 1. **SWASV voltammograms of calibration in electrochemical immunomagnetic assay for ovalbumin – system anti-ovalbumin–ovalbumin–anti-ovalbumin labeled with QDs Q565 in 0.1 M HCl for 2 min heavy metals acumulation**

square-wave anodic stripping voltammetry of quantum dots is presented. This technique takes advantage of that quantum dots are composed of heavy metals such as cadmium and lead, which are easily electrochemically detected.

On the basis of optimal detection conditions, this technique was also used for the evaluation of the conjugation efficiency of secondary antibodies with QDs. This conjugate was subsequently used as secondary antibody for determination of the presence of ovalbumin as model system in the sample. The trend of increasing electrochemical response with increasing concentration of quantum dots and therefore ovalbumin is evident.

The use of magnetic particles of nanometer size enables highly efficient separations of target biomolecules due to their large surface area for specific ligand immobilization. They also allow to preconcentrate and separate target ligands on the surface of transducer with an aid of magnetic field.

4. Conclusions

Nowadays, the quantum dots have many interesting optical features for biosensing applications and have emerged not only in optical sensing strategies, but also in electrochemical sensing approaches. Electrochemical immunomagnetic sensor for detection of ovalbumin as a model protein, which is based on QDs determination, is presented. Such biosensor is attractive due to good availability of screen-printed electrodes, simple use, fast analysis, low detection limits and possibility of miniaturization and can be adopted for another protein detection with slight modification only.

This work was financially supported by the Czech Science Foundation P206/12/0381 and 7. FP EU project „NaDiNe“ No 246513.

REFERENCES

1. Amelia M., Avellini T., Monaco S., Impellizzeri A., Yildiz I., Raymo F. M., Credi A.: Pure Appl. Chem. *83*, 1 (2011).
2. Samir T. M., Mansour M. M., Kazmierczak S. C., Azzazy H.: Nanomedicine *7*, 1755 (2012).
3. Medina-Sánchez M., Miserere S., Marín S., Aragay G., Merkoci A.: Lab Chip *41*, 5728 (2012).
4. Sobrova P., Ryvolova M., Hubalek J., Adam V., Kizek R: Int. J. Mol. Sci. *14*, 13497 (2013).

NEW SENSOR FOR DNA MUTATION DETECTION

VLADIMÍRA DATINSKÁ[a,b], KAREL KLEPÁRNÍK[a], MAREK MINÁRIK[c], and FRANTIŠEK FORET[a]

[a] *Institute of Analytical Chemistry of the ASCR v.v.i., Brno,* [b] *Masaryk University, Faculty of Science, Department of Chemistry, Brno,* [c] *Genomac International, s.r.o., Prague, Czech Republic*
datinska@iach.cz

Summary

We present a design and synthesis of a new sensor intended for the genomic analysis in molecular cancer research. This sensor is based on the Förster resonance energy transfer (FRET) and can be used for the detection of complementary oligonucletide chains based on probe hybridization. Quantum dots (QDs) with their unique optical properties serve as suitable donors of energy in FRET.

1. Introduction

The process of FRET is a photophysical phenomenon through which an energy absorbed by a fluorophore (the energy donor) is transferred nonradiatively by dipole-dipole interactions to the second fluorophore (the energy acceptor)[1]. The efficiency of energy transfer between the donor and acceptor is sensitive to their distance (1–10 nm). The main advantages of QDs, when compared with the conventional organic fluorescent dyes, include absence of photobleaching, wide range of excitation wavelengths and narrow emission the wavelength of which can be modulated by the QD size[2]. Moreover, their high extinction coefficients are prerequisites for absorption of a high amount of energy. The energy is transferred effectively from donor to acceptor and emitted at a longer wavelength.

2. Experimental

We focused on the synthesis of CdTe QDs of a size of 3.2 nm with a maximum emission wavelength of 570 nm passivated by inorganic salts (CdS, ZnS). Mercaptopropionic acid (thiolated ligand) was covalently bonded to the surface to make QDs water soluble. The CdTe QDs were conjugated with a specific oligonucleotide sequence *via* zero-length cross-linkers[3] to form a luminescent probe (donor of FRET). ROX-labelled (6-carboxyrhodamine) PCR fragment from the studied sample serves as an acceptor. The sample-probe hybridization was performed using a standard annealing protocol and followed by fluorescence measurement.

3. Results and discussion

Capillary Electrophoresis with Laser Induced Fluorescence Detection (CE-LIF) was used for analyses of products of conjugation reaction and hybridization reaction. Products of conjugation reaction between QDs and aminated oligonucleotide in ratio 1:1 provided single peak. Thus the absence of peaks of free reactants (QDs) indicates complete conversion.

Hybridization experiments were done in parallel with ROX-labeled complementary and non-complementary oligonucleotides. Each of the oligonucleotides showed a single peak at a 1:1 ratio. By increasing the amount of complementary oligonucleotides a secondary peak was observed. In case of noncomplementary hybridization only single peak remained in various ratios of the reactants. The result indicates nonspecific interaction of both hybrides. After the hybridization experiment with complementary oligonucleotide, an increase of the fluorescence emission spectra at the wavelength of 610 nm confirmed the function of FRET.

4. Conclusions

We present the design, physico-chemical properties and results of the testing of a sensor based on a conjugate of QD and oligonucleotide probe. Hybridization reaction with complementary and non-complementary oligonucleotides resulted in different separation profiles. An increase in fluorescence signal of the hybridized product at the ROX emission wavelength indicates transfer of energy.

This work was supported by Technology Agency of the Czech Republic (TA02010672) and by institutional support RVO 68081715 of Institute of Analytical Chemistry, Academy of Sciences of the Czech Republic, v.v.i. This project is co-financed by the European Social Fund and the state budget of the Czech Republic (CZ.1.07/2.3.00/20.0182).

REFERENCES

1. Forster T.: Naturwissenschaften *33*, 166 (1946).
2. Rajh T., Micic O. I., Nozik A. J.: J. Phys. Chem. *97*, 11999 (1993).
3. Hermanson G.: *Bioconjugate techniques*, Academic Press, San Diego 1995.

PIEZOELECTRIC BIOSENSOR COUPLED TO CYCLONE AIR SAMPLER FOR DETECTION OF MICROORGANISMS

ZDENĚK FARKA[a], DAVID KOVÁŘ[a,b], and PETR SKLÁDAL[a,b]

[a] *Department of Biochemistry, Faculty of Science, Masaryk University, Brno,* [b] *CEITEC MU, Masaryk University, Brno, Czech Republic*
farka@mail.muni.cz

Summary

Even though microorganisms are common part of our lives, some of them are dangerous and must be monitored. The traditional microbiological methods are reliable but slow. In some cases, namely in military, key requirement is fast detection which can be provided by biosensors. In this work, the piezoelectric biosensors providing fast, specific and cheap way of detection are described. Three strains of *E. coli* (BL21, DH5α and K-12) were chosen as safe model microbes and the detection using the developed piezoelectric biosensor was carried out (LOD 10^6 CFU mL^{-1}, total analysis time 20 min). Bioaerosol chamber was constructed to allow safe dissemination of microbes in air and experiments with bioaerosol. The generated bioaerosol was sampled using the cyclone air sampler and analyzed with the on-line coupled piezoelectric biosensor. The levels of 10^6 CFU L^{-1} of *E. coli* in air were successfully detected in less than 26 min which demonstrates possible application of this system for rapid screening of microorganisms in the air.

1. Introduction

Detection of microorganisms by the traditional microbiological procedures is reliable but usually lengthy. In the last years, fast and sensitive methods of detection based on biosensors are being developed. The good specificity of biosensors allows analysis of complex matrices of samples from military and public protection, clinical and food control applications[1].

The importance of detection of microorganisms spread in the air arises with the risk of terroristic attacks. Most of the methods currently used are based on surface-enhanced Raman spectrometry[2] or electrochemical biosensors[3], but new techniques are still being developed[4]. Piezoelectric biosensors are based on changes of the resonant frequency of piezoelectric crystal. This frequency change depends on the amount of mass bound to the sensor surface. Piezoelectric biosensors are sensitive, cheap and easy to use and therefore suitable for label-free detection of microorganisms[5].

2. Experimental

2.1. Microorganisms and antibodies

Escherichia coli was chosen as a safe model microorganism because of its fast and easy cultivation and good availability of commercial antibodies. Three strains (BL21, DH5α and K-12) were tested. Cultivation was done both aerobically and anaerobically using LB Broth (Duchefa Biochemie, Netherlands) over night at 37 °C. The obtained suspension was centrifuged twice at 4500 RCF for 15 min. Each time, the supernatant was discarded and the pellet was resuspended in 50 mM phosphate buffered saline pH 7.4 (PBS). Concentration of microorganisms was determined using the McFarland scale.

Antibody Abcam ab25823 was used for detection of strains BL21 and DH5α. In case of the strain K-12 antibody Serotec 4329-4906 was chosen.

2.2. Piezoelectric immunoassay

To prepare piezoelectric biosensor, gold electrodes of 10 MHz quartz crystals (ICM, USA) were cleaned 30 min in acetone and then incubated in cysteamine (20 mg mL^{-1} in water, 2 hours) to form a self-assembled monolayer. The 1 hour incubation in 5% glutaraldehyde in PBS followed. One type of sensors was subsequently modified for 20 hours by 1 mg mL^{-1} solution of staphylococcal protein A (SpA) which specifically binds the Fc fragment of antibodies. For the other type, antibody was bound directly covalently (100 μg mL^{-1}, 20 hours at 4 °C) after activation with GA. Finally, free reactive aldehyde groups were deactivated using 50 mM ethanolamine for 30 min.

The prepared immunosensor was placed in a flow-through cell and affinity interactions were measured in real-time using QCM Analyzer (Keva, Czech Republic). All measurements were performed in PBS with a flow rate 25 μL min^{-1}. Samples were flown over the sensor for 10 min followed by 10 min dissociation time. Regeneration was done using 50 mM NaOH.

2.3. Bioaerosol chamber

Bioaerosol chamber was a hermetically closed box (volume 1 m^3) made of plexiglass placed on a movable table to allow easy transportation. Air coming in and leaving out of the chamber was filtered by HEPA filters (AirFilters, Czech Republic) connected to air pumps (Hurricane, Italy) that allow fast exchange of air. To measure physical conditions inside the chamber, sensor system Comet 7511 (Comet, Czech Republic) was used.

Humidity was regulated with the help of the humidifier Super Fog (LuckyReptile, Germany).

Aerosol was generated by a vibrating ultrasonic piezoelectric actuator placed in a beaker, where the liquid sample with microbes was injected. Thus formed aerosol was spread using three 12-cm fans (Nexus, Netherlands). Level of particles was measured by the counter Met One 3400 (Hach, USA). The air was gathered by a cyclone air sampler SASS 2300 (Research International, USA) which was connected to the piezoelectric immunosensor. The whole system was controlled remotely by a computer connected through LAN network using router and serial/ethernet adapters.

2.4. Measurement of bioaerosol

Before measurements, the bioaerosol chamber was disinfected using ethanol, closed and air in the chamber was filtered (30 min in/out circulation) to decrease the number of particles inside. Relative humidity was increased to 80 %. Dissemination was done by the piezoelectric actuator; to prevent damage of microbes, 5 shorter cycles (per 60 s with 30 s break) were performed instead of one longer dissemination. During this procedure 1 mL of bacterial suspension (10^9 CFU mL^{-1}) was disseminated giving total concentration in the chamber 10^6 CFU L^{-1}. When dissemination was finished, cyclone was run for 5 min and liquid was captured in a reservoir linked to the piezoelectric biosensor. Piezoelectric immunoassay was done in the same way as mentioned in chapter 2.2.

3. Results and discussion

Interactions of *E. coli* with antibodies were studied using piezoelectric biosensors. Fig. 1 shows the interactions between various concentrations of *E. coli* DH5α and antibody Abcam ab25823 immobilized directly using GA. Limit of detection was 10^6 CFU mL^{-1} and in case of concentration 10^8 CFU mL^{-1} the signal change was 26.6 Hz. Dependence of signal change on concentration of microbe exhibited saturation character. No differences between aerobically and anaerobically cultivated microbes were observed.

Then interactions of the same type of sensor with the strain BL21 were studied, too. The sensitivity was lower than in case of DH5α (signal change 14.4 Hz for 10^8 CFU mL^{-1}) but the same LOD was achieved. Sensor with antibody bound using SpA provided higher changes of resonant frequency for high concentrations (37 Hz for 10^8 CFU mL^{-1}) but LOD was worse ($5 \cdot 10^6$ CFU mL^{-1}). When studying interactions between the strain K-12 and antibody Serotec 4329-4906 analogous results were obtained.

Measurements in bioaerosol chamber have shown that detection down to 10^6 CFU L^{-1} of air is feasible. Results for two experiments with the strain DH5α and one experiment with BL21 can be seen in Fig. 2. In agreement with previous results, DH5α gave approximately twice higher signal than BL21. Comparison of two measurements with DH5α confirms good reproducibility of the method. Similar results were achieved also in case of antibody Serotec 4329-4906 and K-12.

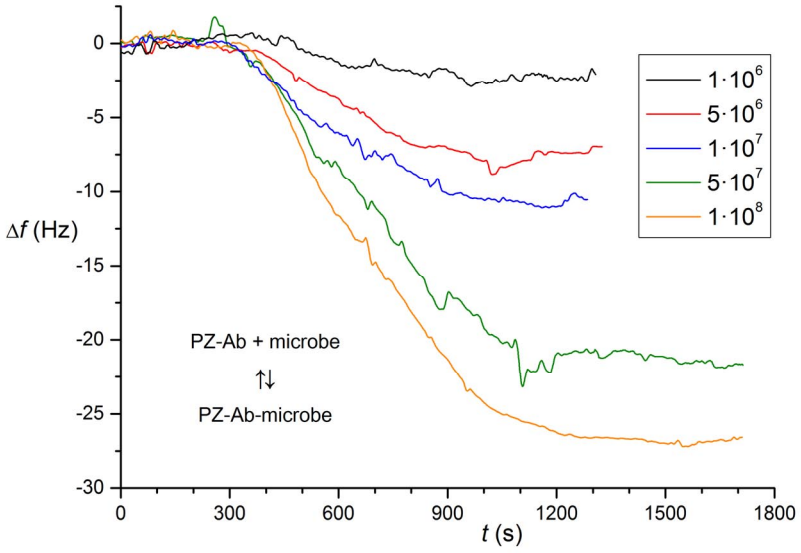

Fig. 1. **The interactions between *E. coli* DH5α and antibody Abcam ab25823 immobilized directly through GA studied using piezoelectric (PZ) immunosensor.** Change of resonant frequency (Δ*f*) in time is shown. Microbe levels are expressed as CFU mL^{-1}

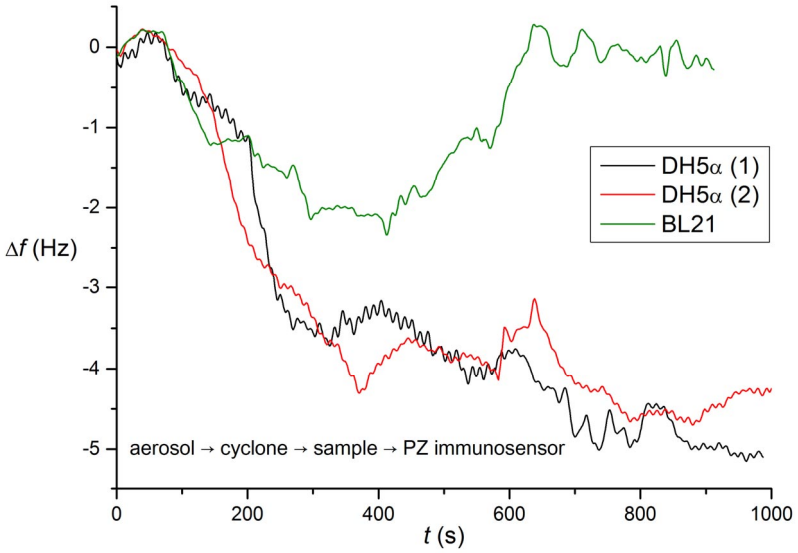

Fig. 2. **The interactions between *E. coli* strains DH5α and BL21 captured from aerosol with antibody Abcam ab25823 immobilized directly through GA.** Change of resonant frequency (Δf) in time is shown. The aerosol contained 10^6 CFU L^{-1} of *E. coli* cells

4. Conclusions

Piezoelectric biosensor for rapid detection of *Escherichia coli* was developed with a limit of detection 10^6 CFU mL^{-1} and total analysis time 20 min. Bioaerosol chamber was constructed to allow safe measurements with aerosolized microorganisms. The aerosol was gathered by a cyclone air sampler and analyzed using piezoelectric biosensor. The level of 10^6 CFU L^{-1} of *E. coli* in aerosol was successfully detected with time for cyclone capturing, sampling and QCM detection less than 26 min making this system a good alternative to other methods for detection of microorganisms in air.

The work has been supported by the Ministry of Defence of Czech Republic (projects no. OVVTUO2008001 and OSVTUO2006003) and by CEITEC – Central European Institute of Technology (CZ.1.05/1.1.00/02.0068) from European Regional Development Fund.

REFERENCES

1. Zourob M., Elwary S., Turner A. P. F.: *Principles of Bacterial Detection: Biosensors, Recognition Receptors and Microsystems*, Springer, New York 2008.
2. Sengupta A., Laucks M. L., Dildine N., Drapala E., Davis E. J.: J. Aerosol Sci. *36*, 651 (2005).
3. Skládal P., Švábenská E., Žeravík J., Přibyl J., Šišková P., Tjärnhage T., Gustafson I.: Electroanalysis *24*, 539 (2012).
4. Švábenská E.: Def. Sci. J. *62*, 404 (2012).
5. Farka Z., Kovář D., Přibyl J., Skládal P.: Int. J. Electrochem. Sci. *8*, 100 (2013).

COMPARISON OF CHIRAL STATIONARY PHASES BASED ON IMMOBILIZED POLYSACCHARIDES IN REVERSED PHASE MODE

RADIM GERYK, DENISA PLECITÁ, KVĚTA KALÍKOVÁ, and EVA TESAŘOVÁ

Department of Physical and Macromolecular Chemistry, Faculty of Science, Charles University in Prague, Prague, Czech Republic
radim.geryk@natur.cuni.cz

Summary

Immobilized polysaccharide-derived chiral stationary phases (CSPs) are a new type of chromatographic columns, which allow using much broader range of solvents. However, these columns are mostly used in normal phase HPLC mode. In this study we worked in reverse phase mode and we used three CSPs that differed in the type of derivatization group or in the nature of the glycosidic linkage of the polysaccharide derivatives. The columns CHIRALPAK IA, CHIRALPAK IB and CHIRALPAK IC are based on tris-(3,5-dimethylphenylcarbamate) of amylose, tris-(3,5-dimethylphenylcarbamate) of cellulose and tris-(3,5-dichlorophenylcarbamate) of cellulose, respectively.

1. Introduction

Chirality is an unique phenomena affecting human life in many aspects. Molecules that are not identical to their mirror images are kinds of stereoisomers called enantiomers. Enantiomers have identical physical properties but could differ in biological activity. Ignorance of pharmaceutical and toxicological differences of the individual enantiomer forms can cause disastrous consequences. As an example can serve chiral compound called thalidomide which was discovered as a sedative to help pregnant women with affects of morning sickness. While *R*-enantiomer had required pharmacological effect, the *S*-enantiomer caused fetal malformations.

High performance liquid chromatography (HPLC) has become a powerful technique for the development of enantioselective separations of chiral drugs and has a significant impact for pharmaceutical, food and agrochemical industries. Nowadays, chiral stationary phases (CSPs) based on polysaccharides (amylose, cellulose) have proven to be one of the most useful tools for separation of a wide range of chiral compounds. Immobilized polysaccharide-derived CSPs are a new type of chromatographic columns, which demonstrate better performance in the areas of enantioselectivity, efficiency and CSP-solvent compatibility[1–3].

2. Experimental

The tested columns CHIRALPAK IA, CHIRALPAK IB and CHIRALPAK IC are based on tris-(3,5-dimethylphenylcarbamate) of amylose, tris-(3,5-dimethylphenylcarbamate) of cellulose and tris-(3,5-dichlorophenylcarbamate) of cellulose, respectively, Fig. 1. The set of diverse chiral compounds including acidic, neutral and basic ones was tested to characterize and understand the principles of chiral recognition. This facilitates the development of new separation methods and accelerate their optimization. In the frame of the separation procedure the various types of mobile phases were tested. The acidic mobile phases were used for acidic analytes to suppress the ionization because charged analytes cannot

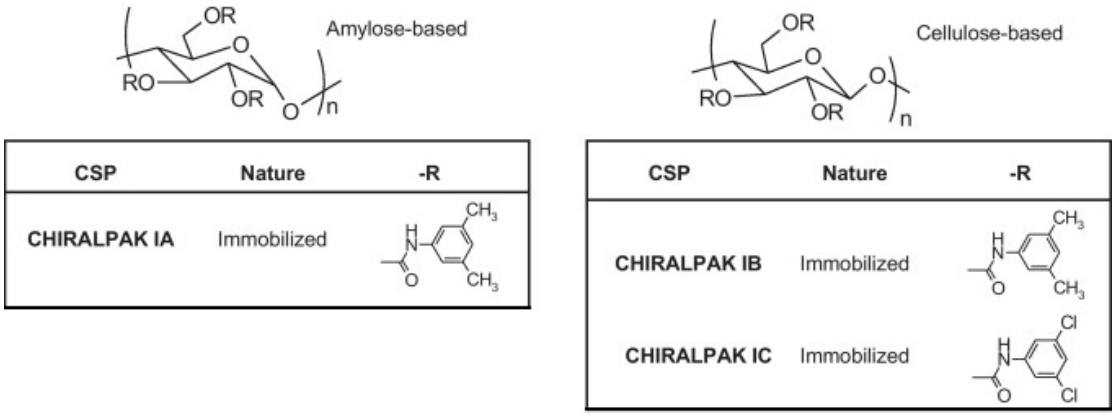

Fig. 1. **Structures of the chiral selectors**[5]

interact efficiently with CSPs (ref.[4]). Basic analytes were separated in suitable basic buffer systems or in the acidic mobile phases with considerable amount of chaotropic reagent (KPF_6, $NaClO_4$) which forms an ion pair with the positively charged analyte.

3. Results and discussion

RP mode mobile phases composed of ACN or MeOH as organic modifiers and suitable buffer systems was chosen for the enantioseparation of selected analytes. The influences of the type and the amount of organic modifier (acetonitrile, methanol) on chromatographic parameters were evaluated. The retention times of the analytes decrease with increasing the amount of organic eluent. Additionally, the same amount of acetonitrile gives a shorter retention than an equivalent amount of methanol. The effect of column temperature on enantioselectivity and resolution of the enantiomers was also studied. The chromatographic parameters of different pharmaceuticals obtained in reversed phase separation systems on three different CSPs were compared. For illustration see Fig. 2 and Fig. 3.

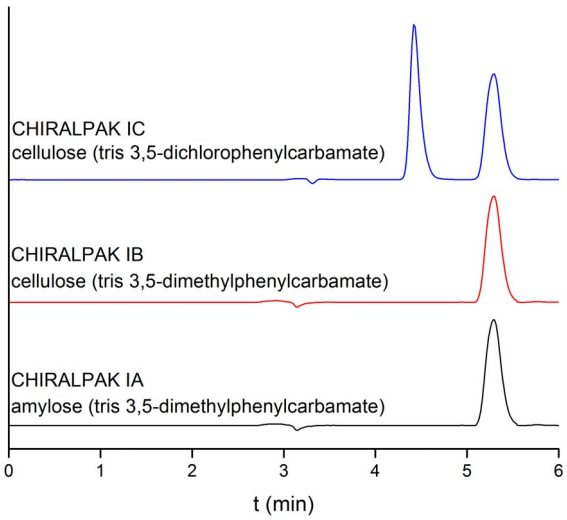

Fig. 2. **Comparison of enantioseparation of fenoprofen on three different CSPs.** Mobile phase composition: ACN/aqueous solution of formic acid, pH 2.10, 60/40 (*v/v*); temperature 25 °C; detection 254 nm

4. Conclusions

The combination of three immobilized CSPs constitutes a powerful column set for resolution enantiomers in reverse phase mode. The reversed phase

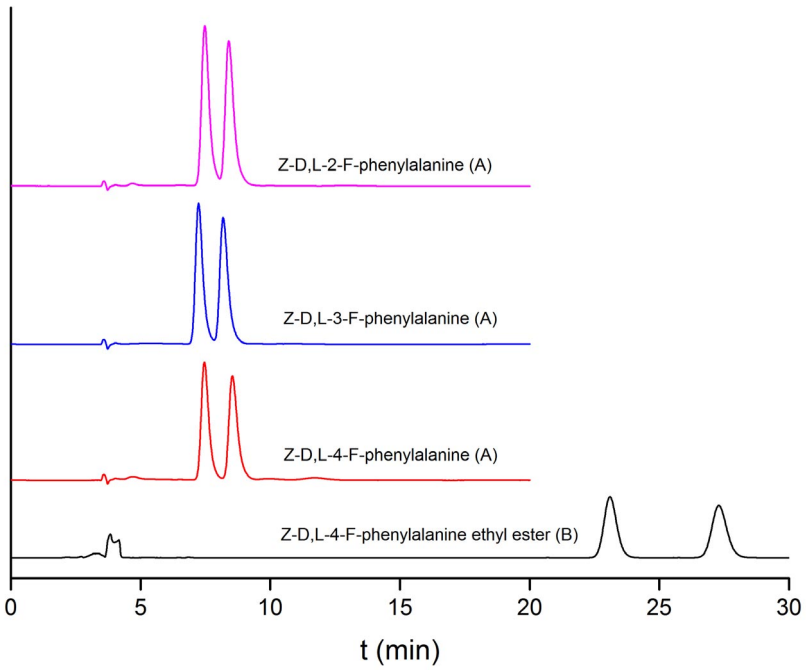

Fig. 3. **Chromatograms of enantioseparation of *N*-blocked analytes on Chiralpak IC column.** A) Mobile phase composition: MeOH/aqueous solution of formic acid, pH 2.20, 70/30 (*v/v*); B) Mobile phase composition: ACN/water 45/55 (*v/v*); temperature 25 °C; detection 254 nm

mode was proved to be suitable for separation of the majority of tested compounds. The results showed that both the polysaccharide type and substituent affect the separation behavior.

The Grant Agency of the Charles University in Prague, project No. 356411, the Ministry of Education, Youth and Sports of the Czech Republic, project Kontakt LH11018, and the long-term project MSM0021620857 are gratefully acknowledged for the financial support.

REFERENCES

1. Zhang T., Nguyen D., Franco P.: J. Chromatogr., A *1217*, 1048 (2010).
2. Zhang T., Nguyen D., Franco P., Murakami T., Ohnishi A., Kurosawa H.: Anal. Chim. Acta *557*, 221 (2006).
3. Franco P., Zhang T.: J. Chromatogr., B *875*, 48 (2008).
4. Tachibana K., Ohnishi K.: J. Chromatogr., A *906*, 127 (2001).
5. Zhang T., Franco P., Nguyen D., Hamasaki R., Miyamoto S., Ohnishi A., Murakami T.: J. Chromatogr., A *1269*, 178 (2012).

AUTOMATED N-GLYCOSYLATION ANALYSIS FOR TRANSLATIONAL GLYCOMICS: QUO VADIS?

ANDRAS GUTTMAN

MTA-PE Translational Glycomics Group, MUKKI, University of Pannonia, Veszprem, Hungary
guttman@lendulet.uni-pannon.hu

Summary

The glycome is the entire set of sugars in a cell, tissue or organism at a certain time, including free and complex forms. Unlike genomes, the glycome is highly dynamic, due to the interplay of those more than 600 enzymes that can be involved in the complex pathways of protein glycosylation. In addition, glycosylation is cell, protein and site specific and epigenetic factors regulating the expression of glycosyltransferases and glycosidases may represent further diversifying mechanisms, influencing the functions of the proteins to which carbohydrates are attached. In the biomedical field, altered glycosylation is frequently associated with pathological conditions. Glycosylation modulation in the biotechnology industry, usually due to changes in bioprocessing / cell culture conditions, may alter the affectivity of biotherapeutics. In both instances, information about specific glycosylation motifs such as the type and number of sugar monomers along with their position and linkage specificity are of high importance. Glycomics, as a subset of glycobiology, systematically studies all glycan structures in a given sample. To fulfill the need of such global glycomics studies, automated, high throughput (preferably in 96 well plate formats) and robust bioanalytical platforms are required to address sample preparation (glycoprotein capture, glycan release and carbohydrate labeling), separation (capillary electrophoresis or liquid chromatography) and data processing (glycoinformatics) issues. This talk will confer the state of the art of analytical glycomics and discuss recent efforts and future prospective of this emerging field in regards to system integration, translational options and their implications in the biomedical and biopharmaceutical arena.

The authors gratefully acknowledge the support of the Hungarian Academy of Sciences via the Momentum Grant #97101 (MTA–PE Translational Glycomics) and the Czech-Hungarian Mobility Support (E277/2/2013).

FAST DETERMINATION OF CATIONS AND ANIONS ON ELECTROPHORETIC MICROCHIP IN CEREBROSPINAL FLUID

JASNA HRADSKI, MARIÁN MASÁR, and RÓBERT BODOR

Department of Analytical Chemistry, Faculty of Natural Sciences, Comenius University in Bratislava, Bratislava, Slovakia
hradski@fns.uniba.sk

Summary

A new analytical method for fast and direct determination of inorganic cations and anions in cerebrospinal fluid by microchip electrophoresis with conductivity detection has been proposed. Samples of cerebrospinal fluid were only diluted appropriately before the analysis. Two different electrolytes were used, one for cationic, and another for anionic separations, at pH 3.1 and 4.3, respectively. Limits of detection were in the range 0.015–0.046 mg L^{-1} and 0.062–0.218 mg L^{-1} for cations and anions, respectively. Repeatabilities of migration times for both cations and anions were up to 1.6 %. Repeatabilities of peak areas for cations were between 2.4 and 4.5 % and for anions between 0.9 and 3.9 %. Recoveries of studied cations and anions in tested samples ranged from 92 to 106 %.

1. Introduction

Cerebrospinal fluid (CSF) analysis is mainly used in diagnostics of central nervous system diseases[1]. It is known that increase or decrease of certain inorganic cations and anions in the CSF can indicate several illnesses, e.g. Alzheimer's disease[2], multiple sclerosis[3], meningitis[4] and Parkinson's disease[5].

Since CSF is a complex matrix the analytical methods with good selectivity and sensitivity are to be used. In addition, in order to achieve fast analysis with minimum sample consumption miniaturized analytical techniques are being used. Microchip capillary electrophoresis fulfills all of these demands.

The simultaneous analysis of cations and anions in complex biological samples is very rare, due to their different concentration levels in such samples. Therefore, microchip electrophoresis methods for separations of inorganic cations (ammonium, calcium, magnesium, sodium and potassium) and anions (chloride, sulfate, nitrite and nitrate) using two background electrolytes (BGEs) on the same microchip were proposed.

2. Experimental

2.1. Instrumentation

Separations were carried out on PMMA column coupling (CC) microchip with integrated conductivity sensors (IonChipTM 3.0, Merck, Darmstadt, Germany). MicroCE analyzer consisted of electrolyte and electronic unit. Main components of an electrolyte unit were peristaltic micropumps and membrane driving electrodes. Peristaltic micropumps were used to transport BGE and sample solutions to the microchip. The membrane driving electrodes were used to suppress disturbances due to the bubble formation during the separation run. An electronic unit delivered the stabilized driving current to the counter-electrode, drove the peristaltic micropumps and interfaced the microCE analyzer to a PC. This unit also included the measuring electronics of the contact conductivity detectors. Monitoring of the analysis as well as collecting the data from conductivity detectors and their evaluation were done using MicroCE Win software, version 2.4 (Merck).

2.2. Chemicals, electrolytes and samples

Chemicals used for the preparation of electrolyte solutions were obtained from Sigma-Aldrich (Steinheim, Germany). Model samples were prepared from chemicals of p.a. purity (Sigma-Aldrich).

CSF samples were collected from three patients with symptoms of neurodegenerative diseases in the 1st Neurological Clinic on Faculty of Medicine, Comenius University in Bratislava and stored at –40 °C in 1.5 mL polypropylene microcentrifuge tubes (VWR, Wien, Austria). Prior to the analysis samples were defrosted, homogenized and after appropriate dilution analyzed.

3. Results and discussion

3.1. Analysis of model samples

Capillary zone electrophoresis (CZE) separations in two different BGEs were performed with model samples during one day on the same microchip. Repeatabilities of migration time and peak area were evaluated from four repeated CZE analyses at three different concentration levels. RSD values of migration times of cations were within 1.2 % and of anions within 0.4 %. RSD values of peak area ranged from 0.3 to 5.6 % for cations and from 0.6 to 5.9 % for anions.

Standard procedure was used for estimation of limit of detection (LOD) based on three time of signal to noise

ratio (3×S/N). LOD was calculated for each of the cations and anions. LOD of cations ranged from 0.015 to 0.046 mg L^{-1} while LOD of anions were from 0.062 to 0.218 mg L^{-1}.

3.2. Analysis of real samples

Electropherograms obtained from analyses of both cations and anions are shown in Fig. 1. Samples were diluted 1500–2500 times for analysis of cations. They were directly analyzed using CZE approach, since under these dilution factors all cations were separated with good resolution.

CZE-CZE approach had to be used in order to determinate anionic micro-constituents since there is excess of chloride in CSF. Initially, CZE separation was performed in the first channel of the microchip and chloride, the most mobile analyte and, at the same time, macro-constituent, was removed into the bifurcation region. Subsequently, by switching the direction of the driving current from the first to the second channel, the rest of chloride and all other analytes migrating behind, were transferred to the second channel, where CZE separation was carried out. Fig. 1 shows that chloride was not completely removed in the first channel which can be ascribed to diffusion driven transfers of chloride from the bifurcation region to the second separation channel.

Three different CSF samples were analyzed on the same microchip. Repeatabilities of migration time and peak area were evaluated from four repeated CZE analyses. RSD values of migration times for cations were from 0.2 to 1.6 % and for anions ranged from 0.2 to 1.0 %. RSD values of peak areas ranged from 2.4 to 4.5 % for cations and for anions were from 0.9 to 3.9 %. Repeatabilities of both migration times and peak areas in CSF samples were similar to those in model samples.

Concentrations of cations and anions obtained from the analyses of CSF samples corresponded to a large extent with concentrations of studied ions found in literature. Recoveries of the cations and anions in CSF samples ranged from 92 to 106 %.

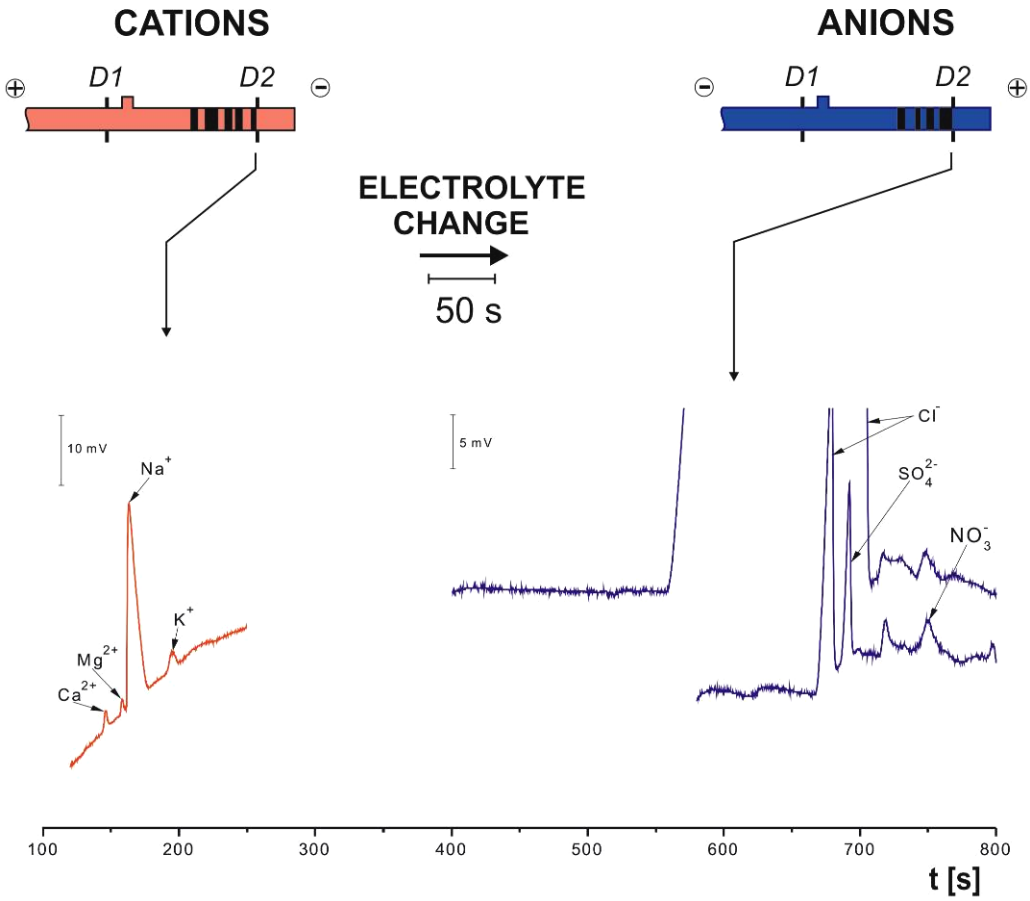

Fig. 1. **CZE separations of inorganic cations and anions present in CSF sample.** Separations were carried out in cationic and anionic BGE at pH 3.1 and 4.3, respectively. Driving current was stabilized at 50 μA for separation of cations and 30 μA for separation of anions in both separation channels

4. Conclusions

This work dealt with separation of cations and anions by CZE in three CSF samples on CC microchip. CSF samples with suspected neurological diseases were analyzed without any pretreatment other than dilution. Given high concentration of chloride in CSF, CZE-CZE approach has been used for determination of anionic micro-constituents, sulfate and nitrate. CZE approach was used for determination of chloride. For determination of cations CZE approach was used.

The employed methods are suitable for fast and sensitive determinations of the studied cations and anions (LOD in the range 0.02–0.05 and 0.06–0.22 mg L^{-1} for cations and anions, respectively) in CSF without any pretreatment.

This work was supported by grants from the Slovak Research and Development Agency (APVV-0583-11) and the Research & Development Operational Programme funded by the ERDF (Industrial research of new drugs based on recombinant proteins, RecProt, 26240220034).

REFERENCES

1. Deisenhammer F., Bartos A., Egg R., Gilhus N. E., Giovannoni G., Rauer S., Sellebjerg F.: Eur. J. Neurol. *13*, 913 (2006).
2. Tohgi H., Abe T., Yamazaki K., Murata T., Isobe C., Ishizaki E.: J. Neural. Transm. *105*, 1283 (1998).
3. Drulović J., Dujmović I., Mesaroš Š., Samardžić T., Maksimović D., Stojsavljević N., Lević Z., Mostarica Stojković M.: Mult. Scler. *7*, 19 (2001).
4. Briem H.: Scand. J. Infect. Dis. *15*, 277 (1983).
5. Kuiper M. A., Visser J. J., Bergmans P. L. M., Scheltens P., Wolters E. C.: J. Neurol. Sci. *121*, 46 (1994).

HILIC: EFFECT OF THE STRUCTURE OF THE MOBILE AND STATIONARY PHASE ON THE RETENTION OF PHENOLIC COMPOUNDS ON THE DIOL BASED COLUMNS

PETR JANÁS, PAVEL JANDERA, and TOMÁŠ HÁJEK

University of Pardubice, Faculty of Chemical Technology, Department of Analytical Chemistry, Pardubice, Czech Republic
petrjanas@seznam.cz

1. Introduction

1.1. HILIC

HILIC, which is a useful method for separation of polar compounds[1], can be characterized as a normal-phase liquid chromatography using the polar columns and water-organic mobile phases, where the range of content of water component is around 2–40 % (ref.[2]). The principle of the method consists in adsorption of molecules water from the water-organic mobile phase onto the surface of the polar stationary phase, where it creates a diffuse layer. The retention is based on the combination of two major mechanisms, partition into the water-rich layer and adsorption onto the surface of a polar stationary phase[3].

1.2. Abraham LSER model

LSER model is the approach, which employs multi-parameter linear correlation between the solvation parameters and the logarithm of the solute retention factor[4]

$$\log k = c + v \cdot V + s \cdot S + a \cdot A + b \cdot B \qquad (1)$$

where V,S,A,B are the structural molecular descriptors and v,s,a,b are the separation system parameters.

2. Experimental

The experiments were carried out on the YMC Triart Column (5 µm, 150 × 2 mm id, organic/inorganic silica particles with bonded dihydroxypropyle groups) and the results were compared to the other two columns with the diol-based columns, Luna HILIC (3 µm, 50 × 3 mm id) and LiChrospher 100 Diol (5 µm, 125 × 4 mm id). All the experiments were carried out at 40 °C at the flow-rate of the mobile phase set to 0.2 mL min^{-1}. The composition of the mobile phase was: 10 mM NH_4Ac in water with the addition of 0,1 % HCOOH/10 mM NH_4Ac in acetonitrile. The standard compounds were phenolic acids and flavonoids.

3. Results and discussion

3.1. Effect of the mobile phase on the retention of flavonoids and phenolic acids

The retention was measured over the full mobile phase composition range-from 2 to 95 percent of buffered water (10 mM NH_4Ac, 0,1% HCOOH) in acetonitrile. The columns showed both reversed phase and aqueous normal phase (HILIC) mechanism and this dual retention mechanism was successfully described by the four parameter equation[5]:

$$\log k = a + m_{RP} \cdot \varphi_{H2O} - m_{HILIC} \cdot \log(1 + b \cdot \varphi_{H2O}) \qquad (2)$$

where a is the logarithm of the retention factor in pure less polar solvent. Parameters m_{HILIC}/m_{RP} characterize the rate of decreasing/increasing retention with increasing volume fraction of buffered water in the mobile phase. All plots of retention factor (k) dependence on the content of water showed "U-shape" (ref.[5,6]).

3.2. Effect of the structure of the mobile and stationary phases on the retention of phenolic acids and flavonoids – Abraham LSER model

The parameters v, s, a, b („v“ characterize the contribution selective non-polar, “s” dipole–dipole and “a

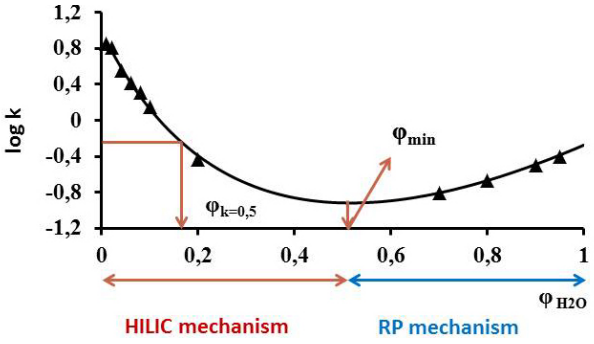

Fig. 1. **Dependence of the logarithm of the retention factor of *p*-hydroxybenzoic acid on the volume fraction of water on the YMC Triart Diol-HILIC column.** The volume fraction of water, φ_{min}, corresponding to the minimum of the U-turn, indicates the transition between the HILIC and RP modes, and $\varphi_{k=0,5}$, corresponds to the volume fraction of water, where the retention of the phenolic acids and flavonoids in the HILIC mode is sufficient. Values of φ_{min} and $\varphi_{k=0,5}$ were compared to the other columns and widest range of composition of the mobile phase, where HILIC mechanism predominates, was on the YMC Triart Diol HILIC

Table I
The comparison of the values of φ_{min} and $\varphi_{k=0,5}$ for the chosen phenolic acids on the YMC Triart Diol HILIC (A), Luna HILIC (B) and LiChrospher Diol (C) columns

A. Compound	φ_{min}	$\varphi_{k=0.5}$
Chlorogenic acid	**0.62**	**0.23**
p-hydroxybenzoic acid	**0.52**	**0.18**
Salicylic acid	**0,41**	**0.09**
B.		
Chlorogenic acid	**0.38**	**0.18**
p-hydroxybenzoic acid	**0.34**	**0.02**
Salicylic acid	**0.35**	**0.06**
C.		
Chlorogenic acid	**0.58**	**0.18**
p-hydroxybenzoic acid	**0.40**	**0.04**
Salicylic acid	**0.44**	**0.06**

and b" hydrogen-bonding interactions) were obtained as a result of multilinear regression analysis fitting the experimental retention factors, k, to the LFER model described by eq. (*1*) and are shown in Table II. Fitting the experimental data with Abraham LFER model was the most successful for flavonoids in the RP mode. For phenolic acids was the experimental fitting as similar in HILIC as in RP mode. The retention of phenolic acids and flavonoids is most affected by the parameter v, which characterizes contribution of the size of the molecule (dispersion interactions) to the retention and b, which characterizes contribution of the hydrogen bonding basicity.

3.3. Comparison of the separation properties of the columns

The separation selectivity was investigated by calculating the separation factors, α, which signify the relation of the retention factors of phenolic acids to the retention factor of 4-hydroxyphenylacetic acid. The separation factors of phenolic acids were the highest in the HILIC mode on YMC-Triart Diol-HILIC (Table III).

4. Conclusions

As a result of the comparison, Ymc Triart Diol HILIC showed better separation selectivity for phenolic acids, higher relative retention in the HILIC mode and wider range of volume fraction of buffered water in the mobile phase, where the HILIC mechanism predominates. The column has acidic properties and the contribution of dipole-dipole interactions is apparent in HILIC mode. The hydrophobic interactions are lesser in RP mode in comparison to other columns.

The financial support of GAČR project P206/12/0398 is gratefully acknowledged.

REFERENCES

1. Alpert A. J.: J. Sep. Sci. *29*, 1784 (1990).
2. Jandera P.: Anal. Chim. Acta *692*, 1 (2011).
3. Soukup J., Jandera P.: J. Chromatogr., A *1245*, 98 (2012).

Table II
The parameters v, s, a, b of the phenolic compounds on the YMC T. Diol-HILIC column

Compounds	Mode	φ_{H2O}	c	v	s	a	b	R^2
Phenolic acids	**HILIC**	**0.10**	**1.08**	**-2.40**	**0.46**	**-0.23**	**2.08**	**0.91**
		0,08	**1,23**	**-2,43**	**0,47**	**-0,21**	**2,09**	**0,91**
		0.06	**1.41**	**-2.48**	**0.53**	**-0.27**	**2.04**	**0.93**
		0.04	**1.56**	**-2.43**	**0.55**	**-0.30**	**1.95**	**0.92**
		0.02	**1.76**	**-2.08**	**0.54**	**-0.33**	**1.51**	**0.92**
	RP	**0.95**	**-1.59**	**1.68**	**-0.38**	**0.20**	**-0.56**	**0.89**
		0.90	**-1.13**	**0.93**	**-0.25**	**0.02**	**-0.19**	**0.90**
Flavonoids	**HILIC**	**0.06**	**-0.25**	**-1.00**	**0.23**	**-0.06**	**0.95**	**0.75**
		0.04	**-0.12**	**-1.01**	**0.22**	**-0.05**	**0.97**	**0.73**
		0.02	**0.04**	**-1.09**	**0.24**	**-0.01**	**1.04**	**0.72**
	RP	**0.95**	**-0.92**	**1.61**	**0.13**	**-0.38**	**-1.30**	**0.97**
		0.90	**-0.89**	**1.23**	**0.12**	**-0.29**	**-1.03**	**0.97**
		0.80	**-0.94**	**0.72**	**0.13**	**-0.20**	**-0.66**	**0.95**
		0.70	**-0.96**	**0.38**	**0.11**	**-0.18**	**-0.35**	**0.92**

Table III
Separation factors for phenolic acids in the RP (95% H_2O) and HILIC (2% H_2O) modes

		YMC Triart Diol-HILIC				LiChrospher DIOL				Luna HILIC			
		95% H_2O		2% H_2O		95% H_2O		2% H_2O		95% H_2O		2% H_2O	
	P. acids	k_{RP}	α	k_{HILIC}	α	k_{RP}	α	k_{HILIC}	α	k_{RP}	α	k_{HILIC}	α
1	**Sal**	0,45	1,52	2,75	3,08	0,53	3,55	1,28	1,88	0,63	2,22	1,32	2,93
2	**Cou**	0,62	2,07	7,02	1,21	0,51	3,45	0,71	1,04	0,69	2,43	0,4	1,13
3	**Phb**	0,39	1,32	6,34	1,33	0,32	2,16	0,74	1,09	0,49	1,71	0,47	1,04
4	**Fer**	0,74	2,50	5,89	1,44	0,61	4,10	0,58	1,17	0,75	2,62	0,32	1,41
5	**Van**	0,48	1,60	6,57	1,29	0,37	2,53	0,51	1,33	0,51	1,79	0,41	1,10
6	**Sin**	0,92	3,07	6,07	1,39	0,66	4,48	0,58	1,17	0,78	2,74	0,33	1,36
7	**Syr**	0,54	1,81	8,48	0,99	0,39	2,65	0,76	1,12	0,60	2,11	0,53	1,18
8	**Hpa**	0,30	1,00	8,46	1,00	0,15	1,00	0,68	1,00	0,28	1,00	0,45	1,00
9	**Gal**	0,26	1,16	/	/	0,19	1,28	4,42	6,50	0,46	1,60	2,19	4,87
10	**Chl**	0,19	1,54	/	/	0,09	1,68	30,61	45,01	0,31	1,10	13,09	29,1

4. Abraham M. H., Rosés M., Poole C. F.: J. Phys. Org. Chem. *10*, 358 (1997).
5. Jandera P., Hajek T.: J. Sep. Sci. *32*, 3603 (2009).
6. Pesek J. J., Matyska M. T., Larrabee S.: J. Sep. Sci. *30*, 637 (2007).

MULTI-STEP SYNTHESIS OF CASPASE-3 SENSOR BASED ON FÖRSTER RESONANCE ENERGY TRANSFER

MARCELA LISKOVA[a], KAREL KLEPARNIK[a], PAVEL PAZDERA[b], and FRANTISEK FORET[a]

[a] *Institute of Analytical Chemistry ASCR, v.v.i., Brno,*
[b] *Centre for Syntheses at Sustainable Conditions and Their Management Department of Chemistry, Faculty of Science, Masaryk University, UKB, Brno, Czech Republic*
liskova@iach.cz

Summary

Programmed cell death or apoptosis is regulated process of cell suicide. The central role in apoptosis play cysteine proteases called caspases. Caspases recognize tetra-peptide sequences Asp-Glu-Val-Asp (DEVD) on their substrates and hydrolyze peptide bonds after aspartic acid residues. Various techniques for the determination of caspase-3 are commercially available e.g. Enzyme Linked Immuno-Sorbent Assay (ELISA), Western blotting or flow cytometric analysis. The products of the cleavage can be detected by spectrophotometry, fluorimetry, chemi-luminescence (CL) or ELISA. In this work, we suggested fluorescent sensor based on Förster Resonance Energy Transfer (FRET) to determine caspase-3 in cell nucleus or cytoplasm by apoptosis for very fast analysis by fluorescence microscopy without sample destroying.

1. Introduction

Programmed cell death (apoptosis) is an essential mechanism to eliminate unwanted cells during the development and homeostasis of multicellular organism[1,2]. Unregulated cell death is implicated in a growing number of clinical disorders. Failure of apoptosis in different way can lead to ischemia damage, neurodegenerative diseases, cancer or autoimmune diseases[3,4]. The central component of apoptosis is a proteolytic system involving a family of proteases called caspases. Caspses are among the most specific of proteases, an unusual and absolute requirement for cleavage of the peptide bond after aspartic acid (C-terminal)[5,6]. Caspase family consists of 15 mammalian members. Caspases are potential targets for therapeutical interventions in the case of tumorigenesis and other pathologies[1,7]. One of the members of caspase family caspase-3 is a key factor in apoptosis which recognizes tetra-peptide sequences DEVD. Currently, the majority of analytical methods for detecting caspase-3 activity are Western blotting, flow cytometric analysis or ELISA with colorimetric/fluorimetric detection[8]. Plenty of techniques were recently developed for detection of caspase-3 in cells with high spatio-temporal resolution e.g. fluorescence resonance energy transfer (FRET) based-assay[9,10].

Förster (fluorescence) resonance energy transfer (FRET) is a widely prevalent photophysical process that occurs between a donor (D) molecule in the excited state and an acceptor (A) molecule in ground states. Energy transfer occurs without the appearance of a photon and is the result of long range dipole-dipole interactions between D and A. This physical transfer of energy usually takes place over a D-A separation of 0.5–10 nm (ref.[11–13]). FRET is one of the few experimental techniques that are able to detect and define distance between molecules, molecular dimensions, proximities change with time, heterogeneous molecular conformations etc.[13].

Luminescent semiconductor nanocrystals called quantum dots (QDs) have unique photophysical properties e.g. high photostability, high emission quantum yield, narrow emission peaks and size – dependent wavelength tunability. QDs have already been used successfully in cellular imaging, immunoassay, DNA hybridization and optical barcoding. QDs with high photostability and wavelength tunability are very suitable to use in FRET based assay as a donor of transferred energy[14].

2. Experimental

For QDs preparation was used one-step synthesis described elsewhere[15]. For organic quencher preparation was used synthesis described in US patent[16].

2.1. Chemicals

As a linker chain were used cysteamine (98%) and *O*-(3-Carboxypropyl)-*O*′-[2-(3-mercaptopropionylamino) ethyl]-polyethylene glycol (PEG) (M_w 3000), as a cross-linkers were used *N*-(3-Dimethylaminopropyl)-*N*′-ethylcarbodiimide hydrochloride (EDC) (99%) and *N*-hydroxy-2,5-dioxopyrrolidine-3-sulfonicacid sodium salt (sulfo-NHS) (99%), as a DEVD sequence was used *N*-Acetyl-Asp-Glu-Val-Asp *p*-nitroanilide (97%) and for deacetylation of terminal *N*-acetyl group was used Penicillin amidase from Escherichia coli (M_r ~70 000). Chemicals mentioned above were purchased from Sigma-Aldrich. Conjugation reaction were done in sodium carbonate buffer (pH 10.5; c = 50 mM) and precipitation including purification of conjugation product was carried out in isopropanol (*i*-Pr). Both, Na_2CO_3 (p.a.) and *i*-Pr (99.7%) were purchased from Lach-Ner. Sodium hydroxide (NaOH) (p.a.) was purchased from Lach-Ner, too. Sodium dithionite ($Na_2S_2O_4$) (99%), for moderate reduction of DEVD *p*-nitroanilide, was purchased from PENTA. 18.2 MΩ × cm ultrapure water was produced by

Neptune Purite Ultimate. For TLC detection we used TLC Silica gel 60 (Merck) and mobile phase was methanol (for UV-VIS spectroscopy) from PENTA.

2.2. Conjugation reactions of QDs and linkers

At first, QDs were conjugated with cysteamine as a linker. QDs (5 mg) were dissolved in 1 ml of 50 mM carbonate buffer at pH 10.5. Then 5 mg EDC and 2 mg sulfo-NHS were add and gently vortexed. This mixture then reacted with 15 mg cysteamine to produce conjugate with terminal thiol group for subsequent reactions. This conjugate was precipitate using *i*-Pr and dried in vacuum in Concentrator 5301 (Eppendorf) at 30 °C. Dried conjugate of QDs and cysteamine was dissolved in 0.5 mL carbonate buffer (pH 10.5). This solution then reacted with 78 µl of PEG (1 mg mL^{-1} in 50 mM carbonate buffer, pH 10.5). Reaction mixture reacted for 2 hours at 37 °C to produce disulfide bridges. Reaction product was precipitate using *i*-Pr and dried in vacuum in Concentrator 5301 at 30 °C.

2.3. Reduction and purification of DEVD sequence

Nitro group from *p*-nitroanilide in DEVD sequence was moderately reduced using sodium dithionite. 2.5 mg DEVD was dissolved in deionized water with addition of 6 µl sodium hydroxide (c = 1.25 M) in order to increase DEVD solubility. 11 mg of $Na_2S_2O_4$ was then added into alkalized solution of DEVD and reduction reaction occurred immediately. Successful reduction of nitro group in DEVD sequence was checked by TLC at 254 nm and by ninhydrin reaction. As a mobile phase was used methanol. Desalting of reduced DEVD was done by Zip-Tip C18 from Millipore.

3. Results and discussion

We have designed sensor for caspase-3 determination in individual apoptotic cells. This sensor is based on FRET, were oscillating electrons, in donor in our case quantum dot, exchange energy with acceptor dipole (BHQ-2 modified quencher) with similar resonance energy via the chain of linker. Our modified BHQ-2 quencher absorbs transported energy and is able to quenched fluorescence. But after cleavage of the bond between quencher and DEVD sequence in presence of caspase-3 in real samples, there is no non-radiative FRET transfer, quencher doesn´t absorb energy and QD emits light at given wavelength (Fig. 1). We used CdTe QDs with maximum emission wavelength 600 nm and with mercaptopropionic acid as a surface ligand.

QDs were modified for DEVD bonding at first by cysteamine (as short linker) and at second by PEG to achieve efficient and optimal Förster distance. Products analyses of conjugation reactions were checked by capillary zone electrophoresis with laser induced fluorescence detection (CZE-LIF). Quencher was successfully synthesized according US patent[16]. We succeed in solving problems with QDs precipitation during sensor synthesis and problems with purification of particular conjugation products. We successfully desalted reduced DEVD and checked it by MALDI-TOF. All results will be presented.

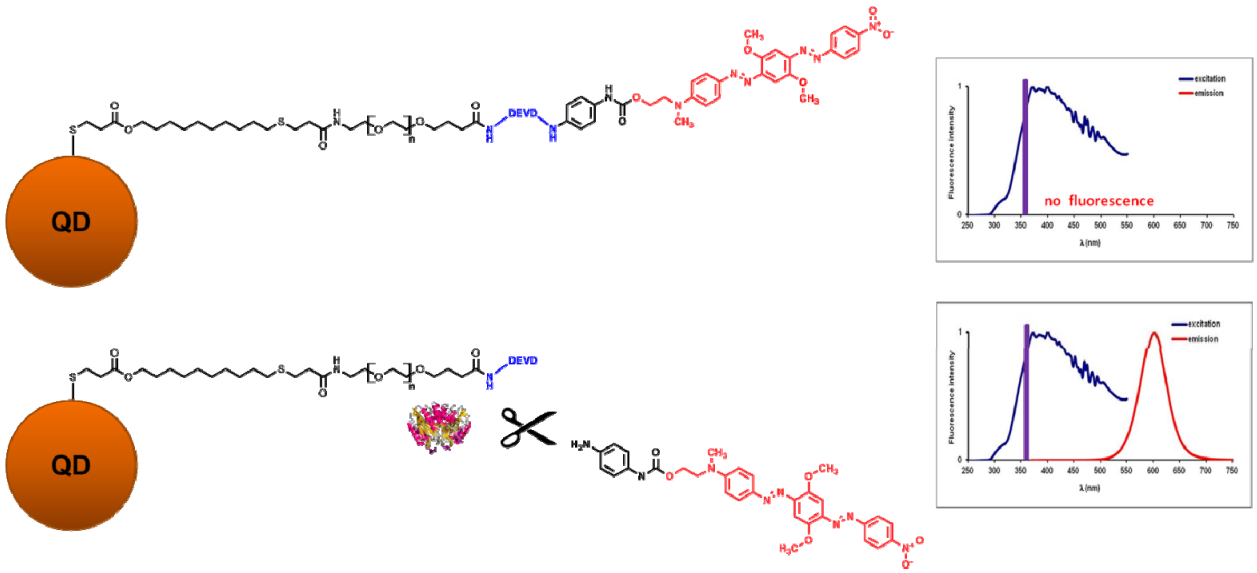

Fig. 1. **Model of caspase-3 sensor with DEVD sequence. A) Model of caspase-3 sensor, without cleavage of DEVD chain and FRET transfer with quenching of fluorescence, B) Cleavage of bond between DEVD and quencher and no FRET transfer with QD´s emission of light**

4. Conclusions

We designed new sensor based on FRET to determined caspase-3 in individual apoptotic cells especially to determine caspase-3 in cell nucleus or cytoplasm. Using of this sensor offer us possibility for very fast analysis of samples by fluorescence microscopy. This method allow reusing of samples in comparison with other detection techniques of caspase-3 like ELISA where samples are destroyed e.g. by cell lysis.

This work was supported by The Grant Agency of the Czech Republic (P301/11/2055, P206/12/G014 and P206/11/2377), Ministry of Industry and Trade (2A-1TP1/090), and institute research plan AV0Z40310501. This project is co-financed by the European Social Fund and the state budget of the Czech Republic (CZ.1.07/2.3.00/20.0182).

REFERENCES

1. Raff M.: Nature *396*, 119 (1998).
2. Jacobson M. D., Weil M., Raff M. C.: Cell *88*, 347 (1997).
3. McIlwain D. R., Berger T., Mak T. W.: Cold Spring Harbor Perspect. Biol. *2013*, 5.
4. Li J., Yuan J.: Oncogene *27*, 6194 (2008).
5. Thornberry N. A., Lazebnik Y.: Science *281*, 1312 (1998).
6. Rupinder S. K., Gurpreet A. K., Manjeet S.: Vascul. Pharmacol. *46*, 383 (2007).
7. Strasser A., Cory S., Adams J. M.: EMBO J. *30*, 3667 (2011).
8. Li Y.: Microchim. Acta *177*, 443 (2012).
9. O'Brien M. A., Daily W. J., Hesselberth P. E., Moravec R. A., Scurria M. A., Klaubert D. H., Bulleit R. F., Wood K. V.: J. Biomol. Screen. *10*, 137 (2005).
10. Sha S., Jin H., Li X., Yang J., Ai R., Lu J.: Protein Cell *3*, 392 (2012).
11. Saini S., Singh H., Bagchi B.: J. Chem. Sci. *118*, 23 (2006).
12. Rev. Mol. Biotechnol. *82*, 177 (2002).
13. Clegg R. M.: Curr. Opin. Biotechnol. *6*, 103 (1995).
14. Clapp A. R., Medintz I. L., Mauro J. M., Fisher B. R., Bawendi M. G., Mattoussi H.: J. Am. Chem. Soc. *126*, 301 (2003).
15. Duan J., Song L., Zhan J.: Nano Res. *2*, 61 (2009).
16. Gharavi et al.: US 7205347 B2, 2007.

CAPILLARY ELECTROPHORESIS WITH CONTACTLESS CONDUCTIVITY DETECTION FOR AMINO ACID PROFILING OF HUMAN AND URINE SAMPLES

ALES MADR, ANDREA CELA, JINDRA MUSILOVA, MARTA ZEISBERGEROVA, and ZDENEK GLATZ

Department of Biochemistry, Faculty of Science and CEITEC, Masaryk University, Kamenice 5, 625 00 Brno, Czech Republic
175764@mail.muni.cz

Summary

Analysis of amino acids in their native form using conventional detection techniques is hindered by lack of chromophores or fluorophores in the structure of the most amino acid. As a result, amino acids are prior the detection derivatized by suitable agents. Derivatization step can be omitted when conductivity detection method is employed. Benefits of capillary electrophoresis and contactless conductivity detection were merged and resulted in analytical method that was tested for amino acid profiling of human plasma and urine samples.

1. Introduction

Quantitative amino acid (AA) analysis is a significant tool for many scientific areas ranging from the characterization of protein to the description of natural products attractive for food and pharmaceutical industry. AAs are not only building blocks of proteins but they also act as precursors of several neurotransmitters, porphyrins and nucleic acids. Quantification of AAs in biological fluids can reveal metabolic disorders affecting synthesis or degradation of AAs. Since AAs play complex role in a living organism, they can reflect health-sate of the organism thus AA profiling can be used for supplementary diagnostic purposes in medical practice where determination of proper diagnosis is unclear or when specific markers are not discovered yet.

2. Experimental

Agilent G7100 Capillary Electrophoresis System with integrated A/D converter using in-cassette-built in-house assembled contactless conductivity detection (CE-C^4D) was used for analysis of AAs in their native form. C^4D was derived from the one presented by Gas *et al.*[1] differing mainly in an operational frequency of a crystal oscillator used. Data acquisition and integration were performed by Agilent ChemStation software.

2.1. Separation conditions

Separation conditions follow from the articles published earlier[2–5] and were refined to obtain the best performance for separation of human plasma, serum and urine samples. Background electrolyte (BGE) consists of 8 % (v/v) acetic acid and 0.1 % (m/m) (hydroxyethyl)-cellulose. Separations were carried out in a bare fused-silica capillary of 50/375 μm inner/outer diameter and 80.0/65.6 cm total/effective length. Cassette with capillary was kept at constant 30 °C and a driving voltage was set to +30 kV with a typical current 12 μA (anode at a sample introduction side). Sample was introduced into the capillary by 50 mbar (0.725 psi) pressure drop for 30, 24 and 12 seconds for human plasma, urine and for creatinine (CR) determination in urine, respectively.

2.2. Sample treatment

Samples of human plasma and urine were stored frozen at –70 °C. On the day of the analysis they were thawed at a room temperature. Proteins were precipitated by an addition of acetonitrile in the volume ratio 1:2, thoroughly stirred and centrifuged at 10 000×g for 10 minutes. Supernatants of human plasma samples were enriched by an addition of guanidineacetic acid (GAc; internal standard) giving final concentration of 50 μM of GAc, 3.1× diluted sample in the 66 % (v/v) acetonitrile. Supernatants of urine samples were analyzed without GAc due to co-migration of GAc with other unidentified peaks, thus the urine samples were only 3× diluted in 66 % (v/v) acetonitrile. Determination of CR in the urine samples demands additional dilution due to a high concentration of CR in the urine. Urine samples were diluted in 66 % (v/v) acetonitrile giving final dilution 100–200×. Presence of acetonitrile in the samples reduces sample conductivity and results in better peak shapes.

3. Results and discussion

3.1. Plasma samples

Twenty-six human plasma samples were collected from patients diagnosed with *i*) cancer, *ii*) cystic fibrosis, *iii*) coagulation defects, purpura and other hemorrhagic conditions, *iv*) other venous embolism and thrombosis. Samples were both from men and women on average 31 years old (range 1–66 years). Quantification of 18 AAs was possible in the all samples. Measured concentrations of AAs were submitted to principal component analysis using OriginPro software resulted in a partial grouping of the samples with the same diagnosis.

3.2. Urine samples

Four early urine samples were provided voluntarily by women 21–24 years old. Prior to storage, the urine samples were passed through membrane filter with 0.2 μm porosity to remove cells and concretions. One urine sample was provided by a woman suffering from epilepsy seizures (cause untold) and the rest were from healthy women and served as a control group. There were found significant differences in levels of the most quantified AAs. However, no solid conclusion can be stated because of a small statistical sample.

4. Conclusions

Presented CE-C^4D method proved to be sensitive and reliable for analysis of AAs their native form in human plasma and urine samples. Multivariate statistical analysis resulted in a partial grouping of the human plasma samples with the same diagnosis thus AA profiling can provide supplementary information about the health-state of the organism. Urine analyses showed sensitivity and precision of the CE-C^4D method. Fact that both plasma and urine can be analyzed at the same condition differing only in the sample introduction times benefits for easy automation of the method.

Financial support granted by the Czech Science Foundation (Project No. P206/11/0009) and the European Social Fund (Project No. CZ.1.07/2.3.00/20.0182 administered by the Ministry of Education, Youth and Sports of the Czech Republic) is highly acknowledged.

Special thanks belong to the Associate Professor Josef Tomandl, Ph.D. from Department of Biochemistry of Faculty of Medicine, Masaryk University for an arrangement of the human plasma samples.

REFERENCES

1. Gas B., Zuska J., Coufal P., van de Goor T.: Electrophoresis *23*, 3520 (2002).
2. Coufal P., Zuska J., van de Goor T., Smith V., et al.: Electrophoresis *24*, 671 (2003).
3. Samcova E., Tuma P.: Electroanalysis *18*, 152 (2006).
4. Tuma P., Samcova E., Andelova K.: J. Chromatogr., B *839*, 12 (2006).
5. Tuma P., Malkova K., Samcova E., Stulik K.: J. Sep. Sci. *33*, 2394 (2010).

ANALYSIS OF TISSUE-BOUND CELLS: NOVEL APPROACHES USING LASER CAPTURE MICRODISSECTION

EVA MATALOVÁ[a,b], EVA ADAMOVÁ[b,c], and KAREL KLEPÁRNÍK[c]

[a] *Institute of Animal Physiology and Genetics CAS, v.v.i., Brno,* [b] *Faculty of Veterinary Medicine UVPS, Brno,* [c] *Institute of Analytical Chemistry CAS, v.v.i., Brno, Czech Republic*

Summary

Recent biomedical research prefers analysis of homogenous samples obtained from primary cells to cell lines. Moreover, attention is paid to cells of low number but high biological impact, such as signalling centres in embryonic development, stem cells or tumour cells. To localize cells of interest within an organ/tissue, histological sections are widely used. However, the methods of choice for further analysis of such samples are mostly limited to histochemistry, immunohistochemistry and *in situ* hybridization.

The repertoire of methodical tools for specific analyses of tissue bound cell populations was considerably enriched by introduction of laser capture microdissection (LCM)[1]. The LCM system represents a modified microscopic technique and above other applications allows for selection of cells within histological sections and their contact-free laser-mediated catapult into a test-tube. This approach yields homogenous cell samples for further analyses. The basic principle operates with stained or unstained histological sections placed on a common or membrane coated slides. The LCM microscope allows visualisation of the section on a computer screen where the cells of interest can be gated. In the next step, laser beam cuts the area and catapults selected cells into a test tube.

Many significant results have been achieved using LCM technique during the last decade. However, as LCM usually provides small amount of biological materials, most of the results are related to the nucleic acid level where amplification methods are available. However, in the case of proteins, where the amplification step is not possible, the great benefits of LCM fade. Therefore, LCM applications in proteomics lack behind genomic and transcriptomic studies.

To overcome the disadvantage of low quantities of tissues and cells for protein evaluation, a novel approach based on flow cytometry (FC) of laser micro-dissected samples was designed. The technique combines LCM providing homogenous samples of tissue bound cells and flow cytometry allowing for evaluation of individual cells. To obtain intact cells, thick cryopreserved sections are used for LCM and the sample undergoes enzymatic and/or mechanical disintegration prior to FC. The method was verified using two populations of cells, apoptotic and proliferating, analysis was performed at DNA and protein levels. LCM-FC results were confronted with biochemical and immunohistochemical findings[2].

To go further, towards even more specific investigation, LCM has been considered with focus on single cells analysis and investigation of post-translationally modified proteins. As a model, caspase-3 was used. This cystein protease represents one member of the cell death trio during apoptotic execution. Caspase-3 as an proenzyme is in general continuously expressed in cells and must be cleaved to become active. Three steps were followed in the development of novel precise methods. First, to evaluate the amount of active caspase-3 per cell in apoptotic vs. non-apoptotic cells, second to quantify caspase-3 in one single cell separated from a population, and last to detect caspase-3 in one cell obtained from the tissue using LCM.

To achieve the first goal, micromass cultures were challenged by camptothecin to stimulate apoptosis. Simultaneously, developmentally induced apoptosis was followed in digital and interdigital cell populations during mouse front limb digitalisation. A modified chemiluminiscence technique clearly showed quantitative differences in caspase-3 activation during naturally *vs.* experimentally induced apoptosis, increased amount of caspase-3 per apoptotic cells vs. non-apoptotic cells and was able to provide results with femtogram accuracy[3]. To further precise the methods, micromanipulation system was used to select just one cell for analysis[4].

Recently, we have tackled the last step – to combine this novel precise technique and laser capture microdissection and thus design an elegant system for selection of one exact cell from the tissue and for analysis of this single cell. To make the method even more attractive, not only cryopreserved tissues but also fresh tissue slices have been tested. Tissue slices as designed a couple of years ago[5] can be prepared using a tissue chopper and were successfully applied in several studies dealing with tracing of translocating cells within tissues[6]. Therefore, the novel methodical combination appears promising for basic research as well as several biomedical branches.

Recent research of tissue interactions is supported by the Grant Agency of the Czech Republic (P302/12/J059). Novel methodical approaches are granted by the project GACR P206/11/2377.

REFERENCES

1. Emmert-Buck M. R., Bonner R. F., Smith P. D., Chuaqui R. F., Zhuang Z., Goldstein S. R., Weiss R. A., Liotta L. A.: Science *274*, 998 (1996).
2. Matalová E., Dubská L., Fleischmannová J., Chlastáková I., Janečková E., Tucker A. S.: Arch. Oral. Biol. *55*, 570 (2012).
3. Chlastáková I., Lišková M., Kudělová J., Dubská L., Klepárník K., Matalová E.: In vitro Cell Dev. Biol.: Anim. *48*, 545 (2012).
4. Lišková M., Klepárník K., Matalová E., Hegrová J., Přikryl J., Švandová E., Foret F.: Electrophoresis *34*, 1772 (2013).
5. Matalová E., Kovářů F., Míšek I.: Physiol. Res. *55*, 183 (2006).
6. Diep L., Matalová E., Mitsiadis T., Tucker A. S.: J. Exp. Zool., Part B *312B*, 510 (2009).

DETERMINATION OF ORGANIC ACIDS IN COMPLEX SAMPLES BY USING UV AND MS/MS DETECTION WITH/WITHOUT HPLC SEPARATION

ĽUDOVÍT SCHREIBER, IVETA HUKELOVÁ, and RADOSLAV HALKO

Department of Analytical Chemistry, Faculty of Natural Sciences, Comenius University in Bratislava, Bratislava, Slovakia
hukelova@fns.uniba.sk

Summary

The aim of this talk is to study different HPLC detectors for determination of both aliphatic and aromatic organic acids in complex mixtures. Due to the fact that suitable separation of these groups of compounds is requiring ion-exclusion chromatography (IEC) stationary phases, flow injection method was developed and tested for triple quadrupole MS detector.

1. Introduction

Separation, identification and quantitative analysis of aliphatic and aromatic acids are important due to their widespread presence in the environment and the use of both in medicine, agriculture and industry.

Free form aliphatic acids are found in various fruits e.g. malic acid in apples, citric acid in citrus fruits or tartaric, lactic and malic acids in grapes which concentration is necessary to know in winemaking. In the food industry are used as preservatives, for example benzoic acid as the sodium salt, which has the characteristics of an inhibitor for microorganisms. Carboxylic acids also serve as indicators of certain diseases, when their higher concentration e.g. in urine evokes a metabolic disorder called organic aciduria, which belongs to the hereditary metabolic disorders. The best known acidurias are propionic, glutaric, methylmalonic and pyroglutaric acid. Determination of carboxylic acids is very important for patients with diabetes, kidney disease and other metabolic disorders.

2. Experimental

2.1. Chemicals

All analytical standard-grade organic acids were obtained from Merck (Darmstadt, Germany) as the methanol (< 99% (v/v) for liquid chromatography). Stock standard solutions were obtained by dissolution of the acids in Simplicity water or methanol. The Simplicity water was purified by passage through a Simplicity® Ultrapure Laboratory Water Systems (Molsheim – France). Potassium dihydrogen phosphate (KH_2PO_4) and 85 % (v/v) phosphoric acid (H_3PO_4) supplied by Merck (Darmstadt, Germany), 0.1 and 0.05% (v/v) formic acid (HCOOH) supplied by Merck (Darmstadt, Germany) were used for the preparation of mobile phase. Hydrochloric acid 37% (v/v) (Merck – Darmstadt, Germany) and ethyl acetate (Chemapol Group – Prague, Czech Republic) were used for human urine sample pretreatment.

2.2. Apparatus

Separation was carried out on a liquid chromatography Elite LaChrom (Merck – Hitachi, Darmstadt, Germany) equipped with pump L-2130, autosampler L-2200, thermostat L-2300, diode array detector L-2450, and Agilent 1290 UHPLC (Agilent Technologies, Waldbronn, Germany) equipped with binary pump, thermostated autosampler, thermostated column compartment, diode array detector, triple quadrupole MS/MS detector. Organic acids were separated on a silica based analytical column with specially modified reversed-phase functional group Alltech Prevail™ organic acid 5 μm (150 × 4.6 mm, I.D) with an Prevail organic acid 5 μm (7.5 × 4.6 mm, I.D) guard column (Grace – Deerfield, USA).

3. Results and discussion

The composition of the separation buffer solution and gradient experimental conditions have been optimized to achieve the best separation of organic acids. Aliphatic and aromatic acids were simultaneously separated using mobile phase composed of (A) 25 mmol L^{-1} KH_2PO_4 with pH 2.3 and (B) methanol with 25 mmol L^{-1} H_3PO_4 in ratio 80:20. The separation was performed with gradient elution at 25 °C and flow rate of 1 mL min^{-1}. Injected volume of standard solutions mixture was 20 μL. The organic acids were detected with DAD at 220 nm.

The composition of mobile phase for MS detection was optimized using (A) 0.05% (v/v) formic acid and (B) methanol with 0.05% formic acid in ratio 80:20. Multi-mode ionization (ESI-APCI) in negative polarity mode was used for MS detection.

Flow injection analysis was performed restriction capillary (0.17 mm ID), and modified flow rate of mobile phase at 0.1 mL min^{-1}.

The quantification of organic acids in samples was carried out by using the method of calibrations curve and standard addition method. We used the standard addition method to determine whether the matrix of a sample changes the analytical sensitivity.

4. Conclusions

The proposed HPLC method with DAD detection meets validation criteria for chromatography methods (ICH proposed criteria for validation of chromatography methods). MS/MS detection using triple quadrupole detector shows improvements of LOD, LOQ and provides valuable qualitative information further analysis including selectivity for coeluting compounds. Risk of false positive or negative identification and quantification is also improved using QQQ detection. Flow injection analysis with mass spectrometry detection shows perspectives in reducing analysis time significantly, further focus should be important for increasing sensitivity for biological fluids analysis. Work will be focused in the future on automated techniques for clinical laboratory purposes.

This work was supported by the grant of project VEGA 1/0852/13 and the grant of project APVV-0583-11. This work is partially outcome of the project VVCE-0070.

SUPPRESION OF PROTEIN SAMPLE LOSSES IN AUTOSAMPLER VIALS

KAREL STEJSKAL[a,b], DAVID POTĚŠIL[a,b], and ZBYNĚK ZDRÁHAL[a,b]

[a] *RG Proteomics, CEITEC MU, Masaryk University, Brno,* [b] *National Centre for Biomolecular Research, Faculty of Science, Masaryk University, Brno, Czech Republic*
karel.stejskal@ceitec.muni.cz

Summary

In the present study, we assessed peptide losses during sample storage in autosampler vials. We evaluated the possibility to suppress the adsorption effects by changing the composition of the sample solution injected into the liquid chromatography coupled with tandem mass spectrometry system (LC-MS/MS) and by use of different material of autosampler vials. As a model sample, a tryptic digest of six bovine proteins (B6E) in the amount of 1 fmol per protein was used for comparative experiments. The combination of a polypropylene vial and solution of poly(ethylene glycol) (PEG) (0.001%) or a mixture of high concentrated urea and thiourea (5M and 1M) as injection solutions provided the best results in terms of number of significantly identified peptides ($P < 0.05$). These conclusions were confirmed by analyses of a real sample with intermediate complexity. Addition of PEG into the real sample solution proved to prevent higher losses, concerning mainly hydrophobic peptides, during up to 48 h storage in the autosampler in comparison with a formic acid solution and even with a solution of highly concentrated urea and thiourea[1].

1. Introduction

The last step in sample processing consists in peptide mixture preparation into sample vial prior LC-MS/MS analysis. Nonspecific adsorption of peptides on solid surfaces, such as autosampler vials, pipette tips and instrumentation parts, is a known problem. This problem became of high importance with development of highly sensitive mass spectrometric instrumentation capable to detect peptides in attomol amounts. Mainly in case of these low abundant components also quantitative analysis is accompanied with decreased repeatability due to adsorption losses[2]. Moreover, it was reported that adsorption occurs in a relatively short time[3] (in 15 minutes) and prediction of peptide adsorption on specific surfaces, based on their biochemical characteristics, is not reliable[4,5].

2. Experimental

2.1. Vial materials

Autosampler vials from seven different materials were tested. We included 3 plastic-based and 4 glass-based commercially available autosampler vials: polypropylene (PP), polyethylene (PE), polymethylpentene (PMP), borosilicate glass (GL), Kimshield™, glass (KIM), silanized glass (SIL), and RSA™ glass (RSA).

2.2. Sample injection solution

Effect of FA was compared with effects of other sample injection solutions: chaotropic agent urea (Urea), combination of urea with thiourea (U/T), dimethyl sulfoxide (DMSO), Anionic Acid Labile Surfactant I (AALS I), and polyethylene glycol (PEG).

2.3. LC-MS/MS analysis

All MS/MS analyses were performed under identical conditions using an UltiMate 3000 RSLCnano system (Thermo Scientific) on-line coupled with a HCTultra PTM Discovery System ion trap mass spectrometer equipped with a nanospray (Bruker Daltonik). After injection (10 out of the total of 12 µl present in the sample vial), peptides were concentrated and desalted on a trap column (100 µm ID × 30 mm length; filled with 3.5-µm X-Bridge BEH C18 (Waters) according to a previously described procedure[6]. FA (0.1%) was used as loading solvent (loading speed 4 µL min^{-1} for 6 min). Peptides were then eluted using a water/ACN gradient onto the separation column (75 µm ID × 150 mm length; 300 nL min^{-1}) filled with Acclaim PepMap RSLC C18 (Dionex).

3. Results and discussion

Our results indicate that significant peptide losses occur immediately after placing the peptide sample into the autosampler vial or, possibly, within the LC system during sample injection and loading on the trap column (Fig. 1). We propose the use of PEG (0.001%) which effectively decreases sample losses probably due to competition in adsorption with the peptides and it has no adverse effects to chromatographic separation or LC-MS system (2 years of continuous use).

Type of the vial material did not play as crucial role as compared to SIS composition especially in combination with PEG (see Fig. 2). Commonly available PP vials were selected for further experiments as one of the best of the tested materials.

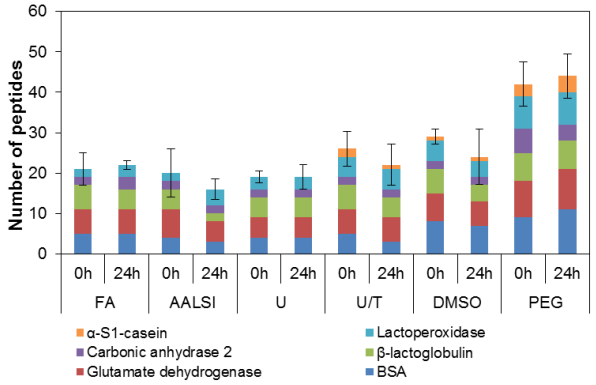

Fig. 1. **Number of significantly identified peptides identified in the model sample after mixing with sample injection solution in polypropylene autosampler vial**

In contrast to the model sample, time of storage played more important role in case of FA solution. While the number of identified peptides did not change dramatically over the tested time period for samples in U/T and PEG, the number of peptides was reduced by 34 % and 44 % after 24 h and 48 h of storage using FA, respectively. To assess the nature of peptides being likely to be preserved in the solution in presence of particular SISs, we investigated their retention times. In general, peptides are eluted by reversed-phase chromatography according to their increasing hydrophobicity. We observed significant decrease in the number of hydrophobic peptides (peptides with RT > 25 min) in FA after 24 h in comparison with the other two solutions (see Fig. 3).

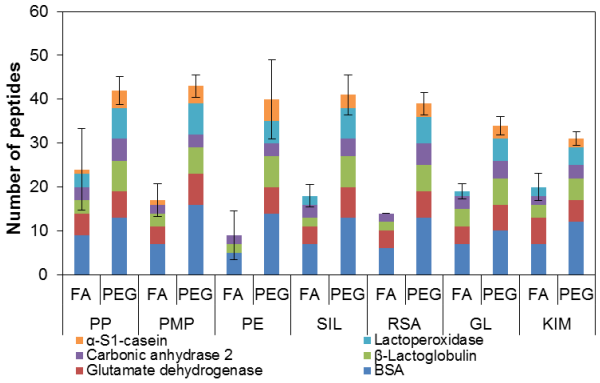

Fig. 2. **Number of significantly identified peptides ($P < 0.05$; MASCOT score > 40) identified in the model sample after mixing with 0.1% formic acid (FA) and 0.001% polyethylene glycol 20,000 (PEG) in different types of autosampler vials**

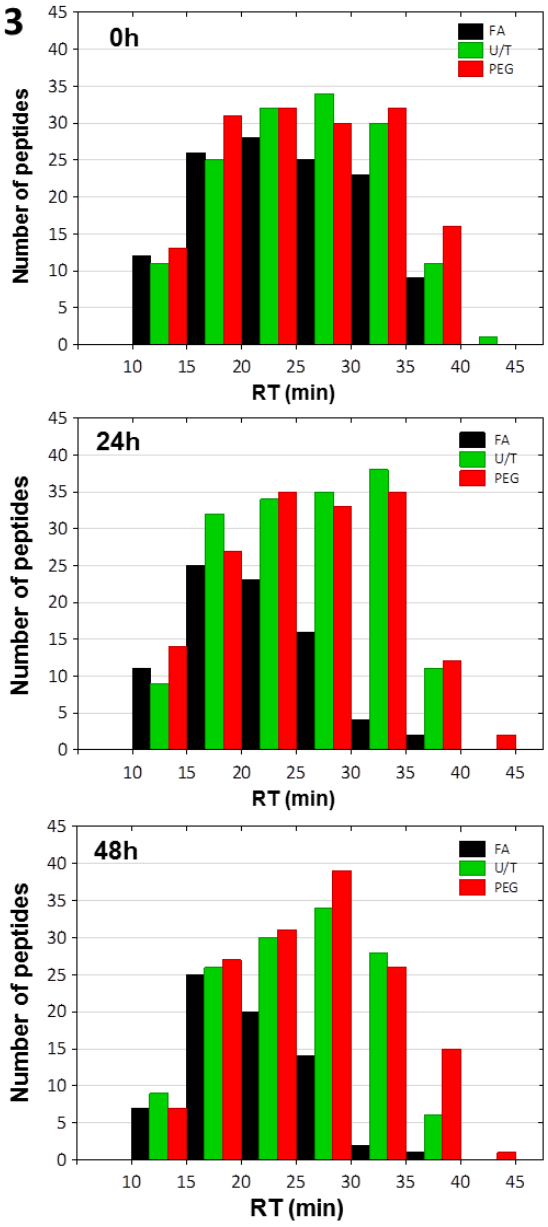

Fig. 3. **Histograms of distribution of peptides in real sample during LC-MS/MS analysis according their retention time (RT).** Real sample was before injection diluted in solutions of formic acid (FA), urea and thiourea (U/T), or polyethylene glycol 20,000

4. Conclusions

Composition of sample injection solution was found to play important role even if samples were immediately analyzed. Compared to other tested additives, PEG represents a simple and cheap solution improving the overall coverage of real sample. No substantial

quantitative losses up to 48-hours storage under studied conditions and no compromising of the LC-MS/MS system performance was observed. We therefore propose the use of 0.001% PEG as an additive into sample injection solution for efficient reduction of adsorptive losses of peptides in autosampler vials.

This work was supported by CEITEC (Grant CZ.1.05/1.1.00/02.0068) and by Czech Science foundation (Project No. P206-12-G151).

REFERENCES

1. Stejskal K., Potěšil D., Zdráhal Z.: J. Proteome Res. *12*, 3057 (2013).
2. Van Midwoud P. M., Rieux L., Bischoff R., Verpoorte E., Niederländer H. A. G.: J. Proteome Res. *6*, 781 (2007).
3. Bark S. J., Hook V.: J. Proteome Res. *6*, 4511 (2007).
4. Goebel-Stengel M., Stengel A., Taché Y., Reeve J. R.: Anal. Biochem. *414*, 38 (2011).
5. Ovesen R. G., Göransson U., Hansen S. H., Nielsen J., Hansen H. C. B.: J. Chromatogr., A *1218*, 7964 (2011).
6. Planeta J., Karasek P., Vejrosta J.: J. Sep. Sci. *26*, 525 (2003).

PRACTICAL ASPECTS OF COMPLEXATION OF BUFFER CONSTITUENTS WITH NEUTRAL COMPLEXATION AGENTS IN CAPILLARY ELECTROPHORESIS

JANA SVOBODOVA[a,b], MARTINA RIESOVA[a], MARTIN BENES[a], EVA TESAROVA[a], and BOHUSLAV GAS[a]

[a] *Charles University in Prague, Faculty of Science, Department of Physical and Macromolecular Chemistry, Prague, Czech Republic,* [b] *University of Heidelberg, Institute of Organic Chemistry, Heidelberg, Germany*

Summary

The complexation of buffer constituents with the complexation agent present in the solution can very significantly influence the buffer properties, such as pH, ionic strength or conductivity. These parameters are often crucial for selection of the optimal separation conditions in analytical separation techniques, particularly for capillary electrophoresis. We demonstrate that even commonly used buffers significnatly complex with usual chiral selectors as neutral cyclodextrins. This type of complexation and the subsequent change in properties of the buffer can have subsequent practical aspects in capillary electrophoresis; namely on determination of complexation constants, development of system peaks and last but not least can deterioritate the results of electrophoretic separation.

1. Introduction

Capillary electrophoresis (CE) is a widely employed separation technique. It offers many useful modifications that make use of the presence of complexation agents in background electrolyte (BGE). The fact that interactions between analytes and complexation agents are reflected in changes of electrophoretic behavior of the respective compounds can be advantageously used to determine complexation constants or for other studies of non-covalent binding in chemistry or biology. The complexation of analyte(s) with complexation agent(s) is described in detail in the literature nowadays. However, possible changes of the BGE properties due to the complexation of buffer constituents with the complexation agent are mentioned rarely. Rawjee *et al.*[1] utilized the complexation of buffer constituent with complexation agents to affect the electrophoretic mobility of the co-ion in order to minimize electromigration dispersion of the analyte. Chen *et al.*[2] observed system peaks originating from the interaction of neutral α-, β- and γ-cyclodextrins with *N*-cyclohexyl-2-aminoethanesulfonic acid (CHES) buffer during the cyclodextrin (CD) assisted separation of underivatized gangliosides. Fang *et al.*[3] noticed the induction of an additional peak registered by electrochemiluminescence detection when sulfated β-cyclodextrin and acetonitrile were simultaneously present in BGE. They attributed the presence of the induced peak to the physical interaction between CD and acetonitrile. Potential changes of the basic buffer properties, such as pH or ionic strength that can appear after the addition of a neutral complexation agent are considered rarely. Just a few authors proposed to control the pH of the buffer after the addition of a ligand[4].

2. Results and discussion

The complexation of buffer constituents can result in substantial changes in buffer properties[5]. The impact of complexation of buffer constituents with a neutral complexation agent can be demonstrated theoretically using our software Simul 5 Complex[6–8] as well as experimentally for common buffers. We were able to observe the significant pH changes for the buffers frequently used in separation techniques, see Fig. 1.

The substantial changes of pH also have the practical impact on electrophoretic results; namely complexation constant determination, system peak development and proper separation of analytes[9]. As the result, the complexation parameters determined in the interacting buffers cannot be regarded as thermodynamic ones and may provide misleading information about the strength of complexation of the compound of interest.

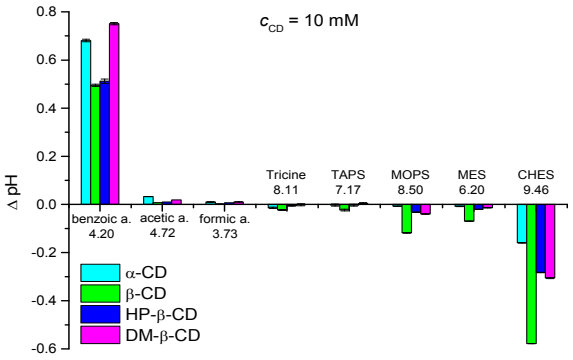

Fig. 1. **Shifts in pH (ΔpH) after addition of 10 ± 0.5 mM α-CD (cyan), β-CD (green), HP-β-CD (blue) or DM-β-CD (magenta) in six commonly used buffers and the model system (benzoate buffer).** Groups of columns are marked by the name of the buffering compound and pH value of the original buffer (without addition of CD). Error bars represent standard deviation of the measured value

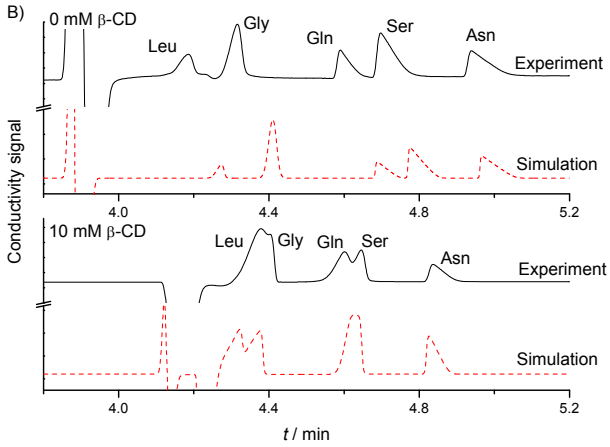

Fig. 2. **Comparison of the separation of a set of amino acids (Leu, Gly, Gln, Ser, Asn) in 10 mM CHES/ 5 mM LiOH buffer, both pH 9.41 and IS 5 mM.** Upper picture, pure buffer marked as 0 mM β-CD; Lower picture: 10 mM concentration of β-CD. Black solid curves: Experiment; Red dashed curve simulations obtained by PeakMaster and Simul 5 Complex, for cyclodextrin free BGE and BGE at a 10 mM concentration of β-CD, respectively. Individual aminoacids are labeled by their respective abbreviation

We also demonstrate that the development of system peaks in interacting buffer systems significantly differs from the behavior known for non-complexing systems, as the mobility of system peaks depends on the concentration and type of neutral complexation agent.

Finally, we show that the use of interacting buffers can totally ruin the results of electrophoretic separation because the buffer properties change as the consequence of the buffer constituents' complexation, see Fig. 2.

4. Conclusions

We demonstrate that complexation of buffer constituents with neutral complexation agents has to be always considered in selection of optimal separation conditions or determination of complexation constants in capillary electrophoresis. Complexation of buffer constituents changes the fundamental properties of the buffer such as pH, ionic strength or conductivity. Thus, we recommend check pH of the buffer solution before and after addition of neutral complexation agent to exclude the effect of complexation of buffer constituents on the electrophoretic results.

The support of the Grant Agency of the Czech Republic, Grant No. P206/12/P630, Grant Agency of Charles University, Grant No. 323611, the project Kontakt LH11018, and the long-term research plan of the Ministry of Education of the Czech Republic (MSM0021620857), are gratefully acknowledged.

REFERENCES

1. Rawjee Y. Y., Williams R. L., Vigh G.: Anal. Chem. *66*, 3777 (1994).
2. Chen Y. R., Ju D. D., Her G. R.: J. High Resolut. Chromatogr. *23*, 409 (2000).
3. Fang L., Yin X. B., Wang E.: Anal. Lett. *40*, 3457 (2007).
4. Evans C. E., Stalcup A. M.: Chirality *15*, 709 (2003).
5. Riesova M., Svobodova J., Tosner Z., Benes M., Tesarova E., Gas B.: Anal. Chem. *85*, 8518 (2013).
6. Hruska V., Benes M., Svobodova J., Zuskova I., Gas B.: Electrophoresis *33*, 938 (2012).
7. Svobodova J., Benes M., Hruska V., Uselova K., Gas B.: Electrophoresis *33*, 948 (2012).
8. Svobodova J., Benes M., Dubsky P., Vigh G., Gas B.: Electrophoresis *33*, 3012 (2012).
9. Benes M., Svobodova J., Riesova M., Tesarova E., Dubsky P., Gas B.: Anal. Chem. *85*, 8526 (2013).

MALDI MS AND SALD ICP MS: COMPLEMENTARY DETECTION TECHNIQUES FOR METALLOPROTEOMICS

IVA TOMALOVÁ, PAVLA FOLTYNOVÁ, VIKTOR KANICKÝ, and JAN PREISLER

CEITEC – Central European Institute of Technology, Masaryk University, Brno, Czech Republic
tomalova@mail.muni.cz

Summary

Matrix-assisted laser desorption/ionization mass spectrometry (MALDI MS) and substrate-assisted laser desorption inductively coupled plasma (SALD ICP) MS are proposed as complementary detection techniques that allows acquisition of both molecular and element specific information from a single capillary electrophoresis (CE) run recorded on a custom-designed sample target. The whole concept is demonstrated on the analysis of rabbit-liver metallothionein (MT) isoform mixture.

1. Introduction

Metals play a crucial role in physiology and pathology of biological systems. It has been estimated that the metalloproteins encompass about one third of all proteins[1]. Therefore, the studies focused on the comprehensive characterization of the metal-protein or metal-metabolite complexes are becoming increasingly important[2].

In this contribution, we present a novel approach for comprehensive multidimensional analysis of metalloproteins. This method is based on an off-line coupling of a single CE run to both MALDI MS and SALD ICP MS. The effluent fractions are collected on an Au-coated polyethylene terephthalate glycol (PETG) sample plate that is compatible to both MS methods.

2. Experimental

CE was carried out in uncoated fused silica capillaries (Polymicro Technologies, USA) of 70 cm (length) and 75 μm (i.d.) using a laboratory-built system. MT isoforms were separated in 20-mM NH_4HCO_3/HCOOH, pH 7.4 at 20 kV. The samples were injected hydrodynamically from unbuffered solution. A fiber optic UV detector was used for the immediate monitoring of the separation process. Fraction collection for the following MALDI MS/SALD ICP MS analyses was carried out using a liquid junction interface and sub-atmospheric deposition chamber. CE fractions were collected on a PETG sample plate coated with 5-nm Au layer, and covered with MALDI matrix, 26.5 mM α-cyanohydroxycinnamic acid (CHC), in 50% ACN and 1% TFA or 65 mM 2,5-dihydroxybenzoic acid (DHB) in 50% ACN and 0.05% ammonia solution. MALDI mass spectra were acquired using MALDI TOF/TOF mass spectrometer (Autoflex Speed, Bruker Daltonics). Afterwards, the Au-PETG sample plate was inserted into an ablation system (model UP 213, New Wave Research, USA) and SALD ICP MS was performed with ICP mass spectrometer (model 7500 CE, Agilent Technologies, USA).

3. Results and discussion

A novel approach (see Fig. 1 for method workflow) for complementary molecular and element-specific detection that combines two methods developed previously, CE□MALDI MS (ref.[3]) and CE-SALD ICP MS (ref.[4]), is proposed. The compatibility of the both MS methods is ensured by the use of a PETG sample plate coated with a golden nanolayer for fraction collection. While the PETG acts as an efficient substrate for SALD ICP MS, the Au nanolayer provides necessary conductivity for MALDI time-of-flight MS. The optimal Au-layer thickness was determined to be 5 nm. Overall performance of the sample plate for the both MS methods as well as the effect of MALDI MS on consequent SALD ICP MS measurement was investigated and the separation and deposition conditions were optimized.

MT mixture (14 ng, corresponding to 2 pmol in total) was injected and separated under the optimal conditions. Fractions at migration time t_{mig} = 7–12 min were collected in 2-s intervals on the Au-PETG target, and covered with

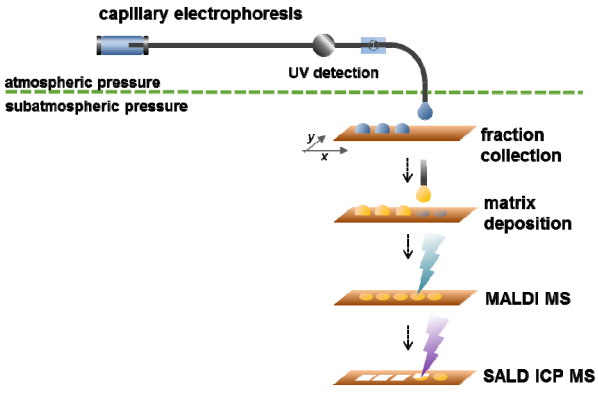

Fig. 1. **Experimental workflow of the CE(UV)-MALDI MS/SALD ICP MS**

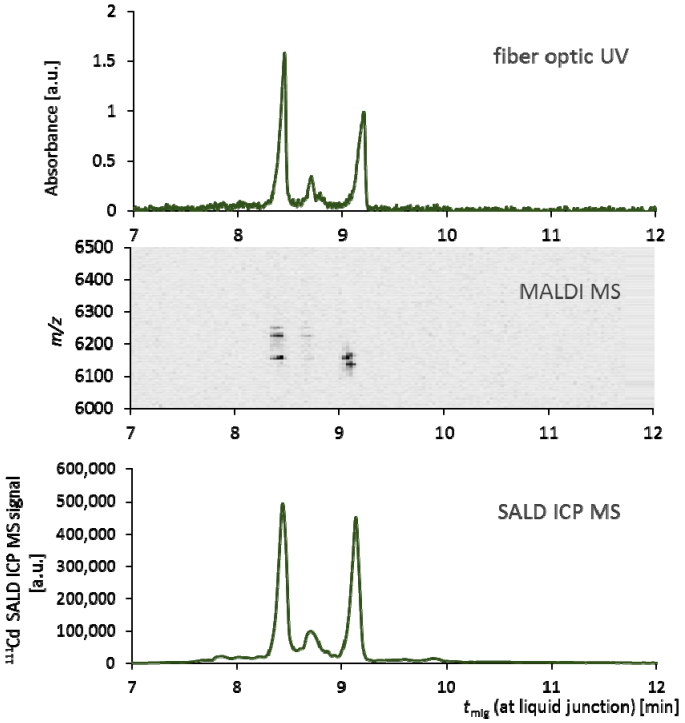

Fig. 2. **CE-UV (214 nm) electropherogram, 2D MALDI MS-electropherogram and SALD ICP MS-electropherogram (^{111}Cd) of a single CE run of MT isoform mixture**

the MALDI matrix solution. The separation record was then subjected to consecutive MALDI MS and SALD ICP MS analyses. The UV-trace, MALDI MS and ICP MS electropherograms recorded from a single separation are shown in Fig. 2.

To take full advantage of the off-line coupling potential, two different MALDI matrices, CHC and DHB in acidic and neutral pH, respectively, were applied on the adjacent spots corresponding to the MT peaks. Thus additional information can be obtained: While the information about protein apoforms is revealed under acidic condition, the un-dissociated metal-protein complexes can be detected at neutral pH.

4. Conclusions

A novel method for metalloprotein analysis based on off-line coupling of capillary electophoresis to both MALDI MS and SALD ICP MS is proposed. We believe it represents a viable alternative to common on-line coupling which employs electrospray ionization and nebulizer ICP MS. The off-line hyphenation allows decoupling separation and both detection processes in time and space and offers further options, such as re-analysis or archiving of the separation record, laser-induced fluorescence detection or on target protein digestion.

We thankfully acknowledge the Czech Science Foundation (GAP206/12/0538) and CEITEC – Central European Institute of Technology (CZ.1.05/1.1.00/02.0068).

REFERENCES

1. Finney L. A., O'Halloran T. V.: Science *300*, 931 (2003).
2. Mounicou S., Szpunar J., Lobinski R.: Chem. Soc. Rev. *38*, 1119 (2009).
3. Rejtar T., Hu P., Juhasz P., Campbell J. M., Vestal M. L., Preisler J., Karger B. L.: J. Proteome Res. *1*, 171 (2002).
4. Peš O., Jungová P., Vyhnánek R., Vaculovič T., Kanický V., Preisler J.: Anal. Chem. *80*, 8725 (2008).

SEPARATION OF TRYPTIC DIGEST OF *CYTOCHROME C* WITHIN A LONG NANOELECTROSPRAY TIP

ANNA TÝČOVÁ[a,b] and FRANTIŠEK FORET[a]

[a] *Institute of Analytical Chemistry of the ASCR, v. v. i., Brno,* [b] *Masaryk University, Brno, Czech Republic*
tycova@iach.cz

Summary

Capillary electrophoresis coupled to mass spectrometry (CE-MS) posses powerful tool for separation and detection of wide range of ionic species. To avoid complicated constructions of interfaces we have conducted the separation within a long and thin nanoelectrospray tip[1]. We have investigated main properties of such an experimental design on a complex sample of tryptic digest of *cytochrome c*.

1. Introduction

This work is aimed at optimization of electrophoretic separation within a long nanoelectrospray tip with mass spectrometric detection. The potential drop needed for sufficient resolution was reached by using system with high resistance.

2. Experimental

The electrophoretic separation was performed in 100 cm × 10 μm I.D. silica fused capillary ended by sharp polished ESI tip. The ESI tip was positioned approximately 2 mm in front of the mass spectrometer sampling orifice (LTQ Velos Pro, Thermo Fisher).

The sample of tryptic digest of *cytochrome c* from equine heart (Sigma Aldrich, ≥ 95%) was prepared by common procedure. To make solution free of ammonium bicarbonate used as a buffer it was evaporated at 37 °C and dissolved again in 0.01% formic acid. Sample of concentration 0.12 mg mL^{-1} was loaded from a gas pressurized chamber used also to assist the liquid flow inside the capillary during the experiments with nanoelectrospray. As a background electrolyte 0.01% HCOOH was used.

3. Results and discussion

At our simple experimental design of interfacing a voltage is applied only at the beginning of the capillary and there is no direct control over the voltage at capillary end, which is ended by an nanoelectrospray tip[2].

If worked with this type of interface, it is the most challenging to adjust sufficient potential drop within a separation channel and reach optimal voltage on the nanoelectrospray tip at the same time. To meet such conditions it is crucial to work with system of high resistance.

Conductivity of background electrolyte is one of the most important factor influencing resistance. We investigated wide range of potential background electrolytes and eventually 0.01% HCOOH (σ = 265 μS cm^{-1}, pH 3.20) has been chosen as the most appropriate. Not only that it has low conductivity but it still has acidic pH which is desirable for charging of analytes.

For further increase of resistance capillary of I.D. 10 μm was used. At the end of the capillary sharp tip was fabricated. There is several ways for fabrication of nanoelectrospray tip (e.g. pulling, etching and grinding). The most promising results were obtained for grinded tips. However, thin capillary brings more than high resistance. Other upsides are ability to create fine electrospray plume, low theoretical plate is reached and it posses more robust system for electrospraying[3].

Velocity of ions during the separation is given by contribution of hydrodynamic flow rate and electrophoretic mobility. To reduce the first named contribution the separation was run for 12 minutes at voltage of 30 kV with no flow rate. Later the conditions were changed to stable plume could be formed. Voltage was decreased to 5 kV and flow rate of 5 nL min^{-1} was developed (Fig. 2).

At such experimental conditions we have reached promising resolution and sensitivity. What is more loaded amount of sample was only 0.93 fmol, which predestine this type of interfacing for analysis of small amount of sample.

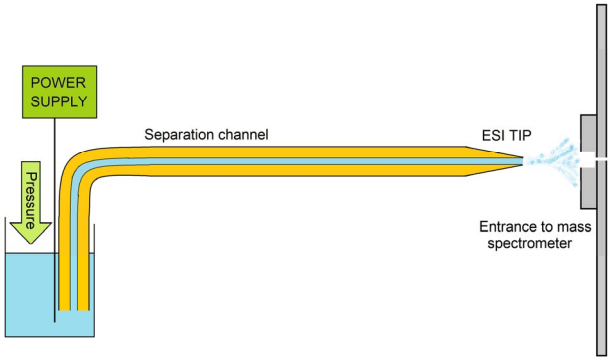

Fig. 1. **Scheme of used interfacing**

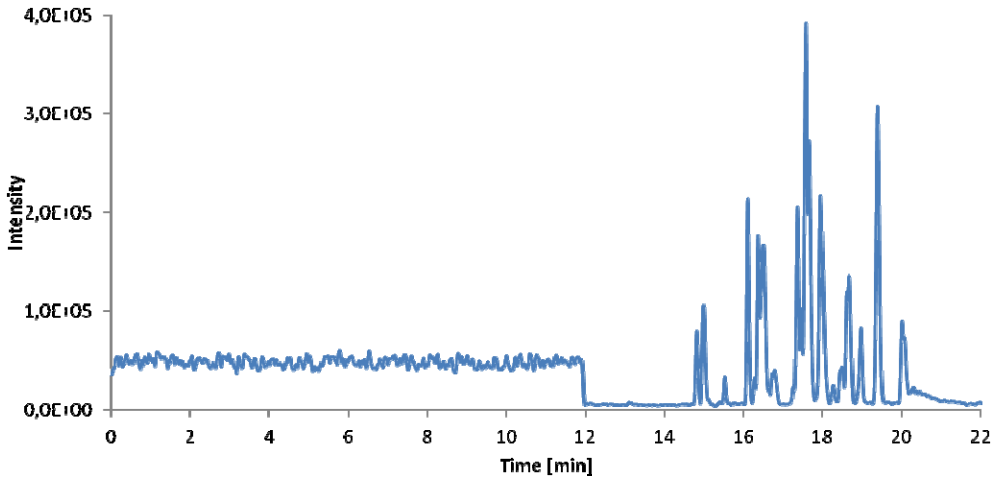

Fig. 2. **Base peak electropherogram of tryptic digest of *cytochrome c* conducted in 100 cm × 10 μm I.D. capillary.** Gradient voltage in two steps was applied –30 kV (12 min) and 5 kV (12–22 min). Flow rate 5 nL min^{-1} was developed only during 5 kV step

4. Conclusions

On a model sample of tryptic digest of *cytochrome c* was shown that this type of interfacing is viable. In comparision to other approaches it brings construction simplicity and potential to work with small amount of sample.

The work has been supported by GACR P206/12/G014. This project is co-financed by the European Social Fund and the state budget of the Czech Republic (CZ.1.07/2.3.00/20.0182).

REFERENCES

1. Maxwell E. Jane, Chen David Y. E.: Anal. Chim. Acta *627*, 25 (2008).
2. Mazereeuw M., Hofte A. J. P., Tjaden U. R., et al.: Rapid Commun. Mass Spectrom. *11*, 981 (1997).
3. Reschke Brent R., Timperman Aaron T.: J. Am. Soc. Mass Spectrom. *22*, 2115 (2011).

APPLICATION OF PRESSURIZED HOT WATER FOR ETCHING OF MICROFLUIDIC STRUCTURES

MICHAL VAŠINA[a], JAKUB GRYM[b], PAVEL KARÁSEK[b], and FRANTIŠEK FORET[b]

[a] *Gymnasium of Mathyas Lerch, Brno,* [b] *Institute of Analytical Chemistry, v. v. i., Brno, Czech Republic*
michalvasina@yahoo.com

Summary

The subject of this study is a new method of glass etching and its application in microfluidics. Commonly, hydrofluoric acid is used for glass etching. In this study we have tested a new method of glass etching using pressurized hot water. Test motives were prepared using photolitography and metal sputtering on the glass substrate and the etching was performed in a newly developed device capable to compress and heat water to its critical point. Electron microscopy and profilometry have been used for analyzing the surface of the etched glass substrate.

1. Introduction

Commonly, hydrofluoric acid is used for glass etching. However, its toxicity represents a significant health and environmental risk factor. This study focuses on the development of a new etching procedure using the recently developed device with temperature controlled high pressure chamber, providing a wide range of pressures and temperatures up to the critical point of water[1]. Glass chips with metallized surface were prepared and the test pattern was photolitographically etched in the metal protection layer prior to the glass etching. Series of experimental data obtained under different pressures, times and temperatures were evaluated by electron microscopy and optical profilometry.

2. Experimental

2.1. Testing of new etching method

The glass slides were sputter coated by a 200 nm layer of Cr followed by spincoating a 1 μm layer of a positive photoresist. The test pattern was created by a direct laser writer (Heidelberg Instruments μPG 101) on 48 glass substrates. After etching by hot water the surface structures of all substrates were analyzed by electron microscope Helios Nanolab 600i (FEI, Brno) and in an optical profilometer ContourGT – X8 (Bruker, FRG).

2.2. Application of new etching method

The object of the second part was to produce a fully enclosed microfluidic chip using the previously described etching protocol. Suitable conditions for etching were chosen, according to the results from surface structure analysis, and the cover glass was bonded to the etched substrate in the oven (Řevnice, Classic – 3013-S) at 600 ° C. Finally, the chip was cut using Precision CNC Dicing / Cutting Saw SYJ-400 supplied by MTI Corporation (USA).

3. Results and discussion

The structure analysis showed that the surface properties of the etched substrate were changing depending on either etching pressure or etching temperature.

3.1. Dependency on etching pressure

The lines accompanied with arrows define the width (w) of underetching. With growing pressure, the substrate is more underetched. The etching water pressure had no

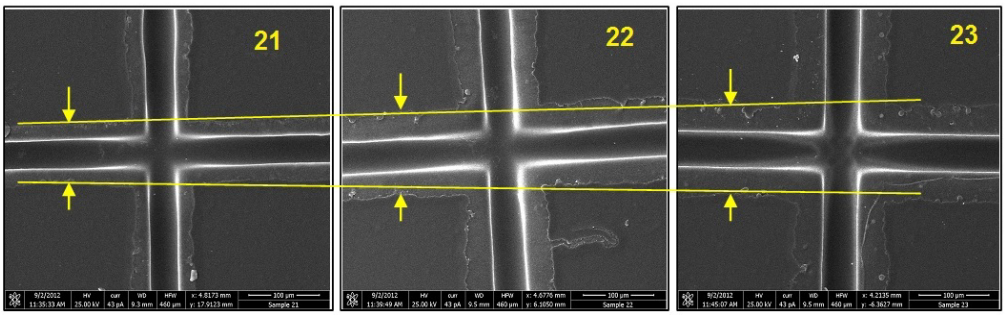

Fig. 1. **Electron microscope images, magnification 300×.** Following pressures (P) of water used for etching: Substrate 21: P = 250 bar; substrate 22: P = 350 bar; substrate 23: P = 450 bar. The etching water temperature (T) was constant: 374 °C

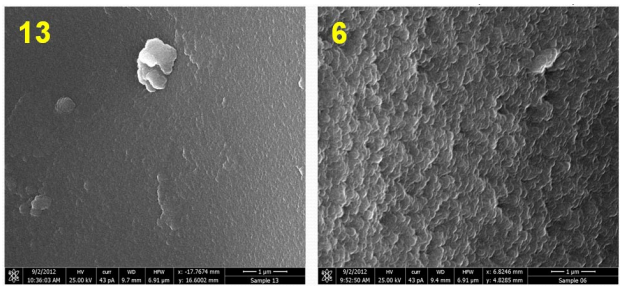

Fig. 2. **Electron microscope images, magnification 20 000×.** Substrate 13: T = 300 °C; channel depth = 18 μm; substrate 6: T = 340 °C, channel depth (d) = 43 μm, Constant pressure was used: P = 400 bars

influence on the channel depth; however, the surface roughness was highly influenced by the etching temperature as shown in Fig. 2.

The difference of 40 °C made the surface of substrate 6 more porous. Furthermore, the etching water temperature influenced the channel depth, with growing temperature, the channels were deeper.

3.2. The final microfluidic device

After evaluation of the etching parameters a fully enclosed microdevice was prepared by thermal bonding of the cover glass on top of the substrate with the etched microchannel. Fig. 3 shows both the channel structure and the final microfluidic chip after dicing.

A suitable (porous) channel surface (second picture of Fig. 3) was chosen for the etching of the microfluidic device that can be used in further research e.g. for immobilization of enzymes such as trypsin.

4. Conclusions

The achieved results prove that the new glass etching method allows substituting the HF based toxic process by the eco-friendly hot water etching. The developed protocol enables good control of the surface properties and the new etching method may become a viable alternative to commonly used methods.

This project is co-financed by the European Social Fund and the state budget of the Czech Republic (CZ.1.07/2.3.00/20.0182). The support of the Grant Agency of the Czech Republic (P206/12/G014) and the institutional research plan (RVO 68081715) are also gratefully acknowledged.

REFERENCE

1. Karasek P., Planeta J., Roth M.: Anal. Chem. *85*, 327 (2013).

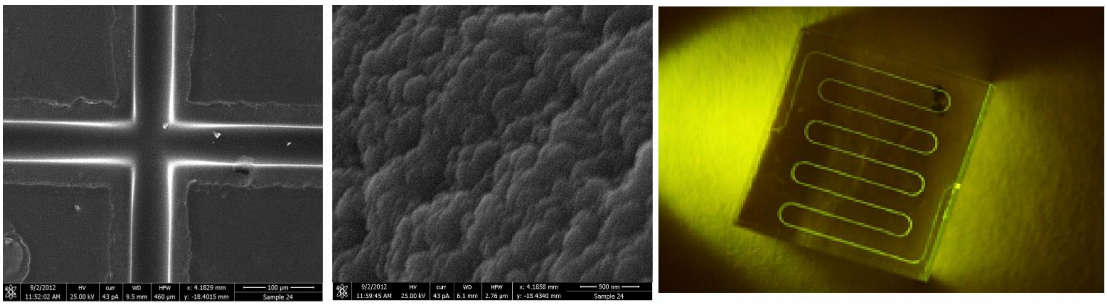

Fig. 3. **Electron microscope images, magnifications 300× and 20 000×, and the final microfluidic device (1×1 cm);** T = 380 °C, P = 450 bar, w = 53 μm, etching time (t) = 5 min

AN INSIGHT INTO THE RETENTION MECHANISM ON CYCLOFRUCAN-BASED CHIRAL STATIONARY PHASES

JIŘÍ VOZKA, KVĚTA KALÍKOVÁ, and EVA TESAŘOVÁ

Department of Physical and Macromolecular Chemistry, Faculty of Science, Charles University in Prague, Hlavova 2030, 128 43 Prague, Czech Republic
tesarove@natur.cuni.cz

Summary

Cyclofructan-based chiral stationary phases were shown as a promising possibility for separation of chiral compounds in HPLC. In this work retention mechanisms of cyclofructan-based chiral stationary phases are described. Additionally, the retention mechanism of dimethylphenyl-carbamate cyclofructan 7 was studied under the conditions of supercritical fluid chromatography. A linear free energy relationship model was utilized for characterization of retention interactions.

1. Introduction

In 2009 Armstrong et al. introduced chiral stationary phases (CSPs) based on native and derivatized cyclofructans (CFs) (ref.[1]). Since that time CFs as chiral selectors found applications in many separation techniques including HPLC, GC, and CE (ref.[2–5]). The structure of CF molecule is composed of six, seven or eight D-fructofuranose units connected via β (2→1) linkage[6]. The connected saccharide units form a crown-ether ring, which significantly determinates chromatographic behavior of CFs. Common abbreviations CF6, CF7 and CF8 indicates a number of saccharide units forming the ring. Native CFs have their crown-ether skeleton sterically blocked by intramolecular hydrogen bonds, therefore their separation abilities are quite limited. As a result of introducing of derivatization groups into the CF molecule the CF molecule relaxes and crown-ether core becomes more accessible and the enantioselective potential significantly increases. Character of the derivatization moiety has substantial impact, since aliphatic derivatization moieties particularly improve enantioselectivity especially for amines, while aromatic derivatization groups improve enantioselectivity among various compounds.

The aim of our work was to reveal retention interaction occurring on CF-based CSPs, namely isopropyl carbamate CF6 (IP-CF6 CSP), *R*-naphthylethyl carbamate CF6 (RN-CF6 CSP) and dimethylphenyl carbamate CF7 (DMP-CF7 CSP) under the conditions of normal phase mode HPLC and last mentioned CSP also under the condition of supercritical fluid chromatography (SFC). In the first article introducing CF-based CSPs was mentioned the possibility of use CF-based CSPs in SFC. However, the detailed study has never been done.

2. Experimental

To determine and quantify the interactions participating in the retention process a linear free energy relationship model (LFER) was employed. This model is based on the idea that retention (expressed as log k, where k is a retention factor) is composed of independent contribution according to the involved interaction type. The most common LFER equation works with five type of interactions (dispersion interactions, hydrogen bond acidity, hydrogen bond basicity, polarity/polarizibility, and ability to interact via n- and/or π-electron pairs).The LFER set contained 35 compounds, whose chemical features were described. The description is based on the physical measurements/calculations and expressed as a number (a descriptor). After analysis of LFER set, logarithms of obtained retention factors undergo multilinear regression analysis (log k against the descriptors). Results of multilinear analysis, regression coefficients, indicate whether the particular interaction type is dominant in the stationary phase (positive value of the regression coefficient) and thus increases the retention or in the mobile phase (negative value of the descriptor) and decreases retention or the same in both phases (statistically insignificant regression coefficient). Despite the fact that LFER model does not take into account the phenomena of chirality, it provides valuable information about the interaction mechanisms.

3. Results and discussion

At first, individual CF-CSPs were compared (see Table I). The same types of interactions in a different extent were shown to be preferred by all three CSPs, i.e. hydrogen bond acidity and dipolarity/polarizibility. Also the effect of hydrophobicity as the retention reducing factor plays a role with all tested CF-based CSPs. Hydrogen bond basicity and interactions with n- and π-electron pairs seemed to be insignificant.

The same model as for HPLC was used for the characterization and further comparison of retention interaction on DMP-CF7 CSP under HPLC and SFC conditions. LFER model confirmed that different interactions participated to different degrees in the retention process on DMP-CF7 CSP in SFC and HPLC

Table I
Comparison of regression coefficients of the LFER equation and correlation coefficient *R* for systems wiht three CF-based CSPs under normal phase mode HPLC

Column	Mobile phase	Model	*e*	*s*	*a*	*b*	*v*	*c*	*R*
CF6-RN	**hex/IPA/TFA**	**O.M**	**x**	**1.128**	**x**	**1.596**	**-1.169**	**-0.944**	**0.953**
	80/20/0	± 95% CI		0.298		0.302	0.382	0.307	
	v/v/v	*p*- value		0		0	0	0	
CF6-IP	**hex/IPA/TFA**	**O.M**	**x**	**0.518**	**x**	**1.573**	**-0.887**	**-0.401**	**0.963**
	80/20/0	± 95% CI		0.228		0.211	0.282	0.232	
	v/v/v	*p*- value		0		0	0	0.001	
CF7-DMP	**hex/IPA/TFA**	**O.M**	**x**	**0.803**	**x**	**1.729**	**-0.703**	**-1.048**	**0.95**
	80/20/0	± 95% CI		0.305		0.287	0.391	0.315	
	v/v/v	*p*- value		0		0	0.001	0	
CF6-RN	**hex/IPA/TFA**	**O.M**	**x**	**0.891**	**x**	**1.535**	**-0.918**	**-0.892**	**0.965**
	80/20/0.5	± 95% CI		0.244		0.231	0.316	0.254	
	v/v/v	*p*- value		0		0	0	0	
CF6-IP	**hex/IPA/TFA**	**O.M**	**x**	**0.594**	**x**	**1.486**	**-0.821**	**-0.553**	**0.957**
	80/20/0.5	± 95% CI		0.242		0.226	0.311	0.254	
	v/v/v	*p*- value		0		0	0	0	
CF7-DMP	**hex/IPA/TFA**	**O.M**	**x**	**0.927**	**x**	**1.622**	**-0.765**	**-1.11**	**0.956**
	80/20/0.5	± 95% CI		0.287		0.267	0.368	0.3	
	v/v/v	*p*- value		0		0	0	0	

CI represents ±95% confidence interval. x, insignificant interaction; O.M., optimal model of the LFER equation; *p*, statistical *p*-value. The *p*-values express probability of the error that the individual coefficient does not contribute to the model, i.e., *p*-values represent the significance of the individual coefficients

Table II
Comparison of regression coefficients of the LFER equation and correlation coefficient *R* for DMP-CF7 CSP in SFC and HPLC

Method	Mobile phase	Model	*e*	*s*	*a*	*b*	*v*	*c*	*R*
HPLC	**Hex/IPA/TFA**	**O.M.**	**x**	**0.789**	**x**	**1.597**	**-0.810**	**-0.881**	**0.95**
	80/20/0.0	± 95% CI		0.277		0.310	0.389	0.330	
	v/v/v	*p*- value		0.000		0.000	0.000	0.000	
HPLC	**Hex/IPA/TFA**	**O.M.**	**x**	**0.933**	**x**	**1.516**	**-0.917**	**-0.940**	**0.96**
	80/20/0.5	± 95% CI		0.254		0.274	0.348	0.296	
	v/v/v	*p*- value		0.000		0.000	0.000	0.000	
SFC	**CO_2/IPA/TFA**	**O.M.**	**0.459**	**0.514**	**x**	**0.949**	**-1.011**	**-0.410**	**0.94**
	80/20/0.0	± 95% CI	0.250	0.263		0.251	0.494	0.359	
	v/v/v	*p*- value	0.001	0.000		0.000	0.000	0.026	
SFC	**CO_2/IPA/TFA**	**O.M.**	**0.537**	**0.472**	**x**	**0.936**	**-1.204**	**-0.227**	**0.94**
	80/20/0.5	± 95% CI	0.253	0.267		0.255	0.501	0.364	
	v/v/v	*p*- value	0.000	0.001		0.000	0.000	0.212	
SFC	**CO_2/MeOH/TFA**	**O.M.**	**0.557**	**0.495**	**0.891**	**1.020**	**-0.806**	**-0.685**	**0.97**
	95/5/0.0	± 95% CI	0.308	0.351	0.279	0.314	0.735	0.512	
	v/v/v	*p*- value	0.001	0.007	0.000	0.000	0.033	0.010	
SFC	**CO_2/MeOH/TFA**	**O.M.**	**0.627**	**0.553**	**0.795**	**1.113**	**-1.165**	**-0.422**	**0.93**
	95/5/0.1	± 95% CI	0.446	0.508	0.404	0.455	1.064	0.741	
	v/v/v	*p*- value	0.007	0.034	0.000	0.000	0.033	0.254	

CI represents ±95% confidence interval. x, insignificant interaction; O.M., optimal model of the LFER equation; *p*, statistical *p*-value. The *p*-values express probability of the error that the individual coefficient does not contribute to the model, i.e., *p*-values represent the significance of the individual coefficients

(see Table II). The results suggested that the adsorption of some components of the mobile phases is more important in SFC than in HPLC. The lower content of alcoholic modifier in the mobile phase, the higher the adsorption, which significantly changes the characteristics of the separation system in SFC.

4. Conclusions

The LFER model was used to describe interactions participating in the retention and separation process on the CF-based CSPs in normal mode HPLC and on DMP CF7 CSP in SFC. Although LFER does not take into account chirality and spatial arrangement of analytes, it proved which forces take part in the interaction mechanism. The same types of interactions in a different extent were shown to be preferred by all three stationary phases, i.e. hydrogen bond acidity and dipolarity/polarizibility in HPLC. Also the effect of hydrophobicity as the retention reducing factor plays a role with all tested CF-based CSPs. Hydrogen bond basicity and interactions with *n*- and π-electron pairs seemed to be insignificant. Furthermore, the LFER model confirmed the different distribution of interactions influencing the retention process on DMP-CF7 CSP in SFC and HPLC.

The Grant Agency of the Charles University in Prague, project No. 356411, the Ministry of Education, Youth and Sports of the Czech Republic, project KONTAKT AM 2010 project LH11018, and the long-term project MSM0021620857 are gratefully acknowledged for the financial support. Furthermore, Prof. Ch. Roussel and Dr. N. Vanthuyne from the Chirosciences team of Aix-Marseille University are thanked for their kind help during the SFC experiments.

REFERENCES

1. Sun P., Wang Ch., Breitbach Z. S., Zhang Y., Armstrong D. W.: Anal. Chem. *81*, 10215 (2009).
2. Sun P., Wang Ch., Padivitage N. L. T., Nanayakkara Y. S., Perera S., Qiu H., Zhang Y., Armstrong D. W.: Analyst *136*, 787 (2011).
3. Zhang Y., Breitbach Z. S., Wang Ch., Armstrong D. W.: Analyst *135*, 1076 (2010).
4. Jiang Ch., Tong M., Breitbach Z. S., Armstrong D. W.: Electrophoresis *30*, 3897 (2009).
5. Gondová T., Petrovaj J., Kutschy P., Armstrong D. W.: J. Chromatogr., A *1272*, 100 (2013).
6. Immel S., Schmitt G. E., Lichtenthaler F. W.: Carbohydr. Res. *313*, 91 (1998).

AN EASY SURFACE MODIFICATION IN HETEROGENEOUS NANO- AND MICRO-FLUIDIC DEVICES

THI THU VU[a,b], MARC FOUET[c], ANNE-MARIE GUE[c], and JAN SUDOR[a,b]

[a] *Université Paul Sabatier, Université de Toulouse, Toulouse,* [b] *Institut de Recherche pour le Développement (IRD), Toulouse,* [c] *Laboratoire d'Analyse et d'Architecture des Systèmes (LAAS), Toulouse, France*
thuvu.edu86@gmail.com

1. Introduction

The homogenization of surface properties in multicomponent or hybrid fluidic devices, integrating silicon, glass, metals, photoresists (e.g., SU8) and elastomers (e.g., polydimethoxysilane, PDMS) requires the innovations of universal techniques which are independent of the nature of surfaces. It was recently reported that dopamine (DOPA) spontaneously oxidizes under alkaline conditions, and forms highly reactive products, that further forms thin-layer coating which can be additionally modified with various molecules of interest[1]. This inspired a new strategy in surface science, namely mussel-inspired surface modification, regardless of the structural similarity between DOPA and catecholic compounds existing in mussel proteins[2]. In this study, amine terminated polyacrylamide (AmPAM) was end-tethered on different fluidic materials (Si, glass, metals, SU8, PDMS) via mussel inspired surface mofication in a one-pot approach[3], that is easily applicable to nano- and microfluidic devices. Modified surfaces were thoroughly characterized. It was found that the bio-antifouling DOPA-AmPAM surfaces were formed on any substrates with very high homogeneity. These findings provided important applications in nano- and micro-fluidic systems.

2. Experimental

The widely used materials for microfluidics such as SiO_2, glass, Cu, Au, SU8, Si and PDMS were modified with AmPAM by one-pot mussel inspired surface modification. The surfaces of interest are simply modified when in contact with an alkaline buffer (50 mM Tris.HCl, pH 9.0) solution that contains DOPA (2 mg mL^{-1}), AmPAM (1 mg mL^{-1}) and ammonium persulfate (1 mg mL^{-1}). AmPAM (MW of 15 100 Da) was synthesied and well characterized in our laboratory. We also modified various surfaces with DOPA coatings only. In general, a freshly prepared solution of DOPA with or without the acrylamide chain is injected into a microfluidic channel and/or flat substrates are immersed into this solution for several hours, then the channels are flushed (and the flat substrates rinsed) with deionized water and dried in a nitrogen stream prior the use or further characterization.

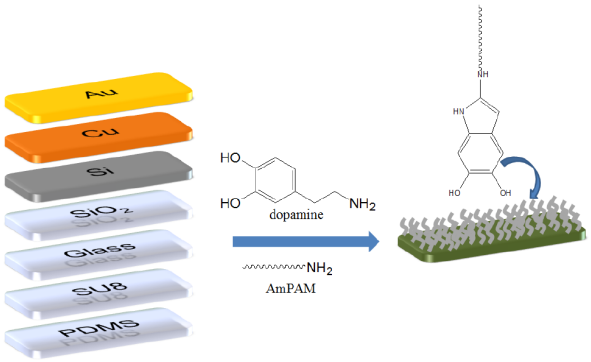

3. Results and discussions

3.1. Water contact angle (WCA)

The static WCA measurements (Fig. 1) show that the DOPA coating adhere to all employed wetting surface, and that independently of the value of the WCA before modification, all the materials become alike (θ = 50.5–53.9°) after the surface coating. This value decreases (θ = 31.5–36.6°) when AmPAM is added to the DOPA solution prior contact with the solid material, suggesting that the polyacrylamide chains get end-tethered onto the surface

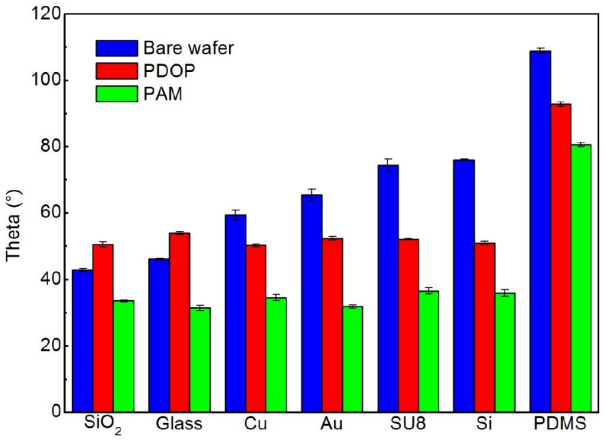

Fig. 1. **Static water contact angle on various surfaces. In blue are shown water contact angles for unmodified surfaces, in red for DOPA only modified surfaces and, in green, for DOPA-AmPAM modified surfaces**

most probably via the primary amino group. In case of very hydrophobic PDMS surface (θ0 >110°), a significant decrease in WCA was also observed, but at much higher values, comparing to the other surfaces (θDOPA=92.8° and θAmPAM-DOPA=80.6°).

3.2. Oxidation kinetics and roughness

The most important factor that controls the surface morphology and uniformity is the dopamine oxidation kinetics[4–8] that can be influenced by the initial dopamine concentration, the pH of employed buffer and the presence of an oxidizing agent. It has been reported recently[7] that highly homogeneous, thin layer films are formed at the higher oxygen concentration via accelerated reaction kinetics. This inspired us to use an oxidizing agent to promote oxidation of dopamine in order to achieve thin films with high uniformity.

Dopamine consumption was determined from UV spectra for the three different conditions (air, oxygen and ammonium persulfate initiation). Surprisingly, the complete dopamine consumption (~ 98 %) was observed after 1h of oxidation in the presence of ammonium persulfate, whereas the highest dopamine consumption was only 38 % in the air bubbled and 60 % in the oxygen bubbled solution. These results suggested that the oxidant induced oxidation of dopamine is irreversible reaction instead of reversible reaction as in case of pH induced oxidation (air and oxygen bubbling).

AFM measurements were performed to study morphology of the surface of AmPAMDOPA as well as DOPA deposited films on silicon oxide surface. Modified substrates in air and bubbled oxygen were also characterized. AFM images (Fig. 2) showed that all modified surfaces are well-covered. The same results were obtained by cyclic voltammetry curves of DOPA and DOPA-AmPAM modified gold electrodes, no redox peaks of electroactive probe was observed in accordance with the shielding effect by well-covered organic films. The thickness of AmPAM-DOPA after 3 h of deposition determined from AFM to be around 10 nanometers.

The root mean square roughness was used to evaluate roughness of deposited coating. We observed the significant decrease in roughness of organic films in the presence of ammonium persulfate. The roughness of AmPAM-DOPA and DOPA are determined to be 1.05 and 0.96 nm, instead of 2.44 and 1.92 nm in air, or 1.63 and 1.17 nm in bubbled oxygen. Alternatively, the density of aggregation considerably decreased in addition of oxidant (only several 102 nm sized grains on 10 μm2). It was

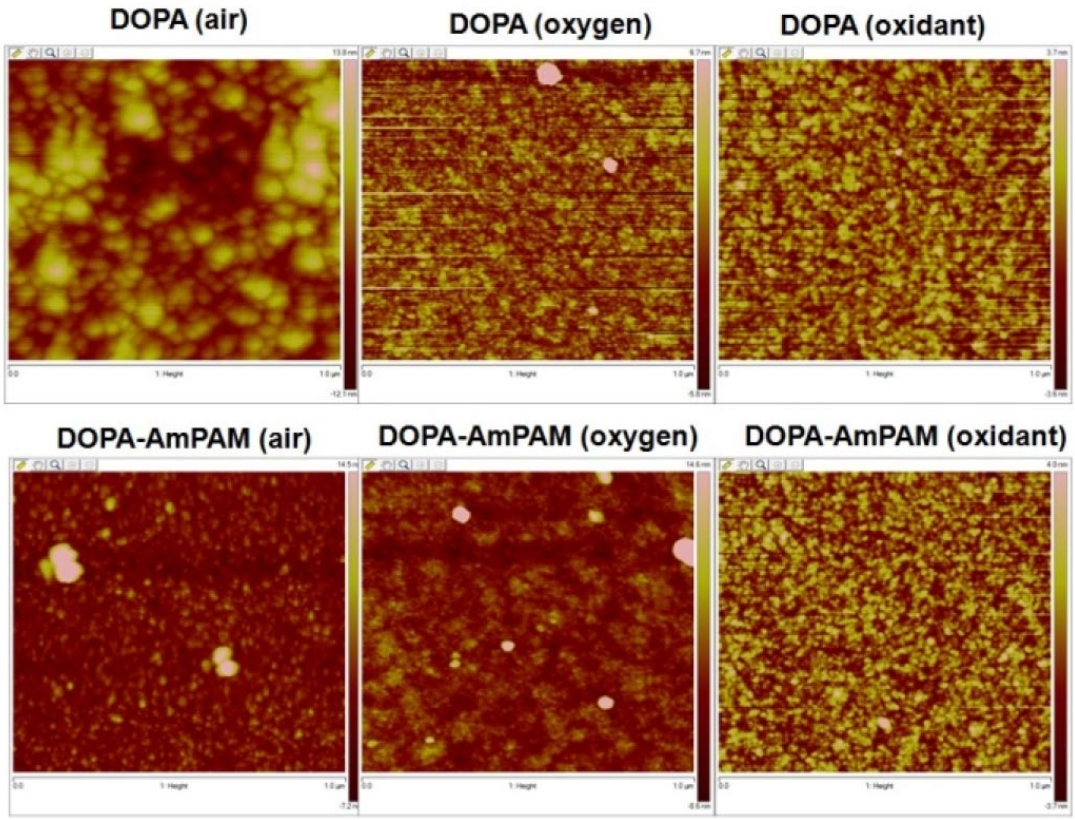

Fig. 2. **AFM images of unmodified and modified silicon oxide surfaces**

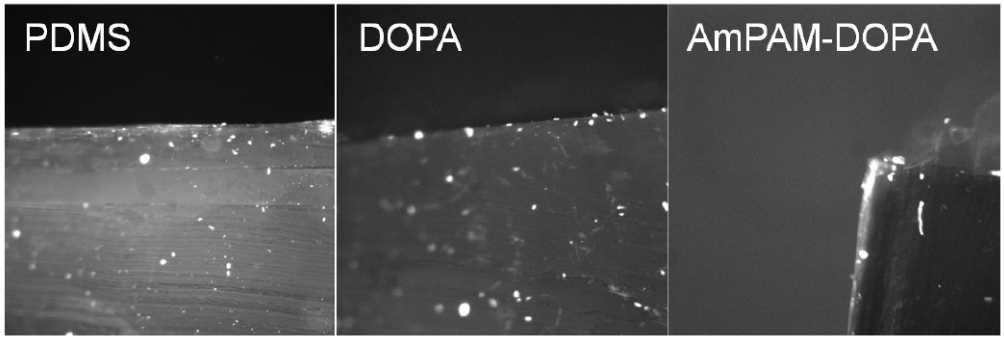

Fig. 3. **Protein absorption on unmodified DOPA coated and DOPA-AmPAM coated PDMS surfaces**

believed that the deposition of films containing DOPA is initiated by adsorption of oxidized radicals (mostly 5,6-dihydroindole and its derivatives) on surfaces[4], then continues by curing process in which the cross-linking net of these molecules are formed through either covalent binding[8] or non-covalent binding[9]. The fact is the use of oxidant created more initial radicals and the surfaces became more uniform with an decreased size of aggregates. Consequently, these organic depositions containing DOPA are spontaneously formed in a densely structural state on surfaces. This explains the important increase in homogeneity of modified surfaces in the presence of oxidant.

3.3. Protein adsorption

The non-fouling properties of our surfaces were studied with fluorescein (FITC)-albumin conjugate. The unmodified and modified PDMS surfaces were dipped into the FITC-albumin solution (1 mg mL^{-1} in PBS pH 7.4) and incubated at room temperature for 18 hrs. After the incubation was completed, the surfaces were washed with deionized water and dried in a stream of nitrogen. Compared to bare and DOPA modified PDMS surfaces, the fluorescence was dramatically decreased on the DOPAAmPAM surface (Fig. 3), suggesting that the hydrophilic PAM brush is necessary to minimize the protein adsorption.

4. Conclusions

We have demonstrated the versatility of our approach for the modification and functionalization of surfaces of any solid material. In this work, we were interested to exploit the non-fouling properties of the modified surfaces prepared from hydrophilic polymer brushes. We applied our strategy to the modification and homogenization of surfaces inside nano- and microfluidic channels. The advantage of the developed strategy is inherited in the substrate independent chemistry and low viscosity of the modifying medium. The formation of DOPA and DOPA-AmPAM films on all the studied materials was clearly demonstrated in our work. The adsorption studies with the FITC-albumin conjugate showed that the adsorption was dramatically decreased on the PDMS-DOPA-AmPAM substrate due to the presence of the PAM polymer brushes.

This work was financially supported by a doctoral grant from Hanoi University of Science and Technology.

REFERENCES

1. Lee H., Shara M. D., William M. M., Phillip B. M.: Science *318*, 426 (2007).
2. Heather G. S., Francisco F. R.: Mar. BioTechnol. *9*, 661 (2007).
3. Sung M. K., Nathaniel S. H., Jihyeon Y., Sung Y. P., Phillip B. M., Insung S. C., Robert L., Daniel G. A., Lee H.: Adv. Funct. Mater. *22*, 2949 (2012).
4. Falk B., Arnaud P., Christian R., Joseph H., Jesus R., Burkhard B., Jean-Claude V., Pierre S., Vincent B.: J. Phys. Chem., C *113*, 8234 (2009).
5. Vincent B., Doriane D. F., Valérie T., David R.: J. Colloid Interface Sci. *386*, 366 (2012).
6. Falk B., Vincent B., Frédéric A., Arnaud P., Marc M., José J.G., Valérie T., David R.: Langmuir *27*, 2819 (2011).
7. Hyo W. K., Bryan D. M., Tae H. C., Changho Lee, Min-Joung K., Benny D. F., Ho B. P.: Appl. Mater. Interfaces *5*, 233 (2013).
8. Daniel R. D., Daniel J. M., Benny D. F., Donald R. P., Christopher W. B.: Langmuir *28*, 6428 (2012).
9. Seonki H., Yun S. N., Sunghwan C., In T. S., Woo Y. K., Lee H.: Adv. Funct. Mater. *22*, 4711 (2012).

INFORMATION ENTROPY APPROACH AS A METHOD OF ANALYSING BELOUSOV-ZHABOTINSKY REACTION WAVE FORMATION

ANNA ZHYROVA, DALIBOR STYS, and PETR CISAR

University of South Bohemia in České Budějovice, Institute of Complex Systems, Nové Hrady, Czech Republic
zhyrova@frov.jcu.cz

Summary

This work is aims to develop a method of analysis for self-organized systems such as living cells culture or herds in native ecosystem. In the selection of the appropriate model was chosen a simpler approach – the Belousov-Zhabotinsky reaction (chemical clock).

Proposed method based on the information theory of mutifractal objects. We use the Renyi information entropy equation for calculation of information gain by which a point contributes to the total information in the image, the point information gain. Obtained values present unique information about object structure. Method allows highlight tiny features in investigated sample structure and characterizes system behavior in dynamic.

1. Introduction

The Belousov-Zhabotinsky (BZ) reaction was devised as a primitive model of citric acid cycle. When performed in a thin – few centimeters thick – layer, it creates easily observable travelling waves which may be captured by ordinary colour camera and analysed. The system behavior in time indicates existence of a sequence of distinct states stable for certain period of time. The experimenter has control of mechanical constraints imposed on the system. States in the course of the reaction may be identified in all cases when the geometry of the experimental vessel allows creation of travelling waves.

2. Material and methods

Experiments were performed with the oscillating bromated-ferroin-bromomalonic acid reaction type (kit were provided by Dr. Jack Cohen)[1]. The reaction mixture was composed out of following solutions: 0.34 M sodium bromate, 0.2 M sulphuric acid, 0.057 M sodium bromide, 0.11 M malonic acid as substrate and redox indicator 0.12 M 1,10-phenantroline ferrous complex. All reagents were coherently mixed under temperature 22 °C and added into Petri dish. Images were captured by Nikon D90 camera in regime Time lapse shooting in interval 10 second between snapshots.

In our practical approach[2,3] we calculate the Renyi entropy contribution of each of the points in the image. We calculate the Renyi entropy difference for the data set containing the examined point and the dataset in which the examined point was excluded. This is the Point Information Gain ($\gamma_\alpha(x,y)$) for given entropy of the order α:

$$\gamma_\alpha(x,y) = \frac{1}{1-\alpha} ln\left(\sum_{i=1}^{n} p_{i,x,y}^{\alpha}\right) - \frac{1}{1-\alpha} ln\left(\sum_{i=1}^{n} p_i^{\alpha}\right) \qquad (1)$$

where $\rho_{i,x,y}$ and ρ_i are probabilities of occurrence of given intensity for given point *x, y* coordinate of camera pixel at given α in the image without and with the examined point.

In the next step number of points of given intensity is summed and normalized – we obtain Point Information Gain Entropy (H_α):

$$H_\alpha = \sum_{x=1}^{x=n} \sum_{y=1}^{y=m} \gamma_\alpha(x,y) \qquad (2)$$

And on the final step of image processing were calculated Point Information Gain Entropy Density (Ξ_α):

$$\Xi_\alpha = \sum_{i=1}^{i=o} \Gamma_{\alpha,i}(x,y) \qquad (3)$$

For given dataset, i.e. image, the ordered set of H_α and Ξ_α tuples a unique characteristic of the image, i.e. each two different images will have different sets, provided that the image is caprured with infinite precision and the calculation is perfomed for all α values form 0 to infinity. In real case the precicion is defined by the digital camera and the set of α values is chosen arbitrarily.

Using statistical approaches such as principal component analysis (PCA)[4] we may construct orthogonal spaces which best fit the observed dataset. All data divided on the clusters depend on the value of the PCA-components. Each cluster of the trajectory present the one of the states of the BZ reaction.

3. Results and discussion

The set of H_α were used for describing the evolution of the system as a multi-fractal object. The state evolution is split in logical sequence of clusters in the new orthogonal, although still phenomenological, state space. On the Fig. 1 is shown decomposition of the system trajectory of the Belousow-Zhabotinsky reaction into series of states which are for distinct period of time

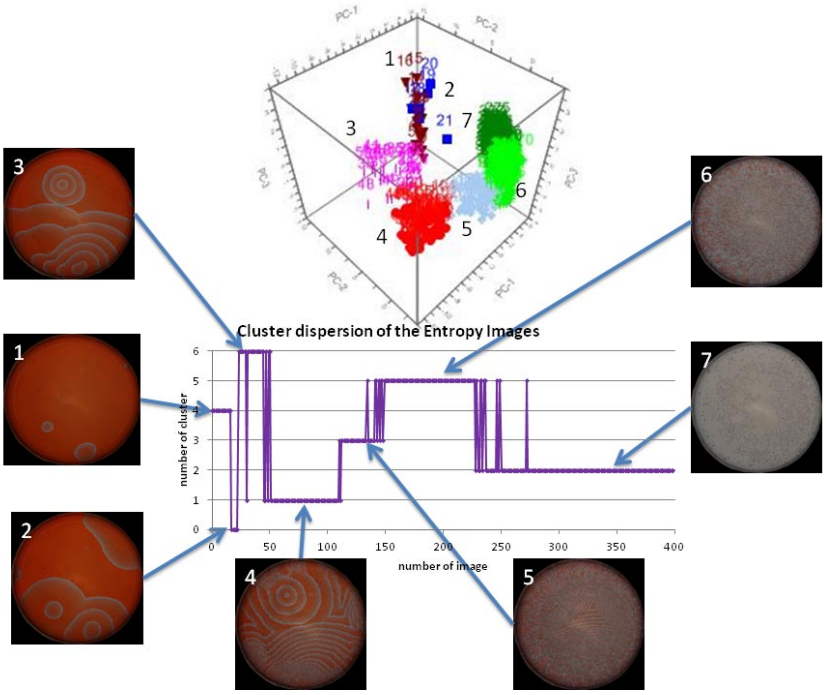

Fig. 1. **The state trajectory of the BZ reaction performed in the Petri dish.** Principle component analysis of the H_α allows to designate different states of the system (changes in waves structure during the reaction evolution), from the point of view of the method clusters of points in the state space. Scores differ significantly between clusters oriented and form logical trajectory in the principal coordinates space

asymptotically stable under current conditions. Clusters (series of images) are very well separated and consistent in time, for each of group could find characteristic image represented the state of the system in their developing process. Moreover, each of the clusters states should have its own spectrum of H_α values which characterizes it.

4. Conclusions

Applying the information entropy as the basic characteristics of the image is a promising area for further research, with the ultimate aim of which is to create the reliable method of automated segmentation of the self-organizing system state space obtained by non-invasive imaging method. And the trajectory segmentation may be used despite to the fact that we do not know the proper manifold in the internal orthogonal coordinate space.

This project was supported and co-financed by the GA JU 134/2013/Z and by the CENAKVA CZ.1.05/2.1.00/01.0024.

REFERENCES

1. Dr. Jack Cohen at http://drjackcohen.com/BZ01.html.
2. Štys D., Urban J., Levitner T.: Mater. Struct. Chem., Biol., Phys. Technol. *18*, 1211 (2011).
3. D. Štys at http://www.expertomica.eu/software.php.
4. http://www.camo.com/rt/Products/Unscrambler/unscrambler.html.

PATHOPHYSIOLOGICAL ROLE OF ABERRANT GLYCAN EXPRESSION IN TUMORIGENESIS AND CANCER PROGRESSION

BERNADETT BARKASZI[a] **and ANDRÁS GUTTMAN**[b]

[a] *Semmelweis University 2nd Department of Pathology, Budapest,* [b] *MTA-PE–Translational Glycomics Research Group, University of Pannonia, Veszprém, Hungary*
baushatee@gmail.com

Summary

Glycan structures are involved in tumor progression and metastasis formation (See Fig. 1) by affecting cell proliferation and survival, adhesion, migration, angiogenesis and immunogenic mimicry. Investigation on glycosylation could help to establish high-sensitivity screening methods based on unique pattern. Rational drug design could also target glycosylation pathways.

1. Introduction

Glycosylation is the most diverse post-translational modification[1]. Many glycosylation changes in cell surface proteins have been observed to facilitate tumor cells in hematogenous spread and invasion. Besides, glycans are responsible for organizing cell surface microdomains[2,3]. Growth factor receptors are prone to accumulate within these structures, where the interaction with microdomain molecules affects their kinase activity. Membrane distribution of epithelial growth factor receptor (EGFR) is also influenced by tri- and tetra-antennary *N*-glycan cell surface lattice that can decrease constitutive endocytosis of the receptor[4]. The recently recognized phenomenon of *O*-GlcNAcylation of nuclear proteins also contributes to the malignant phenotype. A large number of chromatin associated proteins, RNA polymerase II and many nuclear oncogenes and tumor suppressor genes are all reportedly *O*-GlcNAcylated[5,6].

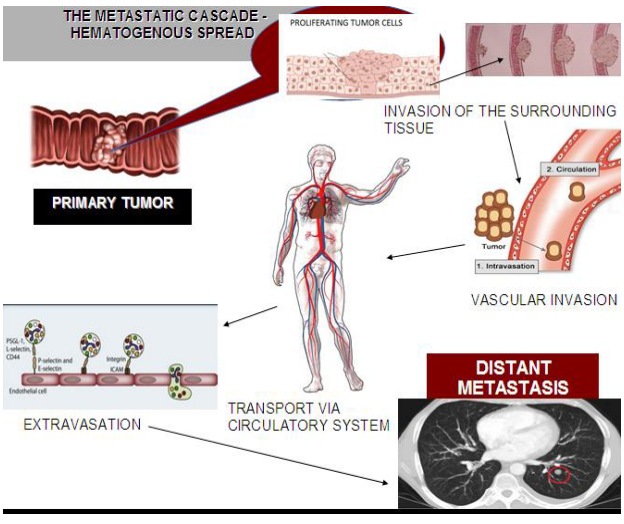

Fig. 1. **Hematogenous spread and metastasis-forming is a cascade of events.** Tumor cells have to detach from their stromal environment, intravasate in the blood stream, survive in the circulation and after extravasation, proliferate in the target organ to form a metastasis

2. Experimental

Glycans can be analyzed after chemical or enzymatic release. Chemical release is performed by hydrazinolysis, which releases both *N*-glycans and *O*-glycans. *O*-glycans can be selectively released beta-elimination. *N*-glycans can be obtained by PNGase F digestion[7]. Native glycans do not ionize efficiently in MS and have low UV/VIS absorption coefficients, preventing efficient spectroscopic detection. Therefore, derivatization, such as permethylation or chromophore / fluorophore labeling is essential before mass spectrometric and liquid chromatography or capillary electrophoresis analysis[7].

3. Results and discussion

3.1. Branched *N*-glycans

Increased β1,6-branching of *N*-glycan content and elevated MGAT5 level is widely observed in cancer cells[8] to inhibit integrin clustering, reducing the adhesion and thus inducing migration[9]. Besides, affinity of *N*-glycans to galectins increases the proportion of branching[8]. Tri- and tetraantennary *N*-glycans are ligands of galectins that regulate surface level of glycoproteins by forming a molecular lattice preventing endocytosis. Glycoproteins rich in *N*-glycans exhibit hyperbolic responses to stimuli[10] and constitutive endocytosis is slow[8], promoting surface retention of EGFR (ref.[4]).

3.2. Increased sialylation and fucosylation

Selectins contribute to cancer-metastasis. The presence of E-selectin ligands on cancer cells correlates with increased adhesion to endothelial cells[11]. They mediate cell tethering and rolling through the recognition of sialyl-fucosylated Lewis carbohydrates (See Fig. 2). Overexpression of these is associated with cancer

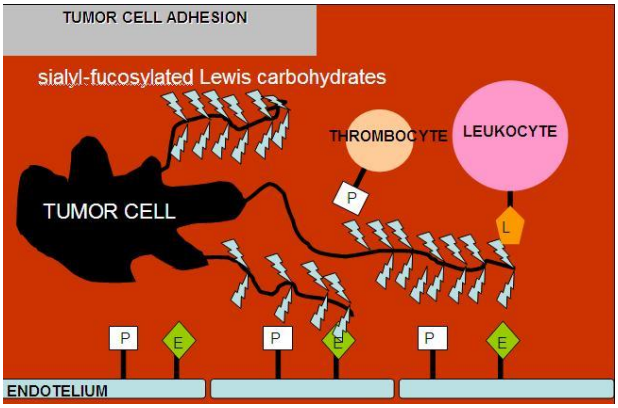

Fig. 2. **Selectins are carbonhydrate-binding molecules expressed by endothelial cells, platelets and leukocytes.** Selectins mediate cell thethering and rolling through the recognition of sialyl-fucosylated Lewis carbonhydrates that are frequently overexpressed in malignant tumors

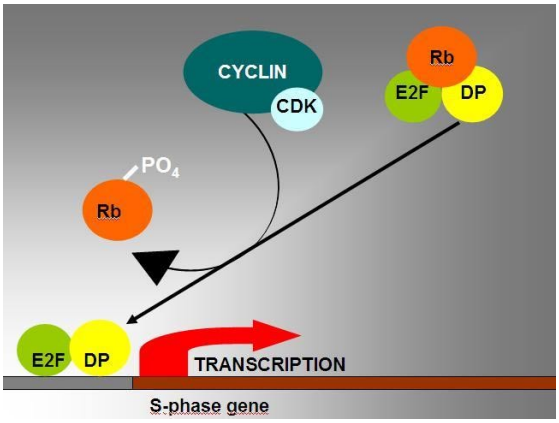

Fig. 3. **In the G0/G1 phase of the cell cycle, hypophosphorylated pRb complexes with transcription factors of the E2F family (indicated as E2F and DP) inhibiting their ability to activate transcription.** Cell cycle dependent phosphorylation of pRb by cyclin/cdk complexes releases E2F to activate transcription of target genes required for S-phase of the cell cycle

metastasis forming[12].

3.3. Glycosylation on growth factor receptors

Monosialodihexosylganglioside (GM3) acts via binding to the EGFR through carbohydrate interactions that require both glycosylation of the EGFR and sialylation of GM3. GM3 is observed to act as a membrane microdomain (lipid raft) organizer[13], in which receptors are able to associate. GM3 interferes with caveolin-1 function and inhibits microdomain formation. Binding of caveolin-1 to the EGFR inhibits EGF-induced proliferation and migration, while dissociation from caveolin-1 facilitates EGFR activation[14].

3.4. *O*-GlcNAcylated nuclear proteins

A large number of chromatin associated proteins, nuclear oncogenes and tumor supressor genes are *O*-GlcNAcylated[15]. Transcription factor cellular-myc has Threonin58 in the transactivation domain that is the major site of both *O*-GlcNAcylation and phosphorylation[16,17]. This mutation hot spot region Thr58 of c-Myc is *O*-GlcNAcylated, but the same site is rapidly phosphorylated when the cells are stimulated to grow[17]. Phosphorylated retinoblastoma protein (pRB) acts is through its interactions with the E2 promoter binding factor transcription factor. E2F mediates the G1/S transition of the cell cycle. In G1, pRB binds to E2F, while in late G1, pRB becomes hyperphosphorylated and E2F is released allowing the co-activator binding (See Fig. 3). An interesting reciprocal relationship was observed between phosphorylation and *O*-GlcNAcylation level[18].

4. Conclusions

Describing detailed glycosylation in cancer is of practical importance in future diagnostics and rational drug design with biomarker-mediated delivery of therapeutic agents. Many glycoproteins are already clinically utilized as tumor markers; however, most diagnostic tests only measure the expression of the polypeptide epitope. Diagnostic tests that recognize specific glycoforms of a protein would be of higher sensitivity and specificity. Fucosylated α-fetoprotein has already been clinically approved as a diagnostic marker of primary hepatocarcinoma[19,20]. Anti-tumor glycan antibodies bound to anti-cancer drugs are also an option in developing highly selective therapies with minimal toxicity to healthy cells.

This work was supported by the MTA-PE Translation Glycomics grant #97101.

REFERENCES

1. Spiro R.G.: Glycobiology *12*, 43R (2002).
2. Wang et al.: J. Biol. Chem. *278*, 48770 (2003).
3. Wang et al.: Glycobiology *11*, 515 (2001).
4. Dennis et al.: Traffic *10*, 1569 (2009).
5. Hart et al.: Annu. Rev. Biochem. *80*, 825 (2011).
6. Wells et al.: Amino Acids *40*, 877 (2011).
7. Ruhaak et al.: Anal. Bioanal. Chem. *397*, 3457 (2010).
8. Lau D.: Glycobiology *18*, 750 (2008).
9. Gu Taniguchi: Cell Adh. Migr. *2*, 243 (2008).
10. Lau et al.: Cell *129*, 123 (2007).
11. Barthel et al.: Proc. Natl. Acad. Sci. *106*, 19491

(2009).
12. IP Witz et al.: Immunol. Lett. *116*, 218 (2008).
13. Simons K., Ikonen E.: Nature *387*, 569 (1997).
14. Wang et al.: Cancer Res. *67*, 9986 (2007).
15. Comer Hart: Biochemistry *40*, 7845 (2001).
16. Chou et al.: Proc. Natl. Acad. Sci. *92*, 4417 (1995).
17. Kamemura et al.: J. Biol. Chem. *277*, 19229 (2002).
18. Wells et al.: Amino Acids *40*, 877 (2011).
19. Nouso et al.: J. Gastroenterol. Hepatol. *26*, 1195 (2011).
20. Moriya et al.: Anticancer Res. *33*, 997 (2013).

AMINO ACID PROFILING OF HUMAN PLASMA SAMPLES USING CAPILLARY ELECTROPHORESIS WITH CONTACTLESS CONDUCTIVITY DETECTION

ANDREA CELA, ALES MADR, JINDRA MUSILOVA, MARTA ZEISBERGEROVA, and ZDENEK GLATZ

Department of Biochemistry, Faculty of Science and CEITEC, Masaryk University, Brno, Czech Republic
323512@mail.muni.cz

Summary

Quantification of amino acids is a significant task for many scientific areas. Amino acids play a complex role in a living organism thus amino acid profiling of human biological fluids can be used for supplementary diagnostic purposes. Capillary electrophoresis coupled with in-house assembled contactless conductivity detection showed to be reliable and sensitive enough for quantification of 18 amino acids in 26 human plasma samples. Principal component analysis resulted in a partial grouping of the plasma samples with the same diagnosis proving potential use of presented method for supplementary diagnostic purposes.

1. Introduction

Amino acids (AA) are important biochemical compounds. AA are building blocks of proteins, they are involved in a synthesis of several neurotransmitters, porphyrins and nucleic acids. Quantification of AA in human biological fluids can reveal metabolic disorders which disrupt metabolic pathways of AA leading to accumulation of certain AA, intermediates or by-products. AA profiling can also reveal health-state of a living organism thus can be used for supplementary diagnostic purposes.

2. Experimental

2.1. Method

Capillary electrophoresis coupled with in-house assembled contactless conductivity detection (CE-C^4D) was chosen for AA analyses. Separation conditions follow the articles published earlier[1–4] and were optimized for human plasma samples. Background electrolyte (BGE) was composed of 8 % (v/v) acetic acid with 0.1 % (m/m) (hydroxyethyl)-cellulose. BGE was filtered using nylon membrane filters with 0.45 μm porosity and degassed in an ultrasonic bath for 10 minutes. Fused-silica capillary of 80.0 cm total length and 50/375 μm inner/outer diameter was used. Length from sample introduction side to a detector was 65.6 cm. Capillary was kept at 30 °C and separation voltage was set at 30 kV (anode at a capillary inlet side). Sample was introduced into capillary using pressure drop of 50 mbar for 30 seconds (equals to 0.5 psi for 43.5 seconds).

2.2. Sample treatment

Human plasma samples were stored in a freezer at –70 °C. The sample was thawed at a room temperature on the day of measurement. Proteins in the human plasma samples were precipitated by an addition of acetonitrile in the volume ratio 1:2, then thoroughly mixed and centrifuged for 10 minutes at 10 000×g. Supernatant was enriched by an addition of guanidineacetic acid (internal standard) giving final concentration of 50 μM and 3.1× diluted plasma sample. The addition of internal standard serves for correction of imprecision of sample introduction and potential sample concentration due to evaporation.

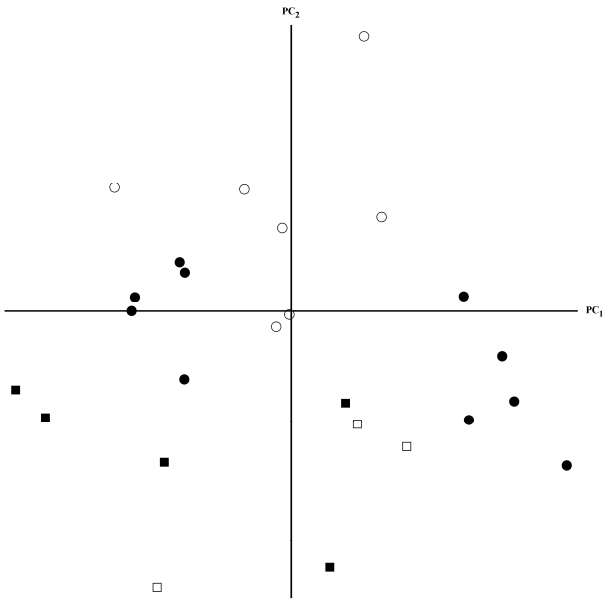

Fig. 1. **Graph of the 1st and 2nd principal scores.** Same symbols represent the same diagnosis; *i*) empty circle cancer, *ii*) filled circle cystic fibrosis, *iii*) empty square coagulation defects, purpura and other hemorrhagic conditions, *iv*) filled square other venous embolism and thrombosis

3. Results and discussion

Twenty-six human plasma samples were collected from patients diagnosed with *i*) cancer, *ii*) cystic fibrosis, *iii*) coagulation defects, purpura and other hemorrhagic conditions and iv) other venous embolism and thrombosis. Samples were both from men and women, 1–66 years old (31 years old on average).

There were quantified 18 AA in the all samples. Concentrations of these AA were submitted to principal component analysis and the first, the second and the third principal component scores were extracted. Visualization of the extracted principal component scores in the 3D space showed partial grouping of the plasma samples with the same diagnosis. Partial grouping can be ascribed to large differences in patient ages and generic definition of the diagnosis.

4. Conclusions

Presented CE-C^4D method is suitable for reliable and sensitive analysis of human plasma samples. Sample treatment is simple and inexpensive. Analysis of 26 human plasma samples differing in age and diagnosis showed changes in AA profiles. There were quantified 18 AA in total resulting in partial grouping of the same diagnosis. It can be considered that AA profiling based on CE-C^4D can be used for supplementary diagnostic purposes in medical practice where determination of proper diagnosis is unclear or when specific markers are not discovered yet.

No ethical standards were violated.

Financial support granted by the Czech Science Foundation (Project No. P206/11/0009) and the European Social Fund (Project No. CZ.1.07/2.3.00/20.0182 administered by the Ministry of Education, Youth and Sports of the Czech Republic) is highly acknowledged.

REFERENCES

1. Coufal P., Zuska J., van de Goor T., Smith V., Gas B.: Electrophoresis *24*, 671 (2003).
2. Samcova E., Tuma P.: Electroanalysis *18*, 152 (2006).
3. Tuma P., Samcova E., Andelova K.: J. Chromatogr., B *839*, 12 (2006).
4. Tuma P., Malkova K., Samcova E., Stulik K.: J. Sep. Sci. *33*, 2394 (2010).

DEVELOPMENT OF LC/MS/MS METHOD FOR DETERMINATION OF ACETAMINOPHEN METABOLITES

PETR ČESLA[a], TOMÁŠ ROUŠAR[b], ERIKA NÝDLOVÁ[a,b], MARTINA VRBOVÁ[a,b], LENKA ČESLOVÁ[a], and JAN FISCHER[a]

[a] *University of Pardubice, Faculty of Chemical Technology, Department of Analytical Chemistry, Pardubice,* [b] *University of Pardubice, Faculty of Chemical Technology, Department of Biological and Biochemical Sciences, Pardubice, Czech Republic*
Petr.Cesla@upce.cz

Summary

A liquid chromatography-tandem mass spectrometry method for the determination of two acetaminophen metabolites, i.e. acetaminophen-glutathione and acetaminophen-cysteine conjugates was developed. The octadecyl silica gel column has been used together with the gradient elution of methanol/water for fast separation of metabolites in less than four minutes. Tandem mass spectrometry in multiple reaction monitoring mode was applied for identification and quantitation of metabolites using deuterated acetaminophen as the internal standard.

1. Introduction

Acetaminophen (paracetamol) represents most common antipyretic and analgesic drug being sold in almost all countries around the world. When it is used within therapeutic limits, it is metabolized by sulfation or glucuronidation pathway. After overdose, the oxidation pathway of acetaminophen (Fig. 1) becomes more important yielding *N*-acetyl-*para*-benzoquinone imine (NAPQI), which is further rapidly metabolized to acetaminophen-glutathione conjugate (APAP-SG). Recently, we have shown that APAP-SG can also play possible pathological role[1–3].

For the monitoring and quantitation of acetaminophen metabolites, the fast and efficient analytical tools are needed. Liquid chromatography with tandem mass spectrometry (LC/MS/MS) is usually used for the determination of acetaminophen and its metabolites[4–9]. In present work, we have developed fast and accurate method for identification and quantitation of acetaminophen and its two metabolites, acetaminophen-glutathione and acetaminophen-cysteine conjugates employing separation on octadecyl silica gel column packed with porous shell particles coupled to triple quadrupole tandem mass spectrometer operated in multiple reaction monitoring mode. Both the conditions of separation and the mass spectrometric detection parameters were optimized and the developed method is presented herein.

2. Experimental

Acetaminophen (*N*-(4-hydroxyphenyl)acetamide, APAP) and its deuterated analogue (APAP-D4) used as internal standard, acetic acid and methanol was purchased from Sigma-Aldrich (St. Louis, MO, USA). The reagents used for the synthesis of acetaminophen-glutathione

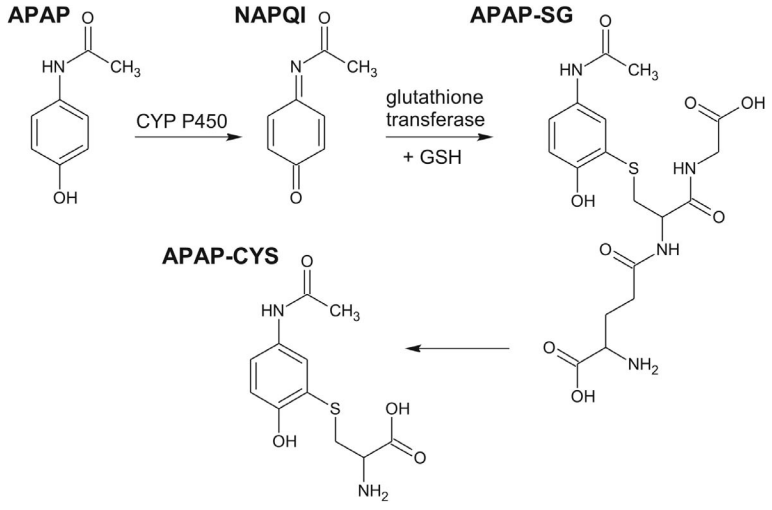

Fig. 1. **Oxidation metabolic pathway of acetaminophen**

Table I
Optimized conditions for MS/MS detection of acetaminophen and its two metabolites

	APAP	APAP-SG	APAP-CYS
MRM transition	152.0/109.9	454.9/271.9	271.0/140.0
Polarity mode	positive	negative	positive
Declustering potential, DP [V]	71	–65	62
Collision energy, CE [V]	21	–22	33
Collision exit potential, CXP [V]	8	–9	10
Dwell time [ms]	100	100	100

conjugate (APAP-SG) and acetaminophen-cysteine conjugate (APAP-CYS) were purchased from Lachema (Czech Republic). APAP-SG and APAP-CYS were synthesized as described elsewhere[1,3].

The LC/MS/MS analyses were performed on Shimadzu modular binary gradient LC system consisted of two LC-20ADXR pumps, autosampler SIL-20ADXR (Shimadzu, Kyoto, Japan), column thermostat LCO 102 (ECOM, Prague, Czech Republic) coupled with QTRAP 4500 MS instrument operated in electrospray mode (AB SCIEX, Framingham, MA, USA). The separation was performed on Kinetex C18 column packed with porous shell particles (100 × 3.0 mm, 2.6 μm; Phenomenex, Torrance, CA, USA) maintained at 40 °C. The mobile phase consisted from water with addition of 0.1 % (v/v) acetic acid (A) and methanol (B) with flow rate of 0.4 mL min^{-1}. The gradient profile was 0 min – 10 % B, 5 min – 70 % B, 7 min – 70 % B, 8 min – 10 % B.

3. Results and discussion

For the precise and accurate determination of APAP and its metabolites APAP-SG and APAP-CYS, the separation and detection conditions were optimized. The employing of octadecyl silica gel column packed with

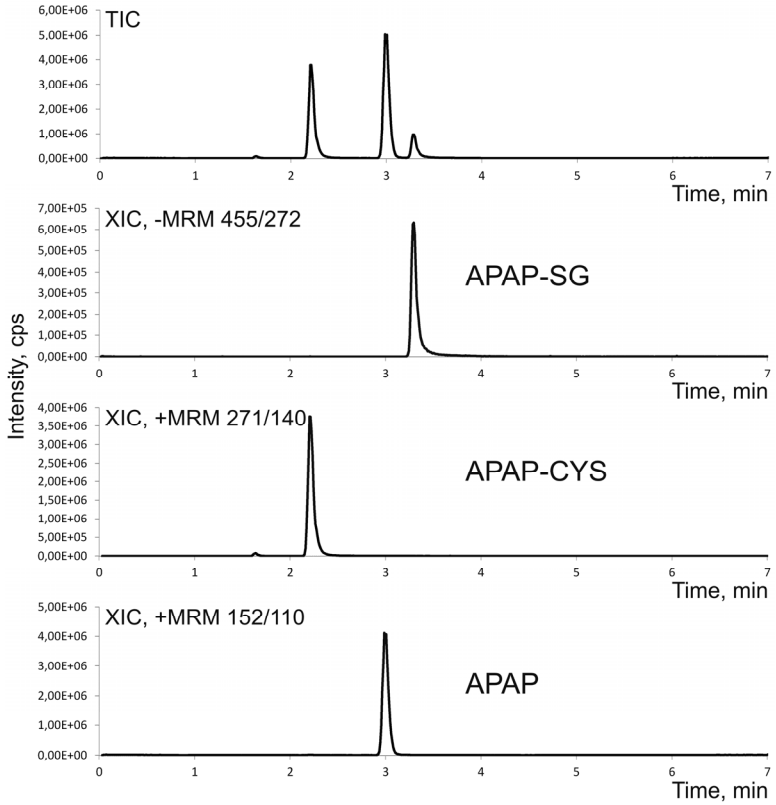

Fig. 2. **LC/MS/MS analysis of acetaminophen and its two metabolites using developed method.** TIC – total ion current, XIC – extracted ion chromatograms for multiple reaction monitoring transitions of metabolites

porous shell particles significantly decreased the time of the analysis and improved the efficiency and detection limits. The MS/MS detection conditions were optimized by direct injection of appropriate standards to the mass spectrometer and by measuring the signal intensity in dependence on the optimized parameters. The optimized MS/MS conditions are shown in Table I. The MRM transition for APAP corresponds to the most intense fragment ion $[M+H-CH_2=C=O]^+$ *m/z* 109.9, followed by the $[M+H-CH_3-CO-NH_2]^+$ ion *m/z* 93 in the positive ion mode. The fragmentation of APAP-SG and APAP-CYS yielded in the cleavage of the glutathione/cysteine chain, with the most intense fragment ion *m/z* 271.9 for APAP-SG and the less intense fragment ions *m/z* 181.9 and 143.0, all in the negative ion mode.

The separation of APAP and its metabolites APAP-SG and APAP-CYS using MS/MS detection under optimized conditions with total ion current and extracted ion currents for corresponding MRM transitions is shown in Fig. 2. The quantitation of all compounds was carried out using deuterated acetaminophen as internal standard. The developed LC/MS/MS method has been applied for the purity control of the synthesized standards of APAP metabolites and for the analysis of the metabolites in liver rat mitochondria samples.

4. Conclusions

The method for determination of acetaminophen, acetaminophen-glutathione metabolite with possible toxic role, and acetaminophen-cysteine has been developed. The optimized separation conditions employing porous shell particle packed column and tandem mass spectrometric detection in multiple reaction monitoring mode was used for the fast and accurate identification and quantitation of the compounds in biological samples.

This work was financially supported by the Ministry of Health of the Czech Republic, project No. NT14320-3/2013.

REFERENCES

1. Roušar T., Nýdlová E., Česla P., Staňková P., Kučera O., Pařík P., Červinková Z.: Physiol. Res. *61 (Suppl. 2)*, S103 (2012).
2. Roušar T., Pařík P., Kučera O., Bartoš M., Červinková Z.: Physiol. Res. *59*, 225 (2010).
3. Nýdlová E., Vrbová M., Česla P., Jankovičová B., Ventura K., Roušar T.: J. Applied. Toxicol. in print, doi:10.1002/jat.2914 (2013).
4. Ohta M., Kawakami N., Yamato S., Shimada K.: J. Pharm. Biomed. Anal. *30*, 1759 (2003).
5. Wen B., Fitch W. L.: J. Mass Spectrom. *44*, 90 (2009).
6. An J. H., Lee H. J., Jung B. H.: Biomed. Chromatogr. *26*, 1596 (2012).
7. Tonoli D., Varesio E., Hopfgartner G.: J. Chromatogr., B *904*, 42 (2012).
8. Hairin T., Marzilawati A. R., Didi E. M. H., Mahadeva S., Lee Y. K., Rahman N. A., Mustafa A. M., Chik Z.: Anal. Methods *5*, 1955 (2013).
9. Taylor R. R., Hoffman K. L., Schniedewind B., Clavijo C., Galinkin J. L., Christians U.: J. Pharm. Biomed. Anal. *83*, 1 (2013).

NAPHTALENE-2,3-DICARBALDEHYDE DERIVATIZATION OF AMINO ACIDS – AN IMPROVED TECHNIQUE FOR MINIMIZATION OF BENZOIN CONDENSATION

TEREZA DEDOVA, ANDREA CELA, ALES MADR, and ZDENEK GLATZ

Department of Biochemistry, Faculty of Science and CEITEC, Masaryk University, Brno, Czech Republic
terezadedova@gmail.com

Summary

The capillary electrophoresis coupled with fluorescence detection is a very powerful tool for analysis of amino acids in biological samples such as urine, plasma, liquor, etc. It can be also used for an additional diagnosis of various metabolic disorders. Labelling with fluorophore molecule is necessary in order to detect amino acids (AA) with a fluorescence detector. For this purpose various derivatization techniques have been introduced over the years. Naphtalene-2,3-dicarbaldehyde (NDA) reaction with a primary amine group in the presence of a cyanide ion is often used to form fluorescent 2-substituted 1-cyanobenz[*f*]insodoles. Nevertheless, to the best of our knowledge, no unified method was described in research publications. In this study, various mixing schemes were tested to propose the best technique for the derivatization reaction in high yield and reproducibility.

1. Introduction

In our research, we have discovered that the order of the addition of reagents is crucial to minimize undesired benzoin condensation reaction of NDA. Benzoin condensation is a reaction catalysed by a nucleophile, in which two aromatic aldehydes react to form alfa-hydroxyketons[1]. An example is a reaction of two benzaldehyde molecules catalysed by a cyanide ion which results in production of benzoin. A similar reaction occurs when NDA is mixed with cyanide in the absence of amine, resulting in formation of several side products (Fig. 1)[2]. Our contribution deals with undesired benzoin condensation reaction of NDA and investigates the influence of addition order of reactants on labelling outcome.

2. Experimental

2.1. Material and methods

The commercially available Agilent G7100 CE system (Agilent Technologies, Santa Clara, CA, USA) equipped with an in-house-assembled Led-IF detector and integrated UV detector was used. The Led-IF detector uses

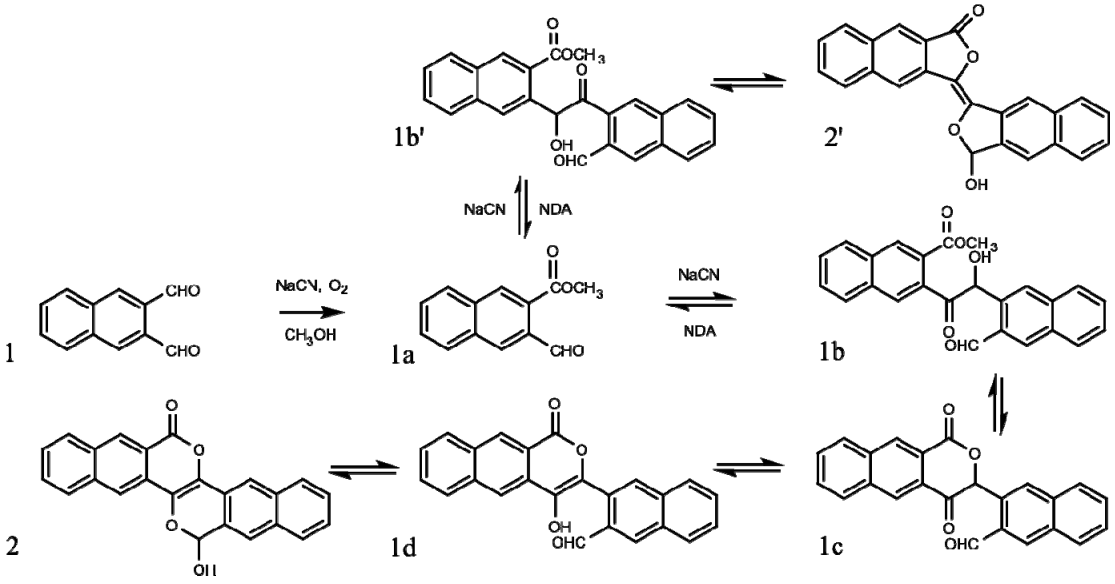

Fig. 1. **Reaction scheme of the NDA benzoin type condensation.** NDA (1) in a methanolic solution reacts in the presence of air and cyanide to form several products

a blue LED diode with the emission maximum at 450 nm. Agilent ChemStation software was used for data acquisition and integration. Separations were carried out on bare fused silica capillaries with 50 μm inner and 375 μm outer diameters and polyimide protective coating. The total and effective lengths of the capillary were 68.5 cm and 50 cm, respectively.

2.2. Kinetics of NDA condensation

Reaction kinetics of benzoin condensation of NDA and benzaldehyde were compared. Changes in levels of NDA and benzoin were quantified as a change in absorbance at 250 nm. The reaction mixtures were thoroughly stirred and then maintained at 37 °C for 180 minutes at 450 rpm. Samples were collected in 10 minutes intervals during the first hour and then in 30 minutes intervals. The reaction was stopped by direct analysis of the aliquots.

2.3. Effect of reactants mixing order

Four different mixing schemes of NDA labelling reaction were studied. All reactions were conducted in amber microtubes to protect light sensitive NDA derivatives of AA. In first mixing scheme[3] (Reaction 1) AA, $Na_2B_4O_7$, NaCN and NDA were added in this order. In the second reaction (Reaction 2) AA, $Na_2B_4O_7$, NDA and NaCN were mixed. For the third reaction (Reaction 3), based on paper published by Siri research group[4], a reaction mixture containing $Na_2B_4O_7$, NDA and NaCN was prepared in advance and subsequently added to AA. In all cases the reaction mixtures were thoroughly vortexed and kept at 25 °C for 30 minutes at 450 rpm. The reaction was then stopped by freezing the samples at –70 °C. Based on the results obtained from these measurements, new mixing scheme (Reaction 4) was designed where AA were mixed with a prepared mixture of $Na_2B_4O_7$ and NaCN, followed by NDA. This simplifies the labelling procedure and prevents the unwanted side reaction.

3. Results and discussion

3.1. NDA condensation kinetics

Our experiment indicates that the NDA benzoin type condensation reaction is more rapid than benzoin condensation of benzaldehyde (data not shown). Significant changes in NDA levels were detected already after 10 minutes of incubation time when the level of NDA dropped to less than 50 %. After 50 minutes only 2 % of initial NDA level was detected. A pale yellow solution after 60 minutes and a formation of brown precipitate after 120 minutes of incubation were observed. The precipitation was significantly enhanced when the temperature was decreased to 4 °C. Based on these results it was assumed that the addition order of reactants can play an important role during the labelling procedure due to the consumption of NDA.

3.2. Effect of reactants mixing order

There was observed no significant difference between Reaction 1 and Reaction 2 ($P < 0.05$). Both of these reactions had a good output, although the amount of pipetting steps is more likely to cause random errors. Reaction 3 is easier to perform, however the decrease in yield for Reaction 3 was significant compared to Reaction 1 ($P < 0.05$). Additionally the difference between Reaction 1 and Reaction 4 was insignificant ($P < 0.05$), thus we prefer Reaction 4, considering the advantage of reducing the amount of pipetting steps.

4. Conclusions

Based on our results, it is possible to simplify the recommended labelling reaction by preparing mixture consisting of $Na_2B_4O_7$ and NaCN without unwanted effect on the outcome of the reaction. Reaction 4 will be used for further optimization. Other conditions such as the effect of pH and the incubation temperature will be tested in further studies along with derivatization of biological samples and evaluation of stability of AA-NDA derivatives.

The financial support granted by the Czech Science Foundation (Project No. P206/11/0009) and the European Social Fund (Project No.CZ.1.07/2.3.00/20.0182 administered by the Ministry of Education, Youth and Sports of the Czech Republic) is highly acknowledged.

REFERENCES

1. McMurry J.: *Organic Chemistry.* 6th ed., p. 1243. Pacific Grove: Brooks/Cole publishing company, 2004.
2. McGill C. M., Swearingen K. E., Drew K. L., Rasley B. T., et al.: J. Heterocycl. Chem. *42*, 475 (2005).
3. Roach M. C., Harmony M. D.: Anal. Chem. *59*, 411 (1987).
4. Siri N., Lacroix M., Garriques J. C., Poinsot V., et al.: Electrophoresis *27*, 4446 (2006).

COMBINATORIAL GLYCOMICS 1: SYNTHESIS OPTIONS

BOGLÁRKA DÖNCZŐ[a], LÁSZLÓ KALMÁR[a], JÁNOS KERÉKGYÁRTÓ[b], ZOLTÁN SZURMAI[b], and ANDRÁS GUTTMAN[a]

[a] Horvath Laboratory of Bioseparation Sciences, MMKK, University of Debrecen, Debrecen, [b] Institute of Biology and Ecology, University of Debrecen, Debrecen, Hungary
boglarka1112@gmail.com

Summary

The viral-surface envelope glycoproteins of HIV are abundantly decorated with complex and high mannose type *N*-glycans (> 20 glycosylation sites). Synthesis of a large number of closely related structural determinants of high mannose antennae was carried out by means of the combination of conventional and combinatorial carbohydrate chemistry. The chitobiose part of the core structure was replaced by a simple octyl aglycone. The pseudo tetra- (**2**) and penta- (**3**)-saccharides were prepared by standard carbohydrate chemistry. The β-mannosidic linkage was created by the oxidation-reduction technique. Random mannosylation of acceptors **2** and **3** resulted in a mixture of predominantly pseudo penta- and hexasaccharides, respectively. After removal of the protecting groups, the interaction of the synthesized mixture of oligosaccharides and gp120 binding proteins will be investigated.

1. Introduction

N-glycoproteins are ubiquitous on eukaryotic cell surfaces and in body fluids. The dynamically growing field of glycobiology is devoted to defining structural and functional roles of glycans in numerous biological recognition processes, including, for example, viral and bacterial infection, tumor metastasis, immune response and many other receptor-mediated signaling processes[1,2]. Chemical synthesis provides a valuable means to produce glycans, which serve as model compounds to gain insight into *N*-glycoprotein structure and function, as tools to study biomolecular interactions and as effectors to evoke biological responses[3]. However, due to the large number of possible connections, chemical preparation of oligosaccharides is much more complicated than the synthesis of other biopolymers such as peptides or nucleic acids. The synthesis of oligosaccharides can be characterised as the regio- and stereoselective formation of interglycosidic linkages. To date, there are no general applicable methods or strategies for synthesis of complex large oligosaccharides and consequently the preparation of oligosaccharides is very time consuming.

All *N*-glycans share a common core sugar sequence of αMan-(1→6)-[αMan(1→3)]-βMan-(1→4)-βGlcNAc-(1→4)-βGlcNAc-(1→Asn-X-Ser/Thr. In the case of oligomannose type, only mannose residues are attached to the core. Among complex types, this type of glycans are also found decorating viral-surface envelope glycoproteins of HIV[4].

Based on the experience of the last 30 years[5–9] our research program focuses on the preparation of large number of closely related structural determinants of high mannose antennae by means of the combination of the conventional and combinatorial carbohydrate chemistry. After removal of the protecting groups the generated mixture of random oligosaccharides will be evaluated with their interaction with gp120 binding proteins.

2. Experimental

The ^{1}H NMR (200, 360 and 500 MHz) and ^{13}C NMR (50.3, 90.54 and 125.76 MHz) spectra were recorded with Bruker WP-200 SY, Bruker AM-360 and Bruker DRX-500 spectrometers. The MALDI measurements were carried out with a Bruker MALDI-TOF mass spectrometer, equipped with a 337-nm nitrogen laser. The accelerating voltage was 20.0 kV. 2,5-Dihydroxybenzoic acid was used as matrix and 100–200 laser shots were applied for each spectrum. The reactions were monitored by TLC on Kieselgel 60 F_{254} (Merck, Darmstadt) with detection by charring with sulfuric acid. Kieselgel 60 (Merck) was used for short-column chromatography.

3. Results and discussion

The key compound of our synthetic route was octyl 3-*O*-allyl-2,4-di-*O*-benzyl-β-D-mannopyranoside **1,** which can be considered as a selectively protected pseudo core trisaccharide, containing β-mannosidic linkage and the chitobiose part is replaced by a simple octyl aglycone.

Compound **1** was prepared by conventional carbohydrate chemistry starting from a *gluco* compound in 9 synthetic steps. The β-mannosidic linkage was created

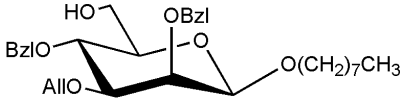

Compound **1**

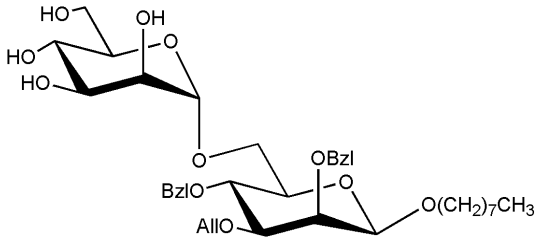

Compound **2**

by C-2 epimerization of the initially introduced β-D-*gluco* unit *via* oxidation followed by stereoselective reduction. Condensation of **1** and acetylated mannose imidate followed by deacetylation gave pseudo tetrasaccharide acceptor **2** bearing 4 free OH-groups.

Removal of the allyl function of compound **1** resulted in a diol which was glycosylated with acetylated mannose imidate to yield a pseudo pentasaccharide. Deacetylation of this latter derivative resulted in acceptor **3** with 8 free OH-groups.

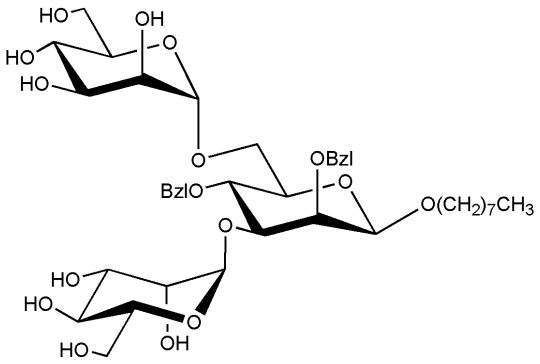

Compound **3**

"Random glycosylations" of pseudo tetra- (**2**) and pentasaccharide (**3**) acceptors with various mannosyl donors yielded the mixtures of predominantly pseudo penta- and hexasaccharides, respectively.

The biological experiments will be carried out after removal of the protecting groups from the synthetic products.

4. Conclusions

The combination of the classical and combinatorial carbohydrate chemistry seems to be a very promising approach for the preparation of random oligosaccharide libraries of biochemical interest.

The authors acknowledge the support of the MTA-PE Translation Glycomics Grant # 97101.

REFERENCES

1. Dwek R. A.: Chem. Rev. *96*, 683 (1996).
2. Varki A.: Glycobiology *3*, 97 (1993).
3. Mandal M., Dudkin V. Y., Geng X., Danishefsky S. J.: Angew. Chem. *43*, 2557 (2004).
4. Scanlan C. N., Offer J., Zitzmann N., Dwek R. A.: Nature *446*, 1038 (2007).
5. Kerekgyarto J., Kamerling J. P., Bouwstra J. B., Vliegenthart J. F., Liptak A.: Carbohydr. Res. *186*, 51 (1989).
6. Lichtenthaler F. W., Klares U., Szurmai Z., Werner B.: Carbohydr. Res. *305*, 293 (1997).
7. Kerekgyarto J., Agoston K., Batta G., Kamerling J. P., Vliegenthart J. F. G.: Tetrahedron Lett. *39*, 7189 (1998).
8. Szurmai Z., Janossy L., Szilagyi Z., Vekey K.: J. Carbohydr. Chem. *17*, 417 (1998).
9. Kalmar L., Agoston K., Szurmai Z., Donczo B., Kerekgyarto J.: J. Carbohydr. Chem. *31*, 203 (2012).

CAPILLARY ELECTROPHORETIC SCREENING OF TOXIC METABOLITES IN VARIOUS BODY FLUIDS – A SIMPLE DIAGNOSTIC TOOL TO DIFFERENTIATE METHANOL AND ETHYLENE GLYCOL POISONING

PAVOL ĎURČ[a], PETR KUBÁŇ[b], MIROSLAVA BITTOVÁ[a], and FRANTIŠEK FORET[b]

[a] *Institute of Chemistry, Masaryk University, Brno,*
[b] *Bioanalytical Instrumentation, CEITEC, Masaryk University, Brno, Czech Republic*
379660@mail.muni.cz

Summary

A new, simple and rapid capillary electrophoretic method with contactless conductivity detection for screening of formate, oxalate and glycolate in various body samples (blood serum, saliva, urine, exhaled breath condensate) is presented. The target analytes are separated in less than 6 minutes in an electrolyte composed of 50 mM L-histidine and 50 mM 2-(*N*-morpholino) ethanesulfonic acid at pH 5.9. A short (33 cm) fused silica capillary with 25 μm ID is used. LODs range from 0.4 to 1.25 μM. The method provides a simple and rapid diagnostic test in suspected intoxication of industrial chemicals and is able to distinguish the ingested liquid, based on its metabolite trace providing a fast screening tool that can be applicable in clinical practice.

1. Introduction

Intoxication by short chain alcohols belongs to the most common intoxication that occurs repeatedly worldwide. Methanol and ethylene glycol ingestion is the most common and it is a medical emergency that requires prompt diagnosis and intervention to prevent morbidity or mortality. The parent alcohols are much less toxic then their metabolites, notably formic, glycolic and oxalic acids that are responsible for various symptoms including loss of vision, CNS depression, renal failure etc.[1]. Unfortunately, there is presently no simple and fast analytical method that could be used in clinical practice for simultaneous determination of all three metabolites. Therefore the development of a new, fast and simple analytical method able to selectively analyze these metabolites in various human body samples is of paramount importance. In this contribution, we show capillary electrophoresis with contactless conductivity detection as a suitable technique.

2. Experimental

2.1. Instrumentation, samples and electrolytes

Analyses were performed using Agilent CE system (Model G1600AX) at −15 kV. A fused silica capillary (25 μM ID/375 μM OD, 33/18 cm total/effective length, Microquartz GmBH, Germany) was used. The analytes were detected by a custom made C4D detector, ADMET (Ver. 5.06, ADMET, Prague, Czech Republic).

The optimized BGE consisted of 50 mM 2-(*N*-morpholino)ethanesulfonic acid (MES) and 50 mM L-histidine (HIS).Various body samples were diluted with DI water and injected into the CE system hydrodynamically: exhaled breath condensate (EBC, no diluton), blood serum (1:100), saliva (1:100) and urine (1:500).

3. Results and discussion

3.1. Optimization of the separation electrolyte system

An optimization of the separation electrolyte system was conducted to separate the peaks of oxalate, formate a glycolate from the other peaks of the compounds that can be present in the various body fluid samples. With the help of PeakMaster 5.3 freeware, several background electrolytes were simulated to separate the analytes of interest. Initially, an electrolyte consisting of 15 mM Glu/10 mM HIS and 30 μM CTAB was applied[2], but unlike in the simulations, the oxalate peak in experiment was seriously tailing. Its shape was improved by selecting another separation electrolyte with a high ionic strength and excluding the positively charged EOF modifier (CTAB). Best results were obtained with electrolyte consisting of 50 mM MES, 50 mM HIS at pH 5.9. The separation using this electrolyte was tested experimentally and electropherograms showed efficient separation of oxalate, formate and glycolate from the other peaks. A short separation capillary of 33 cm total/18 cm effective lengths allowed a rapid separation (under 6 min) even in the counter-EOF mode and a separation of model mixture of 15 inorganic anions and organic acids is shown in Fig. 1.

3.2. Analytical parameters of the method

The analytical parameters of the developed CE method for oxalate, formate and glycolate were investigated. The calibration curves using an internal

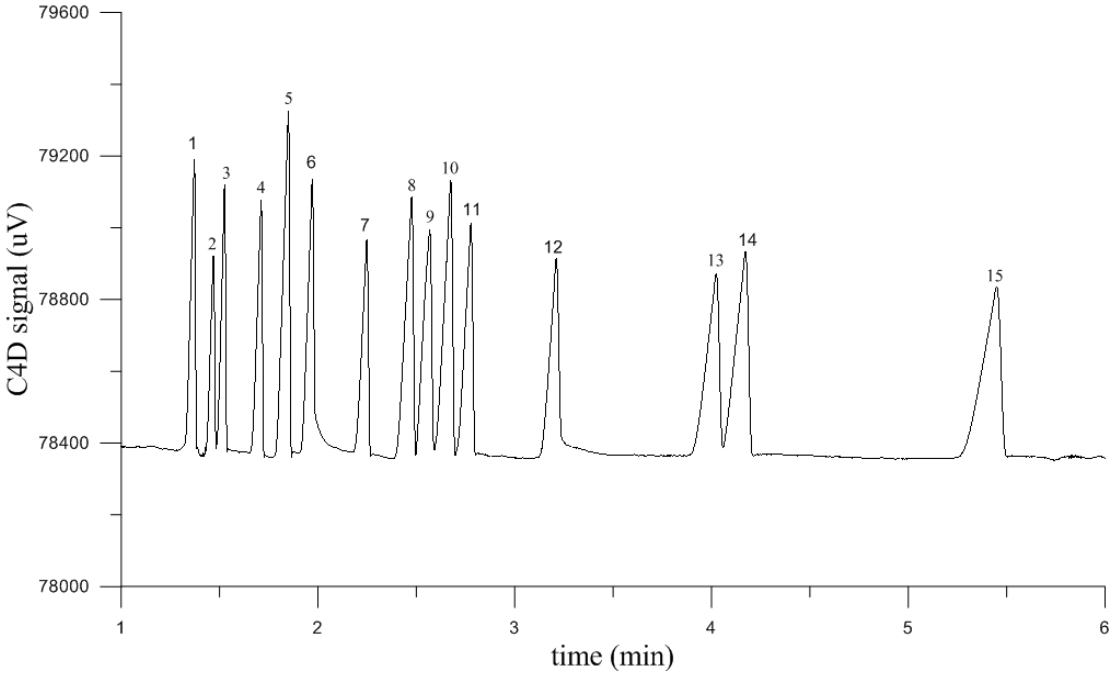

Fig. 1. **The separation of model mixture of 15 inorganic anions and organic acids;** 1 – chloride, 2 – nitrite, 3 – nitrate, 4 – thiocyanate, 5 – sulfate, 6 – oxalate, 7 – formate, 8 – fumarate, 9 – malonate, 10 – tartrate, 11 – maleate, 12 – citrate, 13 – glycolate, 14 – acetate, 15 – lactate

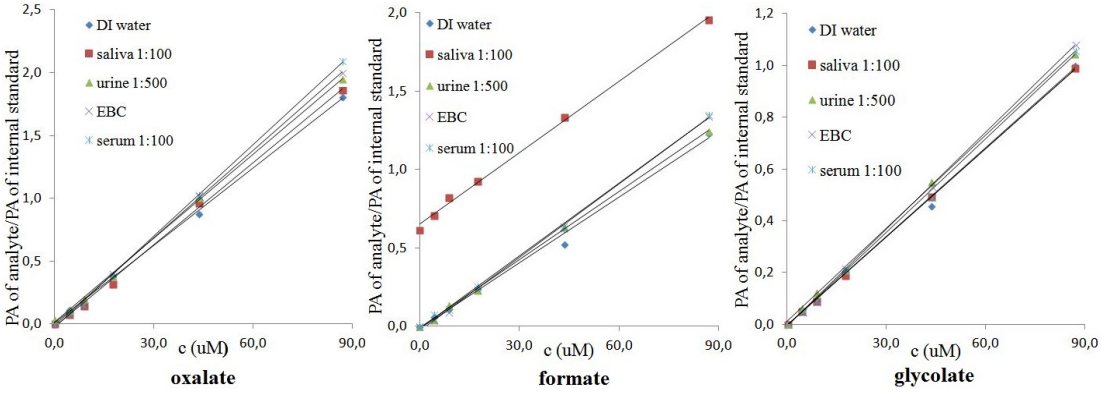

Fig. 2. **Calibration curves for oxalate, formate and glycolate in various body fluid samples and DI water**

standard (fumarate) were strictly linear in the range of 0–90 μM and were similar in all matrices. They are shown in Fig. 2. The R^2 ranged from 0.9971 to 0.9998. The formate calibration in saliva had the same slope but was shifted due to the presence of large concentration of formate in saliva.

The limits of detection were 0.4, 0.5 and 1.25 μM for oxalate, formate and glycolate, respectively and limits of quantitation were 1.3, 1.7, 4.2 μM. Repeatability (n=10) of migration times ranged from 0.3 to 0.7 % RSD and repeatability of peak areas ranged from 2.9 to 3.1 % RSD. The recoveries were also investigated. The recoveries were calculated after addition of known amount of analyte (35 and 70 μM) and internal standard – fumarate (70 μM) into each sample. The recovery values ranged between 89.3 and 108.9 %.

3.3. Analysis of real samples

Various body fluid samples were analyzed using the developed method. The samples were retrieved from

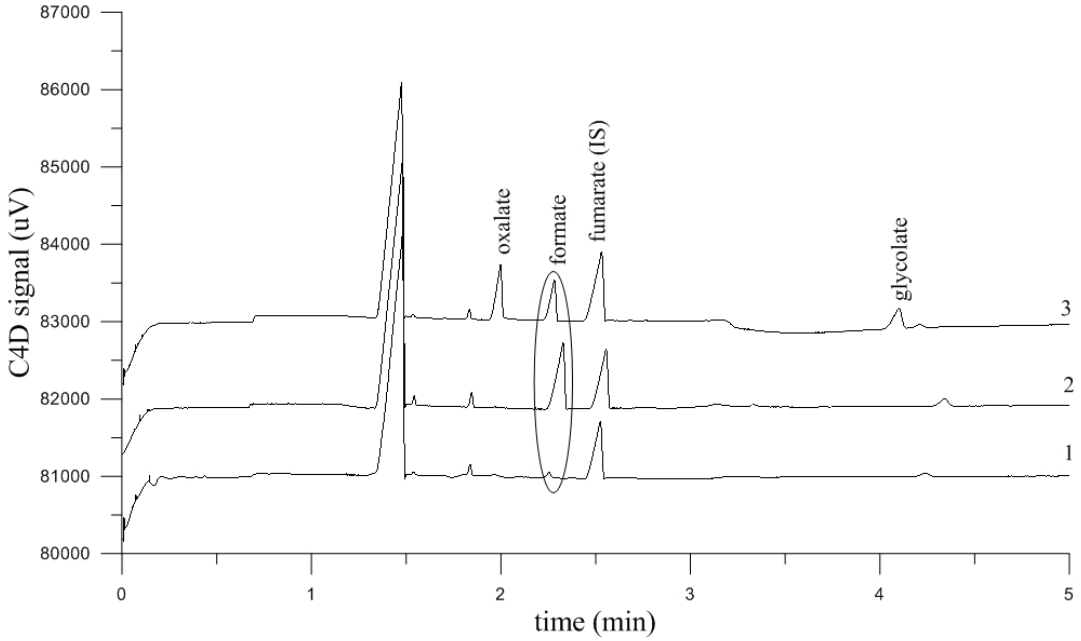

Fig. 3. **Separation of human serum samples;** 1 – lyophilized serum (1:100), 2 – serum of patient intoxicated with methanol (1:100), 3 – lyophilized serum with spiked oxalate, formate, glycolate and IS. CE conditions the same as in Fig. 1

healthy volunteers at the Masaryk University and some of the clinical samples were retrieved from the Department of Anesthesiology and Resuscitation, Havirov Hospital, Czech Republic. The samples of healthy volunteers contained small amounts of formate (saliva, serum, urine), oxalate (serum) and glycolate (urine), all within the physiological ranges. The blood serum samples of patients intoxicated with methanol during the methanol outbreak in 2012 contained significantly elevated concentrations of formate.

To demonstrate the applicability of the developed method, the electropherograms of diluted lyophilized blood serum (1), blood serum sample of patient who has been hospitalized with serious methanol intoxication (2) and diluted lyophilized blood serum with addition of 10 μM oxalate, formate, glycolate and 50 μM fumarate (internal standard) (3) is shown in Fig. 3.

The spiked model serum sample shows that all toxic metabolites can be sensitively detected and can indicate the type of toxic alcohol that has been ingested by the patient. In methanol intoxication (Fig. 3-2) from the three possible metabolites only formate peak occurs, which points to methanol as the source of intoxication. Should the person be intoxicated by ethylene glycol, peaks of glycolate and oxalate could be sensitively detected. The spiked metabolites could also be detected in all other, non-invasive samples (exhaled breath condensate, urine, saliva).

4. Conclusions

A rapid CE-C4D method for determination of oxalate, formate and glycolate in various body fluid samples was developed. The method is fast (< 6 min) and simple because only sample preparation is dilution with distilled water. Mentioned toxic metabolites can be determined in various samples both, invasively and noninvasively taken. Especially those noninvasively taken samples may be attractive from the point of a fast screening and diagnostic tool.

The authors acknowledge the financial support from the Grant Agency of the Czech Republic (Grant No. P206/13/21919S). Part of the work was realized in CEITEC – Central European Institute of Technology 355 with research infrastructure supported by the project CZ.1.05/1.1.00/02.0068 356 financed from European Regional Development Fund.

REFERENCES

1. Jacobsen D., McMartin K. E.: Med. Toxicol. Adverse Drug Exp. *1*, 309 (1986).
2. Kubáň P., Foret F., Bocek R.: J. Chromatogr., A *1281*, 142 (2013).

NEW ISOELECTRIC FOCUSING POWER SUPPLY BASED ON FEATURES OF VOLTAGE MULTIPLIER

FILIP DUŠA[a,b] and KAREL ŠLAIS[a]

[a] *Institute of Analytical Chemistry of Academy of Sciences of the Czech Republic, v. v. i., Brno,* [b] *Department of Biochemistry, Faculty of Science, Masaryk University, Brno, Czech Republic*
dusa@iach.cz

Summary

Present electrophoretic separation methods rely on sophisticated high-voltage power supplies capable of programing a voltage / current time course during an analysis. In this paper we suggest design of a simple high-voltage power supply for isoelectric focusing composed from affordable and commonly available electrical parts. It is based on features of the voltage multiplier invented by Cockcroft and Walton. Electrical characteristics of the power supply enabled power load controlled isoelectric focusing analysis thus eliminating need for programing voltage time course and reducing analysis total time.

1. Introduction

Since their invention, electrophoretic methods have become powerful separation techniques used in life science. With the increase in popularity came plenty of power supplies with ever improving control of the voltage, electric current and power load. From this three quantities power load is especially important for isoelectric focusing (IEF). Applied power is the main factor influencing Joule heat generation during an IEF run and hence it is very important to control it throughout a whole IEF analysis.

Although there are commercially available power supplies with power load limitation for gel and capillary electrophoresis formats this is not true for strip IEF format. Instead of units or tens of watt limitation suitable for gel and capillary geometry, limitation with tens of Milliwatt is needed for strip format. For that reason we suggest a new simple electrophoretic power supply based on features of a voltage multiplier which is able to maintain power load limit demanded for strip IEF.

2. Experimental

The novel power supply was assembled from diodes rated for 1 A / 1000 V and 10, 15, 22, 33, 47, 68, and 100 nF capacitors rated for 250 V AC according to the circuit diagram shown in Fig. 1. In a recent work we have developed a strip IEF device with a separation bed made from nonwoven fabric[1] which was used for a testing of the suggested power supply. Please see the given reference for details of the device design and a composition of testing model IEF mixture. Completed power supply circuit was then installed into the IEF device and outputs were connected to the electrodes and inputs were connected to 220 V AC cable, which was plugged to the power line before analysis. Finally the IEF device with the new power supply was switched on and electrodes were loaded with resistors covering range of resistance from 10 kΩ to 1 GΩ. At the same time, electric current was monitored and voltage and power load were calculated from obtained values. Subsequently, a graph including mentioned quantities was produced. The power supply was run with model IEF mixture and electric current was registered through the whole separation. Relevant voltage, power load, and resistance were calculated using extrapolation function and plotted into a time dependence graph.

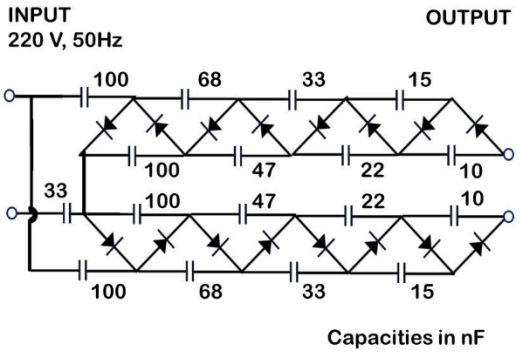

Fig. 1. **Circuit diagram of the developed IEF power supply**

3. Results and discussion

Firstly, the suggested power supply was constructed and electrode outputs were loaded by set of resistors of known resistance. The resistance range was chosen with regard to the common IEF mixture conductivity during an IEF run in strip geometry. After the collection, values of the electric current were plotted to a graph (see Fig. 2A). One can see that through the range of the tested resistances the power supply maintained the power load below 90 mW with even lower limit of 25 mW at very low resistances. Maximum voltage, defined by circuit design, was 5 kV. These data indicated that the power supply should be able

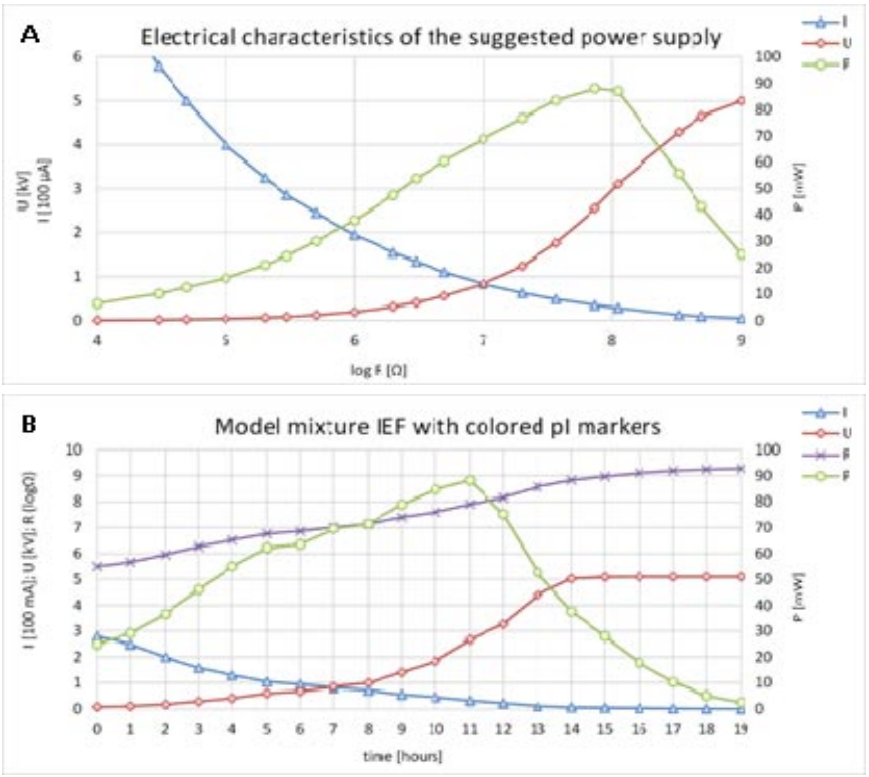

Fig. 2. **A – electrical characteristics of the suggested power supply after loading it with set of resistors, B – electrical characteristics of IEF of the model mixture which was run by the power supply**

to handle power load limited IEF analysis. This was tested by connection of the power supply electrodes to a nonwoven strip IEF device and IEF was run with a model mixture containing colored p*I* markers[1]. Electrical characteristics of the analysis are shown in Fig. 2B. Voltage reached 5 kV after 14 hours of focusing while power load increased slightly from 25 mW to 88 mW and then decreased quickly as focusing approached to a steady state. Application of low power load in the beginning of IEF was important due to high conductivity of the unresolved sample. This limitation becomes crucial when samples with high salt concentrations are employed. As a result, the power load controlled power supply enables focusing sample of unknown composition and moreover no optimization of a voltage time course was necessary.

4. Conclusions

We proposed a new power load controlled power supply for isoelectric focusing in strip geometry. The power supply was based on features of Cockcroft Walton voltage multiplier. Advantageously, it was made from readily available parts and was easy to construct. A monitoring of power supply electrical characteristics showed that power load was kept below 0.1 mA during testing with set of defined resistors. Moreover, the power supply was tested with model IEF mixture including colored p*I* markers. As a result, the obtained data suggests that the power supply can be easily utilized in IEF strip format analyses.

This work was supported by the Ministry of the Interior of the Czech Republic (Project No. VG20102015023), by the Academy of Sciences of the Czech Republic (institutional support RVO: 68081715). This project is co-financed by the European Social Fund and the state budget of the Czech Republic (CZ.1.07/2.3.00/20.0182).

REFERENCE

1. Duša F., Šlais K.: Electrophoresis *34*, 1519 (2013).

MONITORING OF SELECTED ORGANIC ACIDS DURING THE PRODUCTION OF TRADITIONAL MORAVIAN WINE BY CAPILLARY ZONE ELECTROPHORESIS (CZE)

MILOŠ DVOŘÁK, HANA ŠURANSKÁ, and MILENA VESPALCOVÁ

Institute of Food Science and Biotechnology, Faculty of Chemistry, Brno University of Technology, Purkyňova 118, 61200 Brno, Czech Republic
mil.dvorak@seznam.cz

Summary

This paper describes application of capillary zone electrophoresis for determination of selected short-chain organic acids in wine must during the controlled fermentation process by inoculation of fresh must by autochthonous (isolated) S. cerevisiae strain. In order to determine organic acids indirect photometric detection (254 nm) was used. We separated six basic organic acids with short chain and identified in real samples. Separation system contained 3,5-dinitrobenzoic acid and cationic surfactant (CTAB). Separation took place on uncoated fused silica capillary. We focused on monitoring of organics acids amount during fermentation process.

1. Introduction

Determination of major organic acids in wine must is an important control step for biotechnological productions and microbiological tests. Their composition and changes are an indicator of the state of the process, as an indicator of sensory and quality characteristics of the product. In the field of microbiology carboxylic acids are an important parameter that helps the taxonomically classify the microbes or to monitor the impact of changes in conditions on the behavior of microorganisms[1]. Quick and easy alternative with sufficient efficiency offer electromigration methods. In particular, capillary zone electrophoresis and their arrangement is the most suitable principle for rapid analysis of biological samples containing short-chain organic acids[2].

2. Experimental

All reagents were of analytical grade (p.a). Standards of organic acids and cetyltrimethylamonium bromide (CTAB) were from Sigma-Aldrich, 3,5-dinitrobenzoic acid (3,5-DNB) from Penta. Standard stock solutions were prepared with purified water (Milli-Q).

Capillary electrophoresis system was used PrinCE 460 (PrinCE Technologies B.V., Emmen, Neederland) with UV-VIS detector Spectra SYSTEM UV2000 (Thermo Separation Products Inc., San Jose, USA) and fused silica capillary, I.D 50 μm (MicroSolv Technology Corporation, Long Branch, NJ, USA). Registration of signal was realized by CSW 1.7 (DataAppex, Praha, Czech Republic).

All solutions were before used filtered through a 0.45 μm membrane. Backgound electrolyte (BGE) contained 10 mmol L^{-1} 3,5-dinitrobenzoic acid with 0,2 mmol L^{-1} CTAB. pH was set up at 3,2 (NaOH). Fused silica capillary had total length 75 cm, effective length 25 cm. Before first analysis capillary was conditioned with 1 mol L^{-1} NaOH (1200 mBar, 20 min), Milli-Q water (1200 mBar, 10 min), and BGE (1200 mBar, 10 min) with elektrokinetic flush (+25 kV). Between analyses capillary was reconditioned BGE with elektrokinetic reflush (1200 mBar, +25 kV, 5 min). The electrophoretic system was operated with inverted polarity and constant voltage of –30 kV. Indirect photometric detection was set up 254 nm. Temperature of all systems was constant at 25 °C (ref.[3]).

Samples of wine must at different stages of fermentation for analysis were filtered (0.45 μm porous membrane) and diluted MQ-Water.

Samples of wine must were fermentated by different strains of yeast – commercial and isolated "in situ" from vineyard. Different strains of yeast were applied to the wine must from vineyard differing of agricultural processing – ecological and integration process. Isolation of yeast and prepare of fermented must are not subject of this research[4].

3. Results and discussion

27 samples of white wine must was measured ("Sauvignon blanc" variety) and 46 samples of red wine must ("Pinot noir" variety). "Sauvignon blanc" must was obtained from ecological agriculture process and "Pinot noir" must were obtained from ecological and integrated agriculture process. Both musts were fermented by commercial and autochthonous S. cerevisiae strain.

We determined tartaric, citric, malic, lactic, succinic and acetic acids during the process of fermentation. Significant differences were observed only in the case tartaric and malic acid (decrease of amount in the time) and lactic acid (increase of amount). Results of changes amount determined acids white and red must correlated. It was observed, that acetic, citric and succinic acid are not utilized.

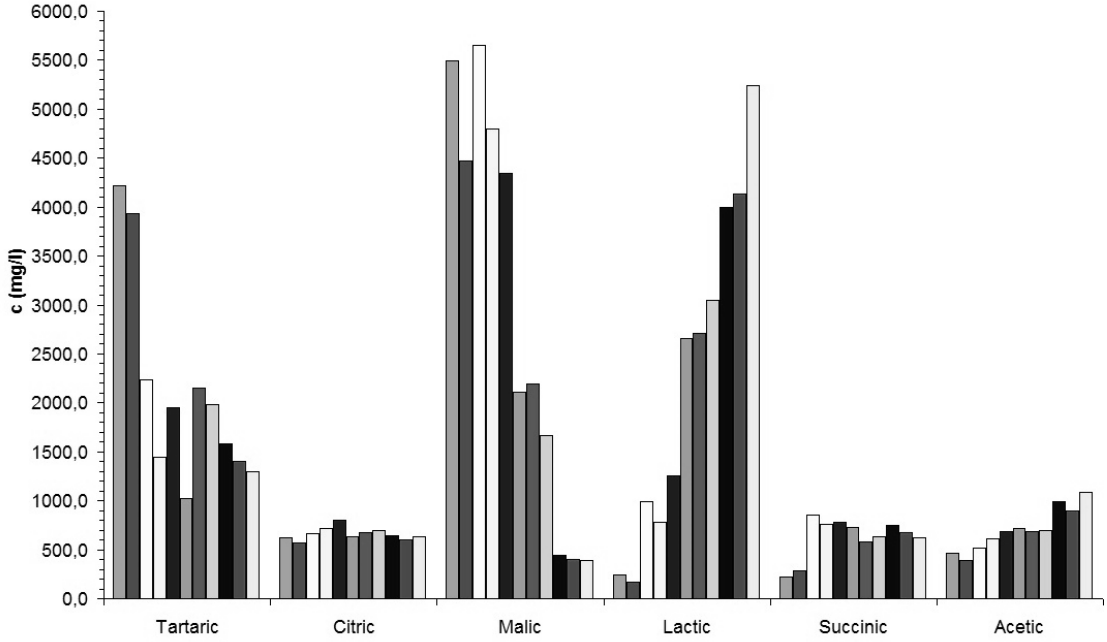

Fig. 1. **Example – Determined concentration of organic acids (mg L^{-1}) in the time.** Samples: "Pinot noir" variety obtained from ecological agriculture vineyard, must was inoculated by commercial yeast

4. Conclusions

Capillary zone electrophoresis with indirect photometric detection and chosen separation system is shown to be sufficient and effective tool for monitoring of the content of carboxylic acids in the wine must. Method was fast enough, economical and effective. It reflected a sufficient reproducibility. We determined amount of selected organic acids in wine musts, the amount of organic acids seems to be independent of yeast strains and mode of grape agriculture.

REFERENCES

1. Sádecká. J., Polonský. J.: J. Chromatogr., A *880*, 243 (2000).
2. Molnár-Perl. I.: J. Chromatogr., A *891*, 1 (2000).
3. Peres R. G., Moraes E. P., Micke G. A., Tonin F. G., Tavares M. F. M., Rodriguez-Amaya D. B.: Food Control *20*, 548 (2009).
4. Šuranská H., Vránová D., Omelkova J., Vadkertiová R.: Chem. Pap. *66*, 861 (2012).

CONJUGATION OF ANTIBODIES FIXED TO SOLID PHASE WITH QUANTUM DOTS FOR AMPLIFICATION OF SIGNAL IN ELECTROCHEMICAL IMMUNOSENSOR

VERONIKA DVORAKOVA, MICHAELA CADKOVA, BARBORA JANKOVICOVA, LUCIE KORECKA, and ZUZANA BILKOVA

Department of Biological and Biochemical Sciences, Faculty of Chemical Technology, University of Pardubice, Pardubice, Czech Republic
veronika.dvorakova1@student.upce.cz

Summary

The aim of this work was conjugation of quantum dots (QDs) with IgG antibody molecules fixed through antigen bound on solid phase and subsequent elution of resulting conjugate. Antibody labeled with QDs can be applied for amplification of signal detected by electrochemical biosensor in routine screening of different clinically important substances such as tumor markers.

1. Introduction

Among serious cancerous diseases with high incidence in today population belongs ovarian or colorectal cancer. Development of rapid, specific and available method for detection of such cancerous diseases is the goal in today research. System which provides all these qualities is represented by ultrasensitive biosensor based on QDs conjugated with antibodies specific to target antigen. This biosensor should be able to detect very low levels of tumor markers in variety of human body fluids[1].

QDs are tiny particles of semiconductor material, usually based on selenides or sulfides of metals like cadmium or zinc, which are only a few nanometers in size. They have unique optical and electrical properties and that is reason why QDs enable to amplify measured signal of target structures[2].

New approach of conjugation of antibodies with QDs could improve biosensor's sensitivity. Our experiment consists of five main steps: covalent binding of model antigen ovalbumin (OVA) on solid phase, blocking of free carboxylic groups on solid phase, immobilization of anti-OVA IgG, conjugation of IgG with QDs and effective elution of labeled IgG (Fig. 1). Final product is detected by voltammetric method (SWV – square wave anodic stripping voltammetry) by using interface PalmSens with miniaturized screen-printed electrode (SPE). Superparamagnetic microparticles were used as solid phase for their popular qualities which are mainly easy manipulation and separation of conjugated and free QDs.

2. Experimental part

Antigen ovalbumin (OVA, Albumin from chicken egg white, Sigma-Aldrich, St. Louis, MO, USA) in amount of 50 μg and 25 μg was bound overnight at 4 °C to 1 mg of magnetic particles SiMAG-Carboxyl (1 μm, Chemicell GmbH, Berlin, Germany) in 0.1 M MES buffer pH 5.0 after 30 minutes activation by EDC (*N*-(3-dimethyl-aminopropyl)-*N*′-ethylcarbodiimide hydrochloride, Sigma-Aldrich, St. Louis, MO, USA) in combination with sulfo-NHS (*N*-hydroxysulfosuccinimide sodium salt, Sigma-Aldrich, St. Louis, MO, USA) at room temperature (RT). Amount of EDC and sulfo-NHS was used in following ratio: 7.5 mg of EDC and 1.25 mg of sulfo-NHS per 1 mg of particles. Sodium dodecylsulphate-polyacrylamide gel electrophoresis (SDS-PAGE) was used as control technique for determination of OVA immobilization efficiency. Then biofunctionalised particles were blocked by 1 M ethylenediamine (Sigma-Aldrich, St. Louis, MO, USA) or 1 M ethanolamine (Sigma-Aldrich, St. Louis, MO, USA) for 1 hour at RT. Blocking reagents were properly washed out by 0.1 M phosphate buffer pH 7.3. Subsequently immobilization of rabbit anti-OVA antibodies (Tetracore, MD, Rockville, USA) was realized.

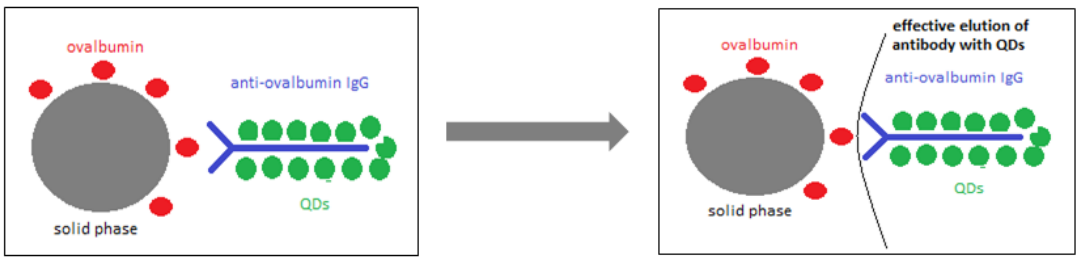

Fig. 1. **Principle of conjugation experiment**

0.5 mg of blocked magnetic particles with bound OVA was incubated with 25 μg of antibodies for 1.5 hour at RT in 0.1 M phosphate buffer pH 7.3 with 0.15 M NaCl with constant rotation. Washing of particles by using 0.1 M phosphate buffer pH 7.3 in combination with 0.1 M phosphate buffer pH 7.3 with 0.2 M NaCl followed. SDS-PAGE was also used for control of immunocomplex creation between target antigen molecules and antibodies. For conjugation of anti-OVA 2.3 μl of 8 μM QDs (CdSe/ZnS, Qdot® 565 ITK™ carboxyl quantum dots, Invitrogen, USA) were used. Overnight binding of QDs at 4 °C was carried out after 30 minutes activation of antibodies by EDC. Finally effective elution of labeled antibodies was realized by using 0.05% trifluoroacetic acid (TFA). Electrochemical detection was used as confirmatory technique for detection of our target product. Native gel electrophoresis (native PAGE) combined with measuring of fluorescence, SDS-PAGE and microscopic detection were used as supplementary detection methods.

3. Results and discussion

OVA and anti-OVA were used as model system for optimization of this experiment. Preparation of biofunctionalised magnetic particles, which is key step, was successful. OVA should be bound in monolayer which represents the best conditions for immobilization of anti-OVA. Anti-OVA are in this case ideally distributed on the particle surface for effective conjugation of QDs. We carried out conjugation of antibodies with QDs by well-known carbodiimide technique. We used very low amount of EDC (0.1–0.5 mg of EDC) to activation of amino groups of target antibodies to prevent unwanted cross-linking and aggregation of particles with antibodies and QDs. The main goal of using blocking reagents before conjugation of IgG with QDs was to prevent binding of QDs with free amino groups situated on biofunctionalised magnetic particles surface. New approach of conjugation presented in this work is based on using solid phase (in our case biofunctionalised magnetic particles) for fixing labeled antibodies which brings better and easier manipulation with whole conjugate and mainly possible separation of conjugated and unconjugated QDs which is using other conventional approaches usually complicated. For elution we applied acidic pH which allows releasing of conjugate from immunocomplex and after separation of particles with OVA using magnetic separator we obtain pure conjugate. Finally conjugate was monitored by wide range of different detection techniques from which detection by electrochemical biosensor was the most important. In this case we reached required amplification of measured signal corresponding to prepared conjugate.

4. Conclusions

We prepared conjugate formed by specific anti-OVA antibodies and CdSe/ZnS-QDs, which can be used for amplification of measured electrochemical signal. In our next work we would like to apply this protocol for preparation of conjugate with specificity against HE4 and pepsinogen, which are significant tumor markers.

This work was supported by Czech Science Foundation (project GACR P206/12/0381) and by the Ministry of Education, Youth and Sports of the Czech Republic (project CZ.1.07/2.3.00/30.0021 "Enhancement of R&D Pools of Excellence at the University of Pardubice").

REFERENCES

1. Lin J., Ju H.: Biosens. Bioelectron. *20*, 1461 (2005).
2. Samir T. M., Mansour M. M., Kazmierczak S. C., Azzazy H. M.: Nanomedicine *11*, 1755 (2012).

SIMULTANEOUS HYBRIDIZATION AND SEPARATION OF SMALL NUCLEIC ACID FRAGMENTS WITH COMBINATION CAPILLARY ISOTACHOPHORESIS AND CAPILLARY ZONE ELECTROPHORESIS

MILAN FRAŇO[a], MICHAELA GALLEE[b], JOZEF MARÁK[c], and PAVOL KOIŠ[b]

[a] *Department of Molecular Biology, Faculty of Natural Sciences, Comenius University in Bratislava, Bratislava,* [b] *Department of Organic Chemistry, Faculty of Natural Sciences, Comenius University in Bratislava, Bratislava,* [c] *Department of Analytical Chemistry, Faculty of Natural Sciences, Comenius University in Bratislava, Bratislava, Slovak Republic*
frano@fns.uniba.sk

1. Introduction

The analysis of nucleic acids (NA) is widely applied and routine in many molecular biology laboratories. NA hybridization techniques are important tools in the variety of diagnostic and biological applications, for example disease detection. However, for nucleic-acid based diagnostic applications more sensitive and faster methods are required. In the last decades microRNA (miRNA) is on the top of the clinical diagnostics research. The miRNA is a type of short (22 nt) non-coding ribonucleic acid molecule found in eukaryotic and some prokaryotic genome. miRNAs are a group of post-transcriptional regulators at the level of mRNA. The human genome may encode over 1100 miRNAs. miRNAs are estimated to regulate at least 30% of all protein coding genes. The miRNAs are involved in most major biological processes in cell like differentiation, proliferation, apoptosis and many others. Except miRNAs role in the normal functioning of cells, so miRNAs has been associated with many human diseases, for example cancer (oncomiRs). miRNAs are aberrantly expressed in cancer and different types of cancer have different expression profiles of miRNAs compared with normal cells, which may ultimately lead to a novel cancer-specific and cancer type-selective treatment and diagnostic strategy[1,2]. New ways for miRNAs quantification are methods based on capillary electrophoresis (CE) techniques, especially capillary isotachophoresis (ITP) and capillary zone electrophoresis (CZE). The ITP is a modern analytical technique which allows subnanomolar analysis and huge preconcentration (approx. 1 million times) of miRNA samples. We are proposing a combination of ITP with CZE to the analysis of small fragments of nucleic acid by principle hybridization target with the oligonucleotides detection probe by UV-VIS detection.

2. Experimental

2.1. Materials and buffers

For hybridization study we used DNA oligonucleotides synthesized in our laboratory (targets-probes) with no secondary or secondary (hairpin) structure. All DNA oligonucleotides used in hybridization study were full complementary. We used the concentration range of oligonucleotides from 1 pM to 100 nM. For the ITP-CZE experiments, we used 2-amino-2-hydroxymethyl-propane-1,3-diol based electrolytes[3] with $MgCl_2$, and 0,1% hydroxyethyl cellulose (HEC) and 0,2–1 % hydroxymethyl ethyl cellulose (MHEC). We used HEC for suppression of electroosmotic flow (EOS), MHEC such as separation sieving matrix, and equimolar concentrations of Mg^{2+} to promote of hybridization. All chemicals were obtained from Sigma-Aldrich, and all solutions were prepared in ultrapure millipore water, and stored at 4 °C. Synthesized oligonucleotides were stored at –20 °C in nuclease free deionized water.

2.2. ITP-CZE experimental model

For our experiments, we used ITP-CZE (Villa Labeco) with 180 mm long, and 80 μm inner diameter separation capillary with double-jacket water cooling, and with UV-VIS detector. Measurements of ITP-CZE parameters were performed under a 100 μA constant current.

3. Results and discussion

We experimentally demonstrate the hybridization and separation models for on-line combinations ITP-CZE with used the model DNA oligonucleotides. We are able to separate model DNA non-complementary oligonucleotides with an identical length, but the different base composition (Fig. 1). For demonstrated model hybridization assay we used model self-hybridization DNA oligonucleotides with melting points 61 °C (Fig. 2).

Efficiency of hybridization of oligonucleotides depends mainly on their structure and concentration, temperature and salt concentration. Addition of different additives to electrolytes, for example HEC, MHEC, acrylamide, improved the separation of single-stranded (ss) and double-stranded (ds) DNA forms. The high temperature can be reached in ITP-CZE columns during the separation process what can have a destabilizing effect on the duplex formation. This can be suppressed by using active cooling of capillaries. Optimization of the driving

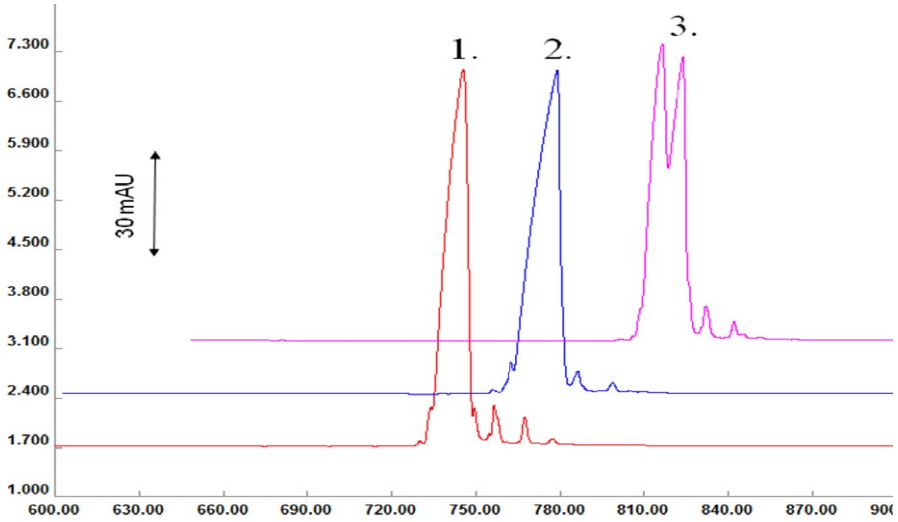

Fig. 1. **Initial demonstration of the ITP–CZE separations of model non-complementary oligonucleotides with addition of 0.2% MHEC to the electrolytes, (1) oligo-110036 (2) oligo-110037 (3) separation of oligo-110036 and 110037.** UV-VIS detection at λ = 260 nm, shift in X and Y axis

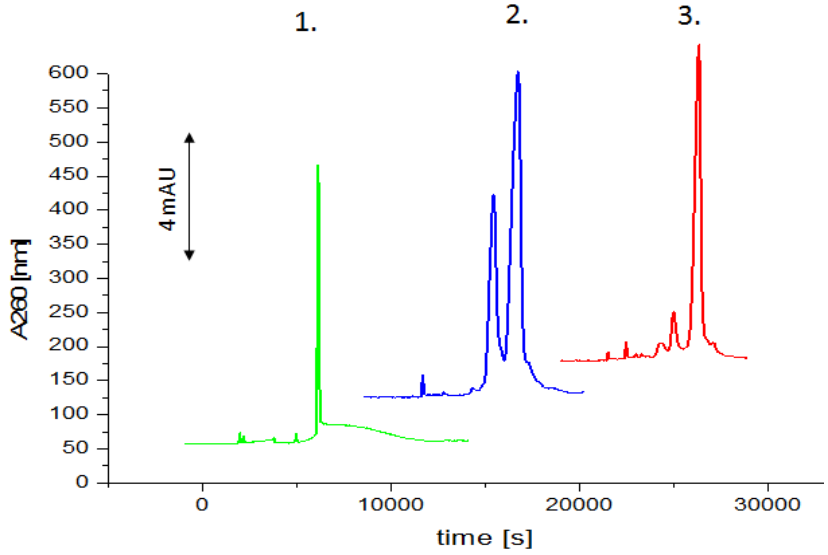

Fig. 2. **Initial demonstration of the ITP-CZE hybridization assay of model self-hybridization oligonucleotides with addition of 0.2% MHEC, (1) oligo-11003X (ss- denaturation) (2) oligo-11003X (ss and ds-partial denaturation) (3) oligo-11003X (ds-hybridization).** UV-VIS detection at λ = 260 nm, shift in X and Y axis

current conditions and the composition of electrolytes provided clearly separated ss- and ds-DNA forms what is documented in Fig. 1 and Fig. 2.

4. Conclusions

This paper shows the possibility of analyzing more complex samples (e.g. nucleic acids) with ITP-CZE. It was found, this technique is suitable for the study of hybridization of model short fragment of nucleic acids on the very low detection limit. Our experimental method delivers results in less than 20 minutes with the limit of detection (LOD) of 15 pM. We analyzed hybridization and separation of short DNA oligonucleotides that had similar sequences to mature miRNAs. The control of temperature

was a critical step for the preservation of the double-stranded structure of DNA hybrids in our experiment. This ITP-CZE combination provides sufficient selectivity and sensitivity for nucleic acid quantifications with minimal financial requirements. Improving this method can lead to clinical applications of miRNA as ideal biomarker for cancer diagnostic assay.

This work was carried out with the financial support from the VEGA grants Nos. 1/0962/12, 1/1305/12 and Comenius University Grant No. UK/548/2013.

REFERENCES

1. Brandi N., et al.: J. Biochem. *148*, 381 (2010).
2. Wang Z., Yang B.: Springer. 2010**,** p. 408.
3. Schoch B. R., Ronaghi M., Santiago J. G.: Lab Chip *9*, 2145 (2009).

APLICATION OF FLUORESCENT CHEMOSENSOR FOR ENZYMATIC ANALYSIS

MICHAELA GALLEE[a], MILAN FRAŇO[b], and PAVOL KOIŠ[a]

[a] *Comenius University in Bratislava, Faculty of Natural Sciences, Department of Organic Chemistry, Bratislava,*
[b] *Comenius University in Bratislava, Faculty of Natural Sciences, Department of Molecular Biology, Bratislava, Slovak Republic*
michaela.gallee@gmail.com

Summary

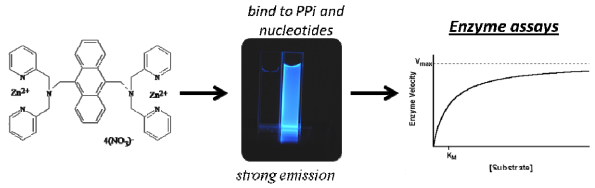

1. Introduction

Over the last years the selective detection of the anion pyrophosphate (PPi) seems very required. PPi is a biologically important target, mainly is a component of all nucleotides, which are a major component of DNA and RNA. Many a time nucleotides or nucleosides are results of enzymatic reactions, especially reactions, which are catalyzed by kinases or phosphatases and glycosyltransferases. The binuclear zinc complex-based fluorescent probe for detection PPi appears useful[1–3]. This chemosensor strongly bind to PPi and emit increased fluorescence intensity. Fluorescent chemosensors have multiple advantages, primarily high sensitivity, low cost, easy of application, and versatility. This work is focused on synthesis of 9,10-bis[(2,2-dipicolylamino)methyl] anthracene-zinc complex, its fluorescent properties and applications.

2. Synthesis of the Zinc complex 1

Fluorescent chemosensor 9,10-bis[(2,2'-dipicolyl-amino)methyl]anthracene-zinc complex **1** was prepared by three-step synthesis (Fig. 1). The first step was synthesis of 9,10-bis(chloromethyl)anthracene by chloromethylation of anthracene[4]. The second step was nucleofilic substitution of 9,10-bis(chloromethyl) anthracene with 2,2'-dipicolylamine to provide 9,10-bis [(2,2'-dipicolylamino)methyl]anthracene. The chemosensor **1** was prepared by complex-forming reaction of 9,10-bis [(2,2'-dipicolylamino)methyl]anthracene with $Zn(NO_3)_2$ (ref.[2]). Fluorescence spectra were recorded on a Tecan Safire 2 Microplate Reader.

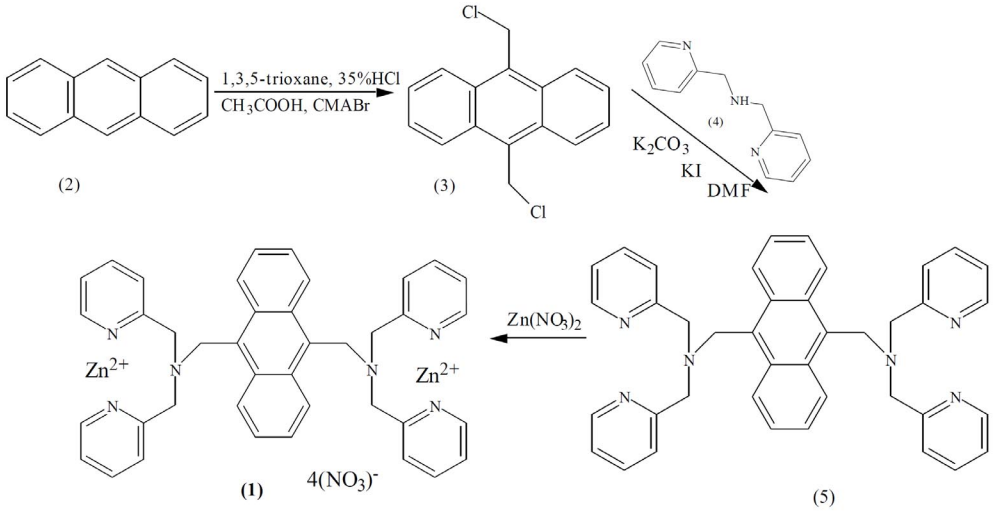

Fig. 1. **Synthesis of fluorescent chemosensor 1**

3. Results and discussion

Prepared fluorescent probe **1** was tested in the presence of various molecules, which are common parts of the enzymatic reactions. A remarkably large fluorescence enhancement was observed when PPi was added to the neutral aqueous solution of **1** (Fig. 2, 3).

Glycosylated nucleotides are typical substrates for glycosyltransferases, whereas non-glycosylated nucleotides are products of these enzymes. For this reason, we tested effect of UDP, UDP-glucose and GDP, GDP-mannose on fluorescent of chemosensor **1**. We found that chemosensor **1** is able to recognize and bind free UDP and analogical GDP and markedly increase of fluorescent intensity. On the other hand, glycosylated nucleotides don´t have the same effect on fluorescent intensity, (Fig. 4).

Finally, we applied receptor **1** for determination of activity phosphatidyl-manosyltransferase and flavonol-3-*O*-glucosylransferase. We found that chemosensor is able to recognize and bind UDP and GDP in a dynamic system such as enzymatic reaction (data not shown).

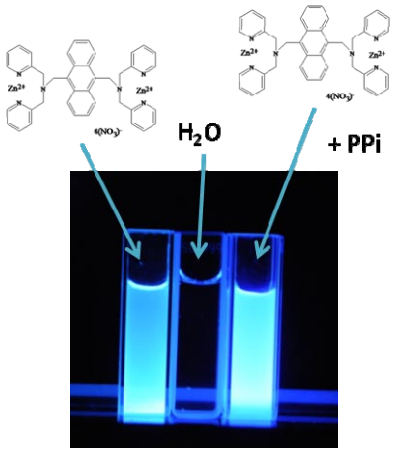

Fig. 2. **Photograph of the increased emission of the receptor 1 in the presence of pyrophosphate (right); the solution of 1 only (left); only water (middle)**

4. Conclusions

Many chemosensors for cations are known, the spectrum of chemosensors for anions is much poorer, despite their important role in biology, clinical diagnostics, and environmental monitoring. This paper shows the possibility of fluorescent analyzing biological anions, concretely pyrophosphate. Prepared binuclear zinc complex based fluorescent probe **1** selectively senses PPi and nucleotides with a large fluorescence enhancement, whereas no detectable fluorescence change was induced by monophosphate species and various other anions. Fluorescence of **1** is greatly intensified by the UDP and GDP, whereas the glycosylated UDP-glucose and GDP-mannose does not induce the fluorescence change. To our knowledge we use this chemosensor for analysis of enzymatic activity manosyltransferase and *O*-glucosyltransferase. The detailed study of prepared chemosensor

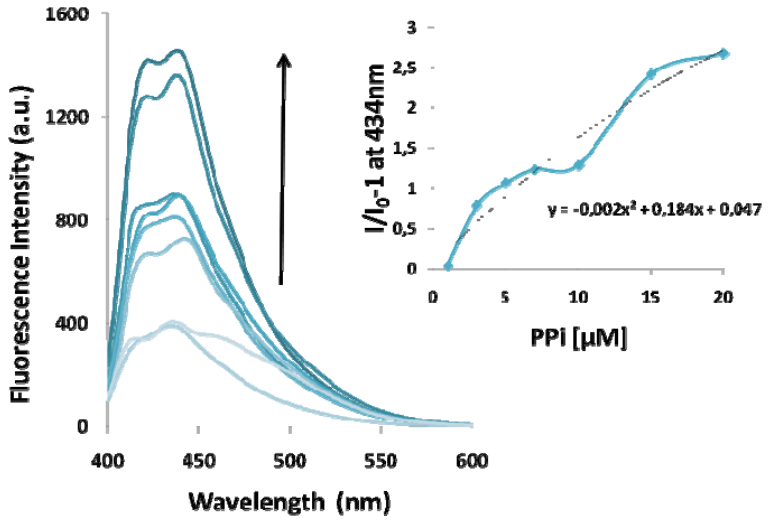

Fig. 3. **Fluorescent spectral change of receptor 1 [5 μM] upon the addition of PPi:** [PPi] = 0, 5, 10, 15, 20 μM; (λ_{ex} = 380 nm, λ_{em} = 400–600 nm). (Inset) Fluorescent titration curve of **1** [5 μM] upon addition of PPi: [PPi] = 0, 5, 10, 15, 20 μM (λ_{ex} = 380 nm, λ_{em} = 434 nm)

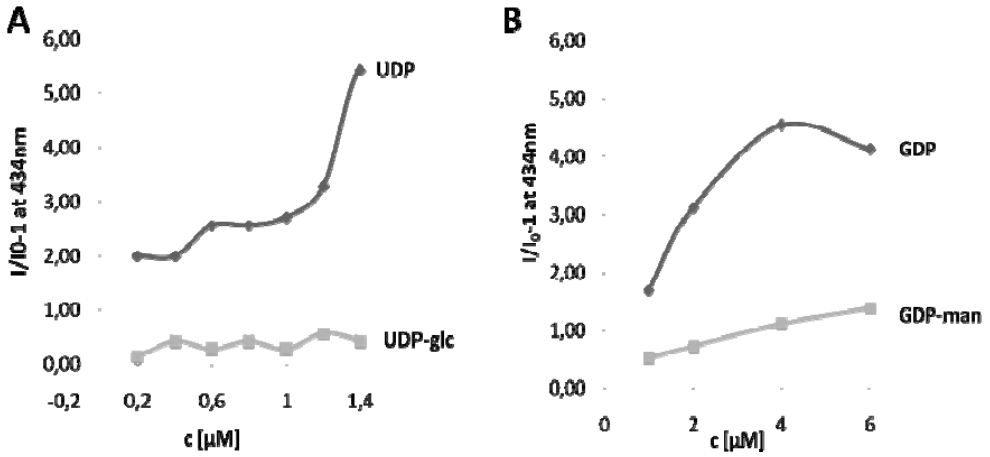

Fig. 4. **(A) Fluorescent titration curves of 1 [1μM] upon addition of UDP and UDP-glucose:** [UDP;UDP-glc]: 0,2; 0,4; 0,6; 0,8; 1; 1,2; 1,4 μM; **(B) Fluorescent titration curves of 1 [2 μM] upon addition of GDP and GDP-mannose** [GDP; GDP-man]= 1, 2, 4, 6 μM; (λ_{ex} = 380 nm, λ_{em} = 437 nm)

is oriented to the development of sensitive and fast real-time method for determination of specific enzymes.

This work was carried out with the financial support from the VEGA grants Nos. 1/0962/12.

REFERENCES

1. Ojida A., Hamachi I.: Bull. Chem. Soc. Jpn. *79*, 35 (2006).
2. Ojida A., Mito-oka Y., Inoue M., Hamachi I.: J. Am. Chem. Soc. *124,* 6256 (2002).
3. Wongkongkatep J., Miyahara Y., Ojida A., Hamachi I.: Angew. Chem. Int. Ed. *45*, 665 (2006).
4. Altava B., Burguete M. I., Escuder B., Luis S. V., García-España E., Muñoz M. C.: Tetrahedron. *53*, 2629 (1997).

IMPROVING THE REPEATABILITY OF SAMPLING PROCEDURES FOR EXHALED BREATH CONDENSATE ANALYSIS

MICHAL GREGUŠ[a,b], PETR KUBÁŇ[b], and FRANTIŠEK FORET[b]

[a] *Department of Chemistry, Masaryk University, Brno,*
[b] *Group of Bioanalytical Instrumentation, CEITEC MU, Brno Czech Republic*
gregus@mail.muni.cz

Summary

A miniature sampler for exhaled breath condensate (EBC) collection was constructed and the repepatability of the collection procedure was studied. The samples were analyzed by CE-C4D home-made instrument. To improve the repeatability of the EBC collection, first the collection tubes, straws and vials require cleanup to remove unwanted interferents. Second, the breathing pattern should be kept uniform. We demonstrate that by adopting these measures, repeatability can be improved from 21.4–186.5 % RSD (non-standardized sampling) to 3.6–80.3 % RSD (standardized sampling) and is comparable than with the commercial device (6.6–75.6 % RSD).

1. Introduction

Exhaled breath condensate (EBC) is a promising diagnostic body fluid that can be applied in lung respiratory research and diagnosis. EBC is obtained by cooling and condensation of exhaled air (non-invasive sampling). Its main components are inorganic ions, small organic molecules and proteins. The utility of EBC in clinical practice has however been hampered by the low repeatability, lack of standardization of both the collection equipment and the breathing techniques, resulting in large spread of the clinical data. In this work we have attempted to improve the repeatability of the sampling by (*i*) designing procedures for proper cleanup and maintenance of the collection devices and by (*ii*) standardization of breathing pattern.

2. Experimental

2.1. Electrophoretic and detection system, injection, electrolytes

A purpose-built CE instrument with C4D detector[1] was employed for all electrophoretic separations. The separation voltages of –15 kV and +15 kV (for cations and anions, respectively) were provided by a high voltage power supply unit (Spellman CZE2000R Start Spellman, Pulborough, UK). The separation capillaries were fused-silica capillaries (50 μm I.D., 360 μm O.D., 44/20 cm total/effective length, Polymicro Technologies, Phoenix, AZ, USA). Standards and EBC samples were injected hydrodynamically at 15 cm for 60 s. The optimized BGE composition[2] used in this work was 20 mmol L^{-1} MES, 20 mmol L^{-1} HIS, 30 μmol L^{-1} CTAB and 2 mmol L^{-1} 18-crown-6 at pH 6 and was used for separation of both anions and cations only by reversing the voltage polarity.

2.2. Samplers for EBC collection

Two types of EBC samplers were used and tested and are depicted in Fig. 1. Laboratory-made sampling device was constructed from a 2 ml polypropylene syringe and a cooled (–20 °C) aluminium cylinder to achieve with maximum simplicity and minimal cost (unit price is about 1 CZK, excl. cooling cylinder). For comparison a commercially available device (R-Tube, www.r-tube.com) was used (unit price is about 500–700 CZK, excl. cooling cylinder). The laboratory-made device was constructed so that it would facilitate the sampling of a single exhaled breath.

3. Results and discussion

To improve the repeatability of the sampling, we have optimized the cleanup and maintenance procedure for the laboratory-made sampler and also standardized the breathing patterns. The EBC was analyzed by CE-C4D and the peaks were identified by spiking with standards.

3.1. Typical electropherogram and identification of peaks

See Fig. 2.

3.2. Cleaning procedures

As a first procedure to improve sampling repeatability, new syringes were washed with DI water and immersed into a large beaker with DI water for 24 hours and sealed to prevent absorption of the components for the laboratory air. After 24 hours, syringes were flushed with deionized water and dried up by clean, dry air. The same procedure was also applied for collection vials (0.25ml volume) and sampling straws. Sealed, pre-cleaned R-tube samplers were used as supplied from the manufacturer. Cleaned vials were also used for storage of EBC collected by R-Tube. This cleaning procedure resulted in significantly improved repeatability of the measured ions

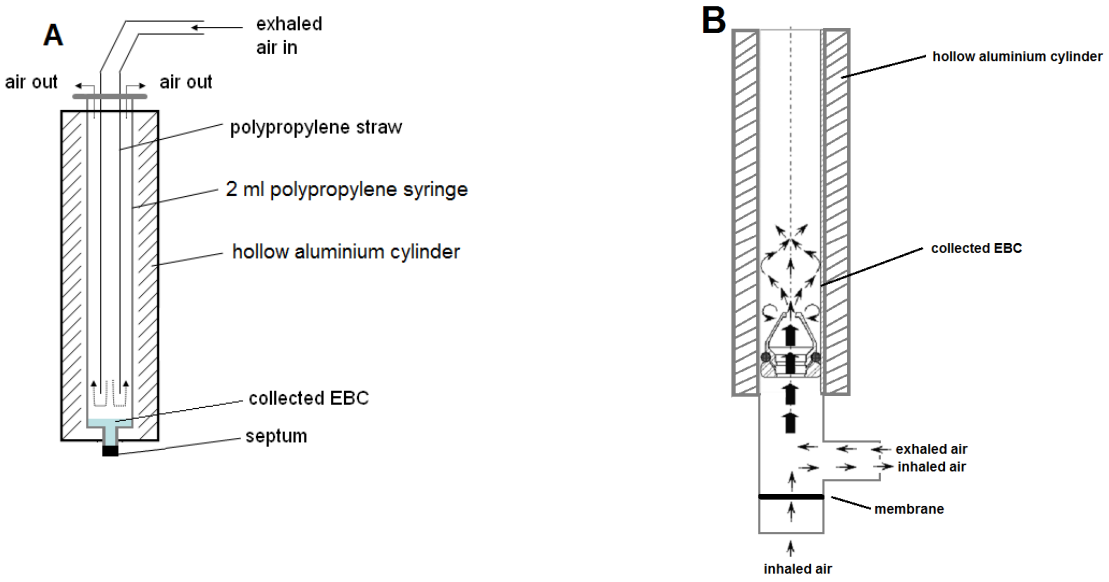

Fig. 1. **Schematic view of the laboratory-made EBC sampler (A) and R-Tube (B) used in the studies**

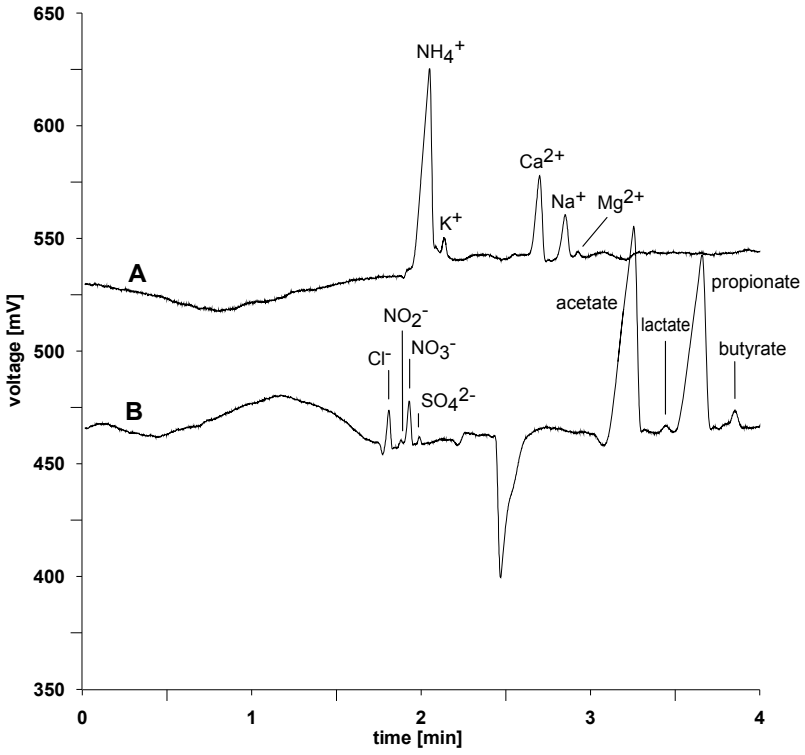

Fig. 2. **Analysis of EBC. Electropherogram of determination of cations (line A) and anions (line B).** CE conditions are the same as in part 2.1.

in the samples. For comparison, non-standardized sampling was used, in which new syringes, vials and straws were tested without any cleanup procedure.

3.3. Breathing patterns

Secondly, the breathing patterns were standardized. Every collected EBC sample was obtained upon three deep

exhales of the same length (eight seconds). This corresponded to the total exhaled volume of 9.6 L (3 × 3.2 L) and the approximate volume of EBC was 60 μL. Prior to collection, the volunteers were asked to calmly breathe for 5 minutes. To maintain similar breathing pattern when using R-tube device, every collected EBC sample was obtained upon three deep exhales of the same length (four seconds, due to the larger ID of the collection tube). The exhaled volume and the collected EBC volumes were thus identical. In non-standardized collection, there was no control of the breathing pattern, exhaled volume and number of exhalations. The results are shown in Fig. 3.

4. Conclusions

A laboratory-made sampler was optimized for analysis of ionic content of EBC. The repeatability of the collection procedure was studied and two important procedures are suggested to improve the overall collection repeatability. First the collection tubes, straws and vials require cleanup to remove unwanted interferents. Second, the breathing pattern should be kept uniform and possibly the total exhaled volume should be the same. We demonstrate that by adopting these measures, repeatability can be improved from 21.4–186.5 % RSD (non-standardized sampling) to 3.6–80.3 % RSD (standardized sampling) and is comparable than with the commercial device (6.6–75.6 % for R-tube). Further, the developed laboratory-made sampler is significantly cheaper and allows collecting the EBC from a single breath. The research and characterization of a single breath is in progress.

The authors acknowledge the financial support from the Grant Agency of the Czech Republic (Grant No. P206/13/21919S). Part of the work was realized in CEITEC – Central European Institute of Technology 355 with research infrastructure supported by the project CZ.1.05/1.1.00/02.0068 356 financed from European Regional Development Fund.

REFERENCES

1. Zhang L., Khaloo S. S., Kubáň P., Hauser P. C.: Meas. Sci. Technol. *17*, 3317 (2006).
2. Kubáň P., Kobrin E. G., Kaljurand M.: J. Chromatogr., A *1267*, 587 (2012).

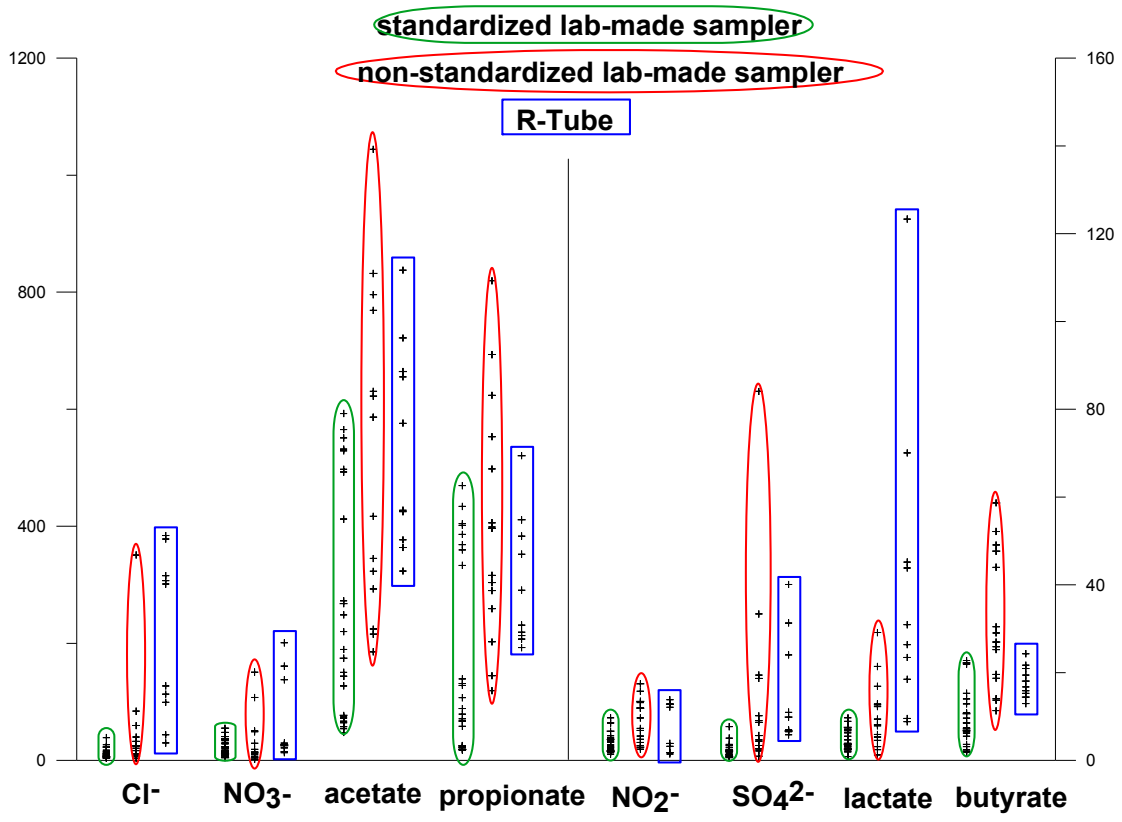

Fig. 3. **Range comparison of values of peaks areas obtained by standardized/non-standardized lab-made sampler and R-Tube**

A PILOT STUDY ON SEPARATION OF NEW DRUGS FOR TREATMENT OF LEUKEMIA BY CAPILLARY ZONE ELECTROPHORESIS

JANA HORSKÁ, PAVLÍNA GINTEROVÁ, JURAJ ŠEVČÍK, and JAN PETR

Regional Centre of Advanced Technologies and Materials – Department of Analytical Chemistry and Department of Analytical Chemistry, Faculty of Science, Palacký University in Olomouc, Olomouc, Czech Republic
januli.hor@centrum.cz

Summary

Imatinib, bosutinib, dasatinib, pazopanib, erlotinib, canertinib and vatalanib are new important anticancer drugs, especially for treatment chronic myeloid leukemia. All of these substances without imatinib are being tested in clinical trials with very promising results. Imatinib is the standard first-line therapy at chronic myeloid leukemia for almost 10 years. The aim of our work was to develop the fastest separation of all these drugs in one run. According to the structure of drugs, capillary zone electrophoresis was chosen. The separation was performed with a background electrolyte containing 100 mM phosphoric acid, adjusted by sodium hydroxide to pH 2.75.

1. Introduction

Imatinib, bosutinib, dasatinib, pazopanib, erlotinib, canertinib and vatalanib (chemical structures are shown in Fig. 1) are newly developed drugs that may successfully be used for the treatment of patients with chronic myeloid leukemia (CML), gastrointestinal stromal tumors (GIST) and other disaeses[1]. CML, the general term for cancers of the blood, is a clonal myeloproliferative disorder of the hematopoietic stem cell, which presents an acquired cytogenetic abnormality, the Philadelphia chromosome (Ph). The Ph, which occurs as a result of reciprocal

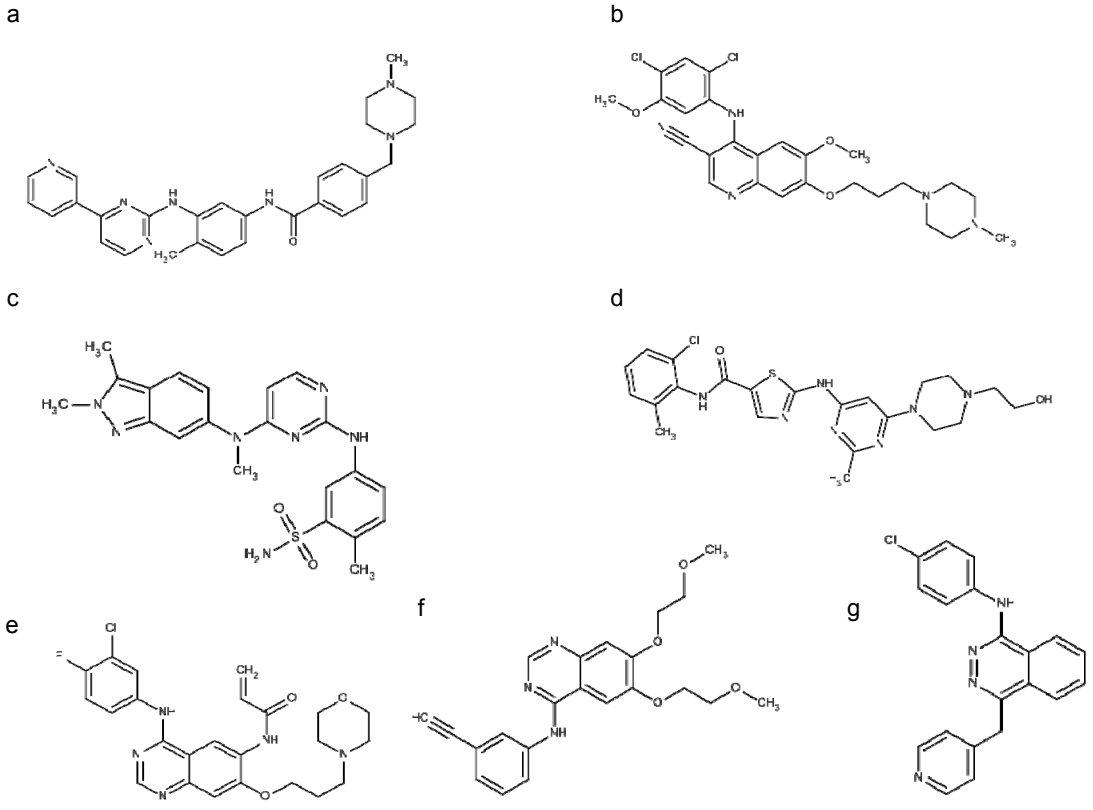

Fig. 1. **Structures of anticancer drugs.** a, imatinib; b, bosutinib; c, pazopanib; d, dasatinib; e, erlotinib; f, canertinib; g, vatalanib

translocation between chromosomes 9 and 22, produces a Brc-Abl gene, which encodes a protein with elevated tyrosine kinase activity which is responsible for the disease pathogenesis[1,2]. All of these drugs are classified as inhibitors of tyrosine kinases[2].

Imatinib (also known as the Gleevec) is the most studied substance of these drugs. Imatinib is the standard first-line therapy at any of the three stages CML (blast crisis, accelerated phase, or in chronic phase after failure of interferon-α therapy) for almost 10 years. Imatinib is a rationally designed oral signal transduction inhibitor that specifically targets several protein tyrosine kinases, Abl, Arg (*Abl*-related gene), the stem-cell factor receptor (c-KIT), the platelet-derived growth factor receptor (PDGF-R), and their oncogenic forms, most notably Bcr-Abl (ref.[3–5]).

In this study, the capillary electrophoresis (CE) method with UV detection was used to separate the anticancer drugs. CE is a powerful analytical separation technique, which is popular in analysis of various drugs in biological samples, pharmaceutical preparations and environmental matrices[6]. The main advantages of CE are the fast and precise separations with lower cost, which includes low solvent, electrolyte and sample consumption[7].

2. Experimental

2.1. Chemicals and reagents

Electrolyte components: phosphoric acid and sodium hydroxide were purchased from Sigma Aldrich (St. Louis, MO, USA). The drugs standards, imatinib, bosutinib, dasatinib, pazopanib, erlotinib, canertinib and vatalanib were bought from the LC Laboratories (Woburn, USA). Bosutinib was bought also from Sigma Aldrich. Stock standard solutions of all drugs were prepared at a concentration of 1 mg mL^{-1} in deionized water and methanol and were appropriately diluted in deionized water for preparation working solutions at concentration of 10 μg mL^{-1}. All solutions were stored under refrigeration at –20 °C in the absence of light.

2.2. Apparatus

All the separations were performed on the capillary electrophoresis system HP 3DCE (Agilent Technologies, Waldbronn, Germany) with the diode array detector; the detection wavelength was 214 nm. Uncoated fused silica capillaries (MicroSolv Technology, NJ, USA) with 50 μm i.d., total capillary length 33.0 cm, effective length 24.5 cm, were used in these experiments. The capillary cassette was thermostated at 25°C. Before each analysis the capillary was rinsed with 0.1 mol L^{-1} NaOH (2 min), deionized water (3 min), and then with the buffer (5 min).

3. Results and discussion

First, dissociation constants (pKa) of the studied analytes were estimated using the MarvinSketch software. According to the calculated pKa values, it was found that all studied analytes are positively charged at low pH values. For this reason, the first experiments were tested in acidic pH (2.0–3.0). As a starting buffer, phosphate buffer at concentration of 100 mM was chosen. Then, the effect

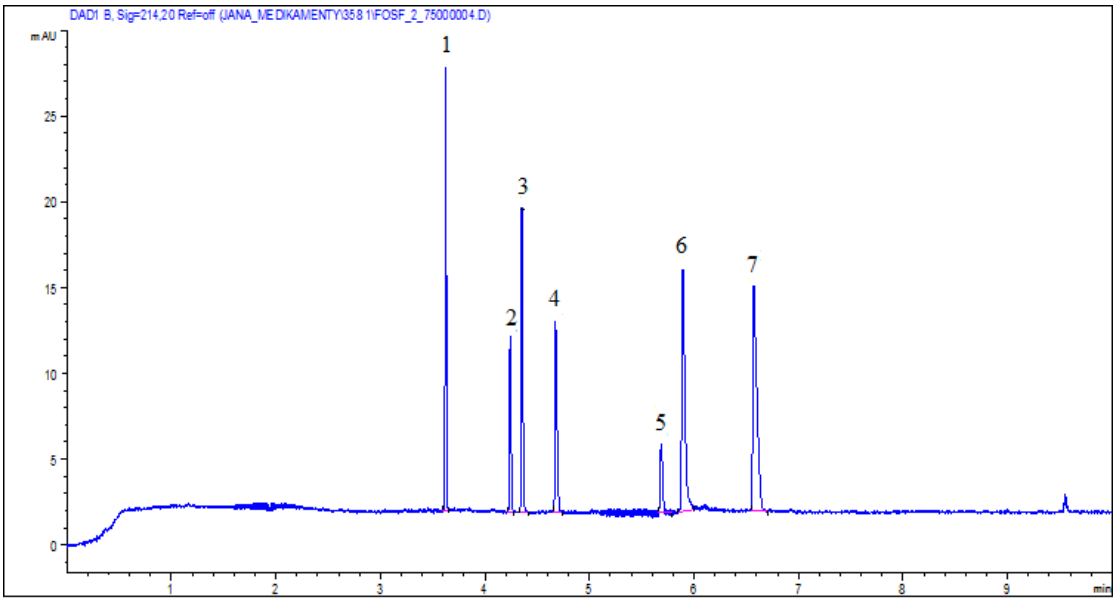

Fig. 2. **Electropherogram of analyzed drugs.** 1, vatalanib; 2, imatinib; 3, bosutinib; 4, canertinib; 5, dasatinib; 6, pazopanib; 7, erlotinib

of pH was evaluated with sodium as counter-ions. The pH of 2.0, 2.25, 2.5, 2.75 and 3.0 was tested. Only partial separation provided the pH values of 2.0, 2.25, 2.5 and 3.0. The best separation was achieved at the pH of 2.75 (Fig. 2). All the analytes were separated in 8 minutes with following migration order: vatalanib, imatinib, bosutinib, canertinib, dasatinib, pazopanib and erlotinib. Relative standard deviations of migration times did not exceed 0.9 %.

4. Conclusion

In this study, an easy and fast CZE method for separation of anticancer drugs was developed. As a consequence, we believe that the proposed method can be an interesting alternative for the determination of these drugs by liquid chromatography.

The financial support of the research by the Operational Program Research and Development for Innovations – European Regional Development Fund (project CZ.1.05/2.1.00/03.0058) and the Operational Program Education for Competitiveness – European Social Fund (project CZ.1.07/2.3.00/20.0018), the Grant Agency of the Czech Republic (project P206/12/1150), and the Student project UP Olomouc PrF_2013_030 is gratefully acknowledged.

REFERENCES

1. Ajimura T. O., Borges K. B., Ferreira A. F., Gastro F. A., Gaitani C. M.: Electrophoresis *32*, 1885 (2011).
2. Khoury H. J., Cortes J. E., Kantarjian H. M., Gambacorti-Passerini C., Baccarani M., Dong-Wook K., Zaritskey A., Countouriotis A., Besson N., Leip E., Kelly V., Brümmendorf T. H.: *Blood 119*, 3403 (2012).
3. Li J., Huang Y., Huang L., Ye L., Zhou Z., Xiang G., Xu L.: J. Pharm. Biomed. Anal. *70*, 7026 (2012).
4. Mumprecht S., Matter M., Pavelic V., Ochsenbein A. F.: *Blood 85*, 3406 (2006).
5. Flores J. R., Berzas J. J., Castaneda G., Rodriguez N.: J. Chromatogr., B *794*, 381 (2003).
6. Alia I., Haquea A., Wania W. A., Saleema K., Zaabib M. A.: Biomed. Chromatogr. *27*, 1296 (2013).
7. Rosemana D. S., Weinbergerb R.: J. Pharm. Biomed. Anal. *85*, 67 (2013).

INFLUENCE OF P53 MUTATION ON RESPONSE OF HUMAN GLIOBLASTOMA TO CYTOSTATIC TREATMENT

HRONEŠOVÁ L.[a], HOLACKÁ K.[a], POLÁŠKOVÁ A.[b], ADÁMIK M.[b], NAVRÁTILOVÁ L.[b], TICHÝ V.[b], HELMA R.[b], BALLOVÁ Ľ.[c], BUSOVA M.[d], BAŽANTOVÁ P.[e], FOJTA M.[b], and BRÁZDOVÁ M.[a,b]

[a] University of Veterinary and Pharmaceutical Sciences Brno, Faculty of Pharmacy, Department of Chemical Drugs, Brno, [b] Institute of Biophysics, v. v. i., Brno, [c] University of Veterinary and Pharmaceutical Sciences Brno, Faculty of Pharmacy, Department of Natural Drugs, Brno, [d] University of Veterinary and Pharmaceutical Sciences Brno, Faculty of Veterinary Hygiene and Ecology, Department of Biochemistry, Biophysics and Chemistry, Brno, [e] University of Ostrava, Faculty of Nature Science, Department of Biology and Ecology, Ostrava, Czech Republic

1. Introduction

Tumor suppressor p53 protein (wtp53) is a transcription factor regulating cell response to cellular and genotoxic stress. Wtp53 function is based on sequence specific interactions with DNA sequences (p53CON) in gene promoters responsible for progression of cell cycle, apoptosis and DNA repair. Mutation in *TP53* gene occurs in about 50 % of cancer cases. Expression of mutant p53 proteins is associated with increased cancer resistance to chemo- and radiotherapy and tumor progression. Mutant p53 protein pro-oncogenic functions are connected to mutp53 conformation, inability to regulate wtp53 target genes, ability to regulate pro-oncogenic mutp53 target genes and blocking of tumor suppressor functions of family members -p63 and p73. Wtp53 conformation is dependent on presence of zinc ion, as an important cofactor of p53 structure. Interestingly, many of mutant p53 proteins contain destabilized protein conformation and are prone to loss of zinc ion. One direction of novel antitumor therapies is focused on p53 reactivation. Recently it was shown that zinc can re-established chemosensitivity in breast cancer cell with R175H mutant p53. The mechanism of reactivation is still not fully understood[1]. In our work we concentrated on investigating of zinc role in mutant p53 biochemistry of glioblastoma cell lines Onda 10, Onda 11 and U251.

2. Experimental

Glioblatoma cell lines U87, Onda 10, Onda 11 and U251 (expressing wtp53, G245S, R273C and 273H) were cultivated and treated with cisplatin or doxorubicin and supplemented by $ZnCl_2$ as described in ref.[1–3]. Colony assay, western-blotting analysis was described in ref.[1–3].

3. Results and discussion

To evaluate whether zinc could affect p53 mutant pro-oncogenic function, we first analyzed the effect of zinc ions on long term survival of glioblastoma cell lines expressing different mutant p53 proteins (G245S, R273C

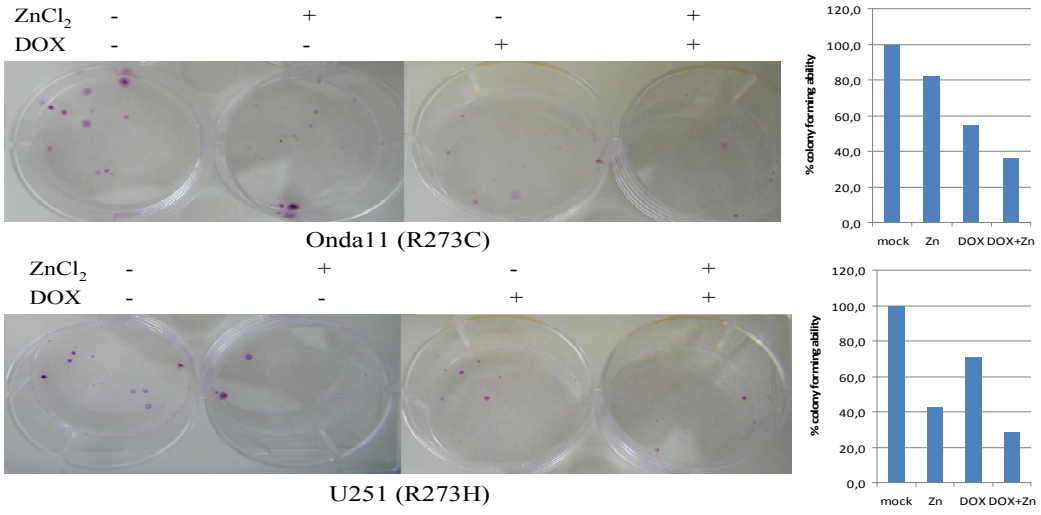

Fig. 1. **Colony forming assay, cell survival after zinc and doxorubicin treatment**

and R273H) in response to doxorubicin and cisplatin treatments. We observed significant enhancement of cell death in U251 and Onda11 cell lines after doxorubicin treatment followed zinc supplementation as shown by quantization of colony assays (Fig. 1). This finding is in agreement with previously observations done with breast cancer cell line expressing R175H (ref.[1]) and suggests that zinc supplementation might affect anti-tumor drug treatment of mutant p53 expressing cell lines. We next addressed the question of whether mutant p53 is stabilized after drug treatment in glioblastoma cell lines. We observed significant induction of p53 protein expression after cisplatin, 5-FU or doxorubicin treatment in all three glioblastoma cell lines, interestingly each cell line reacts uniquely (Fig. 2). Mutant p53 stabilization was observed in U251 by all used drugs (the best response was observed with 5-FU), in the case of Onda11 the best inducing agent was doxorubicin and for Onda10 we observed only weak activation after 5-FU and doxorubicin treatment.

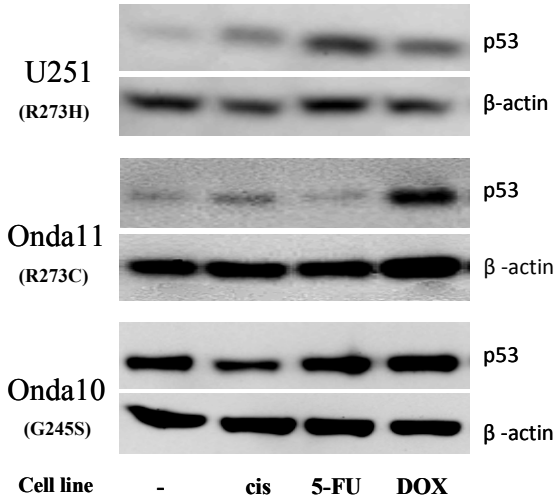

Fig. 2. **p53 analysis after drug treatment**

To determine effect of zinc supplementation on cytotoxicity of tested anticancer drugs we have used MTT assay and the results showed, that zinc enhanced cytotoxicity mainly for doxorubicin treatment. Finally we investigated the effect of zinc ion on p53-DNA interaction *in vitro* and in cells by EMSA and luciferase reporter assay. In agreement with our previous finding[4] we observed using EMSA that zinc ion inhibits binding of purified p53 proteins, zinc inhibition is reversible and can be restored by excess of EDTA or DTT. Interestingly, zinc treatment on cells did not affect p53 binding to DNA as was observed by lucifierase assay. Moreover we observed activation of p53-DNA binding activity by zinc supplementation. So far we were not successful in reactivating of p53-DNA specific activity of studied purified mutant p53 proteins but experiments with mutant p53 proteins directly prepared from glioblastoma cells are still ongoing.

4. Conclusions

Zinc has a crucial role in biology of p53. Our results show that zinc supplementation might affect anti-tumor drug treatment of mutant p53 expression cell lines U251, Onda11 and Onda10.

This study was supported by the IGA VFU Brno 103/2013/FaF, by the Czech Science Foundation 13-36108S and SGS07/PrF/2013 for P.B.

REFERENCES

1. Puca R., Nardinocchi L., Porru M., Simon A. J., et al.: Cell Cycle *10*, 1679 (2011).
2. Brazdova M., Navratilova N., Tichy V., Nemcova K., et al.: PloS One *8*, e59567 (2013).
3. Brazdova M., Quante T., Togel L., Walter K., et al.: Nucleic Acids Res. *37*, 1486 (2009).
4. Palecek E., Brazdova M., Brazda V., Palecek J., et al.: FEBS J. *268*, 573 (2001).

DETERMINATION OF ALIPHATIC AND AROMATIC CARBOXYLIC ACIDS IN DIFFERENT SAMPLES BY ION-EXCLUSION CHROMATOGRAPHY

IVETA HUKELOVÁ, ĽUDOVÍT SCHREIBER, and RADOSLAV HALKO

Department of Analytical Chemistry, Faculty of Natural Sciences, Comenius University in Bratislava, Bratislava, Slovakia
hukelova@fns.uniba.sk

Summary

The aim of this paper was developed a simple liquid chromatography method for determination organic acids in various sample matrixes. For this purpose, ion-exclusion chromatography (IEC) was used and the organic acids were determinate in human urine sample and wine sample.

1. Introduction

Separation, identification and quantitative analysis of aliphatic and aromatic acids are important due to their widespread presence in the environment and the use of both in medicine, agriculture and industry.

Free form aliphatic acids are found in various fruits e.g. malic acid in apples, citric acid in citrus fruits or tartaric, lactic and malic acids in grapes which concentration is necessary to know in winemaking. In the food industry are used as preservatives, for example benzoic acid as the sodium salt, which has the characteristics of an inhibitor for microorganisms. Carboxylic acids also serve as indicators of certain diseases, when their higher concentration e.g. in urine evokes a metabolic disorder called organic aciduria, which belongs to the hereditary metabolic disorders. The best known acidurias are propionic, glutaric, methylmalonic and pyroglutaric acid. Determination of carboxylic acids is very important for patients with diabetes, kidney disease and other metabolic disorders[1–3].

2. Experimental

2.1. Chemicals

All analytical standard-grade organic acids were obtained from Merck (Darmstadt, Germany) as the methanol (< 99% (v/v) for liquid chromatography). Stock standard solutions were obtained by dissolution of the acids in Simplicity water or methanol. The Simplicity water was purified by passage through a Simplicity® Ultrapure Laboratory Water Systems (Molsheim – France). Potassium dihydrogen phosphate (KH_2PO_4) and 85 % (v/v) phosphoric acid (H_3PO_4) supplied by Merck (Darmstadt, Germany) were used for the preparation of mobile phase. Hydrochloric acid 37% (v/v) (Merck – Darmstadt, Germany) and ethyl acetate (Chemapol Group – Prague, Czech Republic) were used for human urine sample pretreatment.

2.2. Apparatus

Separation was carried out on a liquid chromatography Elite LaChrom (Merck – Hitachi, Darmstadt, Germany) equipped with pump L-2130, autosampler L-2200, thermostat L-2300, diode array detector L-2450. Organic acids were separated on a silica based analytical column with specially modified reversed-phase functional group Alltech Prevail™ organic acid 5 μm (150 × 4.6 mm, I.D) with an Prevail organic acid 5 μm (7.5 × 4.6 mm, I.D) guard column (Grace – Deerfield, USA).

3. Results and discussion

The composition of the separation buffer solution and further experimental conditions have been optimized to achieve the best separation of organic acids. Aliphatic and aromatic acids were simultaneously separated using mobile phase composed of (A) 25 mmol L^{-1} KH_2PO_4 with pH 2.3 and (B) methanol with 25 mmol L^{-1} H_3PO_4 in ratio 80:20. The separation was performed with gradient elution at 25 °C and flow rate of 1 mL min^{-1}. Injected volume of standard solutions mixture was 20 μL. The organic acids were detected with DAD at 220 nm. The gradient parameters are listed in Tab. I and obtained chromatogram is shown in Fig. 1.

Calibrations for test acids were obtained by plotting peak area vs. concentration and were linear in the range 0.01–10 mmol L^{-1}. The concentration dependences are linear, with coefficients of correlation better than 0.998 and detection limits (S/N = 3) were from 0.1 mmol L^{-1} to 0.1 μmol L^{-1}. The reproducibility (relative standard deviation, n = 3) from injecting 20 μL of standard solution of test acids ranged between 0.33 % and 3.66 %.

The proposed method was demonstrated for the simultaneous determination of aliphatic and aromatic acids in human urine sample and wine sample. Organic acids were extracted from human urine using ethyl acetate after acidified with 5 mol L^{-1} HCl. The organic solvent was evaporated to dryness and the residues were re-dissolved in 1 mL of phosphate buffer. The white wine (Devín 2012, Topoľčianky s.r.o) was diluted with phosphate buffer in ratio 1:5 and was directly injected into the

Table I
Gradient elution parameters for separation of aliphatic and aromatic acids

Time (min)	0	8	15	36	43	44	45	46	47	57
A (%)	100	100	72	48	30	30	10	10	100	100
B (%)	0	0	28	52	70	70	90	90	0	0

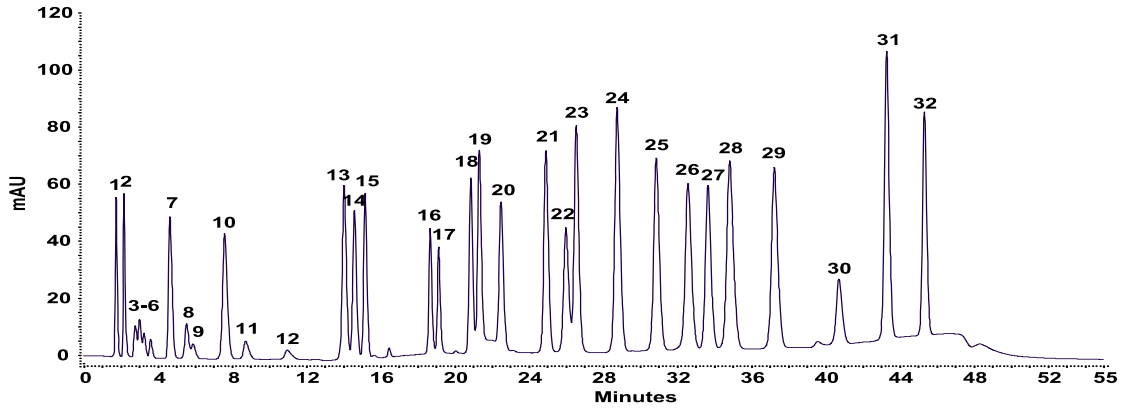

Fig. 1. **Chromatogram of model mixture of 32 organic acids.** Peak identification: (1) oxalic, (2) tartaric, (3) malic, (4) malonic, (5) lactic, (6) acetic, (7) maleic, (8) citric, (9) succinic, (10) fumaric, (11) propionic, (12) levulic, (13) methylsuccinic, (14) pyromellitic, (15) galic, (16) 3,4-dihydroxybenzoic (17) 3,5-dihydroxybenzoic, (18) trimellitic, (19) phtalic, (20) 4-hydroxybenzoic, (21) 2,4-dihydroxybenzoic, (22) vanillic, (23) syringic, (24) 2-methoxybenzoic, (25) trimesic, (26) benzoic, (27) ferulic, (28) salicylic, (29) 3-methoxybenzoic, (30) 2-methylbenzoic, (31) cinnamic, (32) 3-methoxycinnamic

chromatographic system. Fig. 2 and 3 show obtained sample chromatograms.

The quantification of organic acids in samples was carried out by using the method of calibrations curve and standard addition method. We used the standard addition method to determine whether the matrix of a sample changes the analytical sensitivity. The identified organic acids and their concentrations in both samples are listed in Tab. II.

4. Conclusions

The proposed HPLC method with DAD detection could be used for automated analysis of the main and minor organic acid in human urine sample and wine due to the simple sample pre-treatment and the good validation results (LOD, linearity, precision and recovery). Continuing work in our laboratory will be focused on separation of organic acids using HPLC in combination with mass spectrometry.

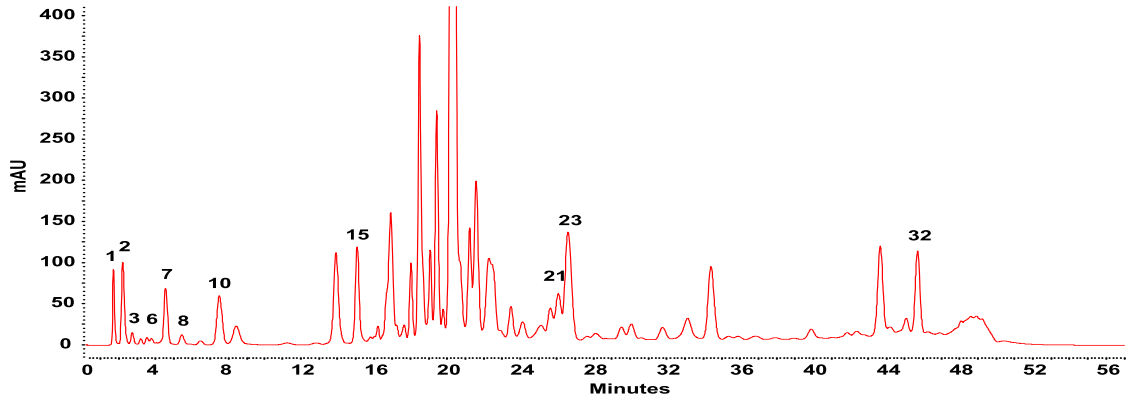

Fig. 2. **Chromatogram of human urine sample.** Peak identification: see Fig. 1

Table II
Concentrations of organic acids in human urine and white wine sample. *SAM – standard addition method

Compounds	Concentration [mmol L^{-1}]			
	human urine		wine	
	calibration curve	SAM*	calibration curve	SAM*
Oxalic	0.356	0.344	0.710	0.721
Tartaric	ND	ND	3.875	4.099
Malic	0.445	0.424	4.054	3.720
Lactic	ND	ND	6.335	6.910
Acetic	1.542	1.011	1.251	1.208
Maleic	0.014	0.015	ND	ND
Citric	0.124	0.130	0.286	0.173
Succinic	ND	ND	1.377	1.420
Fumaric	0.006	0.006	ND	ND
Galic	0.005	0.007	0.007	0.006
3,4-Dihydroxycarboxylic	ND	ND	0.008	0.007
4-Hydroxybenzoic	0.103	0.109	ND	ND
2,4-Dihydroxybenzoic	0.013	0.014	ND	ND
Syringic	0.068	0.069	ND	ND
3-Methoxycinnamic	0.037	0.037	ND	ND

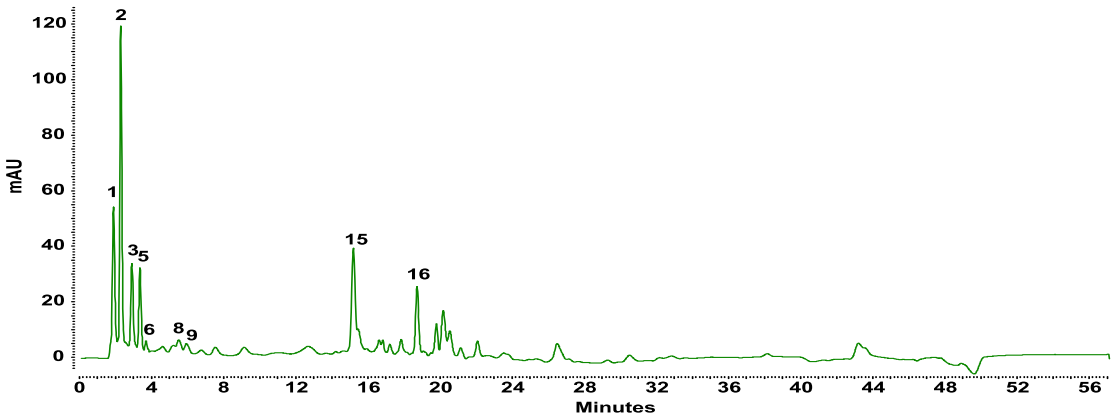

Fig. 3. **Chromatogram of human white wine sample.** Peak identification: see Fig. 1

This work was supported by the grant of project VEGA 1/0852/13 and the grant of project APVV-0583-11. This work is partially outcome of the project VVCE-0070.

REFERENCES

1. Van Hess P. A. W., Vinogradoff S. I.: Soil Biol. Biochem. *35*, 1015 (2003).
2. Waksmundzka-Hanos M.: J. Chromatogr., B *717*, 93 (1998).
3. Goodman L. S., Gilman A.: *The pharmacological basis of therapeutics*. McGraw-Hill, New York 1996.

ON-LINE SCREENING OF ABL1 INHIBITORS BY CAPILLARY ELECTROPHORESIS COUPLED TO MASS SPECTROMETRY

HUI CHEN, ERWIN ADAMS, and ANN VAN SCHEPDAEL

Pharmaceutical Analysis, Faculty of Pharmaceutical Sciences, KU Leuven, Leuven, Belgium
hui.chen@pharm.kuleuven.be

1. Introduction

Phosphorylation mediated by protein kinase is one of the most common post-translational modifications known to regulate biological output[1]. Abl1 is a tyrosine kinase, one of the three main classes of protein kinase. The Bcr-Abl fusion gene is associated with chronic myeloid leukemia[2]. Developing a cost- and time-effective method for screening kinase inhibitors has become very important nowadays. In this report, an on-line screening of Abl1 inhibitors by CE/MS using transverse diffusion of laminar flow profiles (TDLFP)[3,4] for reactant mixing is presented.

2. Experimental

CE/MS experiments were carried out on a Beckman P/ACE MDQ (Beckman Coulter, Fullerton, CA, USA) coupled to an Esquire 3000 HCT ion trap mass spectrometer (Bruker Daltonics, Bremen, Germany) using a sheath liquid co-axial interface from Agilent Technologies (Waldbronn, Germany). CE analyses were performed in fused-silica capillary (85 cm total length, 50 μm i.d.). New fused-silica capillaries were rinsed with 1 M-NaOH for 30 min at 20 psi and water for 15 min at 20 psi. After this treatment, capillaries were coated with a bilayer coating of Polybrene-poly(vinyl sulfonic acid) (PB-PVS). The phosphorylation was initiated in the capillary by mixing three reactant plugs using TDLFP. After reaction, the phosphorylated product was separated using a separation voltage of 30 kV and quantified in the selected reaction monitoring (SRM) mode.

3. Results and discussion

3.1. MS optimization

A sheath liquid of water-methanol (50:50, v/v) containing 0.1% formic acid at a flow rate of 5 μL min^{-1} was used. The positive ion mode was used. By using the SRM mode the sensitivity enhanced about 60 fold compared with MS full scan mode.

3.2. CE system

20 mM ammonium acetate buffer with pH of 6.8 was used as BGE. To conquer the protein adsorption problem, capillary coating was performed. In order to prevent MS contamination and detection interference, static coatings have to be used. In this work, PB-PVS were strongly attached to the capillary surface by adsorption. This coating can be produced simply by flushing the capillary with solutions of PB and PVS.

3.3. Abl1 in-capillary reaction

TDLFP was chosen to mix the reactants in capillary since it can be used for mixing more than two reactants. 2 mM $MgCl_2$ in 20 mM ammonium acetate buffer with pH 6.8 was used as reaction buffer, which was similar to the BGE to avoid reaction and separation problems.

REFERENCES

1. Gratz A., Gotz C., Jose J.: Electrophoresis *31*, 634 (2010).
2. Saglio G., Cilloni D.: Cell Mol. Life Sci. *61*, 2897 (2004).
3. Krylova S. M., Okhonin V., Evenhuis C. J., Krylov S. N.: Trend Anal. Chem. *28*, 987 (2009).
4. Krylova S. M., Okhonin V., Krylov S. N.: J. Sep. Sci. *32*, 742 (2009).

POROUS LAYER OPEN TUBULAR COLUMNS WITH IMMOBILIZED TRYPSIN FOR PROTEIN DIGESTION

RADIM KNOB[a], JANA KŘENKOVÁ[b], JAN PETR[a], and FRANTIŠEK FORET[b]

[a] *Department of Analytical Chemistry, Palacký University in Olomouc, Olomouc,* [b] *Institute of Analytical Chemistry, v.v.i., Brno, Czech Republic*
rknob@seznam.cz

Summary

We have developed a monolithic porous layer open tubular (PLOT) column with immobilized trypsin for protein digestion. The PLOT column was prepared in a 10 μm ID fused silica capillary. Trypsin was immobilized on the monolithic surface and the developed enzyme reactor was used for protein digestion followed by on-line ESI/MS analysis.

1. Introduction

Immobilized microfluidic enzyme reactors (IMER) have shown a high potential in a wide variety of research fields such as medical diagnostics, organic synthesis, drug discovery, or biosensors[1,2]. The use of immobilized enzymes, especially of proteases, has many advantages, e.g., very short digestion time, elimination of autodigestion and therefore absence of undesirable protease fragments in the resulting peptide mixture. The reactors with immobilized enzymes can also be integrated online into the multidimensional systems enabling automated high-throughput protein analysis.

A variety of methods are now available for immobilization of enzymes on the solid supports such as particles or monolithic columns[1]. For extremely small sample volumes, the enzymes can be immobilized directly on the wall of very narrow bore capillary (e.g., 10 μm ID or smaller) characterized by a high surface-to-volume (S/V) ratio[3]. The S/V ratio can be further increased by formation of a monolithic porous layer on the capillary wall providing the larger surface area for enzyme immobilization[4].

In this work, we have developed a methacrylate-based PLOT column prepared in a 10 μm ID fused silica capillary. The monolithic surface was modified with trypsin and the developed capillary IMER was coupled on-line to ESI/MS and used for protein digestion.

2. Experimental

2.1. Preparation of the PLOT column

Briefly, a fused silica capillary (Polymicro Technologies, Phoenix, AZ, USA) with the internal diameter of 10 μm was treated with 3-methacryloxypropyl trimethoxysilane[5]. The treated capillary was washed with the polymerization mixture consisting of 24 % (m/m) glycidyl methacrylate, 16 % (m/m) ethylene dimethacrylate, 20 % (m/m) 1-dodecanol, 40 % (m/m) cyclohexanol, 1 % (m/m) azobisisobutyronitrile (AIBN) (with respect to monomers). Then, the capillary was filled with FC-770, a fully fluorinated liquid immiscible with the polymerization mixture[4]. The capillary was sealed with teflon septa and polymerization was performed at 60 °C for 24 hours. After polymerization, the capillary was washed with methanol.

2.2. Trypsin immobilization

The PLOT column was filled with 0.5 mol L^{-1} sulfuric acid and sealed with septa. After 24 hours, the column was washed with water followed by rinsing with a solution of 0.1 mol L^{-1} sodium periodate. TPCK-trypsin (1 mg mL^{-1}) was dissolved in 25 mmol L^{-1} sodium phosphate buffer pH 7.0 containing 3 mg mL^{-1} sodium cyanoborohydride and 0.1 mg mL^{-1} benzamidine. The enzyme solution was pumped through the PLOT column at room temperature for 3 h, washed with the buffer and stored at 4 °C before further use.

2.3. Protein digestion and MS analysis

A solution of bovine cytochrome c (0.1 mg mL^{-1}) was prepared in 10 mmol L^{-1} ammonium bicarbonate pH 7.8 containing 10% acetonitrile and pumped through the reactor at various flow rates using a syringe pump. The digestion was performed at room temperature.

The trypsin reactor was coupled on-line to the Bruker maXis impact ESI-TOF mass spectrometer (Bremen, Germany). The prepared reactor with a polished tip was used as a nanospray needle. The measurements were carried out in the positive ion mode with a scan range of 400–3000 *m*/*z*. The list of detected ions was used for protein identification by the MS-Fit tool of the Protein Prospector database.

3. Results and discussion

A number of different approaches for preparation of PLOT columns have been reported[6]. Most of them rely on

limitation of polymerization kinetics to obtain a polymer layer at the capillary wall; however, inhomogeneity of the thickness is often observed.

Alternatively, the formation of the polymer layer could be restricted to the capillary wall using two immiscible phases. Therefore, the capillary filled with the polymerization mixture was washed with FC-770, a fully fluorinated solvent. This procedure created a thin layer of the polymerization mixture at the capillary wall. A homogeneous PLOT layer was formed by a thermally initiated polymerization of this thin film wetting the capillary wall (Fig. 1).

Trypsin was immobilized on the monolithic surface by a multi-step binding procedure (Fig. 2). First, the epoxide functionalities of the monolith were hydrolyzed by sulfuric acid followed by oxidation using sodium periodate. Trypsin was immobilized via primary amines and the formed Schiff base was stabilized by sodium cyanoborohydride. The enzyme coupling was performed in the presence of benzamidine in order to prevent undesirable autolysis of the enzyme during the immobilization process.

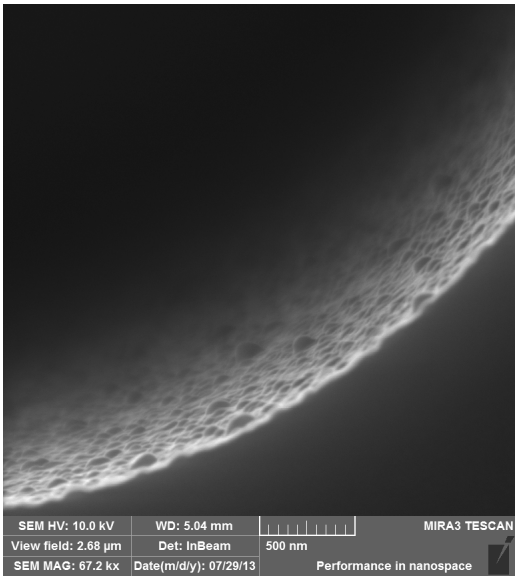

Fig. 1. **Scanning electron micrograph of the PLOT column**

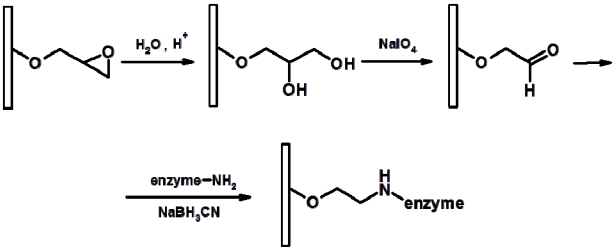

Fig. 2. **Scheme of trypsin immobilization**

Bovine cytochrome c was used as a model protein for digestion using the developed trypsin reactor. The digestion was performed in 10 mmol L^{-1} ammonium bicarbonate pH 7.8 containing 10% acetonitrile in order to minimize non-specific adsorption of protein/peptide on the monolith. The reactor with a polished tip was on-line coupled to the ESI/MS instrument.

The important factor influencing the protein digestion by the trypsin reactor is the protein residence time. Therefore, the protein solution was pumped through the reactor (15 cm, 10 µm ID) at various flow rates (15–100 nL min^{-1}). The corresponding digestion times inside the reactor were 7–50 s. While at the flow rate 15 nL min^{-1} (digestion time: 50 s) the absence of the protein envelope in the mass spectra implied near-complete protein digestion, the appearance of the protein envelope in the mass spectra indicates insufficient digestion at 50 nL min^{-1} (digestion time: 15 s). The sequence coverage obtained with the on-line IMER-MS arrangement was 86.7 % which is comparable with the digestion using soluble trypsin followed by off-line analysis under the same MS conditions (84.8 %).

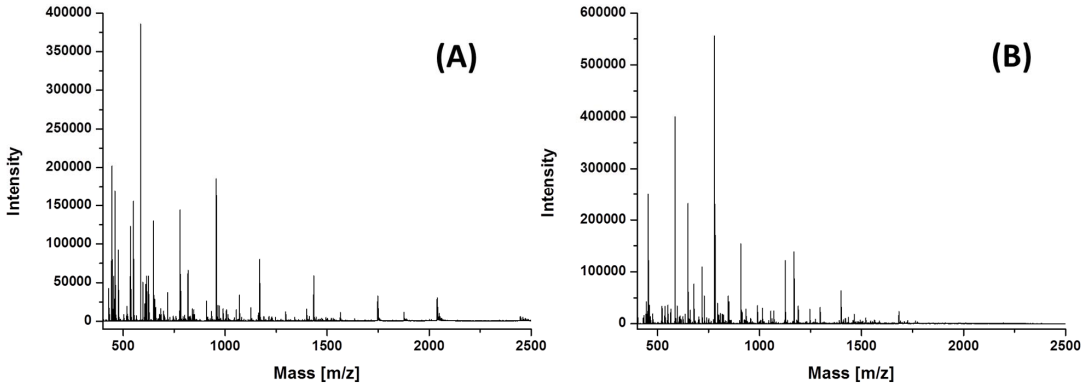

Fig. 3. **Mass spectra of bovine cytochrome c digest.** Digestion time: (A) 15 s, (B) 50 s

4. Conclusions

A monolithic PLOT column with immobilized trypsin for protein digestion was developed. The thin layer PLOT column was prepared using the immiscible phases approach where the formation of the monolith was restricted to the capillary wall by superior wettability of the polymerization mixture after flushing with FC-770. The column was coupled online to ESI/MS and used for digestion of bovine cytochrome c at various flow rates showing near-complete protein digestion in 50 s.

This project was supported by the Operational Programs "Research and Development for Innovations – European Regional Development Fund" (CZ.1.05/2.1.00/03.0058) and "Education for Competitiveness – European Social Fund" (CZ.1.07/2.3.00/20.0018 and CZ.1.07/2.3.00/20.0182). Additional financial support from the Academy of Sciences of the Czech Republic (M200311201) and the institutional research plan (RVO: 68081715) is also acknowledged.

REFERENCES

1. Krenkova J., Foret F.: Electrophoresis *25*, 3550 (2004).
2. Krenkova J., Svec F.: J. Sep. Sci. *32*, 706 (2009).
3. Krenkova J., Kleparnik K., Foret F.: J. Chromatogr., A *1159*, 110 (2007).
4. Knob R., Breadmore M. C., Guijt R. M., Petr J., Macka M.: RSC Advances in press (2013).
5. Rohr T., Hilder E. F., Donovan J. J., Svec F., Frechet J. M. J.: Macromolecules *36*, 1677 (2003).
6. Cheong W. J., Ali F., Kim Y. S., Lee J. W.: J. Chromatogr., A *1308*, 1 (2013).

STUDY OF SEPARABILITY AND DETECTABILITY OF VARIOUS HUMAN INSULIN ANALOGUES AND INSULIN SOLUTION USING RP-HPLC METHOD

VERONIKA KOMOROWSKA and MILAN HUTTA

Department of Analytical Chemistry, Faculty of Natural Sciences, Comenius University in Bratislava, Bratislava, Slovakia
komorowska@fns.uniba.sk

1. Introduction

Human insulin is a peptide hormone consisting of two chains with 21 and 30 amino acids, respectively. These two chains are connected via two disulphide bonds. Its molar mass is 5808 g mol^{-1}. With the latest advances in molecular biology, genomics, proteomics and bioinformatics increased number of biotechnology products which are produced by recombinant techniques. Various recombinant human insulin analogues exist to date. In insulin glulisin two amino acids have been changed in the primary structure. Insulin glargin is characterized by an extension of the B-chain with two additional arginin molecules[1–3]. The various insulin analogues may either show a rapid-acting behavior and are applied directly before the meal or may provide a slow effect which assures a constant basic supply and requires the use one or two times daily.

With the increasing number of these modified analogues, there is a rising need for efficient analysis techniques. A variety of analytical methods, which can be roughly sorted into immunochemical and instrumental analytical methods, had been applied for determination of insulin, e.g.[4]. High performance liquid chromatography (HPLC) is one of the most widely used analytical techniques for the separation of proteins. The aim of our work was initial study of chromatographic behavior of selected recombinant human insulin and its analogues produced by biotechnology process.

2. Experimental

2.1. Chemicals

Formic acid 98–100%, aqueous ammonia 28–30%, methanol (MeOH) 99.9% (v/v), acetonitrile (ACN) 99.9% (v/v), were purchased from Merck (Darmstadt, Germany) all in analytical grade. Samples of human insulin analogues Lantus Solostar (Sanofi Aventis Deutschland GmbH), Apidra (Sanofi Aventis Deutschland GmbH) and sample of regular human insulin Insuman Rapid (Sanofi Aventis, Paris, France), cresol (Lachema, Brno, Czech republic). All aqueous solutions were diluted with ultrapure water purified by Millipore Simplicity (Molsheim, France).

2.2. Chromatography

All chromatographic separations were performed using RP-HPLC C18 column. The HPLC system (Agilent Technologies, Japan) consisted of the following modules: vacuum degasser mobile phases (G1379B), dual-channel high-pressure binary pump (G1312B), auto sampler (G1329B), column thermostat (G1316B), DAD (G1315) and FLD (G1321A). Wavelength range of DAD was set to 190–400 nm. Excitation wavelength FLD was set at 275 nm and emission wavelength at 304 nm. Agilent ChemStation was used for process chromatographic data.

3. Results and discussion

3.1. Study of temperature effect on thermodynamics of separation

For the study were selected temperatures in range from 25 °C to 85 °C and two different organic modifiers (MeOH and ACN) of mobile phase. It is seen from the shown van't Hoff plots in Figs. 1 and 2, that in both types of mobile phases retention behavior of insulin analogues and regular insulin gave nonlinear nature. Nonlinear van't Hoff plots are typical for substances which have a dual retention mechanism, so we can conclude, that for substances under study their complex structure leads to complex interactions in the separation system.

Comparing Figs. 1 and 2, it is clear that the composition of the mobile phase has a considerable influence on the retention behavior of the test compounds at different temperatures. For the separation with a mobile phase consisting of MeOH retention of analytes decreased with increasing column temperature (retention factor varies in the range from 11.34 to 10.83 for insulin glargine, from 11.4 to 11.01 for insulin glulisine and from 11.45 to 10.95 for regular insulin in the temperature range from 25 °C to 85 °C), while the separation with mobile phase consisting of ACN had the opposite trend (retention factor varies in the range from 6.91 to 7.16 for insulin glargine, from 7.00 to 7.37 for glulisine and from 6.99 to 7.31 for regular insulin in the temperature range from 25 °C to 85 °C).

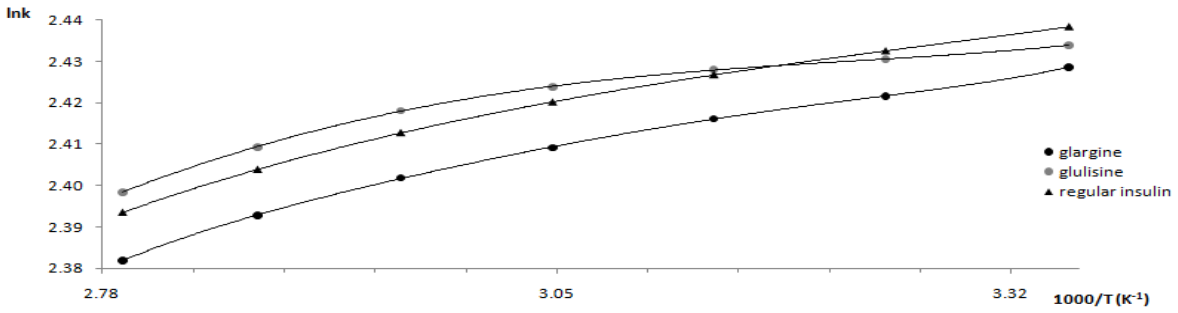

Fig. 1. **Van't Hoff's plot for insulin analogues and regular insulin in mobile phase with MeOH**

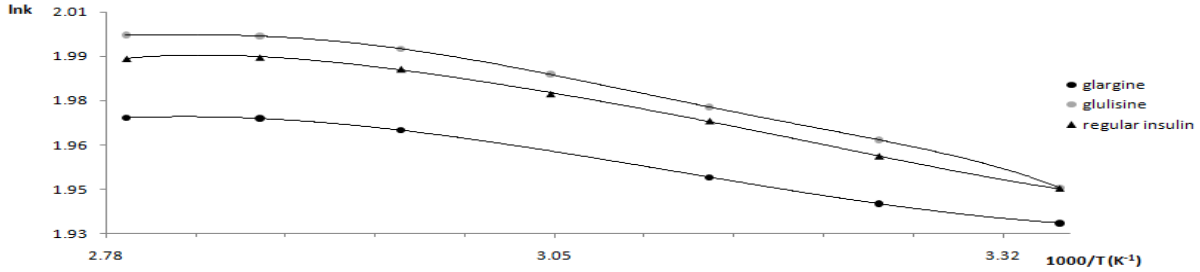

Fig. 2. **Van't Hoff's plot for insulin analogues and regular insulin in mobile phase with ACN**

3.2. Study of organic modifier effect on thermodynamics of sample components separation

Fig. 3 shows that the type of organic modifier has a greater influence on retention of protein nature substance (regular insulin) than on low-molecular weight substance (m-cresol). This result confirms the information given in the literature[5], in which is discussed the fact that an adjustment in thermodynamic conditions of the separation will influence the retention of proteins through changes in the higher protein structures. Therefore it is possible easily influence the selectivity of the separation between the high molecular mass protein substances and low-molecular mass substances with type of organic modifier. The higher selectivity of separation was achieved using MeOH (α = 1.26) than in ACN (α = 1.1).

3.3. Study of detectability of insulin analogues and insulin

For investigation of detectability we used DAD and FLD detector. DAD was set at 280 nm and FLD was set to excitation wavelength at 275 nm and emission wavelength

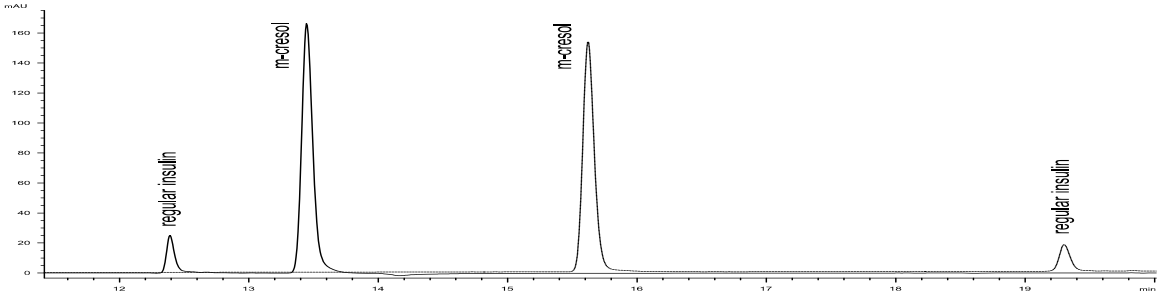

Fig. 3. **Chromatographic results from separation of the sample solution of regular insulin (Insuman Rapid) obtained in two different organic mobile phase modifiers.** Curve with a broken line – the chromatogram obtained with use of MeOH, the curve with the solid line – the chromatogram obtained using ACN. Chromatographic column C18 heated to working temperature (25 °C), the injected volume of sample solutions 50 μL, mobile phase A: buffer from formic acid and amonium formate, mobile phase B: MeOH/H2O (90/10, V/V), appropriate gradient at a flow rate 0.5 mL min^{-1}, UV detection at 280 nm

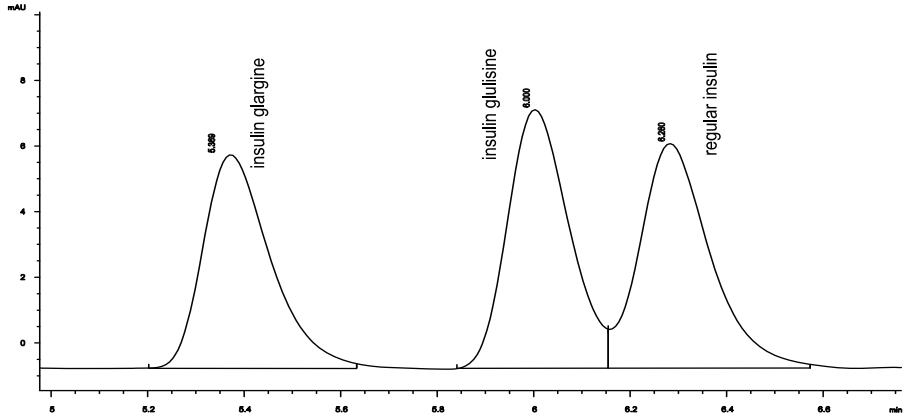

Fig. 4. **Chromatographic results from separation of the mixture insulin analogues and regular insulin.** Chromatographic column C18, the injected volume of sample solutions 50 μL, mobile phase A: buffer from formic acid and amonium formate, mobile phase B: MeOH/H_2O (90/10, V/V), appropriate gradient at a flow rate 0.5 mL min^{-1}, UV detection at 280 nm

at 304 nm. FLD provided better response for all analytes, and thus the lower limits of detection were achieved (data not presented in the paper).

3.4. Separation of mixture insulin analogues and regular insulin

Separation of the mixture was carried out under gradient elution coditions (see Fig. 4). For glargine and human insulin resolution greater than 1.5 was achieved. However, for glulisine and regular human insulin optimization of resolution is still ongoing.

4. Conclusion

In the present work we were able to meet all the objectives of the study. From study we concluded, that there are complex interactions for studied substances even in the RP separation system. With the type of organic modifier of mobile phase is possible significantly affect the selectivity of the separation of the sample components. The higher selectivity was achieved using methanol in the mobile phase. FLD provided better response for the analytes, and thus the lower limit of detection.

This work was generously supported by the grant of project VEGA 1/1349/12 and the grant of project APVV-0583-11.

REFERENCES

1. http://www.drugbank.ca/drugs/DB00030.
2. http://www.drugbank.ca/drugs/DB01309.
3. http://www.drugbank.ca/drugs/DB00047.
4. Ortner K., Buchberger W., Himmelsbach M.: J. Chromatogr., A *1216*, 2953 (2009).
5. Fekete S., Veuthey J. L., Guillarme D.: J. Pharm. Biomed. Anal. *69*, 9 (2012).

UTILIZATION OF LC-MS TECHNIQUES FOR ANALYSIS OF PHENOLIC COMPOUNDS IN VARIOUS TEA SAMPLES

KATARÍNA KRČOVÁ and JOZEF MARÁK

Department of Analytical Chemistry, Faculty of Natural Sciences, Comenius University, Bratislava, Slovak Republic
katarina.krcova@gmail.com

1. Introduction

Phenolic compounds are secondary plant metabolites, which affect organoleptic characteristics of fruits, vegetables and other plants[1,2]. In addition, they show different biological activities such as anti-inflammatory, anti-bacterial, anti-carcinogenic, and play an important role in prevention of osteoporosis and cardiovascular diseases[2–4]. Generally, the term phenolic compounds refers to many different molecules, range from phenolic acids to a complex polyphenols[5]. A plant phenolic compounds posses one or more aromatic or heterocyclic rings, bearing one or more hydroxyl groups[3]. Phenolic compounds are important components mostly present in different sorts of red and white wines, teas, herbals, fruits, vegetables, cereals and spices[1,6,7]. The group of herbal phenols forms: phenolic acids and their derivates, tannins, flavonoids, isoflavonoids, prenylated flavonoids, derivates of coumarin, derivates of stilbene and other phenolic compounds[3]. Tea has been used as an important drink for over 1000 years because of its beneficial effect for the human body. It is one of the most widely consumed soft drinks in the world, next to the water. The content of individual phenolic compounds in tea varieties is highly variable which is caused by using of different fermentation procedure, growing season and different geographical region[8].

The aim of this work was developing and utilization of HPLC-IT-TOF MS method for analysis and identification of phenolic compounds in selected tea samples prepared from various plants, normally grown in the Slovakia (for the list of plants, see Tab. I). The individual plant samples were obtained from Myjava region and the harvesting period was from March to September, 2012.

2. Experimental

2.1. LC-MS analysis

HPLC-MS analyses of selected tea samples prepared from various plants and their phenolic profiles were performed by means of Shimadzu LCMS-IT-TOF™ (Shimadzu, Kyoto, Japan). Chromatographic separations were performed on Kinetex XB-C18 column (100 × 2.1 mm; 2.6 μm) (Phenomenex, Torrance, CA, USA) using gradient elution: water + 0.1% formic acid (A)/ acetonitrile + 0.1% formic acid (B) with 0.2 mL min^{-1} flow rate (0 min: 5% B; 3 min: 10%B; 8 min: 40%B; 10 min: 60% B; 11 min: 90% B; 12 min: 90% B; 12,1 min: 5% B; 20 min: 5% B). The column was thermostated to 40 °C. The MS1-MS3 analyses were performed in automatic data acquisition mode within 50–1000 *m*/*z* range in both positive and negative ionization modes and within 190–400 nm wavelengths used in DAD detection. Data acquisition and data evaluation were performed by using LCMS Solution ver. 3.51 (Shimadzu). Total analysis time was 20 minutes and injected volumes were 2 μL or 5 μL, respectively.

2.2. Chemicals

Chemicals used in this work were obtained from Merck (Merck, Darmstadt, Germany) and Sigma-Aldrich (Sigma-Aldrich, Steinheim, Germany) in analytical grade purity. Acetonitrile and water (both LC-MS purity) were purchased from Merck. Formic acid (LC-MS purity) was purchased from Sigma-Aldrich.

2.3. Samples

22 plant samples analyzed in this work (see Tab. I) were obtained from Myjava region (Slovak republic), with harvesting period March – September 2012. Consequently, the individual samples were dried and stored in cool and dry place. The tea extracts were prepared as follows: Approximately 2.0 g (for accurate weights of individual samples, see Tab. I) of dried sample was extracted with 100 mL of boiling water. Extraction time was 15 minutes. In the following step, the extracts were filtered through 0.8 μm syringe micro filter and cooled to laboratory temperature before their HPLC-MS analyses.

3. Results and discussion

The first part of this work was to find the optimal conditions for chromatographic separation of phenolic compounds in selected tea samples from various plants. Consequently, the mass-spectrometric detection of selected tea samples was performed. Total analysis time was 20 minutes. 22 samples prepared from various plants (see Tab. I) were obtained from Myjava region (Slovak republic). MSXelerator software version 2.4 was used for the visualization of obtained data. Obtained

Table I
Selected tea samples of various plants analyzed in this work

No.	Name of Plant	Name of Plant (Latin)	Mass [g]	Picking period	Analyzed part of plant
1	Breckland Thyme	Thymus serpyllum	2.01	06/2012	blossom, leaves, stem
2	Sage	Salvia officinalis	2.01	06, 07/2012	leaves, stem
3	Common Agrimony	Agrimonia eupatoria	2.00	07/2012	leaves, stem, haulm
4	Lemon Balm	Melissa officinalis	2.00	06, 07/2012	leaves, stem
5	Pot Marigold	Calendula officinalis	2.00	06-09/2012	blossom
6	Eyebright	Euphrasia rostkoviana	1.99	07, 08/2012	haulm, leaves, stalk
7	Chamomile	Matricaria chamomilla	2.00	06/2012	blossom, stem
8	Ribwort Plantain	Plantago lanceolata	2.00	05-08/2012	leaves
9	Lady`s Manthle	Alchemilka xanthochlora	2.02	07, 08/2012	blossom, leaves, stem
10	Garden Thyme	Thymus vulgaris	2.00	07-09/2012	blossom, haulm, stem
11	Coltsfoot	Tussilago farfara	1.99	04/2012	blossom
12	Common Centaury	Centaurium minus	2.02	06-09/2012	leaves, stem, haulm
13	Woodland Strawberry	Fragaria vesca	1.95	05, 06/2012	blossom, leaves, stem
14	Parsley	Petroselinum crispum	2.01	07/2012	haulm
15	Lavender	Lavandula officinalis	1.98	06-08/2012	blossom, leaves, stem
16	Field Horsetail	Equisetum arvense	2.02	06-09/2012	haulm
17	Elderberry	Sambucus nigra	2.00	05/2012	blossom, stem
18	Stinging Nettle	Urtica dioica	1.99	06-09/2012	leaves
19	Lungwort	Pulmonaria officinalis	1.98	03-05/2012	leaves, stem, haulm
20	Yarrow	Achillea millefolium	2.00	07, 08/2012	blossom, stem
21	Cowslip	Primula veris	1.99	03, 04/2012	blossom
22	Small-leaved Lime	Tilia cordata	2.00	06, 07/2012	blossom

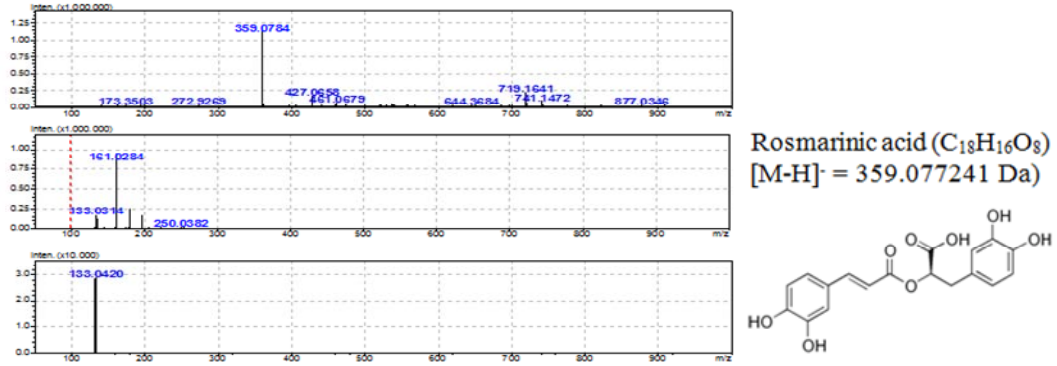

Fig. 1. **TIC and EIC traces obtained from HPLC-MS analysis of 2 μL of tea extract from Melissa officinalis**

chromatograms and MS spectra show the different composition of individual tea samples and their different phenolic profiles. (Fig. 1, Fig. 2).

4. Conclusions

The aim of this work was the development of the suitable method based on the combination high performance liquid chromatography and mass spectrometry and its utilizing for the characterization and

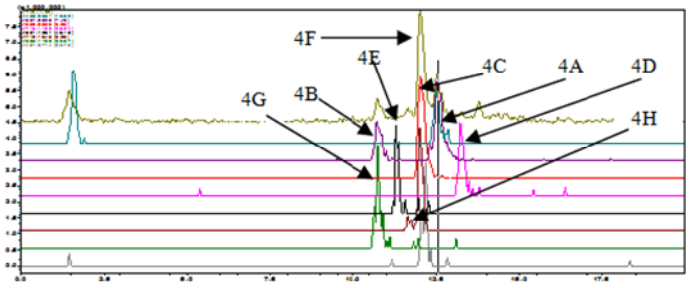

No.	Phenolic compound
4A	Sulphated rosmarinic acid
4B	Lithospermic acid A isomer
4C	Rosmarinic acid
4D	Salvianolic acid C derivate
4E	Rosmarinic acid hexoside
4F	Sagerinic acid
4G	Salvianolic acid K derivate
4H	Luteolin-3'-O-glucuronide

Fig. 2. **MS3 spectra of identified phenolic compound - Rosmarinic acid in extract from Melissa officinalis**

identification of several phenolic compounds present in tea samples prepared from various plants (see Tab. I) obtained from Myjava region. Identified phenolic compounds in extracts from Melissa officinalis are shown on Fig. 2.

This work was financially supported by Slovak Research and Development Agency (Project VVCE-0070-07, APVV-0583-11), Slovak Grant Agency (project No. VEGA 1/1305/12) and Grant UK (UK/608/2013).

REFERENCES

1. Ignat I., Volf, I., Popa V. I.: Food Chem. *126*, 1821 (2011).
2. Boros B., Jakabova S., Dornyei A., Horvath G., Pluhar Z., Kilar F., Felinger A.: J. Chromatogr., A *1217*, 7972 (2010).
3. [Cited: 4. September 2013] < http://web.vscht.cz/koplikr/Rostlinnefenolya flavonoidy.pdf >
4. Ginjom I., D'Arcy B., Caffin N., Gidley M.: Food Chem. *125*, 823 (2011).
5. Jaitz L., Siegl K., Eder R., Rak G., Abranko L., Koellensperger G., Hann S.: Food Chem. *122*, 366 (2010).
6. [Cited: 1. June 2013]<http://referaty.atlas.sk/prirodnevedy/chemia/50908/?pri nt=1>
7. Atoui A. K., Mansouri A., Boskou G., Kefalas P.: Food Chem. *89*, 27 (2005).
8. Zhao Z., Chen P., Lin L., Harnly J. M., Yu L. L., Li Z.: Food Chem. *126* 1269 (2011).

IEF AND HPLC-BASED METHODS FOR EFFICIENT BACTERIAL CHARACTERIZATION

ANNA KUBESOVÁ, JIŘÍ ŠALPLACHTA, DANA MORAVCOVÁ, and MARIE HORKÁ

Institute of Analytical Chemistry of the ASCR, v. v. i., Veveří 97, 602 00 Brno, Czech Republic
kubesova@iach.cz

Summary

Pectobacterium and *Dickeya* species are responsible for blackleg and tuber soft rot diseases on crop and ornamental plants. Recently, a more virulent and aggressive *Dickeya* type of *E. chrysanthemi* was described and it becomes serious problem for potato production in Europe. In this study, we suggest procedures using two commonly available laboratory techniques, gel isoelectric focusing and liquid chromatography, for differentiation and characterization of *Pectobacterium* and *Dickeya* species. We have confirmed that fingerprinting approach can be used for bacterial differentiation, which can be further used in rapid diagnosis of plant disease.

1. Introduction

Bacteria of the genus *Dickeya* cause blackleg and soft rot disease of many plants[1–4]. Recently, *Dickeya* spp. have become serious problem for potato production in Europe. In 2005, new type of *E. chrysanthemi*, was described and named as *Dickeya solani.* This new type is more aggressive than the other *Dickeya* spp.[4,5].

The aim of this study was to discriminate different *Pectobacterium* and *Dickeya* spp., including *D. solani*, using gel isoelectric focusing (IEF) and high performance liquid chromatography (HPLC).

2. Experimental

2.1. Plant pathogens

Strains of *Pectobacterium* and *Dickeya* spp. were obtained from three different collections: La ollection Française de Bactéries associées aux Plantes, Angers, France (CFBP); Plant Research International, Wageningen, Netherlands (PRI); and Czech Collection of Microorganisms, Brno, Czech Republic (CCM).

2.2. Sample preparation

IEF and HPLC were carried out with proteins precipitated from particular cell lysates. Cell lysates were prepared by incubation of bacterial cell suspensions in 8% (w/v) Brij 35 and 20% (v/v) EtOH (ref.[6]). The suspension containing10^{10} cells mL^{-1} was incubated at 30 °C for 16 h. The resulting supernatant was acquired after 60 min of centrifugation at 6000 g on MiniSpin (Eppendorf AG, Hamburg, Germany). The acetone precipitation procedure was used to get proteins from the individual cell lysates.

2.3. IEF

Gel IEF was carried out using apparatus 111 Mini IEF Cell (Bio-Rad) at the pH gradient 3–10 formed by carrier ampholytes. The p*I* markers, 2.0, 3.1, 4.3, 5.3, 6.3, 7.1, 8.0, 9.0, 9.8 (concentration of individual p*I* markers was 1 mg mL^{-1}), and 6 μL of the bacterial sample were loaded onto the gel. The power supply VNZ 22 (Developmental manufactories of ČSAV, Praha, Czech Republic) was used for running of the gel at constant power of 0.6 W, voltage limit 400 V. Brij 35 (0.08% (w/v)) was added into the gel for better solubility of the analyzed proteins[6]. Protein visualization was carried out with CBB G-250 in accordance with manufacturer`s manual. Image of the stained gel was acquired by UMAX Astra 3400 scanner (UMAX Technologies, Dallas, TX, USA) and the gel image was processed using Quantity One Quantification Software (ver. 4.6.0, Bio-Rad).

2.4. HPLC

HPLC experiments were carried out using an Agilent 1200 Series chromatographic system (Agilent Technologies, Santa Clara, CA). Separations were performed on a microbore Poroshell 300SB-C18 column (5-μm particle size, 1 × 75 mm, Agilent Technologies) equipped with a C18 cartridge guard. The elution was run at a flow rate of 20 μL min^{-1} and 70 °C by a binary gradient with acetonitrile as an organic modifier. Solvent A consisted of 0.1 % (v/v) TFA in water and solvent B contained 0.1 % (v/v) TFA in acetonitrile. The used gradient profile consisted of isocratic step (5% solvent B in A) over 5 min and linear gradient elution from 5 to 70 % (v/v) B over 30 min. The detection was performed at 214 nm using a diode-array detector.

3. Results and discussion

A total of 42 strains of *Pectobacterium* and *Dickeya* spp. were subjected to IEF and HPLC analyses. With respect to IEF, each bacterial species provided characteristic protein fingerprint and shows feasibility of the suggested IEF method for reliable characterization and differentiation of the bacteria. These species differ in the p*I* values of the detected protein zones mainly in the p*I* range 4.5–8.0. The samples processed in the same way as

for IEF were further analyzed by HPLC using gradient elution. Under optimized experimental conditions, each individual species owns a unique protein fingerprint. Obtained data shows that this technique is capable to differentiate examined bacteria at the species level as well.

4. Conclusions

Fingerprinting approaches using gel IEF and HPLC have proved effective tools for bacterial differentiation, where the unique IEF patterns or characteristic elution profiles (HPLC) can be used to identify different bacterial species.

This work was supported by the Ministry of the Interior of the Czech Republic (Grant VG20102015023 and Grant VG20112015021) and by the Academy of Sciences of the Czech Republic (Institutional Support RVO:68081715).

REFERENCES

1. Samson R., Legendre J. B., Christen R., Fishcer-Le Saux M., Achouak W., Gardan L.: Int. J. Syst. Evol. Microbiol. *55*, 1415 (2005).
2. Tsror (Lahkim) L., Erlich O., Lebiush S., Zig U., van de Haar J.: Proceedings of the 11th International Conference on Plant Pathogenic Bacteria, 2006, Edinburgh, Scotland, 70.
3. Tsror (Lahkim) L., Erlich O., Lebiush S., Hazanovsky M., Zig U., Slawiak M., Grabe G., van der Wolf J. M., van de Haar J. J.: Eur. J. Plant Pathol. *123*, 311 (2009).
4. Toth I. K., van der Wolf J. M., Saddler G., Lojkowska E., Helias V., Pirhonen M. L., Elphinstone J. G.: Plant Pathology *60*, 385 (2011).
5. Sławiak M., Beckhoven J. R. C. M., Speksnijder A. G. C. L., Czajkowski R., Grabe G., van der Wolf J. M.: Eur. J. Plant Pathol. *125*, 245 (2009).
6. Horká M., Růžička F., Holá V., Šlais K.: Electrophoresis *30*, 2134 (2009).

CONTRIBUTION OF HEVYLITE ASSAYS BY PATIENTS WITH MONOCLONAL GAMMOPATHY

PAVLÍNA KUŠNIEROVÁ[a,b], DAVID ZEMAN[a,b], RADKA ŠIGUTOVÁ[a,b,c], VĚRA PLOTICOVÁ[a,b], FRANTIŠEK VŠIANSKÝ[a], and ZDENĚK ŠVAGERA[a,b]

[a] Department of Clinical Biochemistry, Institute of Laboratory Diagnostics, University Hospital Ostrava, Ostrava, [b] Department of Biomedical Sciences, Faculty of Medicine, University of Ostrava, Ostrava, [c] Department of Biochemistry, Faculty of Medicine, Masaryk University, Brno, Czech Republic
pavlina.kusnierova@fno.cz

1. Introduction

Identification of monoclonal gammopathy is based on protein electrophoresis of serum and urine as well as on the quantification of free kappa and lambda light chains[1]. For detection of monoclonal gammopathy, the levels of immunoglobulin heavy/light chains pairs (Hevylite™) have recently become important[2].

Immunoglobulin heavy chain/light chains assay (Hevylite™) is a new analytical method. It uses specific sheep polyclonal antibodies against junctional epitopes between domains of heavy and light chain in the constant region of immunoglobulin chains[2]. This method enables the individual determinations of the concentrations of k and λ light chains in the intact molecule IgG, IgA, IgM types of monoclonal immunoglobulin. The ratio of Igκ/Igλ is also used as an "index of clonality". This methodology is also independent of the state of renal clearance and variability of blood volume and reflects suppression of non-tumor Ig (ref.[3]). The ratio of Igκ/Igλ provides quick and dynamic information about the degree of therapeutic effect and may be helpful for monitoring the progress of disease. Long-term monitoring of changes in Igκ/Igλ should serve to capture incomplete remission of multiple myeloma (already determined as a negative finding on immunofixation but still exhibiting an abnormal ratio), to detect an incomplete therapeutic effect, and to detect an early stage of relapse (pathological values of Igκ/Igλ appear considerably sooner than positivity of IFE). This method has greater sensitivity with a higher range of measured values and enables accurate diagnosis of unsatisfactory or absent therapeutic effect of chemotherapy. What is more, it has the potential for earlier detection of relapse or disease progression in comparison with electrophoretic monitoring of serum monoclonal immunoglobulin with immunofixation results. In patients with AL amyloidosis, the results of studies also indicated high sensitivity of this method in patients with low levels of monoclonal immunoglobulin. This method could therefore be used for monitoring the effect of treatment in cases which present a normal result in an examination of free light chains in serum. This method could be useful in cases where assessment of disease progression and effectiveness of treatments is difficult to determine[2,4–7]. Studies on malignant lymphoproliferative diseases and the Igκ/Igλ ratio showed higher sensitivity of the method in comparison with conventional electrophoresis in patients with non-Hodgkin lymphoma (48 %), primary macroglobulinemia (100 %), diffuse B-cell lymphoma (65 %), mantle cell lymphoma (63 %), and follicular lymphoma (29 %) (ref.[8]).

2. Experimental

We examined a group of 67 patients suspected of monoclonal gammopathy. The first sample included 27 patients with monoclonal immunoglobulin IgG, the second sample consisted of 23 patients with monoclonal immunoglobulin IgA, and the third group consisted of 17 patients with monoclonal immunoglobulin IgM. Patients were monitored for the following laboratory parameters in serum: total protein and albumin (spectrophotometry, AU 5400, Beckman Coulter, Brea, CA, USA), immunoglobulins G, A, M (nephelometry, BN ProSpec, Siemens Healthcare Diagnostics Inc., Newark, DE, USA), free light chains and light chains kappa and lambda in the intact Ig molecule (turbidimetry, SPA Plus, The Binding Site Group Ltd, Birmingham, UK), serum protein electrophoresis and immunofixation electrophoresis (Hydrasys, Sebia Benelux S.A., Brussels, Belgium). Densitometric values were obtained using a scanner EPSON Perfection V700 Photo and Phoresis software version 7.4.7. (A. L. Instruments, s.r.o., Czech Republic). Statistical evaluation of results was performed using MedCalc software version 11.4 (Frank Schoonjans, Belgium).

3. Results and discussion

We examined the relationship between the densitometrically observed value of monoclonal immunoglobulin and the concentration of light chains kappa or lambda in the intact immunoglobulin molecule (Hevylite™) obtained by the turbidimetric assay. With regard to the non-normal distribution of measured data, the results of analysis were evaluated by Spearman's correlation coefficient "Rho" (r_s) and Kendall´s "Tau" correlation coefficient (r_τ) (Tab. Ia–Ib). The higher values

Table Ia
Results of rank correlations of monoclonal IgG: the densitometrically observed value of monoclonal immunoglobulin vs. the concentration of Hevylite; and total IgG vs. summation of the respective Hevylite pair. Correlations were determined using Spearman's Rho values and Kendall's Tau values

	DM value vs. IgGκ	DM value vs. IgGλ	IgG vs. IgGκ+IgGλ
n	21	6	27
Spearman´s Rho	0.87 p<0.0001	0.94 p=0.0048	0.93 p<0.0001
Kendall´s Tau	0.68 p<0.0001	0.87 p=0.0242	0.77 p<0.0001

Table Ib
Results of rank correlations of monoclonal IgA/IgM: the densitometrically observed value of monoclonal immunoglobulin vs. the concentration of Hevylite; and total IgA/IgM vs. summation of the respective Hevylite pair. Correlations were determined using Spearman's Rho values and Kendall's Tau values

	DM value vs. IgAλ	DM value vs. IgAκ	IgA vs. IgAκ+IgAλ	DM value vs. IgMκ	IgM vs. IgMκ+IgMλ
n	16	7	31	14	14
Spearman´s Rho	0.76 p=0.0007	0.96 p=0.0005	0.95 p<0.0001	0.94 p<0.0001	0.99 p<0.0001
Kendall´s Tau	0.63 p=0.0007	0.91 p=0.0069	0.85 p<0.0001	0.84 p<0.0001	0.96 p<0.0001

Table II
Determination of regression equations (y = a + b×x) for the concentration of IgG and the sum of respective Hevylite pair and for the concentraction of HLC and DM value

x	IgGκ+IgGλ	IgGκ	IgGλ
y	IgG	DM value	DM value
n	27	21	6
Coefficient of determination	0.81	0.79	0.75
Regression equation	y=1.66+1.07·x	y= -3.05+0.97·x	y=1.27+0.69·x

of both correlation coefficients were found between concentrations of IgA kappa (Hevylite^{TM}) and the densitometric value of monoclonal immunoglobulin IgA kappa (r_s=0.964 and r_τ=0.905) (Tab. Ib). The lower values of both correlation coefficients were found between IgA lambda vs. DM value (r_s=0.756, r_τ=0.633) (Tab. Ib). Correlation between DM value and IgM lambda was not evaluated because of the small amount of data. The same procedure was used when evaluating correlations between the concentration of the particular immunoglobulin measured by the nephelometry and the sum of the concentrations of kappa and lambda light chains in the intact immunoglobulin molecule (Hevylite^{TM}) obtained by the turbidimetry assay. The highest correlation was found in the monoclonal protein IgM (r_S=0.991, P<0.0001; r_T=0.956, P<0.0001). The same correlation was found in the remaining two groups (Tab. Ib).

The regression analysis shows that over 90 % of the measured values were explained by the regression relationship. The highest agreement in the group with M-

Table III
Determination of regression equations (y = a + b×x) for the concentration of IgM and IgA and the sum of respective Hevylite pair and for the concentraction of HLC and DM value

x	IgMκ+IgMλ	IgMκ	IgAκ+IgAλ	IgAκ	IgAλ
y	IgM	DM value	IgA	DM value	DM value
n	14	14	31	7	16
Coefficient of determination	0.94	0.86	0.94	0.95	0.53
Regression equation	y=0.48+0.72·x	y=1.71+0.37·x	y=3.03+0.66·x	y=-0.74+0.60·x	y=0.32+0.66·x

protein IgG was found between the concentration of IgG and the sum of IgGκ+IgGλ (r^2=0.81) and the lowest agreement between the concentration of IgG lambda and DM value (r^2=0.75), (Tab. II). In the group with the M-protein of the monoclonal IgM, we again observed very good agreement between the concentration of IgM and the sum of IgMκ+IgMλ (r^2=0.94), (Tab. III). The tightness of fit to the regression line expressed by the coefficient of determination was practically the same in M-protein IgA kappa vs. DM value and the concentration of monoclonal IgA vs. the sum of the concentrations IgAκ +IgAλ (r^2=0.943 and 0.947), (Tab. III). In contrast, the tightness of fit of the measured points by the regression line of M-protein IgA lambda was low (r^2=0.528), (Tab. III).

4. Conclusions

Methods for the determination of free light chains and kappa or lambda light chains in the intact molecule of Ig (HevyliteTM) complement the routine examinations of patients with monoclonal gammopathy, but they cannot replace the routine examination at all. The HLC method appears to be particularly useful in quantifying monoclonal immunoglobulin of the IgA classes. The region of their electrophoretic migration is often at the same site of migration of beta-globulins, causing "overlapping" of M-proteins. The differences between the values determined by HLC, total Ig concentration and densitometrically determined values of M protein may be attributed to the problem of maximum saturation of agarose gel. Furthermore, variations can be induced by the type of dye used and by the differences in reactivity caused by the use of reagents with variable antibody specificity.

REFERENCES

1. Bird J. M., Owen R. G., DęSa S., et al.: Brit. J. Haematol. *154*, 32 (2011).
2. Bradwell A. R., Harding S. J., Fourrier N. J., Wallis G. L. F., Drayson M. T., Carr-Smith H. D., Mead G. P.: Clin. Chem. *55*, 1646 (2009).
3. Alexanian R.: Blood *49*, 301 (1977).
4. Keren D. F.: Clin. Chem. *55*, 1606 (2009).
5. Ludwig H., Harding S., Bradley C., Milosavljevich D., Drayson M., Morgan G., et al.: Blood *114*, (abstract 4879) (2009).
6. Wechalekar A., Harding S., Lachmann H., Gillmore J. D., Wassef N. L., Thomas M., et al.: Amyloid-Journal of protein folding disorders *17*, 188 (2010).
7. Donato L. J., Zeldenrust S. R., Murray D. L., Katzmann J. A.: Clin. Chem. *57*, 1645 (2011).
8. Bradwell A. R., in: (Bradwell A. R.) *Serum Free Light Chain Analysis (plus Hevylite),* Sixth Edition, p. 301–320. Birmingham: The Binding Site Ltd 2010.

KINETIC CHARACTERIZATION OF CYTOCHROME P450 2C9 HYDROXYLATION OF DICLOFENAC BY CAPILLARY ELECTROPHORESIS – MASS SPECTROMETRY

MONIKA LANGMAJEROVÁ, ROMAN ŘEMÍNEK, and ZDENĚK GLATZ

Department of Biochemistry, Faculty of Science and CEITEC – Central European Institute of Technology, Masaryk University, Brno, Czech Republic
langmajerova@ceitec.muni.cz

Summary

The automatized method comprising injection of substrates, incubation, separation of reaction products by CE and their identification and quantification by Qq-TOF mass spectrometry (MS) was successfully used for kinetic measurements of enzymatic reaction. Enzymatic system consisting of cytochrome P450 izoform 2C9 (CYP2C9) and diclofenac (DC) provided these apparent kinetic values: K_m' 4.7 μM and V_{max}' 1.1 nmol min^{-1} nmol^{-1} CYP2C9.

1. Introduction

Cytochrome P450 enzymes represent one of the most important systems involved in drug metabolism[1]. The interactions between these enzymes and drugs are defined by reaction kinetics and drug-drug interactions etc.[2]. An automated system integrating the mixing of reactants, the incubation and the subsequent separation and detection can be advantageously used for such extensive screenings. There are two approaches for CE assay. Off-line CE assay is generally performed in two steps, when a reaction mixture is incubated in the vial and then analyzed by CE. On the contrary the on-line CE assay exploits space inside the capillary as a reaction chamber and as a separation column as well. Moreover, CE combined with MS/MS detection allows target identification and its quantification.

2. Experimental

2.1. Capillary electrophoresis

Analyses were performed on Agilent 7100 CE System. Bare fused-silica capillary (75 cm length, 75 μm i.d., 363 μm o.d.) filled with 30 mM ammonium acetate (pH 8.7) as BGE was used. Separation was carried out by application of voltage –22 kV (293 V/cm) at 37 °C. Linear voltage gradient from 0 kV to –22 kV during first 0.2 min and positive pressure 100 mbar after 6.5 min of analysis was applied.

2.2. On-line reaction

Solutions of CYP2C9 enzyme (E) and mixture of substrate and cofactor (S) dissolved in incubation buffer were injected hydrodynamically by pressure 15 mbar into capillary according previous published work[3] – S solution for 3, 3, 3 and 6 s and E solution three times for 3 s between S plugs. Resulting reaction mixture contained 17.5 nM CYP2C9, 1 mM NADPH and required concentration of DC. Incubation was performed for 10 minutes and the reaction was terminated by voltage application. All steps are visualized by Fig. 1.

2.3. Mass spectrometry

Bruker maXis impact quadrupole time-of-flight MS was coupled to CE. The connection was enabled by sheath liquid co-axial interface from Agilent and sheath liquid (ShL) containing 0.5% ammonia dissolved in isopropanole-water (1:1, v/v) was delivered by flow rate 2.5 μL min^{-1}. Dry gas and drying temperature was set to 5 L min^{-1} and 180 °C. ESI needle voltage was set to 5500 V and nebulization gas pressure was set to 0.2 bar. Spectra were acquired in positive mode in the mass range from 50 to 1600 *m*/*z* and spectra rate 1 Hz.

Fig. 1. **Injection procedure.** A – Injected zones. B – Creation of reaction mixture (RM) by diffusion. C – Separation of product (P) substrate (S) and enzyme (E)

3. Results and discussion

3.1. CE-MS method

The method optimization started by selecting appropriate BGE. Ammonium acetate (15, 30 and 50 mM) in pH range 8.5–9.2 was tested. Best results were achieved with 30 mM ammonium acetate, pH 8.7. Selection of nebulization gas pressure was based on stability of total ion electropherograms and peak intensities and best results provided pressure 0.2 bar. ShL study dealt with composition and flow rate. Usage of acidic or alkaline modifier and the nature and percentage of the organic solvent was examined. Acetic acid and ammonia were tested as modifiers. Methanol, acetonitrile and isopropanol were investigated as organic solvent in 1:1 and 1:2 ratios with water. The mixture of isopropanol-water 1:1 (v/v) with 0.5% ammonia showed the highest peak area response. Flow rate was measured in range 1–4 μL min^{-1} and any significant differences between peak areas or intensities were not observed. Therefore flow rate 2.5 μL min^{-1} was used for subsequent experiments.

3.2. On-line incubation

First step of on-line incubation optimization was determination of optimal CYP2C9 concentration in reaction mixture and optimal incubation time. Typical extracted ion electroforeograms are shown on Fig. 2. Repeatability of metabolite production was verified (RSD = 8.9 %; based on peak areas) and external calibration curve was linear in range 25–250 nM. Quantification was based on external calibration. Finally the dependence of reaction rate on substrate concentration was evaluated (Fig. 3). Identification of compounds was performed using standard of metabolite and also using precise mass of parent and fragment ions from MS^2 spectrum (Fig. 4).

4. Conclusions

The new method allowing identification and quantification of enzymatic reaction products within single analysis in on-line CE mode was introduced. Apparent kinetic values obtained with this method (K_m 4.7 μM and

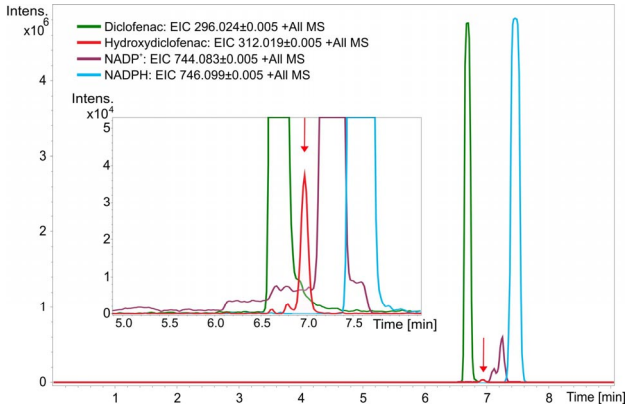

Fig. 2. **Record of analysis after 10 minutes in-capillary incubation of diclofenac**

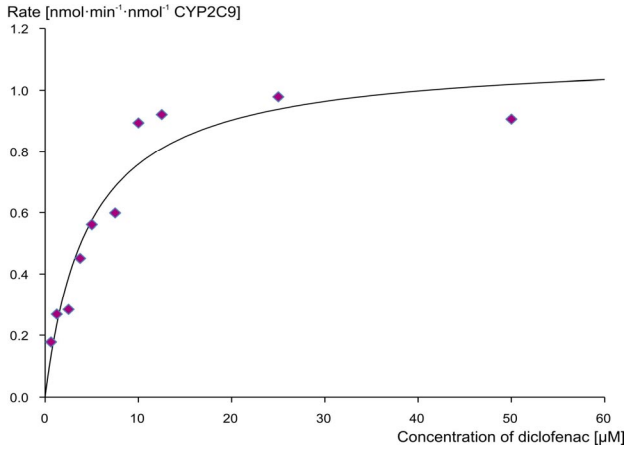

Fig. 3. **Michelis-Menten plot for cytochrome 2C9 reaction with diclofenac**

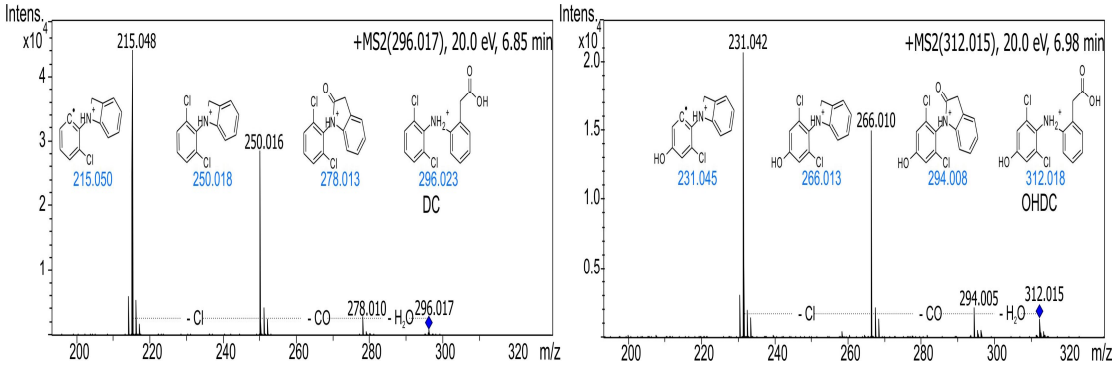

Fig. 4. **MSMS spectrum of diclofenac (DC) and hydroxydiclofenac (OHDC)**

V_{max}' 1.1 nmol min^{-1} $nmol^{-1}$ CYP2C9) were in agreement with previous published data[3]. Principle of reactant's mixing inside capillary based on diffusion and employment of tandem MS detection guarantee generic applicability of method regardless on tested enzyme and substrate.

This study was supported by grant P206/12/G014 financed by Grant Agency of Czech Republic.

REFERENCES

1. Guengerich F. P.: Chem. Res. Toxicol. *21*, 70 (2008).
2. Lin J. H., Lu A. Y. H.: Pharmacol. Rev. *49*, 403 (1997).
3. Řemínek R., Zeisbergerová M., Langmajerová M., Glatz Z.: Electrophoresis *34*, 2705 (2013).

CAPILLARY ISOTACHOPHORESIS OF ANIONS WITH ELECTROSPRAY-IONIZATION MASS-SPECTROMETRIC DETECTION

ZDENA MALÁ, PETR GEBAUER, and PETR BOČEK

Institute of Analytical Chemistry, Academy of Sciences of the Czech Republic, v. v. i., Brno, Czech Republic
mala@iach.cz

Summary

We present ITP-ESI-MS as a powerful tool for selective and sensitive analyses of anionic analytes. Our extended concept of ITP includes besides regular and free-acid ITP also self-maintained ITP in moving boundary systems. Easy theory describes the system properties including their stacking-window diagrams. Simple ESI-compatible electrolyte systems allow flexible tuning with very satisfactory results as demonstrated on the example of analysis of pharmaceuticals in waters.

1. Introduction

The CE-MS combination is a routine technique despite it has lower sensitivity than LC[1]. Replacement of CE by ITP eliminates the dispersion step and analytes remain stacked until they reach the detector and this can enhance the sensitivity by orders of magnitude[2]. Surprisingly the ITP-MS technique was so far applied only scarcely and there are almost no papers about analyses of anions which represent a broad and interesting application field[3]. We present a concept of ITP that allows flexible selection of electrolytes and tuning of their selectivity based on very simple ESI-compatible electrolyte systems, to reach highly sensitive ITP-MS analyses of anions.

2. Experimental

We used a 7100 CE system (Agilent Technologies, Waldbronn, Germany) with a bare fused-silica capillary (100 μm id, 85 cm length) at a running voltage of –20 kV. A commercial CE-ESI-MS interface (Agilent) was used with a coaxial sheath liquid flow (1 % acetic acid + 2 mM ammonium acetate in 50% methanol), supplied via splitter (8 μL min^{-1}). The 6130 single quadrupole mass spectrometer (Agilent) was operated in single ion monitoring negative mode (capillary 3500 V negative; nebulizer pressure 10 psi; drying gas flow 10 L min^{-1}; drying gas temperature 200 °C) for monitoring of $[M\text{-}H]^-$ molecules. Nitrogen was supplied by an NM32LA generator (Peak Scientific, Frankfurt, Germany). The CE and MS instruments were controlled and data acquisition performed by ChemStation software (Agilent). Calculations were performed with the freeware program Simul 5 Complex[4].

3. Results and discussion

We use an extended model of ITP[5–7] as shown in Fig. 1 (involving weak acids HA and HB and a weak base R ionizable to RH^+) where both acids HA and HB may be present in both the L and T zones. The system has moving boundary character and behaves as ITP as long as the L-T boundary remains self-sharpening. The condition of stacking of a minor analyte X (acid HX) is

$$u_{\mathrm{ITP,T}} < u_{\mathrm{X,T}} \quad \text{and} \quad u_{\mathrm{X,L}} < u_{\mathrm{ITP,L}} \qquad (1)$$

where $u_{\mathrm{i,j}}$ is its effective mobility in zone j and $u_{\mathrm{ITP,j}} = v_{\mathrm{ITP}}\kappa_{\mathrm{j}}/i$ is the ITP boundary mobility related to zone j (κ_{j} is the specific conductivity of zone j and i is the current density). This condition can be rewritten to the form

$$u_{\mathrm{ITP,T}}\frac{c_{\mathrm{H,T}} + K_{\mathrm{HX}}}{K_{\mathrm{HX}}} < u_{\mathrm{X}} < u_{\mathrm{ITP,L}}\frac{c_{\mathrm{H,L}} + K_{\mathrm{HX}}}{K_{\mathrm{HX}}} \qquad (2)$$

(u_{X} is the ionic mobility of anion X and $c_{\mathrm{H,j}}$ is the H^+ concentration in zone j) that defines the stacking window of the system. Assuming equality we get two curves which plotted in a u_{X} vs. pK_{HX} network demarcate the region of points (u_{X}, pK_{HX}) of analytes X that are stacked in the given ITP system. An example comparing two ESI-compatible ITP systems (composed of formic and propionic acid and ammonium as counterion) is shown in Fig. 2. The points for model analytes diclofenac (Dic), ibuprofen (Ibu) and salicylate (Sal) show different stacking selectivity as only points lying between curves L and T are stacked in the system.

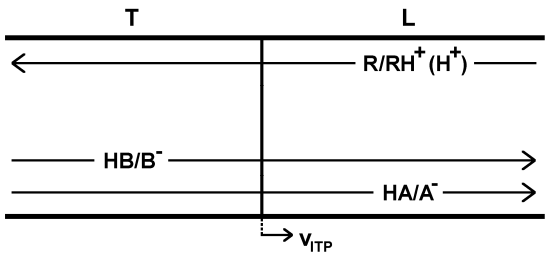

Fig. 1. **Scheme of a moving-boundary ITP system.** L and T are the leading and terminating zones, respectively, and v_{ITP} is the ITP velocity

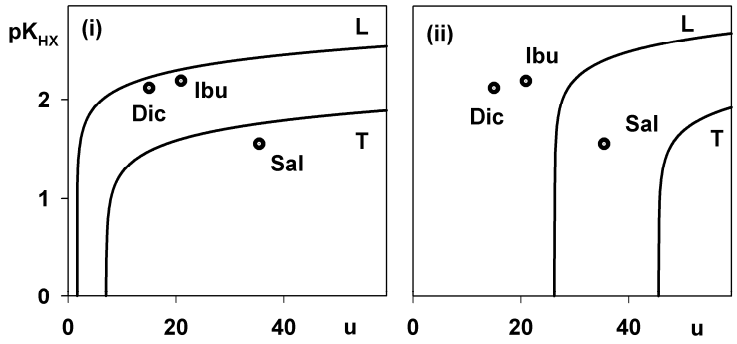

Fig. 2. **Stacking windows of ITP systems.** (i) L: 10 mM formic acid, T: propionic acid; (ii) L: 10 mM formic acid + 8 mM NH_4^+, T: propionic acid (u in 10^{-9} $m^2V^{-1}s^{-1}$)

For simplicity we used the example of regular ITP systems (where HA is missing in zone T and HB is missing in zone L, see Fig. 1) for which the stacking conditions simplify (e.g. condition 1 becomes $u_{B,T} < u_{X,T}$ and $u_{X,L} < u_{A,L}$). Fig. 3a,b show the experimental results of separation of Dic, Ibu and Sal in the systems from Fig. 2. The match well with theory: in system (i) Dic and Ibu are stacked and Sal remains unstacked, in system (ii) the situation is opposite. In Fig. 3c there is the analysis of a real sample (Ibu and Dic in river water) indicating high sensitivity due to ITP stacking in the very simple free-acid system (i) with H^+ as the only counterion.

4. Conclusions

The combination of ITP with ESI-MS allows increasing the sensitivity of electrophoretic analyses by several orders of magnitude. The extended concept of ITP in moving boundary systems brings more flexibility in the selection of electrolyte systems limited by ESI compatibility requirements. Theory allows prediction of the system´s stacking window and easy selectivity tuning. The model allows highly sensitive analyses of anions even in the negative ion mode, e.g. for the analysis of diclofenac and ibuprofen in waters with LOQs on the 10^{-10} M level.

We gratefully acknowledge support by the Grant Agency of the Czech Republic (P206/13/5762) and by Institutional support RVO:68081715 of the Academy of Sciences of the Czech Republic.

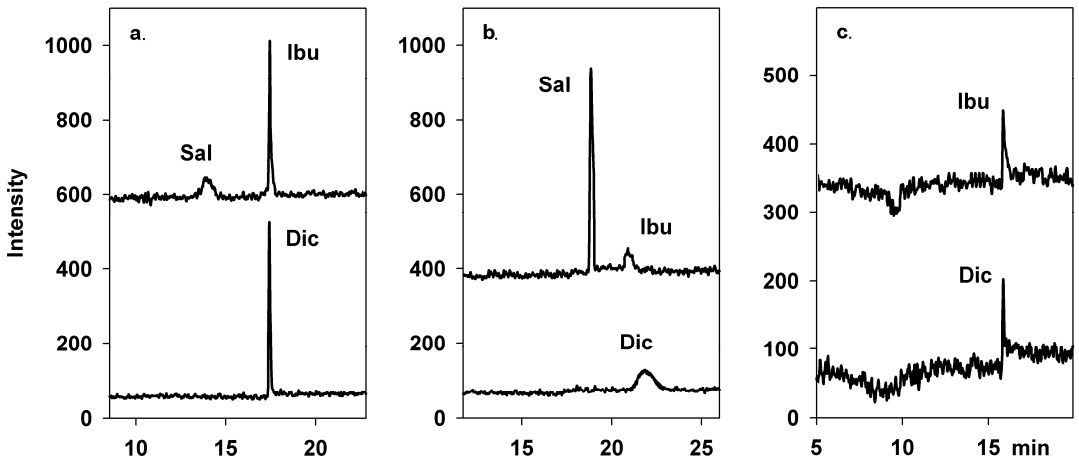

Fig. 3. **Experimental negative single ion monitoring signals for Sal (*m*/*z* 137), Ibu (*m*/*z* 205) (sum in the upper trace) and Dic (*m*/*z* 294, lower trace) of ITP-MS analyses using systems (i) (a,c) and (ii) (b) from Fig. 2.** Sample: (a,b) 10^{-7} M Sal, Ibu and Dic in 2 mM propionic acid, (c) untreated river water (found trace amounts of Dic and Ibuof the order 10^{-10} M). Pressure injection (a,b) 10 mbar for 5 s, (c) 100 mbar for 150 s

REFERENCES

1. Pantůčková P., Gebauer P., Boček P., Křivánková L.: Electrophoresis *30*, 203 (2009).
2. Boček P., Deml M., Gebauer P., Dolník V: *Analytical Isotachophoresis*, VCH Verlagsgesellschaft, Weinheim 1988.
3. Zhao Z. X., Wahl J. H., Udseth H. R., Hofstadler S. A., Fuciarelli A. F., Smith R. D.: Electrophoresis *16*, 389 (1995).
4. Hruška V., Beneš M., Svobodová J., Zusková I., Gaš B.: Electrophoresis *33*, 938 (2012).
5. Malá Z., Pantůčková P., Gebauer P., Boček P.: Electrophoresis *34*, 777 (2013).
6. Malá Z., Gebauer P., Boček P.: Electrophoresis, in press (elps.201300292).
7. Gebauer P., Malá Z., Boček P.: Electrophoresis, in press (elps.201300379).

ADJUSTMENT OF DYNAMIC HIGH RESOLUTION IMAGES OF LIVING CELLS BY COMBINATION OF AN OPTICAL MICROSCOPY IN TRANSMITTING LIGHT, ATOMIC FORCE MICROSCOPY AND IMAGE INFORMATION ANALYSIS

DARIA MALAKHOVA, DALIBOR ŠTYS, and RENATA RYCHTARIKOVA

University of South Bohemia in České Budějovice, FFPW and CENAKVA, Institute of Complex Systems, Nové Hrady, Czech Republic
dmalakhova@frov.jcu.cz

Summary

Presented works is part of the more general project which aims to determine the state of the cell as dynamic self-organizing system. For that, we need to determine position and state of organelles, sub-cellular structures, shape of the cell and events at the cell border. The purpose of current work is to find the solution of the problem of obtaining 3D dynamic images live cell images at maximal resolution and information yield while keeping the cell alive and intact. We combine AFM and optical microscopy in transmitted light. Intermediate results are presented.

1. Introduction

The state of the cell is given by states of its organelles and of the overall organization of the cell. Determination the state of the organelle in the living cell is based on the ability to determine its shape and state. Overall state of the cell is given by its shape, distribution of sub-cellular structures, dynamic processes at cell borders and in its interior.

In order to improve understanding of functioning self organized complex objects we are trying to create the model which help us to get deeper in this problem[1]. For this purpose we are making 3D model of the live cell. This model units in itself combination of image of cell topography with high resolution which have been get by AFM and by in-depth analysis of the stack of images from the optical microscope. The analysis using Rényi information entropy approach[2] enables to eliminate the contribution of the points spread function to the build-up of the image. Theoretical basis of the calculation of the point divergence gain comes from the overall property of the self-organised object, its multifractality. This would solve many basic biological issues, and, in medicinal practice it may serve for identification of abnormalities at different stages of cellular development in artificial fertilization, cancer diagnostics, biocompatibility essays etc.

2. Materials and methods

2.1. Cells cultivation and cells fixation method

For our goals we used cell line MG-63 which bought at Serva cat No.86051601. The cells were grown for the period of the measurement (1–2 days) at 37 °C in a synthetic dropout media with 30% raffinose as the sole carbon source. For AFM scanning cells should be fixed in the petri dish, according to this purpose we fixed cells on the fibronectin using PBS buffer with $Ca^{2+}Mg^{2+}$, Gibco solution and 1 % bovine fetal serum.

2.2. Microscopy

Experiment was done using a versatile sub-microscope – the nanoscope which was developed by the Institute of Complex System FFPW USB in collaboration with Czech fine mechanics and software teams. The optical path are consist of two Luminus 360 light emitted diodes, the condenser system, a firm sample holder and an objective system made of two complementary lenses which allow us to make a change in distance between the objective lens and the sample. The size of the original camera pixel with 40 magnifications was 3434 nm and the size of final pixel after de-mosaicing was 6868 nm. With help of programmable piezo mechanics z-scan was automatically performed and step size was 100 nm.

To identify topography of the cell we have been used atomic force microscope (AFM) NanoWizard 3 produced by JPK Company[3]. Cell scanning was carried in contact mode in liquid. For this type of sample we choose AFM probes MLCT from the Bruker company with resonance frequency 7 kHz and spring constant 0.01 N m^{-1}.

2.3. Point Divergence Gain calculation

The point divergence gain $PDG_{\alpha,x,y}$ is calculated analogously to $PIG_{\alpha,x,y}$ (ref.[4,5]). It is the information increase or decrease achieved by this replacement of the point at position x, y by the point at the same position in the next image $x\,(l+1)$, $y\,(l+1)$.

The respective probabilities are pi, the probability of the occurrence of intensity i in the original image l, and pi, $x(l+1)$, $y(l+1)$ the probability of the occurrence of the given intensity in the image where the examined point of coordinates x, y was replaced by the point at the same location in the next image number $l+1$.

$$PDG_{\alpha,x,y} = \frac{1}{1-\alpha}\, ln\left(\sum_{i=1}^{n} p_i^{\alpha}\right) - \frac{1}{1-\alpha}\, ln\left(\sum_{i=1}^{n} p_{i,x(l+1),y(l+1)}^{\alpha}\right) \quad (1)$$

3. Results and discussion

The comparison of AFM and transmitted light microscopy is complicated by the variance in the points spread function of diffracting object variant in size, shape and interior refractivity index. On the other hand, it has been known for a long time that sub-resolution object may in favorable conditions seen in biological samples[6]. By the method of calculation of the point divergence gain we neglect the point spread function and obtain sharp borders of intracellular objects as they are formed by diffracting elements. In this way we obtain information about the cell at the resolution of one camera pixel, which is in our case 74 nm. Such images may be compared with AFM topographic maps.

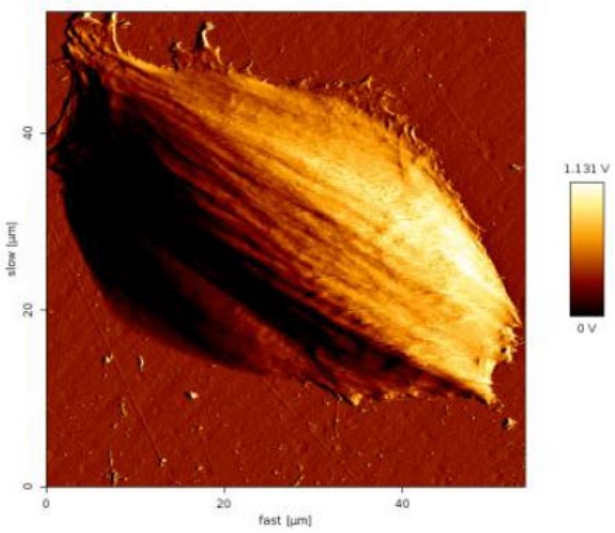

Fig. 1. **AFM image of the living cell MG-63 scanned in contact mode in liquid**

There are a lot of problems occurs during the usage of various AFM set-ups. Fig. 1 shows us one of them. For example it is not clear are we observing cytoskeleton of the cells or it is just some scratches on the cell surface becauce of high force applied during the scanning, or because the cantilever was too stiff for this type of cells.

For comparison of the AFM and optical microscopy information we show the PDG-transformed images from the bright light optical microscope obtained with Rényi coefficient α=4.0 and α=0.5 at the zeroth information change level (Fig. 2). The former enhances shapes of interior objects, the later borders of sub-cellular structures. Theoretical interpretation of these findings is not completed but the technical use is obvious: we identify regions into which the cell is separated (at α=0.5) and identify larger homogeneous object such as organelles (at α=4.0). The former finding has not been reported before, most probably since the information about large-scale unique structures is generally hidden in the dataset until the aspect of general (i.e. non-normal) intensity distribution is implemented in the calculation. The observation at α=4.0 may be to a large extent interpreted in a rather straightforward manner, the level 0 represents objects homogeneously spanning through the two subsequent images, at the level 255 we observe object which either lie only at one level or have mover in the time of positioning of the microscope optics to the next level. However, there are many objects at any intermediate α level which do not have the character of the noise, represent intra-object structures and should be analyzed.

The above mentioned observations, namely the observation of thin objects, is in partial discrepancy with current models of the imaging by the optical microscope. The point spread function spans through the whole space along the optical axis. Thus, the object should be observable at all levels. This we confirm for large object but not in case of smaller and thinner objects. We propose that theory needs to be developed for imaging of

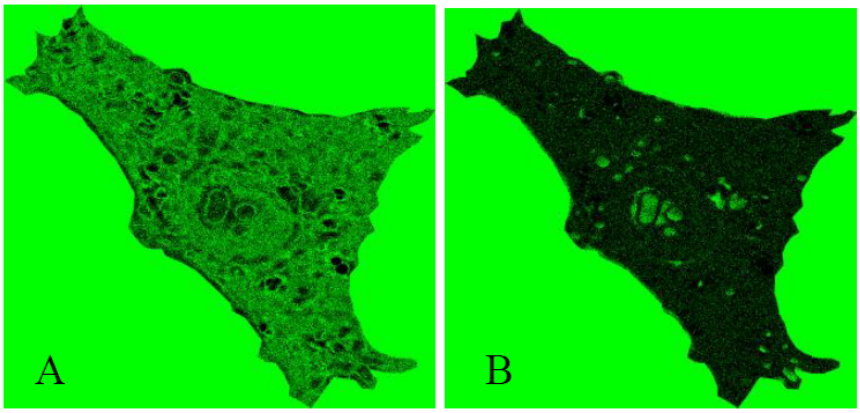

Fig. 2. **Representations of the PDG transformed images at the zeroth level calculated between image 75 and 76 of the cell, with Rényi coefficient at panel A α=0.5 and at panel B α=4.0**

diffracting object, where the diffraction image of the objects is projected on the lens and thus not the image of the point objects gives rise to the interference image, but rays originating from the diffraction image. We do not bring any theoretical solution to the problem, but we believe that is imaginable that along the optical axis, partial re-construction of the original object occurs. And here we bring some evidence, but this needs to be confirmed.

The main aim of the combination of AFM and optical microscopy is calibration of the scale. Any object identified by the transformation of optical microscopy image analysis should lie within the borders of the cell determined by the AFM technology. The report in this article shows technical developments in this direction.

4. Conclusions

In this contribution we present first steps in the avenue towards the complete comparison of the optical microscopy image and AFM topographical image. The final goal is to calibrate the optical image which shall further enable to understand the true state of the living cell without chemical or genetic modification. Moreover, cells are typical example of chemical self-organizing object. The main distinction between cells originating from higher heterotrophic organisms and, for example, the chemical clock, is the existence of "soft" border created by the cell membrane. Thus combination of definition of the border by the AFM and high-resolution dynamic analysis of the state of organelles should only give the answer on origins of cell existence and stability.

This project was supported and co-financed by the GA JU 134/2013/Z and by the CENAKVA CZ.1.05/2.1.00/01.0024.

REFERENCES

1. Zhyrova A., Stys D.: Int. J. Computer Mathematics 2013.
2. Bugrin M.: *Theory of Information: Fundamentality, Diversity and Unification*, World scientific publishing, Singapore 2010.
3. JPK instruments, *NanoWizard Handbook* Version 2.2 02/ 2012.
4. Stys D., Vanek J., Nahlik T., Urban J., Cisar P.: Molecular BioSystems 2011.
5. Stys D., Jizba P., Papacek S., Nahlik T., Cisar P.: *On Measurement of Internal Variables of Complex Self-Organized Systems and Their Relation to Multifractal Spectra*, (Kuipers and Heegaard eds.), Springer, Heidelberg 2012.
6. Stys D., Urban J., Vanek J., Cisar P.: *Analysis of biological time-lapse microscopic experiment from the point of view of the information theory*, Micron 2011.

LIQUID CHROMATOGRAPHY MASS SPECTROMETRY OF SELECTED BENZO-PHENANTHRIDINE ALKALOIDS INCUBATED WITH RAT LIVER MICROSOMES

ADAM MIDLIK[a], KRISTÝNA PĚNČÍKOVÁ[a], IVANA KUŠNYEROVÁ[a], GABRIELA DOVRTĚLOVÁ[b], KRISTÝNA NOSKOVÁ[b], JAN JUŘICA[b], EVA TÁBORSKÁ[a], and ONDŘEJ PEŠ[a]

[a] *Department of Biochemistry, Faculty of Medicine, Masaryk University, Brno,* [b] *Department of Pharmacology, Faculty of Medicine, Masaryk University, Brno, Czech Republic*
379962@mail.muni.cz

1. Introduction

Quaternary benzo[*c*]phenantridine alkaloids (QBAs) belong to a subgroup of isoquinoline alkaloids. They include major sanguinarine (SA) and chelerythrine (CHE) as well as minor QBAs chelirubine (CR), sanguilutine (SL), sanguirubine (SR), chelilutine (CL), and macarpine (MA) (see Fig. 1). The effects of QBAs on biological systems have been studied extensively, especially for commercially available SA and CHE. The results have been summarised in several reviews[1–3]. Limited availability of the minor pentasubstituted QBAs and hexasubstituted MA reduces data concerning their biological effects, yet various anti-proliferative and pro-apoptotic properties have been described[4]. It was shown that although the QBA molecular structures are very similar, the mechanism of their action on the molecular level may be different[5,6]. As pharmacological studies imply that even a small change in the structure may trigger a significant difference in pharmacological activity, it cannot be simply accepted that metabolic routes of all QBAs will be analogous. The metabolic fate of minor QBAs should be intensively studied in order to identify their metabolites, to reveal their toxicity and/or alternate biological effects in different pathways. An approach to reveal the metabolic fate of selected QBAs may employ an *in vitro* model of rat liver microsomes (RLMs) with resulted QBA metabolites to be analyzed by means of liquid chromatography (LC) coupled to hybrid quadrupole time-of-flight (Q-TOF) mass spectrometry (MS).

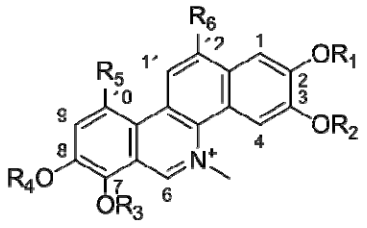

Alkaloid	R_1	R_2	R_3	R_4	R_5	R_6
Sanguinarine (SA)	$-CH_2-$		$-CH_2-$		-H	-H
Chelerythrine (CHE)	$-CH_2-$		$-CH_3$	$-CH_3$	-H	-H
Sangulutine (SL)	$-CH_3$	$-CH_2$	$-CH_3$	$-CH_3$	$-OCH_3$	-H
Chelilutine (CL)	$-CH_2-$		$-CH_3$	$-CH_3$	$-OCH_3$	-H
Sanguirubine (SR)	$-CH_3$	$-CH_2$	$-CH_2-$		$-OCH_3$	-H
Chelirubine (CR)	$-CH_2-$		$-CH_2-$		$-OCH_3$	-H
Macarpine (MA)	$-CH_2-$		$-CH_2-$		$-OCH_3$	$-OCH_3$

Fig. 1. **Benzo[*c*]phenanthridine alkaloid structures**

2. Experimental

2.1. Extraction and isolation of QBAs

SA, CHE, CL, and CR were isolated according to a method described by Slavik et al.[7]. Isolation and purification step was performed by means of semi-preparative reversed-phase (RP) chromatography. The purity of alkaloids was > 90 %.

2.2. Isolation of RLMs

Research male rats (Wistar albino) of the same age and weight were killed by decapitation and subjected to laparotomy. A liver sample (4 g) was homogenized, centrifuged and the total protein was determined by the Lowry method and bovine serum albumin as standard.[8] Aliquots were stored in –80 °C until needed.

2.3. Incubation, extraction and analysis of samples

Each alkaloid (50 μL) was vortexed with 50 μL of RLMs in a buffered (50 mM phosphate, pH 7.4) NADPH generating system (glucose-6P dehydrogenase, glucose-6P) for 30 min. The reaction was stopped by addition of 100 μL of methanol and transferring to an ice bath.

Metabolites were purified by adding 1 mL of MeOH:ACN:formic acid (50:50:0.02) into a 100 μL aliquot of the incubation mixture, followed by vortex and centrifugation. A small portion of the supernatant was five times diluted and injected (20 μL) onto an LC column.

2.4. LC MS

LC MS method was established using Dionex Ultimate 3000RS (Thermo Scientific, Sunnyvale, CA) module. Compound separation was achieved with a 3.0 × 150 mm, 4 μm Synergi RP-Max C18 column at 23 °C and a flow rate of 0.5 mL min^{-1}. A binary mobile phase system

consisted of 0.1% formic acid (A) and LC-MS grade ACN (B). Mobile phase B was increased from 20 % to 40 % for 10 min and then to 80 % for next 10 min. It was kept constant for 10 min followed by equilibration to the initial conditions for 3.0 min. A total HPLC run was 33 min. The HPLC system was connected to a MicrOTOF-QII (Bruker, Germany) mass spectrometer, operated in positive electrospray ionization mode. The ionization conditions were set by the software as the following: Capillary voltage 4500 kV, end plate offset –0.5 kV, source temperature 220 °C, desolvation gas (nitrogen) flow 10 L min^{-1}, nebulizer (nitrogen) pressure 3 bar, collision cell voltage 35 eV.

3. Results and discussion

LC MS and MS/MS spectra were first investigated to obtain the elemental formula of each compound. Identification of target compounds then relied on isotope pattern matching and combination of MS/MS and retention behavior. Products of incubation for each QBA are summarized in Table I. QBAs were found to undergo reduction to dihydro-derivatives (+2 Da) and/or demethylation (–14 Da) of both parent and reduced compounds. *O*-demethylation was proposed since retention times of *N*-demethylated products would have considerably increased due to the loss of the quaternary nitrogen. Identity of reduced compounds was verified by the reaction of the original incubation mixture with an excess of $NaBH_4$, resulting in the pure alkaloid and the *O*-demethylated product to be further reduced to its respective dihydro (DH) compound.

4. Conclusions

Selected QBAs were, when incubated with RLMs, found to provide dihydro-derivatives with CHE, CL, and CR correspondingly metabolizing to mono *O*-demethylated products. Absence of additional metabolites (hydroxylation, ring-opening reactions) might be explained by low activity of cytochrome P450 isoenzymes and/or insufficient time of incubation.

The work was supported by Czech Ministry of Education, Youth and Sports (LH12176-KONTAKT II) and Science Foundation of Masaryk University (MUNI/ A/0818/2012).

REFERENCES

1. V. Simanek, R. Vespalec, A. Sedo, J. Ulrichova, J. Vicar, in *Chemical Probes in Biology: Science at the Interface of Chemistry, Biology and Medicine*, ed. by M. P. Schneider, 2003, Vol. 129, pp. 245-254.
2. Z. Dvorak, V. Kuban, B. Klejdus, J. Hlavac, J. Vicar, J. Ulrichova, V. Simanek: Heterocycles *68*, 2403 (2006).
3. A. Zdarilova, J. Malikova, Z. Dvorak, J. Ulrichova, V. Simanek: Chem. Listy *100*, 30 (2006).
4. I. Slaninova, K. Pencikova, J. Urbanova, J. Slanina, E. Taborska: Phytochem. Rev. DOI 10.1007/s11101-013 -9290-8 (2013).
5. W. C. Tang, I. Hemm, B. Bertram: Planta Med. *69*, 97 (2003).
6. M. L. Colombo, E. Bosisio: Pharm. Research *33*, 127 (1996).
7. J. Dostal, J. Slavik: Chem. Listy *94*, 15 (2000).
8. O. H. Lowry et al.: J. Biol. Chem. *193*, 265 (1951).

Table I
The retention time, exact mass and elemental composition of selected QBAs after 30 min incubation with RLMs

Alkaloid	Detected products	t_r (min)	Ion	Observed m/z	Calculated m/z	error (ppm)	Sum formula [M]
SA		4.4	$[M]^+$	332.0927	332.0923	-1.3	$C_{20}H_{14}NO_4$
	DHSA	22.1	$[M+H]^+$	334.1069	334.1079	3.1	$C_{20}H_{15}NO_4$
CHE		5.7	$[M]^+$	348.1241	348.1236	-1.5	$C_2{:}H_{18}NO_4$
	DHCHE	21.5	$[M+H]^+$	350.1391	350.1392	0.4	$C_2{:}H_{19}NO_4$
	O-demethylated CHE	4.4	$[M]^+$	334.1071	334.1079	2.5	$C_{20}H_{16}NO_4$
	O-demethylated DHCHE	17.5	$[M+H]^+$	336.1235	336.1236	0.2	$C_{20}H_{17}NO_4$
CL		7.1	$[M]^+$	378.1351	378.1341	-2.5	$C_{22}H_{20}NO_5$
	DHCL	21.1	$[M+H]^+$	380.1483	380.1498	3.9	$C_{22}H_{21}NO_5$
	O-demethylated CL	5.7	$[M]^+$	364.1180	364.1185	1.4	$C_2{:}H_{18}NO_5$
	O-demethylated DHCL	16.2	$[M+H]^+$	366.1331	366.1341	2.9	$C_2{:}H_{19}NO_5$
CR		6.1	$[M]^+$	362.1033	362.1028	-1.2	$C_2{:}H_{16}NO_5$
	DHCR	21.9	$[M+H]^+$	364.1168	364.1185	4.7	$C_2{:}H_{17}NO_5$
	O-demethylated CR	4.7	$[M]^+$	348.0865	348.0872	2.0	$C_{20}H_{14}NO_5$
	O-demethylated DHCR	17.8	$[M+H]^+$	350.1027	350.1028	0.4	$C_{20}H_{15}NO_5$

USING DIFFERENT ELECTROPHORETIC METHOD FOR THE DETERMINATION OF THE AFFINITY CONSTANTS OF SALICYLIC ACID AND BSA

LENKA MICHALCOVÁ and ZDENĚK GLATZ

Department of Biochemistry, Faculty of Science and CEITEC – Central European Institute of Technology, Masaryk University, Brno, Czech Republic lenna@mail.muni.cz

Summary

The capillary electrophoresis fontal analysis (CE-FA), Hummel Dreyer methods (HD) and affinity capillary electrophoresis (ACE) were used to study the affinities between salicylic acid (SA) and bovine serum albumin (BSA). The binding constant (Ka) was measured by all these methods. The Ka values obtained from CE-FA (5.66 ± 0.22 × $10^3 M^{-1}$), HD methods with internal (2.83 ± 0.23 × $10^3 M^{-1}$) and external (2.28 ± 0.12 × $10^3 M^{-1}$) calibration are in agreement. The comparison of results and other conditions shows the best measurement methods are CE-FA and HD with external calibration.

1. Introduction

The binding constant (Ka) is commonly used to describe the strength of binding between ligand such as drug and protein. The strength of the interaction has a significant effect on the biological activity of the drug, and knowledge of the nature and extent of drug-protein binding can help us to understand the pharmacokinetics and pharmacodynamics of a drug[1]. The advantage of capillary electrophoresis (CE) is very low sample consumption and a high resolution. It does not require the highly purified samples, immobilization or labelling of any of the interacting species. The investigated interaction takes place in a solution, which can be simulated physiological conditions[2].

The main objectives of this study were to determine the Ka of the model system (BSA – SA) using several CE based methods, compare their results and their requirements – time preparation, time analysis, simplicity of evaluation and repeatability of measurements.

2. Experimental

The uncoated fused silica capillary was 58.5/50 cm (L_{tot}/L_{eff}) with I.D. of 75 μm. Operational voltage of 24 kV was performed in normal polarity and the detection wavelength was set to 214 nm. The temperature of the capillary was maintained at 25 °C. The other conditions of optimized methods are summed in Tab. I.

3. Results and discussion

In order to establish the Ka, three CE based methods – CE-FA, HD, ACE were chosen. Representative electropherograms of the CE-FA method for complex BSA - SA and a standard solution of SA are shown in Fig. 1. CE-FA provides good repeatability and good fitting of data points (Tab. II).

HD was carried out in two forms – with internal or external calibration. Representative electropherograms of the HD method are shown in Fig. 2.

The peak area and peak height were tested for evaluation of binding curve. The peak area was found a better parameter than the peak height. The internal and external calibrations were tested as well, and it is the external calibration that provides better repeatability and lesser scatter of data points (Tab. II).

Table I
Summary of capillary electrophoresis conditions

	CE-FA	HD	ACE
Background electrolyte (BGE)	borate buffer (15mM borax was adjusted to pH 8.5 with 60mM boric acid)		
	neat BGE without additives	with different amounts (0 – 800 μM) of SA	with different amounts (0 – 20 μM) of BSA
Sample	50 μM BSA + 10 -1000 μM SA	50 μM BSA	1 mM SA + 0.05% DMSO
Capillary treatment	Pre-analysis: 2 min 1 M HCl 1 min water 5 min 0.1 M NaOH 1 min water 2 min BGE 3 min 24 kV BGE Post-analysis: 1 min water		Pre-analysis: 3 min 1 M NaOH 2 min water 3 min BGE Post-analysis: 1 min water

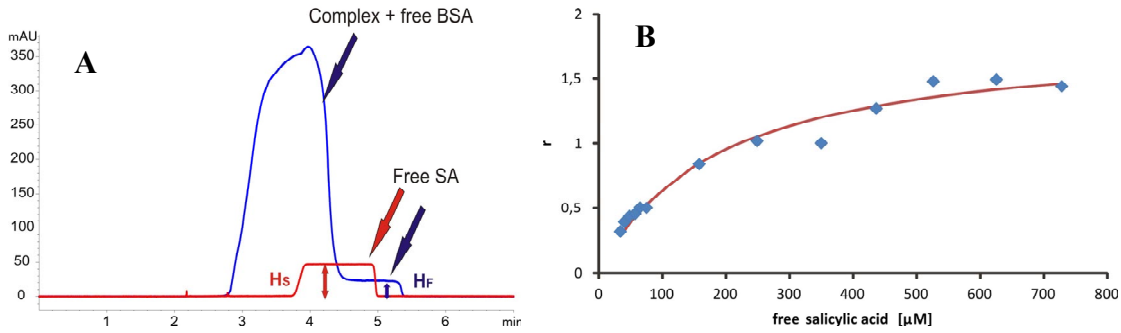

Fig. 1. **Set of representative results obtained with the CE-FA method.** A) Electrophoreograms o free SA for calibration curve and complex BSA – SA. B) Typical binding curve obtained for BSA – SA with CE-FA

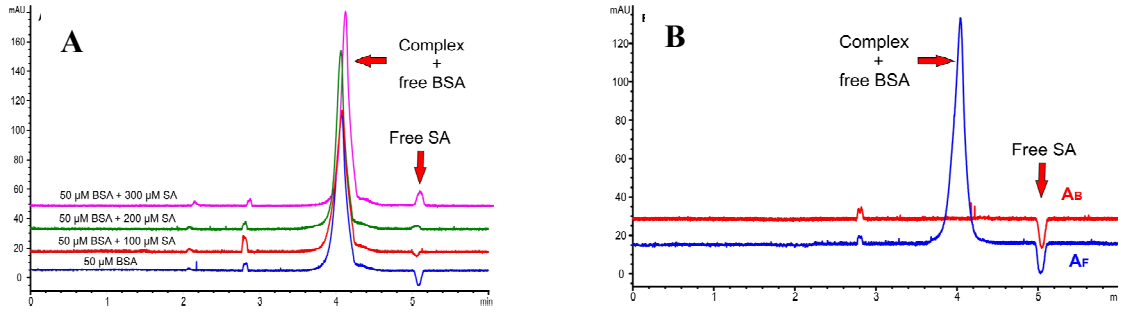

Fig. 2. **Typical results of HD methods. Both examples are measured in BGE with 200 µM SA.** A) Internal calibration. B) External calibration

Table II
Summary of results

	Ka · 10^3 l/mol	n
CE-FA	5.66 ± 0.22	1.8 ± 0.2
HD area internal calibration	2.83 ± 0.23	2.6 ± 0.5
HD area external calibration	2.28 ± 0.12	1.7 ± 0.3

The comparison of data points obtained with different HD modification is shown in Fig. 3. The binding curve obtained with the CE-FA is included as a reference.

The last tested method was ACE. Representative electropherograms of ACE are shown in Fig. 4. The advantage of the method is that it does not require a calibration for measurement of binding constant. The several types of flushing procedure were tested for better repeatability of analysis. The procedure with the smallest RSD for a run to run analysis was chosen as the best washing procedure. However, the repeatability between day to day analyses was insufficient.

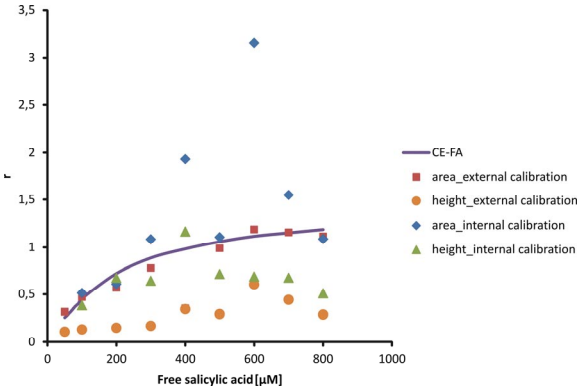

Fig. 3. **Binding curves of BSA – SA obtained by HD methods**

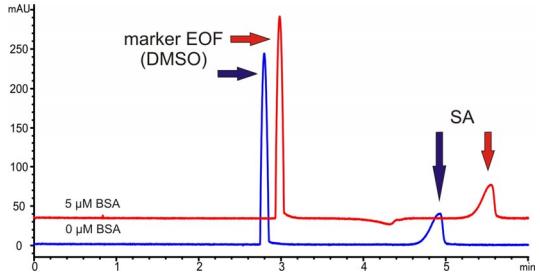

Fig. 4. **Typical electropherograms of ACE**

4. Conclusions

The Ka was measured by several capillary electrophoretic methods. Their comparison shows that the simplest methods (according to amount of different BGEs and different samples) are CE-FA and HD with external calibration. But CE-FA data points contain a lesser scatter than HD data points do. The HD method with internal calibration requires more demanding preparation of sample.

This work was supported by grant P206/12/G014 from the Czech Science Foundation.

REFERENCES

1. Sharma R., Choudhary S., Kishore N.: Eur. J. Pharm. Sci. *46*, 435 (2012).
2. Vuignier K., Schappler J., Veuthey J. L., Carrupt P. A., Martel S.: Anal. Bioanal. Chem. *398*, 53 (2010).

ELECTROPHORETIC MOBILITY MEASUREMENTS OF A MULTIVALENT RED DYE SPADNS

PAVLA PANTŮČKOVÁ, PAVEL KUBÁŇ, and PETR BOČEK

Institute of Analytical Chemistry of the Academy of Sciences of the Czech Republic, v. v. i., Veveří 97, CZ-602 00 Brno, Czech Republic
pantuckova@iach.cz

Summary

Measurements of the electrophoretic mobility of an anionic dye 4,5-dihydroxy-3-(*p*-sulfophenylazo)-2,7-naphthalene disulfonic acid trisodium salt (SPADNS), which is a commonly used anionic dye, are described in this contribution. Electrophoretic mobilities of SPADNS were measured in various buffer solutions covering the pH range of 2.4–9.1. Effective electrophoretic mobilities of SPADNS measured in these buffers varied between 50.5 × 10^{-9} m^2/Vs and 60.5 × 10^{-9} m^2/Vs with an average effective mobility of 55.0 × 10^{-9} m^2/Vs.

1. Introduction

The determination of electrophoretic mobilities of multivalent dyes and determination of their p*K*s is very often neglected in the literature. These measurements are not trivial and usually result into data, which are not easy to interpret and are therefore often not published. Electrophoretic mobility of SPADNS was not published so far. However, SPADNS is often used as an attractive visible compound for measurement of e. g. precise timing for time switching between isotachophoretic and capillary electrophoretic step[1]. The need for the determination of its electrophoretic mobility started to be important in our actual research concerning micro-electromembrane extractions using electrically induced transfer of charged analytes across free liquid membranes[2], since SPADNS is well suitable for observation of the transfer of analytes and it offers intensive colour even at low concentrations. Chemical structure of SPADNS is depicted in Fig. 1.

2. Experimental

Effective mobilities of SPADNS were measured in 5 different buffer solutions within the pH range of 2.4–9.1: 1 M acetic acid (HAc), pH 2.4; 10 mM Histidine (His) + 50 mM HAc, pH 4.1; 20 mM 2-Morpholinoethanesulfonic acid monohydrate (MES) + 20 mM His, pH 6.1; 20 mM Tris-hydroxymethylaminomethane (Tris) + 10 mM HCl, pH 8.1; 50 mM Tris + 5 mM HCl, pH 9.1. Electrophoretic separations were performed in a fused silica capillary of 31.5/24.5 cm total/effective length, 75 μm id/365 μm od, applied voltage of = 8/–8 kV and injection for 3 s at 3 mbar corresponding to the injected sample length of 4 mm. Commercial capillary electrophoresis apparatus, Agilent 7100, was used for the experiments. The calculations of electrophoretic mobilities were done according to ref.[4].

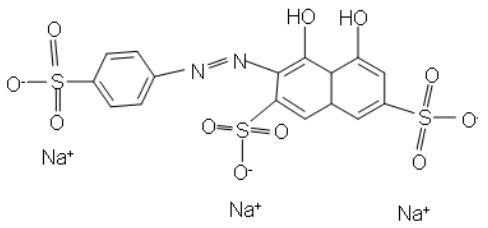

Fig. 1. **The chemical structure of SPADNS** (pK -3.0, -2.0, 3.55 , ref.[3]).

3. Results and discussion

The mobilities of the electroosmotic flow (μ_{EO}) were measured at positive polarity using mesityl oxide as an analyte, which was detected at 254 nm, see Table I. The results of the effective mobilities of SPADNS, which were measured at negative polarity, are summarized in Table I as well. For the measurements of SPADNS mobilities, the apparatus was set at the maximum of its absorbance at 490 nm.

4. Conclusions

Measurements of electrophoretic mobility of SPADNS were performed in various buffer solutions. Mobility of electroosmosis increased with the pH of buffer solutions according to the theory and reached maximum value at pH 9.1 as expected. On the other hand effective electrophoretic mobilities of SPADNS showed no pH dependence within pH range of 2.4–9.1. It means that true p*K* values of SPADNS can be expected below 2. The relative large variation range confirms the empirical experience that mobilities of multivalent dyes are not easy to be measured. A possible explanation may be the sorption effects of the dye ions to capillary wall due to the presence of a lot of polar functional (azo- and hydroxyl) groups. Measurements of effective mobilities of

Table I
Comparison of μ_{EO} and μ_{eff} (SPADNS) in selected buffer solutions

pH	μ_{EO} [$\times 10^{-9}$ m^2/Vs]	μ_{eff}(SPADNS) [$\times 10^{-9}$ m^2/Vs]
2.4	14.6	54.8
4.1	17.2	60.5
6.1	25.1	56.0
8.1	30.4	50.5
9.1	47.5	53.4

The effective mobility of SPADNS varied within the range of 50.5–60.5 × 10^{-9} m^2/Vs. The average effective mobility corresponds to 55.0 × 10^{-9} m^2/Vs.

multivalent dyes are therefore feasible, note however, that these might be dependent on buffer solution composition and pH value.

Financial support from the Academy of Sciences of the Czech Republic (Institute Research Funding RVO: 68081715) and the Grant Agency of the Czech Republic (Grant No. 13-5762S) is gratefully acknowledged.

REFERENCES

1. Pantůčková P., Křivánková L.: Electrophoresis *31*, 3391 (2010).
2. Kubáň P., Boček P.: Submitted for publication.
3. Hirokawa T., Omori A., Yokota Y., Hu J.-Y., Kiso Y.: J. Chromatogr. *585*, 297 (1991).
4. Foret F., Křivánková L., Boček P.: *Capillary Zone Electrophoresis,* pp. 7–19, VCH Weinheim 1993.

POLYDOPAMINE COATED CAPILLARIES FOR CE SEPARATIONS

JAN PARTYKA[a,b], FRANTISEK FORET[a], THI THU VU[c,d], and JAN SUDOR[c,d]

[a] Institute of Analytical Chemistry of the AS CR, v.v.i., Brno, Czech Republic, [b] Department of Chemistry, Faculty of Science, Masaryk University, Brno, Czech Republic, [c] Université de Toulouse; UPS; UMR 152 Pharma-Dev; Université Toulouse 3, Faculté des Sciences Pharmaceutiques, F-31062 Toulouse cedex 09, France, [d] Institut de Recherche pour le Développement (IRD); UMR 152 Pharma-Dev; F-31062 Toulouse cedex 09, France
partyka@iach.cz

Summary

We have tested CE separation of selected samples in capillaries with polydopamine modified surface. The capillaries were modified by polydopamine or polydopamine with an additive. The polydopamine coating with additive represents a simple and effective procedure for capillary alteration by another modificator such as hydroxyethyl cellulose, hydroxypropyl cellulose etc. In this work, we represent separation data from PrinCE system with UV detection for peptides, proteins and oligosaccharides labeled by 2-aminobenzoic acid.

1. Introduction

Commonly used techniques for modification of capillaries require chemicals with a reactive group which allows a binding to capillary wall. Application of these compounds is often problematic because of their reactivity and modification process usually requires some specific conditions such as high temperature or nonaqueous solvent. The represent surface modification was inspired by mussels which polymerize dopamine in water solution to form adhesive[1].

2. Experimental

The capillaries were modified by dopamine in TRIS/ HCl (50 mM, pH 9.0). Ammonium persulfate was added to the dopamine solution to obtain faster polymerization and more uniform surface coatings. We experimented with several additives because of improvement separation properties of capillaries. These additives were added into the dopamine solution before polymerization.

The separations were measured using PrinCE autosampler with UV detection (214 nm). The peptides and proteins were used without any another labeling. A dextran ladder was used as sample of oligosaccharides. Because of absence any chromophore in molecules of oligosaccharides, labeling by 2-aminobenzoic acid was necessary. The all separations were performed in 6-aminocaproic acid/acetic acid (20 mM, pH 4.8) as a background electrolyte[2].

3. Results and discussion

In parallel with the capillaries, we have also modified flat surfaces and characterized them with water contact angle (WCA) measurements, atomic force microscopy (AFM) in a tapping mode, cyclic voltammetry (CV) and by the measurements of the endoosmotic flow. The WCA measurements clearly showed that all studied surfaces (Si, SiO_2, Au, Cu, SU8 and PDMS) were covered with the DOPA film (WCA for the DOPA film was between 50.5–53.9° for all the surfaces). The AFM studies showed an improved uniformity of the DOPA coatings when ammonium persulfate was utilized in the polymerization mixture. The thickness of the deposited films was also measured by AFM and was found to be close to 10 nm after 3 hrs of film deposition. However, we can increase the film thickness by repeating the coating procedure with fresh solutions. The DOPA films were also studied by cyclic voltammetry and it was observed that the oxidation/reduction peaks of an electroactive probe (ferrocyanide) disappeared after a gold surface was treated with DOPA solution.

We have compared separations in bare fuse silica capillary, capillary coated by polydopamine and capillaries coated by polydopamine with additive. Hydroxyethyl cellulose (HEC) from 90 to 1300 kDa, hydroxypropyl cellulose (HPC) from 100 to 1000 kDa and polyvinyl alcohol (PVA) 70 kDa were tested as the additive. Measurement of endoosmotic flow by dimethoxysulfoxide showed prolongation of migration times in polydopamine-coated capillary and in polydopamine-coated capillaries with additive. The endoosmotic flow was suppressed in capillaries coated by polydopamine with additive more than only polydopamine and the migration times were various in dependence on kind of additive, e.g. when HEC (90 kDa) was used, no EOF was observed.

A mixture of seven peptides was used as a model for testing of capillaries. The separation was the fastest thanks to the strongest EOF and at the same time the worse in bare fuse silica capillary. Effective separations were accomplished by coated capillaries. A resolution of each

peak was sufficient but only migration times were various.

Unfortunately, separations of proteins were not successful. We tested a mixture of four proteins, but no clear peaks were observed. These problems were partially suppressed when we used stacking effect because of peaks self-focusing.

The best separations results of 2-aminobenzoic labeled oligosaccharides were accomplished by polydopamine coated capillary and by polydopamine with HPC 100 kDa coated capillary. The separations had better resolution than separation in the bare fuse silica capillary. A small disadvantage can be prolongation of migration times of oligosaccharides but it can be overcome by using higher separation voltage.

4. Conclusions

In this work, we presented a new possibility of capillary coating. The polydopamine coating appears as promising procedure because of simple reaction conditions in water solution. Moreover, it is possible to use polydopamine as resin during grafting of HEC, HPC etc. The capillaries with these coatings are suitable for CE separation of small molecules such as peptides or oligosaccharides.

This work was supported by the Grant Agency of the Czech Republic (P301/11/2055), the Academy of Sciences of the Czech Republic (M200311201) and the institutional research plan (RVO: 68081715). This project is co-financed by the European Social Fund and the state budget of the Czech Republic (CZ.1.07/2.3.00/20.0182). Thi Thu Vu benefitted from the fellowship of the University of Hanoi.

REFERENCES

1. Lee H., Dellatore S. M., Miller W. M., Messersmith P. B.: Science *318*, 426 (2007).
2. Foret F., Szökő E., Karger B. L.: Electrophoresis *14*, 417 (1993).

ISOQUINOLINE ALKALOIDS OF THE CZECH AND CHINESE CULTURE OF *MACLEAYA MICROCARPA* (MAXIM.) FEDDE

KRISTÝNA PĚNČÍKOVÁ[a], ONDŘEJ PEŠ[a], PETR TÁBORSKÝ[b], ZHI-HONG JIANG[c], and EVA TÁBORSKÁ[a]

[a] Department of Biochemistry, Faculty of Medicine, Masaryk University, Brno, Czech Republic, [b] Department of Chemistry, Faculty of Science, Masaryk University, Brno, Czech Republic, [c] State Key Laboratory of Quality of Chinese Medicine Research, Macau University of Science and Technology, AvenidaWai Long, Macao, PLR
k.pencikova@mail.muni.cz

1. Introduction

Macleaya microcarpa (Maxim.) Fedde belongs, together with *M. cordata* (Willd.) R. Br. and their interspecific hybrid *Macleaya x kewensis* Turill, to the genus *Macleaya*, family Papaveraceae. Quaternary benzophenanthridine alkaloids (QBAs) sanguinarine (SA), chelerythrine (CHE), chelirubine (CR), chelilutine (CL) and the rarely occurring macarpine (MA) are the most interesting bioactive substances. While the major benzophenanthridine alkaloids SA and CHE are available commercially and have been the subjects of numerous biological studies, minor QBAs remained unnoticed for a long time due to their limited availability. Not long ago, first biological studies[1–3] described the effects of these alkaloids on cells and identified a number of interesting properties, which puts these alkaloids in the center of interest for further research. Minor QBAs display strong anti-proliferative and apoptotic activity *in vitro*[2]. MA has been reported as promising fluorescent probe for cell nuclei labeling and visualization of various stages of the cell cycle in fluorescence microscopy and flow cytometry[1]. In addition, polycyclic, planar structure of the quaternary form allows intercalation of these alkaloids into DNA[4].

Hence, the essential assumption for further studies of minor QBAs is the necessity to obtain these alkaloids in sufficient quantities. As they are not available commercially and synthesis is rather unsatisfactory[5], isolation from the plant material seems to be the best approach for their production.

M. microcarpa is a perennial herb whose origin is in central China. In conditions of middle Europe, *Macleaya* is successfully grown and reproduced vegetatively. The aim of this presentation is to compare the content of alkaloids in the Czech and Chinese culture.

2. Experimental

M. microcarpa was grown in The Centre of Medicinal Plants of Masaryk University in Brno. One-year-old culture was harvested in September 2009, fourteen years old culture was harvested in July 2010. Chinese *M. microcarpa* was collected in mountains in province Shan'xi in June 2012. It was not possible to determine the age of this culture.

The plant material was wiped, dried, finely grounded and extracted by methanol in FexIKA apparatus (IKA, Germany), which is based on the fluidized bed extraction. The extraction time was 16×15 min. After extraction, the individual extracts were evaporated to 25 mL.

Subsequently, the extracts were diluted 1:1 with HPLC mobile phase and filtered through a 0.45 μm syringe filter. Samples were analyzed by reversed phase HPLC with UV detection. Moreover, identification of alkaloids was confirmed by HPLC-MS/MS.

The HPLC analyses were performed using an HPLC apparatus consisting of a high pressuregradient pump LC-20AD, DAD detector SPD M20A (Shimadzu, Japan), ECOM syringe loading sample injector (ECOM, Czech Republic) with external sample loop 20 μl and C-12 column Synergi Max-RP 80A (4 μ, 150×4.60 mm ID) (Phenomenex, USA). The extract analyses were performed using gradient elution. The mobile phase was prepared from a stock solution containing sodiumheptanesulfonate (0.01 mol L^{-1}) and triethylamine (0.1 mol L^{-1}) in redistilled water, pH 2.5 was adjusted by phosphoric acid. The solution A and B contained 25 % and 60 % (v/v) of acetonitrile, respectivelly. The following elution profile was employed: 0–1 min isocratically 20 % B; 10 min 50 % B; 20 min 100 % B; 20–30 min isocratically 100 % B. The flow rate was set to 0.5 mL min^{-1} and the detection was performed by the DAD detector at 280 nm.

3. Results and discussion

One of the first comprehensive studies of *M. microcarpa* came from Slavík[6]. For a long time, *M. microcarpa* remained unnoticed, while *M. cordata* has been studied and cited as a source of benzophenanthridines SA and CHE. A detailed study of *M. microcarpa* has been published recently; it includes changes in alkaloid content during the entire vegetation period[7].

The results of current analysis showed that allocryptopine (ALL) is the main alkaloid of the underground part from both cultures. Other major alkaloids include protopine (PRO) and CHE (Tab. I), small amounts of berberine and coptisine were detected as well.

Table I
The alkaloid content in the Czech and Chinese culture of *Macleaya microcarpa*. The experiments were performed in a duplicate. The amount of alkaloids is expressed as mass of alkaloid (mg) per a gram of the dry drug ± standard deviation

Age of the plant (years)	PRO mg/g ± SD	ALL mg/g ± SD	SA mg/g ± SD	BER mg/g ± SD	CHE mg/g ± SD	CR mg/g ± SD	CL mg/g ± SD	MA mg/g ± SD
1 (Czech)	13.659±2.089	50.870±9.166	1.886±0.322	0.063±0.015	2.704±0.428	0.826±0.117	0.232±0.046	0.237±0.075
14 (Czech)	10.723±1.360	56.498±4.114	4.713±0.463	0.093±0,012	11.267±2.264	3.242±0.545	1.317±0,254	1.907±0.385
? (Chinese)	3.573±0.456	22.679±3.514	1.832±0.286	0.201±0,028	2.998±0.543	1.864±0.335	0.995±0.182	0.948±0.260

In addition, presence of *N*-methylcanadine was confirmed by HPLC-MS/MS in the Chinese culture and in the one-year-old Czech culture. In the older Czech culture, this alkaloid was not detected at all.

The same minor QBAs - CR, CL and MA were found in both cultures, though their amounts were significantly higher in the older Czech culture (approximately 4-fold for CR, 6-fold for CL and at least 8-fold for MA, see Tab. I). Nevertheless, this culture is 14 years old, which is not perspective for routine harvest and alkaloid isolation.

Despite the unknown age of the Chinese culture of *M. microcarpa*, CR, CL and MA amounts were approximately only 2-fold lower than in older plants encouraging the option to harvest *M. microcarpa* in its natural habitat.

4. Conclusion

Currently, the main source of QBAs is isolation from plant material.Therefore, it is necessary to constantly search for new possibilities and cultures, which are able to accumulate these alkaloids in sufficient quantities.

The financial support of this work by The Ministry of Education of Czech Republic (project KONTAKT II LH12176) and by the Masaryk University Project of Specific Research (SVMUNI/A/0818/2012) is gratefully acknowledged.

REFERENCES

1. Slaninová I., Slanina J., Táborská E.: Cytometry A *71*, 700 (2007).
2. Slaninová I., Slunská Z., Šinkora J., Vlková M., Táborská E.: Pharm. Biol. *45*, 131 (2007).
3. Slunská Z., Gelnarová E., Hammerová J., Táborská E., Slaninová I.: Toxicol. In Vitro *24*, 697 (2010).
4. Hossain M., Kumar G. S.: J. Thermodyn. *41*, 764 (2009).
5. Ishikawa T., Saito T., Ishii H.: Tetrahedron *51*, 8447 (1995).
6. Slavík J., Slavíková E.: Chem. Listy *48*, 106 (1954).
7. Pěnčíková K., Urbanová J., Musil P., Táborská E., Gregorová J.: Molecules *16*, 3391 (2011).

PREPARATION OF LOW-COST MICROFLUIDIC DEVICES USING AN OFFICE LAMINATOR

LENKA VOJTKOVÁ, PAVLÍNA SVOBODOVÁ, ANDREA SUCHOMELOVÁ, and JAN PETR

Regional Centre of Advanced Technologies and Materials, Department of Analytical Chemistry, Palacký University in Olomouc, Czech Republic
secjpetr@gmail.com

Summary

Low-cost microfluidic platforms represent an easy cheap and high-throughput alternative to modern expensive instruments. In our work, we developed a simple platform using an office laminator machine. Three types of channels were studied as a proof of a concept.

1. Introduction

A financial crisis in the world, particularly in Europe affects people's behavior, economy, competitiveness, and politics. Since this crisis seems to affect life of all the people in next years, there is a need for methods/devices/processes that will be highly effective, competitive and cheap. The price will plays one of the most important roles and probably will be highly rated. Low-cost microfluidic platforms are known as an alternative to common instruments which have high prize and low portability. First, the title "low-cost devices" is related mainly to devices that could be developed in many copies with small costs (as PDMS chips). However, there is another possibility to lower the price by using classical filtration papers or nitrocellulose membranes as described by Whitesides et al.[1] or Yager et al.[2]. These "paper-based microfluidic devices" (μPADs) can be easily produced, modified for many purposes, and also commercialized.

In our previous works[3], we designed paper-based chips for determination of ecotoxicologically relevant heavy metals. However, we wanted to cover our chips to avoid any contact of atmosphere with the reagent zones. As described before, a simple transparent adhesive tape can be used for such purposes but this is not really reproducible approach since the tape can be easily detached. Hence, the aim of our work was to overcome problems with the transparent adhesive tape and to find more precise and reproducible approach to cover paper-chips. Recently, the similar work was presented by Cassano et al.[4] who called these devices as "laminated paper-based analytical devices" (LPADs).

2. Experimental

Paper-microfluidic devices were prepared as follows: a design was drawn using the Corel Draw X5 software; then printed by the Xerox ColorQube 8570 wax printer on filter paper Whatman, Grade 1; wax melting was done by ironing using the Tefal Primagliss 2530 iron at highest temperature (205 °C) over a bake paper. Laminating of the devices was done using automatic Fellowes Cosmic A4 laminating machine with using Fellowes Impress A4 Laminating pouches (100 μm). Next micodevices were prepared as cut paper strips (as channels) which were carefully inserted into the laminating pouch by tweezers and directly laminated. Finally, cut laminated pouches were used instead of cut paper strips to form paper-free channels, too. Microscopic observations were done by the optical microscope Motic 102M equipped with a CCD camera.

3. Results and discussion

First, we studied simple coverage of wax-printed paper-based microfluidic device by the laminating pouch. We found that the reagent zone is stable for more than 14 days and the laminating pouch prevent the chip and reagents also against e.g. low and high humidity or accidental spills onto the chips. The same results were achieved also for paper strips laminated in the pouch. The microscopic view of the laminated paper strip is in Fig. 1. As can be seen, the paper is fully covered by the laminating foil.

When the chip should be used, the laminating foil is simply cut in the place where the channel starts or a drop of analyzed liquid is placed onto the chip and the foil is

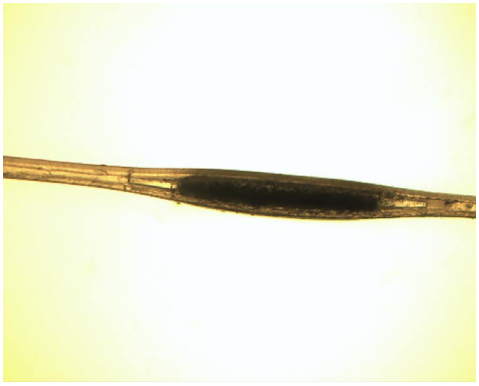

Fig. 1. **Microscopic view of the paper strip laminated in the pouch**

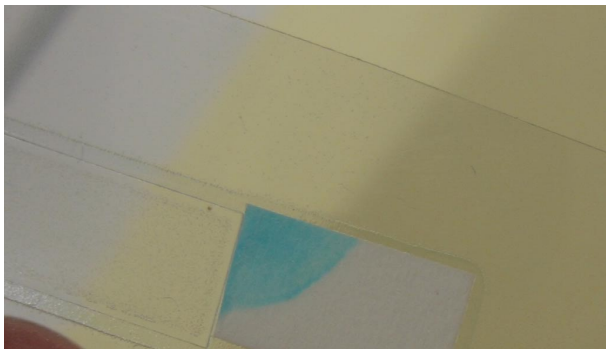

Fig. 2. **Laminated pouch-based channel with a paper-based reagent pad**

perforate by a needle. Channels in the laminating pouch can be also differently crossed allowing division of the flow or they can be bridged using a piece of parafilm between them.

Finally, a pouch laminated in advance was cut and used instead of a cut paper strip to form paper-free channels. This type of channel misses some positive effects of the paper as adhesion or partitioning but the liquid flow is much faster. Moreover, this channel can be also connected with the paper-based fluidics using paper pads as reagent zones (Fig. 2).

4. Conclusions

In this work, we designed low-cost microfluidic platforms based on the use of an office laminating machine that forms cheap and high-throughput types of analytical microdevices. We believe that our work proved the concept of using laminating pouches as covers of the chips as well as the supply for channels fabrication.

Authors gratefully acknowledge the financial support by the Operational Program Research and Development for Innovations – European Regional Development Fund (project CZ.1.05/2.1.00/03.0058) and the Operational Program Education for Competitiveness – European Social Fund (projects CZ.1.07/2.3.00/20.0018 and CZ.1.07/2.3.00/35.0023).

REFERENCES

1. Yager P., Edwards T., Fu E., Helton K., Nelson K., Tam M. R., Weigl B. H.: Nature *442*, 412 (2006).
2. Martinez A. W., Phillips S. T., Butte M. J., Whitesides G. M.: Angew. Chem. Int. Ed. *46*, 1318 (2007).
3. Petr J., Svobodová P., Vojtková L., Suchomelová A., Přibylka A., Knob R.: *MicroTAS 2013 Proceedings*, p. 1902 (2013).
4. Cassano C. L., Fan Z. H.: Microfluid. Nanofluid. *15*, 173 (2013).

THIN METAL FILMS FOR DETECTION AND PRECONCENTRATION

PAVEL PODEŠVA and FRANTIŠEK FORET

Institute of Analytical Chemistry, Brno, Czech Republic
podesva@iach.cz

Summary

Thiol specific sensor, based on measurement of the resistivity change was developed. The sensor can be regenerated many times, has a large dynamic range and its surface can be easily modified by deposition of metal nanoparticles for increased capacity.

1. Introduction

The chemiresistor is the sensor, which changes its resistivity with change of adjacent chemical environment[1,2]. In this work it is the gold thin film sensor[3] interacting with thiols in liquid phase When a thiolated molecule adsorbs on the gold surface[4,5], the covalent bond between the sulphur and gold atom is established with 50 % of C-C bond strength[6] and this effect can be represented by shift in resistance up to 5 % (ref.[7]). After washing the sensor surface, the chemisorbed thiolated compounds can be released by electric current generated by a voltage applied between the gold surface and regeneration electrode and used for further analysis. For enhancement of the retention capacity, the gold surface was modified by Au nanoparticles.

2. Experimental

2.1. Hardware

The device was constructed as a droplet plate with four circuit blocks, each with four sensing elements (spots) arranged in the Wheatstone bridge where only one element in block was used at a time when using as sensor, or as a retention column. The first metal layer was prepared by lift-off lithography and sputtering process using 3'' quartz glass. In next step was using classic lithography process for preparing a hydrophobic coating around the sensor surface. Sample was placed on the test spot by pipette in volume 25–100 μl. The sensing spots were surrounded with hydrophobic coating, keeping the drop in position.

2.2. Chemistry

To enhance the surface capacity the spot was modified by deposition of gold nanoparticles. We used the method according to ref.[8] using the well-known citrate stabilized gold colloid solution mixed with water solution of hydroquinone where 100 ml of the gold colloid was placed on each spot of the selected section, and a disc-shaped counterelectode was in contact of the top of the droplets. After applying the voltage hydroquinone was oxidized into benzoquinone producing H+ ions, canceling the charge of the citrate layer resulting in the formation of Au aggregates.

3. Results and discussion

Experiments have shown, that controlled deposition of a porous film of gold nanoparticles is possible and that the film of the Au aggregates forms much faster on the positive electrode when compared to the unconnected or negative electrode. After deposition the Au film was washed with water and baked in to decompose the remaining organics in the layer.

Financial support from the Grant Agency of the Czech Republic (P301/11/2055) and the institutional support RVO: 68081715 is acknowledged. Part of the work was realized in CEITEC – Central European Institute of Technology with research infrastructure supported by the project CZ.1.05/1.1.00/02.0068 financed from European Regional Development Fund.

Fig. 1. **Detail of the deposited layer of the gold nanoparticles (wide strips) and uncovered counterelectrode (~ 100 μm narrow strip)**

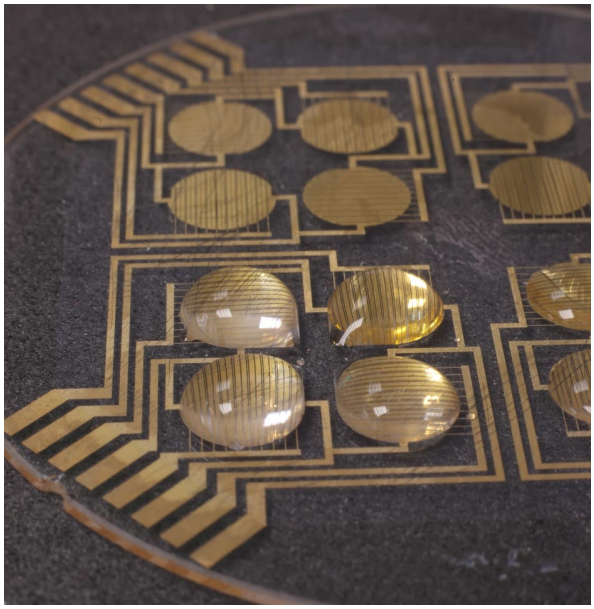

Fig. 2. **Overall view of sensor. Front section is holding droplets on spots**

REFERENCES

1. Podesva P., Foret F.: Curr. Anal. Chem. *9*, 642 (2013).
2. Tucceri R.: Surf. Sci. Rep. *56*, 85 (2004).
3. Tellier C. R.: Active and Passive Electronic Components *12*, 9 (1985).
4. Flynn N. T., Tran T. N. T., Cima M. J., Langer R.: Langmuir *19*, 10909 (2003).
5. Schonenberger C., Jorritsma J., Sondaghuethorst J. A. M., Fokkink L. G. J.: J. Phys. Chem. *99*, 3259 (1995).
6. Fried G. A., Zhang Y. M., Bohn P. W.: Thin Solid Films *401*, 171 (2001).
7. Riu J., Maroto A., Rius F. X.: Talanta *69*, 288 (2006).
8. Xu Y. Z., Zhang Y. R., Zheng J. F., Guo C., Niu Z. J., Li Z. L.: Int. J. Electrochem. Sci. *6*, 664 (2011).

PLASMA FREE METANEPHRINES AS DIAGNOSTIC MARKERS OF PHEOCHROMOCYTOMA

LENKA PORTYCHOVA[a], ZORA NYVLTOVA[b], ALICE BRABCOVA VRANKOVA[c], MICHAL BARTOS[b], MICHAELA PILAROVA[a], IVAN VERMOUSEK[a], MIROSLAV ANTAL[b], and ALES HORNA[a]

[a] RADANAL Ltd., Pardubice, [b] Research Institute for Organic Synthesis Inc., Rybitvi, [c] 3rd Internal Department, 1st Faculty of Medicine and General Teaching Hospital, Charles University in Prague, Czech Republic
Lenka.Portychova@vuos.com

Summary

Quantitative determination of catecholamines and their O-methyl metabolites plays an important role in the diagnosis of pheochromocytoma (PHEO) – adrenal medulla tumour. This kind of tumour synthesizes, stocks, metabolizes and mostly secretes catecholamines. For this reason it is possible to use elevated concentrations of catecholamines and their metabolic products from plasma and urine as diagnostic markers of this tumour. Determination of metanephrines is often preferred against determination of catecholamines regarding the diagnosis of PHEO. Tumour cells produce free metanephrines continuously and irrespective of the release of catecholamines.

The project aims to develop a new kit for the determination of plasma metanephrines. Solid phase extraction (SPE) was used for the pre-treatment of plasma samples. The determination was performed by high performance liquid chromatography with electrochemical detection (HPLC-ED).

1. Introduction

Catecholamines are organic compounds derived from the amino acid tyrosine[1]. Tyrosine is produced in the human body by hydroxylation of phenylalanine[2], the metabolism is shown in Fig. 1. Catecholamines act as hormones or neurotransmitters. These substances are produced by the central nervous system or the adrenal medulla. In a healthy human body there are these compounds and their metabolites represented in very small amounts (pmol L^{-1})[3,4]. Higher levels of catecholamines and their metabolites are in the body caused by stress, physical exertion, pain, emotional distress, etc. Extremely high levels of catecholamines and metabolites are caused by neuroendocrine tumours of the adrenal medulla, which include e.g. pheochromocytoma[5].

PHEO synthesizes, stocks, metabolizes and mostly secretes catecholamines. These compounds and their metabolic products are used as diagnostic markers of the mentioned tumour[4]. The determination of metanephrines, particularly metanephrine (MN), normetanephrine (NMN) and 3-methoxytyramine (3-MT), is often preferred against the determination of catecholamines regarding the diagnosis of pheochromocytoma. Tumour cells produce free metanephrines continuously and irrespective of the release of catecholamines[5,6]. Furthermore, 3-MT indicates tumour metastasis[7].

2. Experimental

2.1. Chemicals and equipment

All chemicals, standards and reagents were purchased from Sigma-Aldrich (St. Louis, MO, USA). Water was deionized and purified in the Select Neptune Ultimate water purification system (Purite, Oxon, UK).

HPLC mobile phase was prepared by mixing prepared solutions A and B (1:1). An acetonitrile was added to the

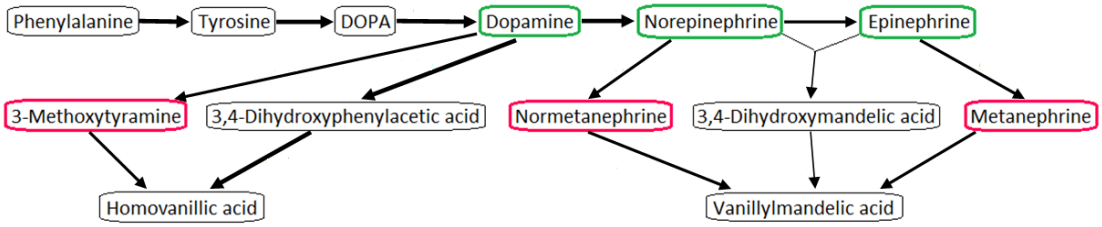

Fig. 1. **Metabolism of phenylalanine** (DOPA = dihydroxyphenylalanine)

mixture, pH of the mobile phase was 2.94 after adjusting. The solution was filtered through 0.22 μm nylon membrane filter (Membrane Solutions, North Bend, OH, USA).

The acidity of the mobile phases was measured by pH meter WTW 526/538 (Wissenschaftlich-Technische Werkstätten, Weilheim, Germany) with SCHOTT chloride electrode (pH 0...14/-5 ... +80 °C / Gel, SCHOTT AG, Mainz, Germany).

Solid phase extraction of metanephrines from plasma was carried out with the equipment Visiprep SPE Vacuum Manifold (Supelco, Bellefonte, PA, USA) using a vacuum pump. The Discovery DSC-SCX cation exchanger and the Discovery DSC-SAX anion exchanger (both from Supelco) were used for a preparation of ion-exchange columns.

Simple apparatus of nitrogen cylinder, equipment for reducing and controlling the gas pressure on the cylinder and system for purifying nitrogen with activated charcoal were used for the evaporation of samples. The samples were placed in the heating block Multi-Blok Heater (Lab-Line Instruments, Inc., Bombay, India) to accelerate the evaporation.

2.2. Instrumentation

The chromatographic system consisted of the Ultimate 3000 Series pump, the Ultimate 3000 Series ACC-3000 autosampler (both from Thermo Fisher Scientific, Inc., Waltham, USA) and a Coulochem III detector containing one conditioning cell (Model 5021A) and one analytical cell (Model 5011A) (ESA, Inc., Chelmsford, USA). The guard column UHPLC C18 4.6 mm ID Column (Phenomenex, Torrance, USA) and the analytical column Kinetex XB-C18 100 × 4.6 mm (5 μm) (Phenomenex) were used.

2.3. Working conditions

2.3.1. Pre-treatment of human plasma sample

To activate the ion-exchange matrix we passed through the extraction columns 5 mL (two times 2.5 mL) of a mixture of a dilution of concentrated ammonium hydroxide and methanol, followed by 2 mL of a phosphate buffer and 2 mL of deionized water. 1 mL volume of plasma with internal standard 4-hydroxy-3-methoxy-benzylamine (HMBA) was passed through the column. The ion-exchange matrix was then rinsed with 2 mL of a phosphate buffer, 2 mL of deionized water and 2 mL of methanol. Metanephrines were eluted from the column with 2 mL of a mixture of the dilution of concentrated ammonium hydroxide and methanol. The eluate was evaporated and the residue was dissolved in 220 μL of mobile phase, of which 150 μL was injected onto the chromatographic column.

2.3.2. HPLC/Coulochem analysis

The column was heated to 28 °C, the autosampler temperature was set at 8.5 °C and a flow rate of mobile phase at 0.7 mL min^{-1}. The potential of conditioning cell was set at +400 mV. The working potentials were +100 mV (1st electrode) and –350 mV (2nd electrode). The sensitivity was set at 50 nA.

3. Results and discussion

During the development of the kit we have progressively optimized the whole method. Pre-treatment of plasma sample, solid phase extraction procedure, mobile phase composition and conditions of the analysis were optimized.

3.1. Optimization of the sample pre-treatment

A centrifugation of plasma sample was tested with different reagents and also without them. As an addition to the plasma sample before centrifugation were tested acetonitrile, ethanol, methanol, isopropanol, and various concentrations of perchloric acid, acetic acid, trifluracetic acid, meta-phosphoric acid, hydrochloric acid and formic acid. Different rotations per minute and various temperature and duration were also tested. None of the examined methods of centrifugation proved. Metanephrines are therefore extracted (using SPE) from untreated plasma samples.

Solid phase extraction was tested by using a range of commercially available SPE columns and several types of sorbents. These sorbents were used for filling empty columns (volume 3 mL). The columns filled with a mixture of Discovery DSC-SCX and Discovery DSC-SAX are the most appropriate to extract metanephrines from plasma samples. The SPE procedure was also optimized to achieve the highest possible yields of MN, NMN and 3-MT.

3.2. Optimization of HPLC/Coulochem analysis

As the mobile phase were tested various types of buffers and different ratios of individual components within them. The most suitable water for preparation of the mobile phase for Coulochem was also chosen based on the tests. Now we use a mixed buffer adjusted to pH 2.94 (containing acetonitrile and water prepared in the Select Neptune Ultimate water purification system).

Metanephrines were separated on several different columns: LiChroCART RP-18 125 × 4 mm (5 μm) (Merck, Darmstadt, Germany); Poroshell 120 SB-C18 150 × 4.6 mm (2.7 μm) (Agilent Technologies, Santa Clara, CA, USA); Poroshell 120 SB-C18 100 × 4.6 mm (2.7 μm) (Agilent); Kinetex XB-C18 100 × 4.6 mm (5 μm) (Phenomenex) and Kinetex Phenyl-Hexyl 150 × 4.6 mm (5 μm) (Phenomenex). The column Kinetex XB-C18 100 × 4.6 mm (5 μm) is the most suitable. The best responses of metanephrines were determined on the column Kinetex Phenyl-Hexyl 150 × 4.6 mm (5 μm) but the internal standard HMBA eluted too close to metanephrine. The

Table I
Comparison of analysis results of plasma samples with increased levels of metanephrines detected in our laboratory and in the laboratory of 1st Faculty of Medicine (Charles University in Prague)

	Measured at the Charles University		Our measurements	
Sample No.	NMN [pg mL^{-1}]	MN [pg mL^{-1}]	NMN [pg mL^{-1}]	MN [pg mL^{-1}]
328	46	317	54	364
368	977	710	1011	623
410	2901	72	2855	92
432	187	41	187	45
449	168	53	179	58
464	1139	284	1153	263

Metanephrine occurs in a healthy human body in the maximum concentration of 100 pg mL^{-1} and normetanephrine in the max. concentration of 160 pg mL^{-1}. At least one of the analytes (NMN, MN) in the tested plasma samples (Table I) exceeds the limit value. Patients (who have been taken plasma samples) have probably the tumour pheochromocytoma in their body.

analysis would have to take at least 35 min to separate these two peaks sufficiently. It would be possible to use e.g. the internal standard 3,4-dihydroxybezylamine instead of HMBA. This is still a subject of research.

The column temperature was chosen 28 °C in order to having a robust method usable also in warmer summer days. Flow rate is set at 0.7 mL min^{-1} to obtain a lower pressure in the system.

A current-voltage curve of MN, NMN, 3-MT and HMBA was measured to optimize the potentials of the detector cells. The potentials were set at +400 mV (the conditioning cell), +100 mV (1st electrode) and –350 mV (2nd electrode).

3.3. Analysis of plasma samples with increased levels of metanephrines

We analyzed plasma samples from the laboratory of 1st Faculty of Medicine (Charles University in Prague) which were evaluated as positive. Comparison of the values that were measured in the Prague laboratory with values that were measured in our laboratory is shown in Table I.

4. Conclusions

The developed method can help identify plasma samples of persons who have the tumour pheochromocytoma. Total analysis time is 22 min (for the determination of metanephrine, normetanephrine and 3-methoxytyramine in plasma samples). Currently we are completing the optimization of our method in order to determining the lowest possible limit of detection and the lowest possible limit of quantification. The project ends in December 2014.

This work was supported by Ministry of industry and trade of Czech Republic (project FR-TI4/331).

REFERENCES

1. Purves D., Augustine G. J., Fitzpatrick D., Hall W. C., LaMantia A. S., McNamara J. O., White L. E.: *Neuroscience,* 4. vyd., Sinauer Associates Inc., Sunderland 2007.
2. Joh T. H., Hwang O.: Ann. N.Y. Acad. Sci. *493*, 342 (1987).
3. Raggi M. A., Sabbioni C. Casamenti G., Gerra G., Calonghi N., Masotti L.: J. Chromatogr., B *730*, 201 (1999).
4. Kršek M.: *Endokrinologie* Galén, Praha 2011.
5. Pacák K.: *Feochromocytom*, Galén, Praha 2008.
6. http://neuroendokrinni-nadory.cz/downloads/diagnostika-nen-vysetreni.pdf, 13. 3. 2013.
7. Eisenhofer G., Lenders J. W. M., Siegert G., Bornstein S. R., Friberg P., Milosevic D., Mannelli M., Linehan W. M., Adams K., Timmers H. J., Pacák K.: Eur. J. Cancer *48*, 1739 (2012).

LOW-COST 3D-PRINTED FLUORESCENCE DETECTOR FOR CAPILLARY ELECTROPHORESIS

JAN PŘIKRYL[a,b] and FRANTIŠEK FORET[a]

[a] *Institute of Analytical Chemistry of the ASCR, v. v. i., Brno,* [b] *Department of Chemistry, Faculty of Science, Masaryk University, Brno, Czech Republic*
prikryl@iach.cz

Summary

We have verified the possibility of Fused Deposition Modeling (type of additive manufacturing) for lab-made construction of inexpensive fluorescence detector for capillary electrophoresis using commercially available optical components. Sensitivity of fabricated and assembled detection system was tested by fluorescein solutions. Limits of detection were determined for several tested arrangements.

1. Introduction

Additive manufacturing, also known as 3D printing, has become an important method of fabrication, especially prototyping. Applications of 3D print ranges from industrial fabrication of prototypes to making of models in architecture, biology or geology. Especially, the usage in medicine is noteworthy, where it is used both for manufacturing of models (pre-surgical preparing) and functional parts (custom-made implants)[1]. Recently, fabrication of fluidic device as an application in the analytical chemistry was published[2].

Fabrication by FDM is one of the least expensive methods of additive manufacturing and therefore it could be taken this advantage to make low-cost fluorescence detection system. Despite of the quite high cost of fluorescence detection, it is widely used and a number of different approaches for construction of low-cost detectors has been described[3,4].

Fluorescence, especially Laser (or LED) induced, provides sensitive and selective detection of analytes often in the sub-picomolar range. In separation methods including liquid chromatography and capillary electrophoresis or in microfluidic devices it is so far the most sensitive detection technique. In capillary techniques and, especially, in the microfluidic devices the spatial limitations predetermine the epifluorescence arrangement to become more favorable when compared to classical orthogonal arrangement, profiting from usage of the same objective lens for sample excitation and for collection of emitted fluorescence[5].

2. Experimental

The chassis of the fluorescence detection system, as well as cover lid and capillary holder, was designed in the user-friendly 3D-modeling software SketchUp (Trimble Navigation, Ltd., USA) and printed by using the FDM printer EASY3DMAKER (AROJA, s. r. o. , Czech Republic) from black PLA (polylactic acid).

Fused silica capillary (75 μm I.D.) was used as a sample cuvette. Other optical elements, such as optical filters and lenses, were purchased from Edmund Optics GmbH (Germany). The collected fluorescence emission was detected either by a photomultiplier tube (R647, Hamamatsu, Japan) or by a photodiode (ODA-6WB-500M, Opto Diode Corp., USA). Blue emitting LED with the emission maximum at 470 nm (Opto Diode Corp., Newbury Park, USA) coupled to a 400 mm optical fiber (Thorlabs, USA) was used as the excitation source.

Testing fluorescein solutions (pH 9.3) consisted of fluorescein (Reactifs RAL, France), sodium tetraborate decahydrate (LACHEMA, Czech Republic) and methanol (99.8%, PENTA, Czech Republic).

3. Results and discussion

The chassis of the fluorescence detector was printed from PLA and optical elements were located in designed slots. For the detector performance characterization we have measured solutions of fluorescein for construction of calibration curves and determination of limits of detection (LODs), which were calculated as a threefold standard deviation of six blank solutions signals. The LOD was 9.2×10^{-11}M with detection by the photodiode and 1.0×10^{-11}M with detection by the photomultiplier tube. It is worth mentioning that expensive photomultiplier tube was only approximately ten-times more sensitive compared one-tenth-price photodiode in our arrangement.

4. Conclusions

In this study, we presented a new possibility for fabrication of inexpensive fluorescence detection system using a 3D printer and tested its performance as a detector for capillary techniques. The 3D printing provides an excellent way to fabricate all mechanical parts with sufficient precision and allows rapid modifications to be made during the system development.

The research was financially supported by Grants of the Grant Agency of the Czech Republic (P206/12/G014), the Academy of Sciences of the Czech Republic (M200311201) and Research Plan of the Institute of Analytical Chemistry of the ASCR, v. v. i. (RVO:68081715). This project is co-financed by the European Social Fund and the state budget of the Czech Republic (CZ.1.07/2.3.00/20.0182).

REFERENCES

1. Giannatsis J., Dedoussis V.: Int. J. Adv. Manuf. Technol. *40*, 116 (2009).
2. Anderson K. B., Lockwood S. Y., Martin R. S., Spence D. M.: Anal. Chem. *85*, 5622 (2013).
3. Novak L., Neuzil P., Pipper J., Zhang Y., Lee S. H.: Lab Chip *7*, 27 (2007).
4. Wu J., Liu X., Wang L., Dong L., Pu Q.: Analyst *137*, 519 (2012).
5. Kuswandi B., Nuriman Huskens J., Verboom W.: Anal. Chim. Acta *601*, 141 (2007).

OPTIMIZATION OF A NEW CLOUD POINT EXTRACTION PROCEDURE FOR DETERMINATION OF TRACE AMOUNTS OF COPPER IN HUMAN URINE

SIMONA PROCHAZKOVA, LENKA OKENICOVA, and RADOSLAV HALKO

Department of Analytical Chemistry, Faculty of Natural Sciences, Comenius University in Bratislava, Bratislava, Slovakia
curmova@fns.uniba.sk

1. Introduction

Copper (Cu) is an essential trace element for humans. It plays an important role in many biological processes. In human body, even a small amount of copper affects various enzymes as a powerful catalyst. In the human organism, Cu ions can exist in both an oxidized, cupric Cu (II), and reduced, cuprous Cu(I), state. The highest concentrations of copper are discovered in the brain and the liver. The central nervous system and the heart have high concentrations of copper as well. About 50 % of copper content is stored in bones and muscles. The total copper content of the adult body is typically between 70 and 80 mg (ref.[1]). Increased copper content in the human body is clearly seen in genetic diseases of metabolism like Wilson's disease. It was found that Cu content in the liver of patients with Wilson's disease is about 25 times higher than in healthy subjects. Wilson's disease requires very specific medication and its late deployment can lead to death of the patient after the age of 30 years[2]. Urinary copper is derived from the so-called free (non-ceruloplasmin-bound) copper circulating in plasma. In Wilson's disease, the 24h urinary copper excretion is increased, and the concentration taken as suggestive of disease is greater than 100 μg per 24h (>1.6 μmol per 24 h). The reference limits for normal 24 h excretion of copper very between laboratories, with many taking 40 μg per 24 h (0.6 μmol per 24 h) as the upper limit of normal[3]. The determination of trace copper in biological samples is particularly difficult because of the complex matrix and the usually low concentration of copper, which requires sensitive instrumental techniques and frequently a pre-concentration step. Micelles and other organized amphiphilic assemble are increasingly utilized in analytical chemistry especially in separation and pre-concentration procedures.

2. Experimantal

2.1. Apparatus

A Perkin-Elmer model 1100B (Norwalk, Connecticut, USA) atomic absorption spectrometer equipped with a copper hollow-cathode lamp as a radiation source was used throughout the measurement. The acetylene flow rate and the burner height were adjusted in order to obtain the maximum absorbance signal, while aspirating the analyte solution in 1% nitric acid in water. Data evaluations are made from integrated absorbance values. CPE experiments were performed using a thermostated bath (Avalier, Czech Republic), maintained at the desired temperature. Phase separation was assisted using a centrifuge mlw T30 (Janetzki, Germany) in 25 mL calibrated centrifuge tubes. pH meter AT 3200P (Agilent Technologies, California, USA) and analytical balances AR 0640 (Ohaus, USA) were used for another analytical procedures. PRO-PS Labconco (Cansas City, USA) was used for producing of deionized water.

2.2. Reagents

All chemicals were of analytical-reagent grade and were used without previous purification. Calibration solutions of Cu(II) were prepared by successive dilution of stock solution of pure Cu(II) (Merck, Darmstadt, Germany). The chelating agent 2,9-dimethyl-1,10-phenanthroline (Neocuproine) from (Sigma-Aldrich, Steinheim, Germany) was prepared by dissolving appropriate amounts in 20% (v/v) methanol. The non-ionic surfacant Triton X-114 (Fluka, Buchs, Switzerland) was used without further purification. The desired pH of the solutions was adjusted by using ascorbic acid (Merck, Darmstadt, Germany) and ammonium acetate (Merck, Darmstadt, Germany).

3. Results and discussion

For the CPE, aliquots of 25 mL solution containing sample or standard solution (0.10 mg L^{-1}) of copper ions, Triton X-114 (1%) and neocuproine (0.10 mmol L^{-1}) buffered at suitable pH (0.05% (v/v) ascorbic acid/0.50% (v/v) ammonium acetate). The mixture is heated in a thermstated bath at 70 °C for 15 min. Separation of the two phases is accelerated by centrifuging at 3500 rev min^{-1} for 10 min. At that point, the initial solution separated into two phases: one bulk containing the surfacant monomers and surfacant-rich phase small volume containing containing the surfacant monomers and surfacant-rich phase small volume containing the trapped metal by micelles. Developed method is based on the reaction of neocuproine with Cu(I) which forms orange-yellow stable and hydrophobic chelate in a neutral or slightly acidic buffer solution. Cu(II) was reduced to Cu(I) ions by ascorbic acid as a weak reducing reagent, which was added to buffer solution. On cooling in an ice-bath for 10 min, the surfacant-rich phase became viscous and was

Table I
Analytical characteristics of the proposed method

Analytical parameters	Copper
Regression equation	A = 0,0487x + 0,0027; R^2 = 0,9998[a];
(*n* = 6)	A =1,9344 x + 0,0017; R^2 = 0,9997
LOD [mg L^{-1}]	0,255[a]; 0,042
Pre-concentration factor	20
Enrichment factor	40

[a] Analytical characteristic for copper without pre-concentration

retained at the bottom of the tubes. The aqueous phases can readily be discarded simply by inverting the tubes. To decrease the viscosity of surfacant-rich phase, methanolic solution of 1% (v/v) HNO_3 was added. The final solution was introduced into the nebulizer of the spectrometer via a manual sample injector. Our results are in Figure 1–4. The effects of experimental conditions such as pH, concentration of chelating agent and surfactant and equilibration temperature on recovery were studied.

A comparison of the basic analytical characteristics of the proposed methods with and without application of pre-concentration by CPE is summarised in Table I.

Optimized CPE approach has been used for the selective determination of Cu(II) in the sample of human urine. The results obtained are shown in Table II. After adding 0.05 and 0.10 mg L^{-1} Cu(II) to these samples were calculated extraction recovery, which ranged 85–90 %.

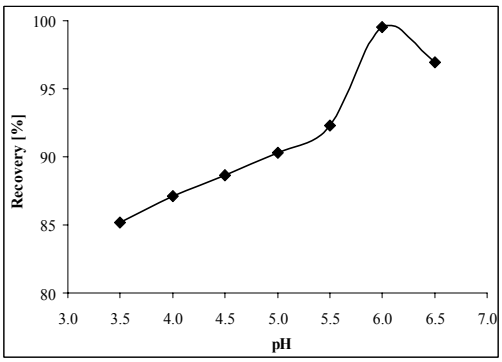

Fig. 1. **Effect of pH**

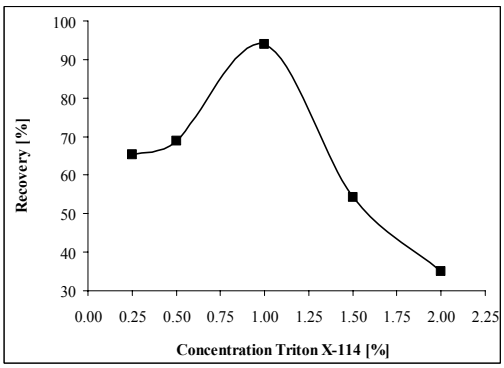

Fig. 3. **Effect of Triton X-114 concentration**

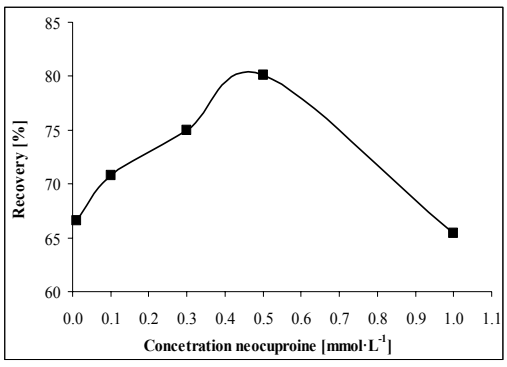

Fig. 2. **Effect of neocuproine concentration**

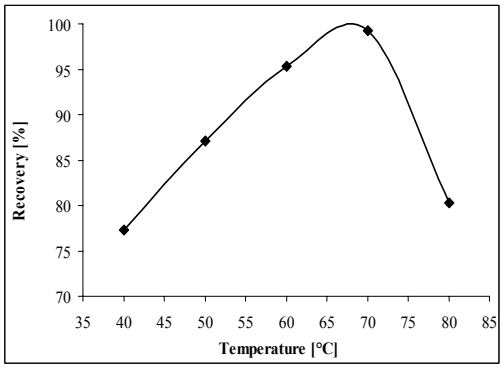

Fig. 4. **Effect of equilibrium temperature**

Table II
The results of the determination of copper in human urine sample

Biological sample	Added Cu(II) [mg L^{-1}]	Determined concentration[a] [mg L^{-1}]	Recovery [%]	RSD [%]
Human urine	0	–[b]	–[b]	–[b]
Human urine	1	0,910 ± 0,002	90	4,56
Human urine	2	1,646 ± 0,003	85	3,74

[a] Mean values (n = 4), pre-concentration factor 20; [b] has not been established

4. Conclusion

Cloud point extraction on nonionic surfactant was developed for the determination and speciation of Cu(II) in human urine samples by FAAS. The procedure is inexpensive, because it consists of much low equipment and running costs such as FAAS, which is available in most laboratories. The methodology offers a simple, rapid, sensitive and inexpensive alternative to other separation pre-concentration techniques with the concomitant benefits from the use of CPE safety, cost, high separation yield, and possibility to select the proper surfactant and versatility.

This work was generously supported by the grant of project VEGA 1/0852/13, Grant Comenius University UK/308/2013 and the grant of project APVV-0583-11. This work is partially outcome of the project VVCE-0070.

REFERENCES

1. Copper Development Association Inc. [Cited: 27. september 2013 < http://www.copper.org/consumers/health/papers/cu_health_uk/cu_health_uk.html >]
2. Huster D.: Best Pract. Res. Clin. Gastroenterol. *24*, 531 (2010).
3. Linder M. C., Hazegh-Azam M.: Am. J. Clin. Nutr. *63*, 797 (1996).

REMOVAL OF ABUNDANT PROTEINS TO ENABLE GLOBAL PROTEOME ANALYSIS OF THE HUMAN PLASMA: QC METHODLOGY DEVELOPMENT USING IMMUNOGLOBULIN AND ALBUMIN AS MARKERS

MÁRTA RÁCZ[a], LÁSZLÓ TAKÁCS[b], ANDRÁS GUTTMAN[a], and JÓZSEF LÁZÁR[b]

[a] *Horvath Laboratory of Bioseparation Sciences, University of Debrecen, Debrecen, Hungary,* [b] *BioSystems International Kft. Debrecen, Hungary*
racz.marta@hlbs.org

Summary

Global proteome analysis is important for the discovery of novel disease specific biomarkers and for the ultimate development of protein based diagnostics. In order to access the proteome at the low ng mL^{-1} (or below) range, abundant plasma proteins need to be removed, and both, affinity and MS based technologies necessitate this step. Removal of abundant plasma proteins is achieved by antibody affinity depletion or specific matrices (i.e. Sepharose blue, and Thiophilic adsorbent resin) that bind abundant plasma proteins. Here, we present albumin and IgG, the most abundant human plasma proteins, as indicators of sample quality for proteome analysis.

1. Introduction

For biomarker discovery, our laboratory deploys monoclonal antibody (mAb) proteomics, which profiles cognate epitope specific changes of the proteome. We have demonstrated earlier that specific changes of epitope dynamics, including but not limited to changes in protein concentration are associated with disease conditions like, cancer or chronic inflammatory disease of the lung[1–3]. During the proximal phase of the mAb-s discovery process (before the development of sandwich ELISAs) technology sensitivity depends on the accessibility of medium-low concentration range fraction of the plasma proteome, and this is achieved by the removal of abundant proteins[4]. Instead of testing each individual protein targeted by the depletion device(s) and to qualify broader specificity affinity resins, we tested albumin (HSA) and IgG, the most abundant plasma proteins for the quality analyis of abundant bprotein depletion.

2. Experimental

2.1. Chemicals

For depletions Blue Sepharose 6 Fast Flow (from GE Healthcare) resin and Pierce Thiophilic Adsorbent (Thermo Scientific) were used. In ELISA experiments Human IgG and Serum Albumin (for calibration) purchased from Sigma-Aldrich (St. Louis, MO, USA), mouse monoclonal antibodies and secondary biotinilated antibodies produced by BioSystems International Kft. (Debrecen, Hungary).

2.2. Depletion of human serum samples, origin of examined samples

1 mL human plasma was depleted with the Blue Sepharose 6 Fast Flow resin. After the albumin depletion immunoglobulins were removed by the Pierce Thiophilic Adsorbent. Before the ELISA experiments the total protein concentration of the samples were also determined by BCA protein assays.

2.3. Sandwich ELISA technology

ELISA plates were coated with the appropriate capture antibody (10 ug mL^{-1} an hour long at 37 °C). After washing (2X) and blocking samples and calibrator protein were applied in serial dilution and incubated for 1 h at 37 ° C. After this, plates were washed 4 times between each step. Next secondary antibody (biotinylated) was applied in 5 ug mL^{-1} concentration then streptavidin-HRP was used in 5000-fold dilution. For the enzymatic reaction TMB substrate were added and the reaction was stopped with 4 normal H_2SO_4. Chemiluminescent signals were measured at 450 nm (Multiscan Ascant Reader,Thermo Scientific, Hudson, NH, USA). Sample concentrations were calculated from the linear equation fitted to the points located on the ascending part of the calibrator curve.

3. Results and discussion

In order to reliably measure HSA and IgG concentration we developed specific sandwich ELISA tests using antigen specific mAb pairs. Figure 1 shows titration curves using the targeted analytes.

As an example, we tested samples of human plasma that has been depleted of HSA and IgG using Sepharose blue, and Thiophilic adsorbent resins[5,6]. With the ELISA test we found that about 99.5 % of IgG were eliminated from the used plasma sample.

Recent developments in the field[7] indicates that depletion of abundant proteins may be done on clinical samples lung cancer diagnostics measurements by MRM-MS and other MS based methodologies. Regulatory agencies do require the development of quality control tests to be applied regularly on the clinical samples for approved diagnostics. We plan to test our simple ELISA

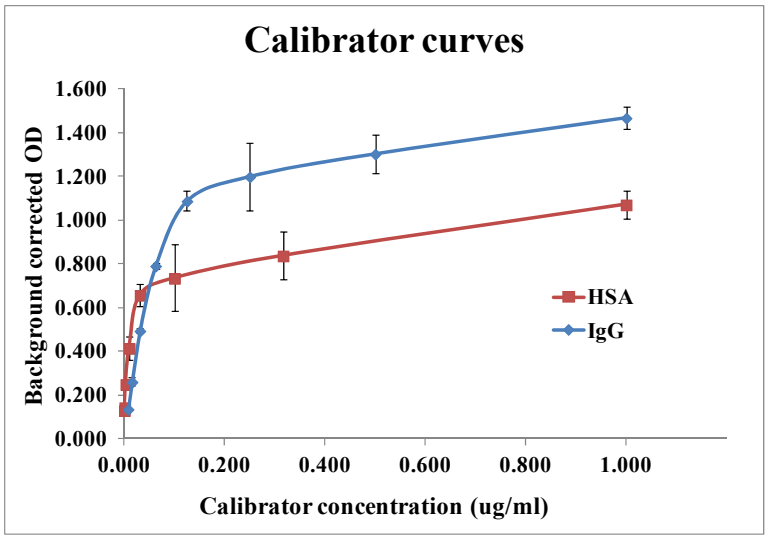

Fig. 1. **Titration curve**

based methodology (including simple devices) in larger scale studies addressing both the research and the potential clinical markets to determine tolerance thresholds for quality acceptance.

4. Conclusions

The simplicity and robustness of the methodology presented here suggest potential wide scale applicability of specific HSA and IgG testing for sample preparation analysis.

REFERENCES

1. Guergova-Kuras M., Kurucz I., Hempel W., Tardieu N., Kádas J., Malderez-Bloes C., Jullien A., Kieffer Y., Hincapie M., Guttman A., Csánky E., Dezso B., Karger B. L., Takács L.: Mol. Cell Proteomics *10,* 10.1074/mcp.M111.010298. (2011).
2. Csanky E., Olivova P., Rajnavolgyi E., Hempel W., Tardieu N., Elesne Toth K., Jullien A., Malderez-Bloes C., Kuras M., Duval M. X., Nagy L., Scholtz B., Hancock W., Karger B., Guttman A., Takacs L.: Electrophoresis *28*, 4401 (2007).
3. Váradi Cs., Mittermayr S., Szekrényes Á., Kádas J., Takacs L., Kurucz I., Guttman A.: Electrophoresis *34*, 2287 (2013).
4. Anderson N. L., Anderson N. G.: Mol. Cell Proteomics *1*, 845 (2002).
5. Kovács A., Sperling E., Lázár J., Balogh A., Kádas J., Szekrényes Á., Takács L., Kurucz I., Guttman A.: Electrophoresis *32*, 1916 (2011).
6. Kovács A., Patai Z., Guttman A., Kádas J., Takács L., Kurucz I.: Electrophoresis doi: 10.1002/elps.201200677. (2013).
7. Park J., Yang J. S., Jung G., Woo H. I., Park H. D., Kim J. W., Huh W., Ko J. W., Kim H., Cho J. Y., Lee S. Y.: J. Proteomics *94*, 302 (2013).

OPTIMIZATION OF ELECTROCHEMICAL OXIDATION OF ERYTHROMYCIN

MONIKA RADIČOVÁ, RÓBERT BODOR, and JOZEF MARÁK

Department of Analytical Chemistry, Faculty of Natural Sciences, Comenius University, Bratislava, Slovak Republic
radicova@fns.uniba.sk

1. Introduction

Several analytical methods have been used to metabolic studies of numerous xenobiotics. *In vivo* experiments with laboratory animals and *in vitro* experiments with liver microsomes belong to the mostly used approaches[1]. Recently, considerable attention has received the using of a method based on electrochemistry/ mass spectrometry (EC/MS) coupling to simulate oxidative phase I metabolism. Mass voltammograms generated by EC/MS technique provide a direct overview of oxidation products that may also be formed in the human body[2]. Electrochemical oxidation is preferable to *in vitro* oxidation using cytochrome P450 enzymes because it does not use any biomolecules (including enzymes or cofactors). Consequently, obtained oxidation products can be separated easily with minimal contamination or detected without the interferences from biological matrix. Numerous xenobiotics, such as antibiotics, emitted into the environment may directly influent the ecosystem. Most of them undergo chemical and microbial transformations after exposure to terrestrial or aquatic system. It is known that important degradation pathways of xenobiotics in the environment usually involve a redox reaction mechanism[3]. Combination of electrochemical techniques with HPLC-MS can constitutes a one way for evaluating and predicting the degradation pathways of various emerging pollutants[4]. Erythromycin is a macrolide antibiotic that has an antimicrobial spectrum comparable to penicillin. A great part of erythromycin is metabolized by demethylation in the liver. Its main elimination route is in the bile and a small amount in the urine[5]. Because of broad using of erythromycin in infection diseases treatment, various methods were developed for its determination. Between often used techniques belongs spectrophotometry in UV-VIS area[6], infrared spectroscopy[7], electrochemistry[8], and liquid chromatography with UV detection[9], electrochemical detection[10] and in combination with mass spectrometry[11]. These techniques were used for determination of erythromycin in different pharmaceutical preparations[6,12], biological samples[13–15], and environmental samples[11,16,17]. The aim of this work was to study and to optimize electrochemical oxidation of erythromycin for flow system connected to mass spectrometry in the next step.

2. Experimental

All measurements were performed on Potentiostat/ Galvanostat PGSTAT128N (Metrohm Autolab B.V., Utrecht, Netherland), which was operated by PC using software NOVA ver. 1.6.010 (Metrohm). Three-electrode system was set in electrochemical cell with glassy carbon electrode (GCE) as working electrode. Stock solution of erythromycin was prepared by dissolving of 10 mg of erythromycin (Sigma Aldrich, Steinheim, Germany) in 1 mL of mixture water: ethanol in 1:1 (v/v) ratio. Before starting electrochemical measurements, nitrogen was bubbled through electrolyte solution, and during measurements, nitrogen was kept above the electrolyte. In this work, two electrochemical methods, i.e. cyclic voltammetry and differential pulse voltammetry, were tested. Measurement conditions for cyclic voltammetry were as follow: an initial potential was –1.9 V and the highest potential was +1.2 V. Measurement conditions for differential pulse voltammetry were as follow: an initial potential was –1.5 V and the end potential was +1.2 V with scan rate 0.05 V/s. Each measurement was repeated 3 times.

3. Results and discussion

Several basic electrolytes were tested for both methods, i.e. sodium hydroxide, sodium carbonate and ammonium acetate. Electrochemical oxidation is possible in all of above mentioned electrolytes and therefore, the choice of the optimal electrolyte was limited by our effort to perform off-line connection of EC with mass spectrometry. Therefore, solution of ammonium acetate was used in next experiments in both cyclic voltammetry (CV) and differential pulse voltammetry (DPV) modes. The records obtained by analyses of blank electrolyte and the electrolyte with the addition of erythromycin to final concentration 81.6 μM using CV and DPV methods, where 10 mM ammonium acetate was used as electrolyte solution, are shown in Figs. 1 and 2. We can see oxidative peak on both records at potential 0.77 V for CV and 0.72 V for DPV respectively. We don't see reductive peak in CV record, therefore we can establish, that oxidation of erythromycin is irreversible.

Various concentrations of ammonium acetate solutions in the range 100–2 mM were tested in both methods. We observed from particular records, that

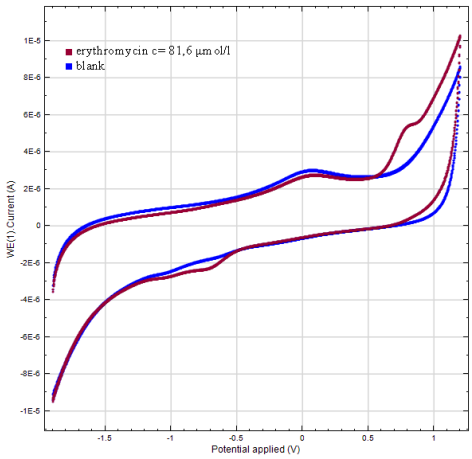

Fig. 1. **Records obtained from CV analysis of blank 10 mM ammonium acetate (pH 8.9) electrolyte and addition of erythromycin to electrolyte to final concentration 81.6 µM**

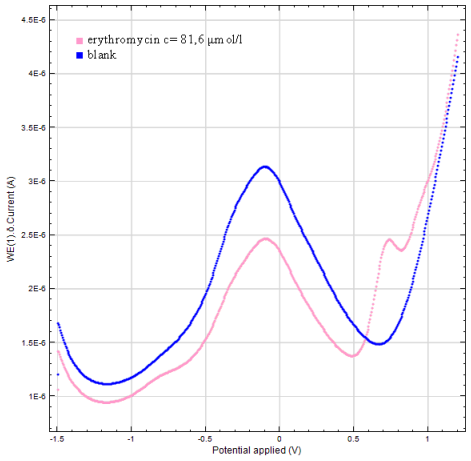

Fig. 2. **Records obtained from DPV analysis of blank 10 mM ammonium acetate (pH 8.9) electrolyte and addition of erythromycin to electrolyte to final concentration 81.6 µM**

optimal concentration of ammonium acetate solution under our experimental conditions is 10 mM. Optimization of scan rate (v) was necessary especially for cyclic voltammetry. Measured values of current in cyclic voltammetry mode increased with increasing scan rate, what was caused by capacitive current. The influence of capacitive current is eliminated in differential pulse technique. We have chosen 100 mV s^{-1} and 50 mV s^{-1} as optimal value of scan rate for CV and DPV, respectively, based on the shape of curve and speed of analysis.

4. Conclusions

Developed method of electrochemical oxidation of erythromycin will be in the next step applied to electrochemical flow cell and further optimized to be suitable for off-line connection with mass spectrometry.

This work was financially supported by the grants of the Slovak Research and Development Agency (project No. VVCE-0070-07 and APVV-0583-11) and the Slovak Grant Agency (grant VEGA No 1/1305/12).

REFERENCES

1. Lohmann W., Karst U.: Anal. Bioanal. Chem. *391*, 79 (2008).
2. Telgmann L., Faber H., Jahn S., et al.: J. Chromatogr., A *1240*, 147 (2012).
3. Tahara K., Nishikawa T., Hattori Y., et al.: J. Pharm. Biomed. Anal. *50*, 1030 (2009).
4. Bussy U., Ferchaud-Roucher V., Tea I., et al.: Electrochim. Acta *69*, 351 (2012).
5. Norouzi P., Daneshgar P., Ganjali M. R.: Mater. Sci. Eng., C *29*, 1281 (2009).
6. Ashour S., Bayram R.: Spectrochim. Acta, Part A *99*, 74 (2012).
7. Qu N., Li X., Dou Y., et al.: Eur. J. Pharm. Sci. *31*, 156 (2007).
8. Avramov Ivić M. L., Petrović S. D., Mijin D. Ž., et al.: Electrochim. Acta *54*, 649 (2008).
9. Van den Bossche L., Lodi A., Schaar J., et al.: J. Pharm. Biomed. Anal. *53*, 109 (2010).
10. de la Huebra M. J. G., Vincent U., von Holst C.: J. Pharm. Biomed. Anal. *43*, 1628 (2007).
11. Dinh Q. T., Alliot F., Moreau-Guigon E., et al.: Talanta *85*, 1238 (2011).
12. Hassib S. T., Farag A. E., Elkady E. F.: Bulletin of Faculty of Pharmacy, Cairo University *49*, 81 (2011).
13. Norouzi P., Daneshgar P., Ganjali M. R.: Mater. Sci. Eng., C *29*, 1281 (2009).
14. Juan C., Moltó J. C., Mañes J., Font G.: Food Control *21*, 1703 (2010).
15. Horie M., Takegami H., Toya K., Nakazawa H.: Anal. Chim. Acta *492*, 187 (2003).
16. Shao B., Chen D., Zhang J., Wu Y., Sun C.: J. Chromatogr., A *1216*, 8312 (2009).

OFF-LINE COMBINATION OF PREPARATIVE ISOTACHOPHORESIS AND SIZE-EXCLUSION CHROMATOGRAPHY IN ANALYSIS OF HUMIC ACIDS

ZDENKA RADIČOVÁ, RÓBERT BODOR, RÓBERT GÓRA, MILAN HUTTA, and MARIÁN MASÁR

Department of Analytical Chemistry, Faculty of Natural Sciences, Comenius University in Bratislava, Bratislava, Slovakia
radicovaz@fns.uniba.sk

Summary

The off-line combination of preparative capillary isotachophoresis (CITP), operating in a discontinuous fractionation mode, and size-exclusion chromatographic method for separation and characterization of humic acids (HAs) was studied in this work. The CITP separations were performed using electrolyte system at pH 10.

The use of three discrete spacers (DSs), injected into the CITP column together with the HAs, allows the spatial separation of humic constituents and their reproducible fractionation using a micropreparative valve (with a volume of 22 μL). The presence of corresponding DSs zones in collected fractions were controlled by analytical CITP in the same electrolyte system as used for preparative CITP.

Individual CITP fractions were off-line analyzed by size-exclusion chromatography (SEC) using 99/1 *N*,*N*-dimethylformamide (DMF)/aqueous phosphate buffer (pH 3.0) with Spheron HEMA 100 stationary phase with photometric (280 nm and 420 nm) and fluorimetric detection (ex. 470 nm/em 530 nm).

1. Introduction

Humic substances (HSs) are ubiquitous natural materials occurring in huge amounts in soils, sediments and waters as a product of the chemical and biological transformation of animal and plant residues. In general, HSs are amorphous, brown or black, acidic and polydisperse, and they have molecular masses in range from several hundreds to tent of thousands[1]. The major extractable components of soil HSs are HAs, which are not soluble in water under acidic conditions but soluble at higher pH (ref.[2]). The importance of separation methods in the chemistry of HAs was recently reviewed by Janoš[3].

Electrophoretic methods have traditionally been employed in investigations of natural polymeric substances[3]. Capillary isotachophoresis (CITP), one of the basic modes of electrophoretic methods, is very useful for micropreparative purposes. Preparative CITP as a discontinuous fractionation technique can be realized by micropreparative valve placed at the end of the capillary. This technique allows isolation of micro amount of ionic analytes to the fractions which could be subsequently analyzed e.g. by chromatographic methods[4]. Among the chromatographic methods those based on size-exclusion effect (SEC) play an important role. SEC is used for measurement of data on relative molecular masses distribution of HAs[5].

2. Experimental

2.1. Instrumentation

An electrophoretic analyzer EA-102 (Villa-Labeco) working in a hydrodynamically closed one-column arrangement (1,5 mm i.d. × 160 mm, made of fluorinated ethylenepropylene (FEP) copolymer) was used for the fractionation of the HAs. The sample solutions were injected by injection valve (150 μL). The micropreparative valve with a volume of 22 μL was placed at the end of column, behind a conductivity detector and used for isolation of the fractions under no current conditions.

An electrophoretic analyzer EA-101 (Villa-Labeco) working in a hydrodynamically closed one-column arrangement (0,3 mm i.d. × 160 mm, FEP) with conductivity detector was used for the analytical CITP control of the collected fractions . Fractions (5 μL) were injected by microsyringe (Hamilton) via the septum.

Preparative and analytical CITP experiments were carried out using chloride at 10 mmol L^{-1} concentration as leading ion. Final pH of leading electrolyte was adjusted with ethanolamine as counter ion to 10.0. Hydroxyethylcellulose (HEC), as a suspensor of electroosmotic flow, present at 0.1% (v/v) in a leading electrolyte (LE) was used. Hydroxide anion was used as a terminating ion.

Individual fractions collected from the preparative CITP were off-line analyzed by SEC using 99/1 DMF/ aqueous phosphate buffer (pH 3.0) with Spheron HEMA 100 stationary phase (filled in a 2.2 mm I.D. column with length 25 mm) and monitored with DAD and fluorimetric detector. Relative molar mass exclusion limits of polymers in Spheron HEMA 100 range from 70 000 to 250 000. Injected volume 20 μL was injected by the autosampler.

2.2. Samples

The stock solution of HAs (number of series: S42944-268, Sigma-Aldrich) was prepared at a 1000 mg L^{-1} concentration and filtered by disposable membrane filters

of 1 μm pore sizes (Millipore) and then diluted to the required concentration. Aqueous stock solutions of the discrete spacers used in this work (aspartic acid – ASP, 2-aminoadipic acid – AAD, taurin – TAU) were prepared at concentration of $1 \cdot 10^{-2}$ mol L^{-1}. The stock solution of HAs with discrete spacers (HDS) consisted of a 100 mg L^{-1} concentration of HAs and $3 \cdot 10^{-4}$ mmol L^{-1} of spacers.

Samples for SEC analysis: (1) standard of HAs prepared by mixing 160 μL of stock solution of HAs and 50 μL of deionized water (Labconco), (2) standard of HAs with added spacers (HDS) prepared by mixing 110 μL of stock solution of HDS and 50 μL of deionized water, (3) fractions obtained by preparative CITP prepared by mixing 50 μL of fractions (pooled from three fractionations) and 10 μL of deionized water.

3. Results and discussion

The use of suitable spacers in preparative CITP allows a very reproducible fractionation realized by micropreparative valve. An appropriate mixture of twenty discrete spacers for CITP characterization of HAs was published by Nagyová and Kaniansky[6]. Based on the results of this work we chosen three spacers (ASP, AAD and TAU) distributing the HAs constituents into CITP zone boundaries relatively uniformly.

Carbonates naturally present in the electrolyte solutions were served also as discrete spacer. The sample of HAs was fractionated in to five fractions based on different effective mobility subintervals. The mobility subintervals were defined by following couples of CITP zones: (1) chloride-carbonate, (2) carbonate-ASP, (3) ASP-AAD, (4) AAD-TAU, (5) TAU-OH-. The correctness of fractionation procedure was verify by presence of corresponding DSs zones on the isotachopherograms from the analytical CITP control of individual fractions.

The SEC chromatographic method with flourimetric and spectrophotometric (DAD) detection was used for analysis of fractions isolated using preparative CITP. Using this method, we were able to divide components of HAs into two peaks. The first peak represents the macromolecular component and the second peak small molecules of the sample. A similar chromatogram was obtained from the fluorescence (Fig. 1) and the DAD (Fig. 2). On the chromatograph acquired from DAD, there is visible a drop of absorbance immediately after second peak. The analysis showed different representation of macromolecules and small molecules in various fractions, but also their different proportion. This fact suggests a different composition of individual fractions.

4. Conclusions

Humic acids are very complex mixture and the exact structure is not known. That is why is important to combine different analytical methods working on different separation principles for characterization of HAs. Preparative CITP combined with SEC should be considered as an alternative way for characterization of humic acids. Differences between chromatographic profiles of the fractions acquired by preparative CITP suggested that individual CITP fractions contained different types of HAs compounds. SEC analysis of CITP fractions indicated that more mobile HAs (fractions F1, F2) are apparently enriched in high-molecular mass components, whereas less mobile fractions of HAs are relatively enriched in low-molecular mass components.

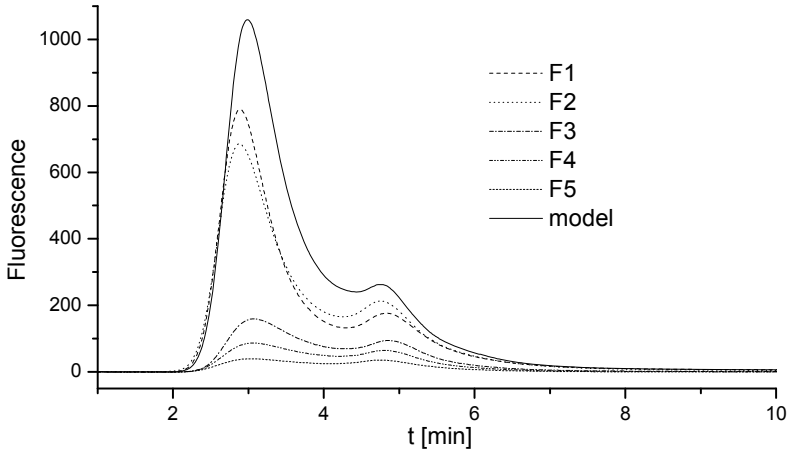

Fig. 1. **SEC profiles of model HAs and CITP fractions of HAs obtained by fluorimetric detection** (ex. 470 nm/em 530 nm). Mobile phase composition was aqueous phosphate buffer (pH 3.00, 50 mmol L^{-1}) containing 1 % (v/v) dimethylformamide (DMF). Flow-rate was 0.2 mL min^{-1}. Injected sample volume was 20 μL of each fraction

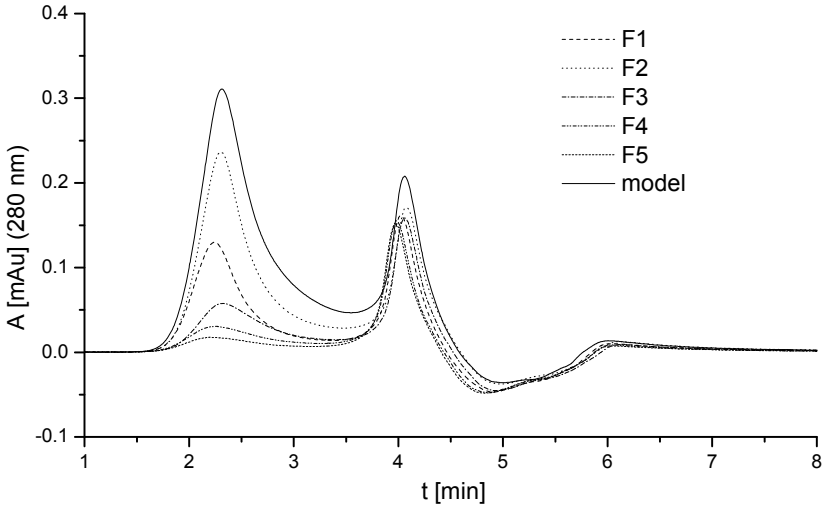

Fig. 2. **SEC profiles of model HAs and CITP fractions of HAs obtained by spectrophotometric detection** (280 nm). Conditions and parameters are the same as in Fig. 1

This work was generously supported by Comenius University in Bratislava (UK/312/2013) and the grant from the Slovak Research and Development Agency (APVV-0259-12).

REFERENCES

1. Stevenson F. J.: *Humus Chemistry: Genesis, Composition, Reactions,* Wiley, New York 1994.
2. Khan S. U.: *Soil Organic Matter*, Elsevier Science, Amsterdam 1975.
3. Janoš P.: J. Chromatogr., A *983*, 1 (2003).
4. Hutta M., Kaniansky D., Kovalčíková E., Marák J., Chalányová M., Madajová V., Šimuničová E.: J. Chromatogr., A 689, 123 (1995).
5. Góra R., Hutta M., Rohárik P.: J. Chromatogr., A *1220*, 44 (2012).
6. Nagyová I., Kaniansky D.: J. Chromatogr., A *916*, 191 (2001).

THE USE OF MICROCHIP ELECTROPHORESIS FOR DETERMINATION OF THE MAIN PHARMACEUTICAL COMPONENTS

MARÍNA RUDAŠOVÁ, MARIÁN MASÁR, and RÓBERT BODOR

Department of Analytical Chemistry, Faculty of Natural Sciences, Comenius University in Bratislava, Bratislava, Slovak Republic
rudasova@fns.uniba.sk

Summary

This work presents use of new analytical method that provides rapid and accurate determination of an active ingredient in various pharmaceutical preparations. Isotachophoretis separations were performed on a poly (methylmethacrylate) microchip with conductivity detection. External calibration and internal standard methods were used for results evaluation in this respect.

1. Introduction

The goal of analytical chemists over the years has been simplification procedures of a chemical analysis. "A total analysis system" (TAS), more often in miniaturized form (μTAS), have been concepts put to address this issue, which has dramatically evolved since its beginning back in 1990 (ref.[1,2]). The μTAS concept aims to develop integrated micro-analytical systems, which perform complete analysis cycles (e.g. sample pre-treatment, chemical reactions, analytical separation, detection, and data handling) on the same micro-device[3,4]. The capillary electrophoresis methods, that play a key role in „lab-on-a-chip", provide easier automation of the analytical procedure, short time of analysis, a possibility to analyze sub-nl sample volumes, reduced consumption of reagents and waste production as well as reduction of financial costs of the analysis, which is also the aim of μTAS concept.

The capillary electrophoresis methods have wide area of application, for example in the pharmaceutical industry. A control of pharmaceutical preparations includes two approaches: (a) the determination of the main components, and (b) the determination of impurities in preparation. This work deals with the determination of the main component of various pharmaceuticals using an isotachophoresis (ITP) with high separation capacity on the microchip with conductivity detection.

N-acetylcysteine is an active ingredient in mucolytics. Its sulfhydryl (-SH) group reacts with disulfide bonds in mucoproteins to split them into smaller units, whereby the viscosity of the mucus becomes reduced[5]. *N*-acetylcysteine is known as an antiviral, anti-tumor and anti-inflammatory agent and also has been used in the treatment of acquired immune deficiency syndrome (AIDS) and hepatitis B, for the prevention of cancer, the treatment of oxidative stress of different origins and paracetamol overdose[6].

The aim of this work was to develop an ITP method for fast and precise determination of the main component, *N*-acetylcysteine, in various pharmaceuticals, such as ACC Long and Solmucol, performed on the michrochip with the conductivity detection.

2. Experimental

Chemicals used for the preparation of electrolyte and model sample solutions were obtained from Merck (Darmstadt, Germany), Sigma-Aldrich (Seelze, Germany), Serva (Heidelberg, Germany) and Lachema (Brno, Czech Republic).

Water demineralized by a Pro-PS water purification system (Labconco, Kansas City, KS, USA) and kept highly demineralized by a circulation in a Simplicity deionization unit (Millipore) was used for the preparation of the electrolyte and sample solutions. Electrolyte solutions were filtered before the use through membrane filters with a pore diameter of 0.8 μm (Millipore).

Stock solutions of *N*-acetylcysteine and Anthranilic acid (used as an internal standard) were prepared at 1000 mg L^{-1} concentrations.

Pharmaceutical preparations (Solmucol 200 and 90, Institut Biochimique SA, Switzerland, and ACC Long, Salutas Pharma GmbH, Germany) were bought in local pharmacy. They were dissolved in demineralized water and filtered through membrane filters (Millipore). No other sample pretreatment was used before the analysis.

Poly(methylmethacrylate) (PMMA) microchip with coupled separation channels (CC) and on-column conductivity detectors (Merck) used in this work was made by technological procedure described in detail in the literature[7].

3. Results and discussion

The ITP separations were performed with suppression of electroosmotic and hydrodynamic flow. Under these working conditions, the RSD values of the zone lengths of *N*-acetylcysteine were in the range 1–8 %, independently of the used microchip. The results are shown in Table I. Repeatabilities of quantitative parameters for corrected zone lengths of *N*-acetylcysteine on internal standard (Anthranilic acid) improved approx. 2-4-fold. The ITP repeated measurements were performed on three

Table I
Repeatibilities of zone lengths of *N*-acetylcysteine

Concentration of *N*-acetylcysteine [mg L^{-1}]	Zone length of *N*-acetylcysteine		Corrected zone length of *N*-acetylcysteine/Antranilate	
	Average	RSD [%]	Average	RSD [%]
50 A	4.02	2.15	0.49	1.30
50 B	4.24	4.29	0.51	1.44
50 C	4.23	7.94	0.51	2.11
100 A	7.60	1.32	0.96	1.14
100 B	8.68	3.34	1.06	0.41
100 C	8.23	1.88	1.01	2.20
200 A	15.55	0.85	1.96	0.39
200 B	16.85	2.88	2.15	0.34
200 C	16.95	2.44	2.14	1.81

A, B, C = ITP measurements performed on 3 microchips (A, B, C), 1 MCE device, and within 3 days; RSD = relative standard deviation. Concentration of anthranilate (internal standard) was approx 100 mg L^{-1}

microchips, at one microchip electrophoresis (MCE) device, and within three days. The internal standard eliminates run-to-run fluctuations in injected sample volume.

The results in Table II show the RSD values of three regression equations for *N*-acetylcysteine present in model samples, in the concentration range 50–200 mg L^{-1}, together with Anthranilic acid used as the internal standard. The concentration of Anthranilic acid was 100 mg L^{-1}. Parameters of the regression equation for calibration solutions were evaluated by methods of external calibration and internal standard.

The contents of *N*-acetylcysteine in pharmaceutical preparations, e.g. Solmucol 200, Solmucol 90 and ACC Long, were evaluated by methods of external calibration and internal standard. The external calibration method showed a higher dispersion of the content of *N*-acetylcysteine in the sample (about 10-fold higher RSD values).

4. Conclusions

The ITP method for determination of *N*-acetylcysteine in various mucolytic pharmaceuticals was developed. The methods of external calibration and internal standard were used for determination of its content in various pharmaceutical samples. The method of the internal standard eliminated run-to-run fluctuations in the sample volume injected on the microchip. The results of this study showed that developed ITP method can be used for fast and precise determination of the active ingredient in pharmaceuticals.

Table II
Parameters of the regression equations for *N*-acetylcysteine with Antranilic acid used as the internal standard

Parameter	External calibration			Internal standard			n	Δc [mg L^{-1}]
	a [s L mg^{-1}]	b [s]	R	a	b	R		
A	0.0721	0.3165	0.9995	0.0095	0.0031	0.9999	19	25–200
B	0.0764	0.1764	0.9993	0.0096	0.0040	0.9997	20	25–200
C	0.0874	0.1333	0.9903	0.0109	0.0052	0.9991	16	50–200
Average	0.0786	0.2087		0.0100	0.0041			

A, B, C = ITP measurements performed on 1 chip (A, B, C), 1 MCE device, and in 1 day; a = slope of calibration curve; b = intercept of calibration curve; R = correlation coefficient; SD = standard deviation; RSD = relative standard deviation; n = number of measurements; Δc = concentration interval. Concentration of anthranilate (internal standard) was approx. 100 mg L^{-1}

This work was generously supported by Comenius University in Bratislava (UK/142/2013) and the grant from the Research & Development Operational Programme funded by the ERDF (Center for Industrial Research of Optimal Method for Synthesis of Highly Effective Drugs, SynAnPharm, ITMS 26240220061).

REFERENCES

1. Manz A., Graber N., Widner H. M.: Senzors Actuat. *1*, 244 (1990).
2. Reyes D. R., Iossifidis D., Manz A.: Anal. Chem. *74*, 2623 (2002).
3. Lichtenberg J., De Rooij N. F., Verpoorte E.: Talanta *56*, 233 (2002).
4. Huikko K., Kostiainen R., Kotiaho T.: Eur. J. Pharm. Sci. *20*, 149 (2003).
5. Tomkiewicz R. P., App E. M., De Sanctis G. T., Coffiner M., et al.: Pulm. Pharmacol. *8*, 259 (1995).
6. Daly F. F. S., Fountain J. S., Murray L., Graudins A., et al.: Med. J. Aust. *188*, 296 (2008).
7. Masár M., Poliaková M., Danková M., Kaniansky D., et al.: J. Sep. Sci. *28*, 905 (2005).

HIGH PRESSURE MODIFICATION OF THE SIMPLE AUTOMATED LIQUID CHROMATOGRAPHIC SYSTEM FOR SPLITLESS NANO COLUMN GRADIENT SEPARATIONS

JOZEF ŠESTÁK[a,b] and VLADISLAV KAHLE[a]

[a] *Institute of Analytical Chemistry, v.v.i., Brno,* [b] *Faculty of Chemistry, Brno University of Technology, Brno, Czech Republic*
sestak@iach.cz

Summary

Our simple liquid chromatographic system for splitless gradient nanocolumn separations at backpressure up to 50 bars was modified to run analysis under the pressure up to 300 bars. Programmable syringe pump was equipped with a 250-μL high-pressure syringe and mobile phase gradients were created and stored in relatively long capillary. Available linear gradients of volumes from 5 to 50 μL traced by uracil are presented. Sample introduction was performed as separate step and real large volume of sample (tens of microliters) could be injected and pre-concentrated on-column. Relative standard deviation of retention times and peak areas were received (RSD < 0.3 % and RSD < 5 % respectively).

1. Introduction

In our previous work[1], we used glass micro syringe retained in inclined position to handle the liquids. Mobile phase gradient was created by successive sucking of four mobile phases with gradually decreasing acetonitrile concentration and due to turbulent mixing occurred at syringe needle-barrel boundary. While the syringe was retained in inclined position, the mobile phase gradient was stable because of different specific weight of acetonitrile rich and water rich part of the mobile phase gradient. Glass syringe was pressure resistant up to 50 bars and its orientation had to be altered when reversed mobile phase gradient was required. Moreover gradient shape changed slightly at different flow rates. Recently we have modified our concept. We replaced glass micro syringe with the high pressure one so our system is now able to work at backpressure up to 300 bars. Further we tried to find a more versatile option of gradient pre-mixing than that we used in the case of the inclined glass micro syringe.

2. Experimental

Experimental configuration consisted of programmable syringe pump (NE-500 OEM, New Era) equipped with a 250-μL high-pressure syringe (FMJ-250, Penn-Century) and selector valve (C55-1340I, Vici Valco). High pressure syringe was connected to central port of selector valve via PEEK capillary (380 μm i.d. × 500 mm) fixed in horizontal position. PEEK capillary here served as gradient generator as well as sample loop. Mobile phase gradients were created by successive sucking of defined volumes of four water-acetonitrile solutions with gradually changing acetonitrile concentration into the PEEK capillary. Uracil (detected at 254 nm) was added to water to visualize the change of mobile phase composition. Stability of gradient profile was tested by delivering of the constant gradient volume at various flow rates. Before preparing gradient, relatively large volume of sample diluted in weak mobile phase was sucked into the PEEK capillary and then injected on column. For assessment of repeatability of the gradient separation a mixture of nitro-explosives was injected on capillary column (100 μm i.d. × 150 mm) filled with Kinetex 2.6 μm C18 particles.

3. Results and discussion

Traces of linear gradients of volumes from 5 to 50 μL are shown in Fig. 1. Different steepness of gradient is controlled by variation of successively sucked volumes of 5, 30, 50 and 80 % v/v acetonitrile into the PEEK capillary. Gradient shape is very smooth because sharp mobile phase boundaries fade out while passing through the valve body and due to the parabolic profile of laminar flow as well as due to diffusion. Mobile phase gradient created this way could be identified as very time-stable. Traces of 10-μL gradient delivered at flow rates 0.2–5 μL min^{-1} are shown in Fig. 2. In front of previous concept[1], no significant deviation of gradient shape was observed. Gradient separation of some explosives is shown in Fig. 3. Relative standard deviation of retention times and peak areas calculated from ten successive runs was below 0.5 % and 5 % respectively.

4. Conclusions

Simple system for splitless nano column gradient liquid chromatography developed in the past was improved. We replaced glass micro syringe with the high pressure one and we used 380 μm i.d. × 500 mm capillary fixed in horizontal position as gradient generator. This configuration is independent on the syringe diameter and syringe orientation. Gradient separation is repeatable, gradient shape is very time-stable and practically

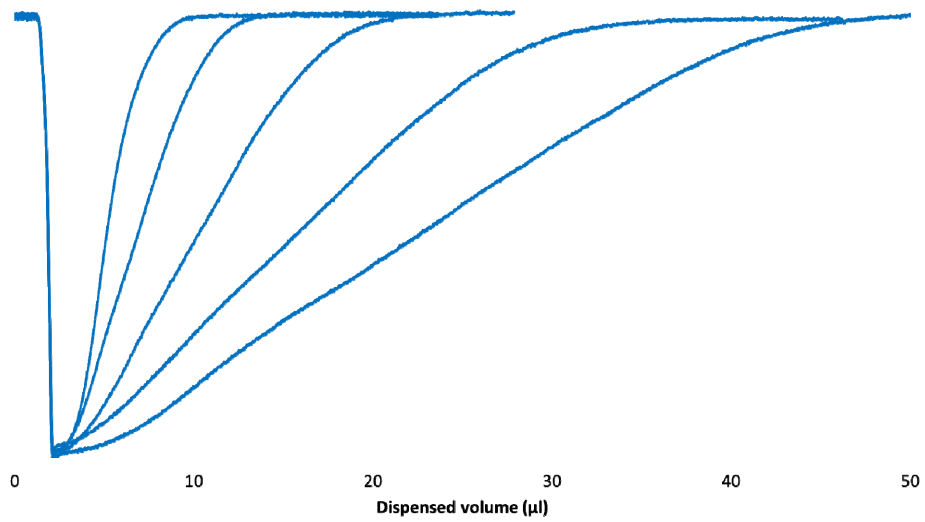

Fig. 1. **Blank water-acetonitrile gradients traced by uracil.** The steepness of gradient is dependent on successively sucked volumes of 5, 30, 50 and 80 % v/v acetonitrile

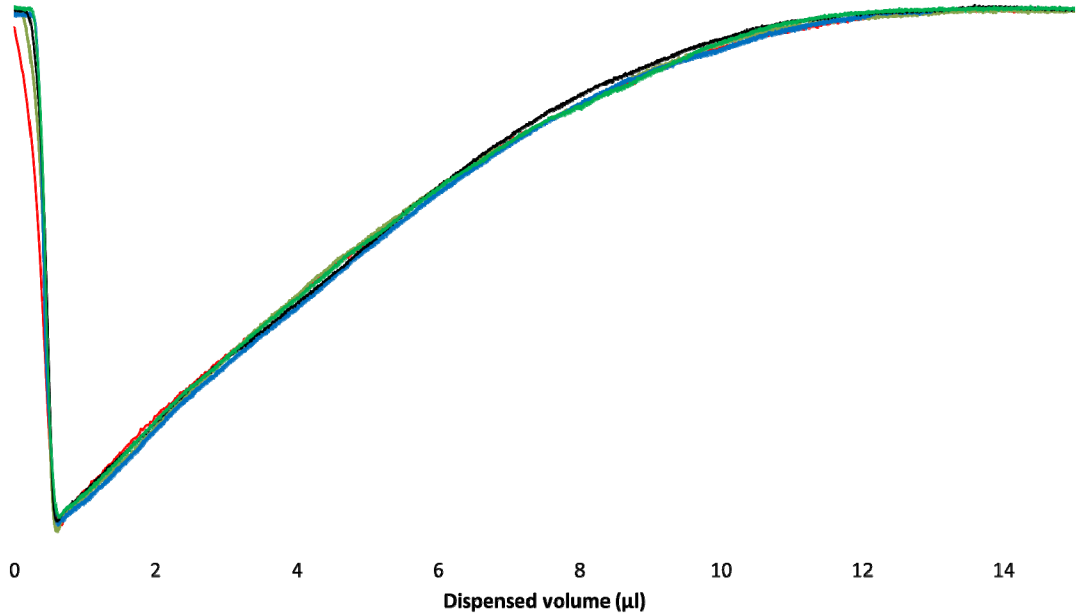

Fig. 2. **Gradient stability test;** 10-µL gradient traced by uracil was delivered at flow rates: 0.2, 0.5, 1, 2 and 5 µL min^{-1}

independent on flow rate. Reversed mobile phase gradient for column regeneration or for HILIC separation mode is also available with no need for change of configuration. Moreover overall capillary could be filled with sample and direct on-column analytes pre-concentration from large sample volume could be suggested.

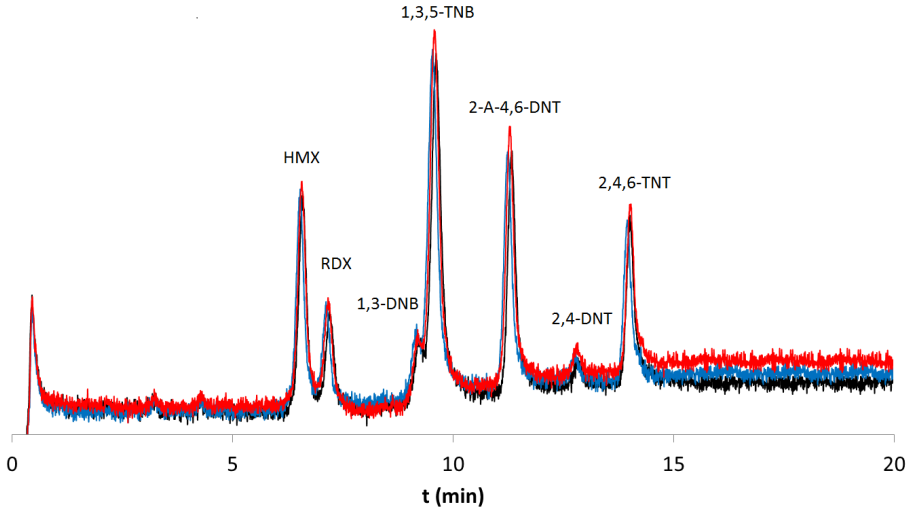

Fig. 3. **Gradient separation of the explosives;** Kinetex 2.6 µm C18 100 µm i.d. × 150 mm, 30–80 % v/v acetonitrile 0–60 min, 0.5 µL min^{-1}; 25 °C, UV detection at 230 nm

This work has been supported by the Ministry of Education, Youth and Sports of the Czech Republic (grant No. FCH-F-13-2087) and by the Ministry of the Interior of the Czech Republic (project No. VG20112015021).

REFERENCE

1. Sesták J., Duša F., Moravcová D., Kahle V.: J. Chromatogr., A *1276*, 26 (2013).

IMMOBILIZED ENZYME REACTOR FOR ON-LINE STUDIES OF DRUG METABOLISM MEDIATED BY CYTOCHROME P450 2C9 ISOFORM

JAN SCHEJBAL, ROMAN ŘEMÍNEK, LUKÁŠ ZEMAN, MARTA ZEISBERGEROVÁ, and ZDENĚK GLATZ

Department of Biochemistry, Faculty of Science and CEITEC – Central European Institute of Technology, Masaryk University, Brno, Czech Republic
358113@mail.muni.cz

Summary

Drug biotransformation mediated by cytochrome P450 enzymes (CYP) is a pivotal factor in the early developmental stages of new drugs. Metabolism evaluation of every hit thus constitutes the integral part of ADME/tox screenings. Enzyme immobilization represents a useful approach in this field because of CYP recycling and simplification of sequential analyses by providing protein-free samples. A new method for immobilization of therapeutically important cytochrome P450 2C9 isoform (CYP2C9) on magnetic microparticles SiMAG-Carboxyl is thus presented.

1. Introduction

Immobilized enzyme reactors (IMERs) represent a promising tool for rapid on-line screenings of drug metabolism. Attachment to carrier enables not only repetitive use of a single batch of the tested enzyme but also simplification of sequential analyses by providing protein-free samples and improvement of its thermal and operational stability. These advantages are especially important in the early stages of a new drug development processes when the extensive numbers of tested candidates are screened for their affinities to drug-metabolizing enzymes such as CYP. For this reason main goal of the presented study was to develop a method for immobilization of the CYP2C9 on the magnetic microparticles and construct IMER allowing on-line screenings of drug metabolism mediated by this therapeutically important enzyme, which forms approximately 20 % of all CYP in human liver and is responsible for metabolism of more than 10 % of commonly prescribed drugs[1].

2. Experimental

2.1. Immobilization procedure

Solutions of all reactants were prepared in immobilization buffer consisting of 30 mM potassium phosphate (pH 8.60). After SiMAG-Carboxyl magnetic microparticles have been washed with immobilization buffer, the solution of 6 mM 1-ethyl-3-(3-dimethylamino-propyl)carboimide (EDAC) and 10 mM *N*-hydroxy-sulfosuccinimide was added and the surface of the microparticles was activated by mixing for 2 hours at 25 °C. Then, the second washing cycle followed. The solution of CYP2C9 containing 40 μM flurbiprofen and 40 μM dapsone was added to the activated microparticles and immobilized by mixing for 20 hours at 5 °C.

2.2. In-capillary reaction

The microparticles with attached CYP2C9 were washed with water and injected into capillary, where they were fixed by two external NdFeB magnets to form the IMER. The enzymatic reaction was started by introduction of a plug of diclofenac at a certain concentration and 1 mM NADPH prepared in 50 mM potassium phosphate (pH 7.40) inside the IMER. The incubation was carried out at 25 °C and the reaction was terminated by application of voltage and separation of reaction mixture components.

2.3. Separation

All the experiments were performed on the Agilent 7100 CE System. An uncoated silica capillary (total length 33.5 cm, effective length 19 cm, 75 μm id) was thermostated at 25 °C. 20 mM sodium dihydrogen phosphate, disodium tetraborate buffer (pH 8.60) was used as a background electrolyte (BGE). Separations were accomplished by application of 27 kV (418.6 V cm^{-1}, positive polarity).

3. Results and discussion

Parameters of immobilization procedure such as attachment scheme, concentration of support surface activators (0.75–6 mM EDAC, 1.25–10 mM NHS), composition, concentration (20–60 mM) and pH (6.6–9.4) of immobilization buffer, attachment time (2–24 hours) and temperature (5–35 °C) and concentration (12.5–250 nM) of CYP2C9 were optimized with respect to its activity and stability. On the basis of results obtained, 30 mM potassium phosphate (pH 8.60) used as an immobilization

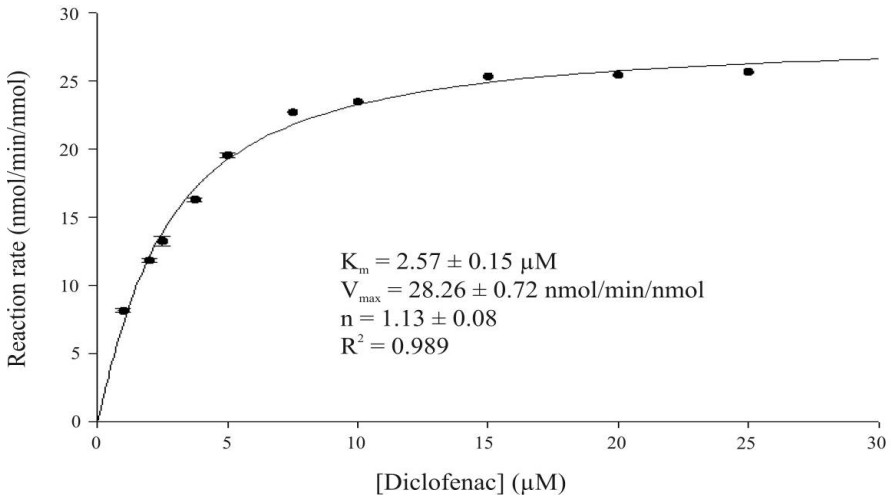

Fig. 1. **Michaelis-Menten plot of immobilized CYP2C9 reaction with diclofenac**

buffer, 6 mM EDAC and 10 mM NHS as a magnetic beads surface activators, 40 μM flurbiprofen and 40 μM dapsone as additives to a solution of 100 nM CYP2C9 and immobilization for 20 hours at 5 °C were chosen as the best procedure parameters. Following off-line experiments proved that the immobilized CYP2C9 can be repetitively used for 12 hours without considerable loss of the activity. What is more, values of basic kinetic parameters of Michaelis constant (K_m) and Hill coefficient (n) obtained within performed kinetic study with model substrate diclofenac (see Fig. 1) were in very good agreement with data found in literature[2,3] obtained with soluble CYP2C9 form proving that binding to the microparticles has no negative effect on its activity.

CYP2C9 immobilized on magnetic microparticles was then used for construction of in-capillary reactor. Cassette of CE system was modified in order to hold two NdFeB magnets which determine position of IMER inside the capillary. The enzymatic reaction was started by injection of a plug of diclofenac and 1 mM NADPH prepared in 50 mM potassium phosphate buffer pH 7.4 and terminated by application of voltage 27 kV (418.6 V cm^{-1}, positive polarity) and separation of CYP2C9 and diclofenac. The electrophoregram obtained is shown in Fig. 2. Subsequent analyses showed a decreasing production of 4‘-hydroxydiclofenac nevertheless. The other optimization of the system thus will be focused on the improvement of CYP2C9 stability inside CE system; the effect of the applied separation voltage on its activity will be primarily examined.

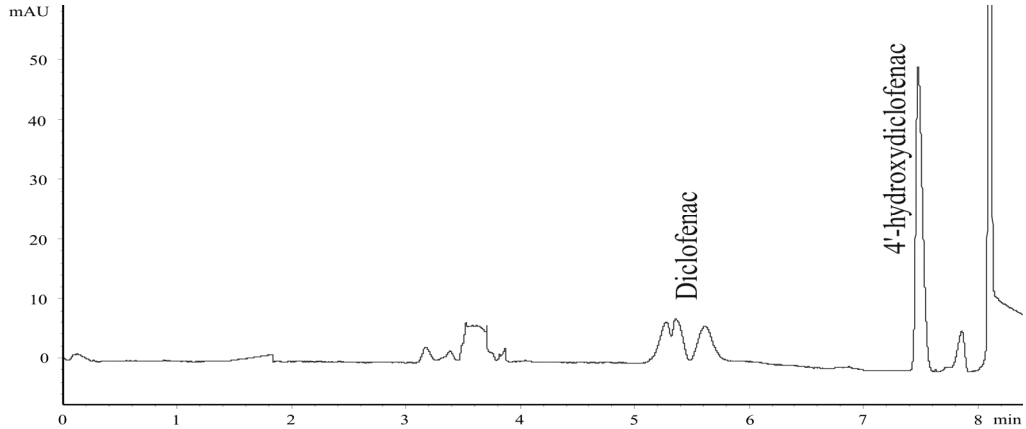

Fig. 2. **Electrophoregram obtained after in-capillary reaction.** Sample: 50 μM diclofenac, 1 mM NADPH prepared in 50 mM Na phosphate buffer pH 7.4, 60 min incubation. Separation conditions: capillary total length 33.5 cm, effective length 19 cm, ID 75 μm; BGE 20 mM sodium phosphate-tetraborate buffer pH 8.6; 25 °C; 27 kV

4. Conclusions

The method for immobilization of CYP2C9 on SiMAG-Carboxyl magnetic microparticles was developed. Experimental results of the off-line method proved that immobilized CYP2C9 can be repetitively used for 12 hours without considerable loss of activity. Performed kinetic study with model substrate diclofenac confirmed that the attachment on magnetic nanoparticles has no negative effect on CYP2C9 activity.

The prepared immobilized CYP2C9 particles were used to form an IMER in order to perform in-capillary reaction. Preliminary experiments, however, revealed progressive loss of enzyme activity of CYP2C9 hold inside separation capillary. The following effort thus will be focused on overcoming of this drawback so that the final system will be applicable for rapid on-line screenings of CYP2C9 inhibitors.

This work was supported by the grant No. GAP206/10/0057 financed by Grant Agency of The Czech Republic.

REFERENCES

1. Miners J. O., Birkett D. J.: Br. J. Clin. Pharmacol. *45*, 525 (1998).
2. Walsky R. L., Obach R. S.: Drug Metab. Dispos. *32*, 647 (2004).
3. Konečný J., Juřica J., Tomandl J., Glatz Z.: Electrophoresis *28*, 1229 (2007).

DETERMINATION OF REFERENCE INTERVALS OF URINARY CYSTATIN C AND ITS RATIO TO URINARY CREATININE IN HEALTHY CHILDREN

RADKA ŠIGUTOVÁ[a,b,c], MICHAL HLADÍK[b,d], FRANTIŠEK VŠIANSKÝ[a,b], PAVLÍNA KUŠNIEROVÁ[a,b], KRISTIAN ŠAFARČÍK[a,b], and ZDENĚK ŠVAGERA[a,b]

[a] *Department of Clinical Biochemistry, Institute of Laboratory Diagnostics, Faculty Hospital Ostrava, Ostrava,* [b] *Department of Biomedical Sciences Faculty of Medicine, University of Ostrava, Ostrava,* [c] *Department of Biochemistry, Faculty of Medicine, Masaryk University, Brno,* [d] *Department of paediatrics, Faculty Hospital Ostrava, Ostrava, Czech Republic*
radka.sigutova@fno.cz

1. Introduction

1.1. Structure and function of cystatin C

Cystatins are parts of cystatin (super)family that is divided into three major groups, namely stefins, proper cystatins and kininogens. For their inability to inhibit cysteine protease, fetuins, the fourth group, are often treated separately[1]. A significant function of cystatins is thus inhibition of proteases such as cathepsins B, H, K, L, and S. Cystatins protect the organism against inadequate activity of these enzymes and reduce the risk of damage. The family of cysteine protease inhibitors also includes cystatin C. Out of all the cystatins, it is the most effective deactivator of cathepsins[4]. Cystatin C is composed of a single polypeptide chain containing 120 amino acid residues. This nonglycosylated basic protein with disulphide bridges between residues 73 and 83 and between 97 and 117 has a molecule weight of 13 343 Da (ref.[2,5]). The cystatin C gene encodes a polypeptide of 146 amino acids; CST3 gene is localised on chromosome 20 (20p11.2). The isoelectric point of cystatin C is 9.3, the form of pI 7.8 has been isolated from urine, and the protein therefore has a positive charge in virtually all body fluids[1].

1.2. Presence of cystatin C

Cystatin C is produced at a constant rate by all cells having a nucleus ('house-keeping' gene). Neither diet nor inflammatory or tumorous processes have an effect on its synthesis. It is present in plasma (0.5–1.2 mg L^{-1}) and cerebrospinal fluid (3–14 mg L^{-1}), seminal plasma (41–62 mg L^{-1}), saliva (0.36–4.8 mg L^{-1}), synovial fluid (approx. 2.0 mg L^{-1}), amniotic fluid (approx. 1.0 mg L^{-1}) and tears (approx. 1.0 mg L^{-1}) (ref.[4]). The level of urinary cystatin C in urine in healthy adult individuals is 0.095 mg L^{-1} (0.033–0.29 mg L^{-1}) and it increases when increasing the age[6]. Cystatin C is freely filtered in glomeruli and re-absorbed by the proximal tubular cells where it is also completely degraded. Increased urinary concentration of cystatin C is a marker of the functionality of cells. Disrupted glomerular filtration can be detected on the basis of increased levels of cystatin C in plasma. Plasma level of cystatin C increases with the age as a result of filtration rate decline[1].

2. Experimental

Physiological levels of urinary cystatin C and their ratio to urinary creatinine levels (CysC-U/Crea-U) were calculated out of a set of 111 samples collected from pre-school and school children (3–15 years old) regardless of gender. Morning urine samples were frozen at –80 °C within 2 hours of collection until analysis.

Urinary cystatin C levels were measured using ELISA kit (Cystatin C Human ELISA, Biovendor – Laboratory medicine, Czech Republic). Urinary creatinine levels were obtained by means of the Jaffe method on AU 5400 biochemical analyser (AU 5420, Beckman Coulter, Inc., USA).

Basic statistical properties (mean, standard deviation, skewness, pointedness) were calculated using QCExpert 3.0 software. Reference intervals were calculated by parametric and nonparametric method with the CBStat ver. 5 software. Parametric method assumes a symmetrical distribution whose feature is the skewness of distribution. In case it is disrupted, the data need to be transformed. Nonparametric method requires no data symmetry as it is based on serial statistics. The number of necessary data for this method is 120. The confidence interval was calculated using the Bootstrap procedure.

3. Results and discussion

The results of basic statistical quantities are given in Tab. I. Obtained urinary cystatin C and its ratio to urinary creatinine showed no normal distribution (Fig. 1); data skewness was considerable (Tab. I).

Reference interval (RI) of urinary cystatin C in 3–5 year-old children calculated by means of the parametric method containing power transformation ranges from 13.68–166.33 μg L^{-1} with the significance level α=5 %. RI obtained using the nonparametric procedure differed only slightly (Tab. II).

Reference values of the CysC-U/Crea-U ratio obtained by means of the parametric method for the given set of children ranges from 1.87–113.1 μg $mmol^{-1}$. The nonparametric method showed a wider reference interval

Table I
Basic statistical properties

Parameters	CysC-U	CysC-U/Krea-U
Mean	57.22 ($\mu g.L^{-1}$)	12.21 ($\mu g.mmol^{-1}$)
Standard Deviation	40.13 ($\mu g.L^{-1}$)	35.74 ($\mu g.mmol^{-1}$)
Skewness	1.54	4.52
Deviation from 0	Significant	Significant
Pointedness	6.64	26.28
Deviation from 3	Significant	Significant

Table II
Reference limits of CysC-U and the CysC-U/Crea-U ratio

Parameters	Procedure	2.50 %	90% CI		97.50 %	90% CI	
CysC-U ($\mu g.L^{-1}$)	Parametric	13.68	10.18	17.85	166.33	140.30	195.20
	Nonparametric	13.55	9.98	17.13	174.96	133.80	216.10
CysC-U/Krea-U ($\mu g.mmol^{-1}$)	Parametric	1.87	1.53	2.30	113.10	57.80	224.30
	Nonparametric	1.77	1.26	2.27	152.30	62.90	241.50

Note: CI = confidence interval

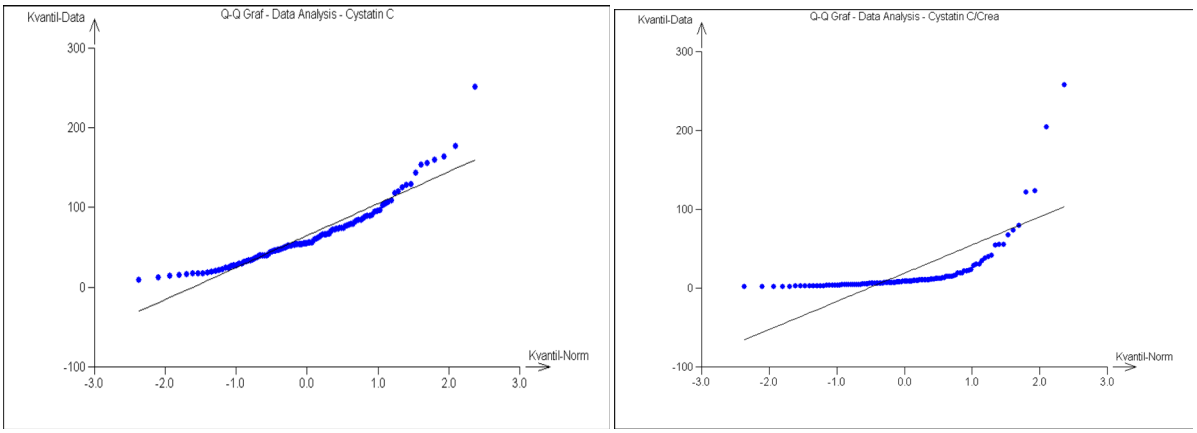

Fig. 1. **CysC-U quantile-quantile plot (left) and CysC-U/Crea-U quantile-quantile plot (right)**

of 1.77–152.30 μg $mmol^{-1}$. For graphic representation of RI see Fig. 2 and 3.

4. Conclusion

We calculated reference limits of urinary cystatin C and its ratio to urinary creatinine. The ratio of urinary cystatin C to urinary creatinine is supposed to guarantee the standardisation of results regardless of the time of

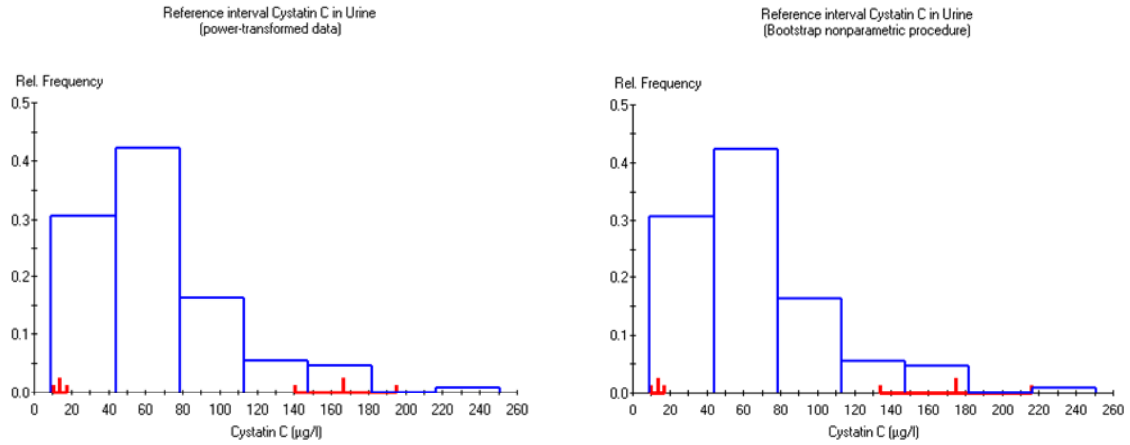

Fig. 2. **Histograms of CysC-U reference values.** Reference limits obtained by the parametric method (left) and the nonparametric method – Bootstrap procedure (right)

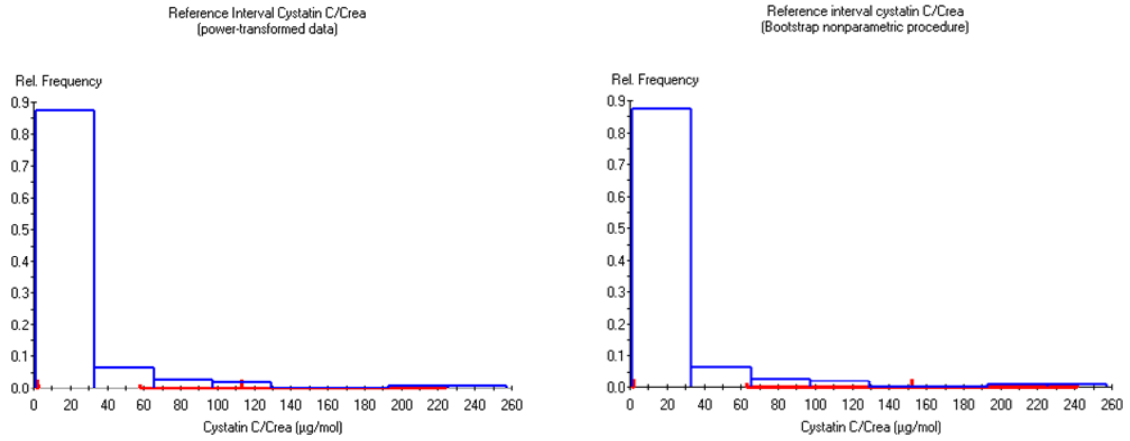

Fig. 3. **Histograms of CysC-U/Crea-U reference values.** Reference limits obtained by the parametric method (left) and the nonparametric method – Bootstrap procedure (right)

urine sampling. Obtained values are expected to enable paediatricians to make right decisions concerning early and adequate treatment of tubular cell damage.

In consequence of the skewness of measured data, the confidence interval upper limit in both methods used to calculate RI is relatively wide. The set of the data should be extended in order to make this limit more accurate.

This study was supported by the Ministry of Health of the Czech Republic (01549/2012/RRC).

REFERENCES

1. Jabor A., a kol.: *Vnitřní prostředí*. Grada Publishing, a.s., Praha 2008.
2. Grubb A.: Adv. Clin. Chem. *35*, 63 (2000).
3. Herget-Rosenthal S., Marggraf G., Husing J., et al.: Kidney Int. *66*, 1115 (2004).
4. Abrahamson M., Alvarez-Fernandez M., Nathanson C. J.: Biochem. Soc. Symp. *70*, 179 (2003).
5. Jabor A., Friedecký B., a spol.: Klin. Biochem. Metab. *10*, 169 (2002).
6. Filler G., Bökenkamp A., Hofmann W., Le Bricon T., Martínez-Brú C., Grubb A.: Clin. Biochem. *38*, 1 (2005).

DETERMINATION OF CHLOROPHENOLS IN ENVIRONMENTAL SAMPLES USING ELECTROMEMBRANE EXTRACTION AND CAPILLARY ELECTROPHORESIS

ANDREA ŠLAMPOVÁ, PAVEL KUBÁŇ, and PETR BOČEK

Institute of Analytical Chemistry of the Academy of Sciences of the Czech Republic, v.v.i., Veveří 97, 602 00 Brno, Czech Republic
kuban@iach.cz

Summary

Combination of electromembrane extraction (EME) with capillary electrophoresis (CE) was used for determination of trace level chlorophenols (CPs) in environmental water samples. The analytes were transported across supported liquid membrane (SLM), composed of 1-ethyl-2-nitrobenzene (ENB), by the application of electrical field. A driving force of 150 V was applied to extract the analytes from neutral sample (donor solution) into strongly alkaline acceptor solutions. The acceptor solutions were subsequently analyzed by CE with UV-Vis detector. Thus chlorophenols were selectively concentrated by one order of magnitude. Recovery values of six CPs were between 14 and 25 % for 5 min and could be further increased up to 20–42 % for 15 min extraction time. The precision of the EME-CE-UV was characterized by relative standard deviation (RSD) values of migration times (0.05–0.16 %) and peak areas (0.7–5.6 %) at concentration level of 10 μg mL^{-1} of CPs, *n*=5. Calibration parameters showed linear relationship between analyte concentration and analytical signal in the concentration range 0.01–10 μg mL^{-1} with correlation coefficients (r^2) better than 0.999. Limits of detection (LODs), defined as 3× signal-to-noise ratio, for standard solutions and environmental samples were below or equal to 5 ng mL^{-1}.

1. Introduction

EME is a sample pretreatment method that employs electric field as a driving force for selective transfer of analytes from an aqueous solution (donor) across a SLM into another aqueous solution (acceptor). CPs are mainly produced in industrial processes such as manufacturing of polymers, drugs, textiles, dyes, pesticides, explosives, paper, and petrochemicals and exist in environmental waters and soils as persistent organic pollutants. Evaluation and monitoring trace levels of these highly toxic and carcinogenic compounds in environmental samples, especially in aqueous samples, are indispensable. EME was shown useful and efficient extraction technique for trace analysis of environmental samples and its potential for determination of CPs was evaluated in the presented contribution[1].

2. Experimental

2.1. Electromembrane extraction

The EME system was described in a previous publication[2].

2.2. Capillary electrophoresis

A P/ACE 5010 CE instrument (Beckman, Fullerton, CA, USA) equipped with UV-Vis absorbance detector was operated at a potential of +15 kV applied at the injection side of the separation capillary. BGE solution for CE of CPs consisted of 20 mM $Na_2B_4O_7 . 10\ H_2O$ and 10 mM Na_2HPO_4 adjusted to pH 9.8 with 1 M NaOH.

3. Results and discussion

EME system using neutral donor and alkaline acceptor solutions (pH values 7 and 12, respectively) was used for efficient extraction of CPs. Highest efficiencies for six selected CPs were obtained in the EME systems using KOH as donor and CsOH as acceptor solutions, and ENB used as SLM. Effect of the sample matrix on the recovery of six CPs was examined based on addition of 10 mM Cl^- to donor solutions, which corresponds to the typical concentration of inorganic anions in environmental samples. Sample matrix had minimal effect on the transport of analytes across the SLM at optimized EME conditions. Determination of real samples confirmed that the developed method is suitable for the determination of CPs in environmental samples, see Fig. 1.

4. Conclusions

Electromembrane extraction followed by capillary electrophoresis was developed as an efficient method for determination of CPs in environmental samples. Transfer of chlorophenols across SLM was dependent on several EME parameters, such as composition of liquid membrane, pH of acceptor and donor solution, applied electric potential and extraction time. Additionally, effects of the composition donor and acceptor solutions on the transfer analytes across SLM was demonstrated for the first time.

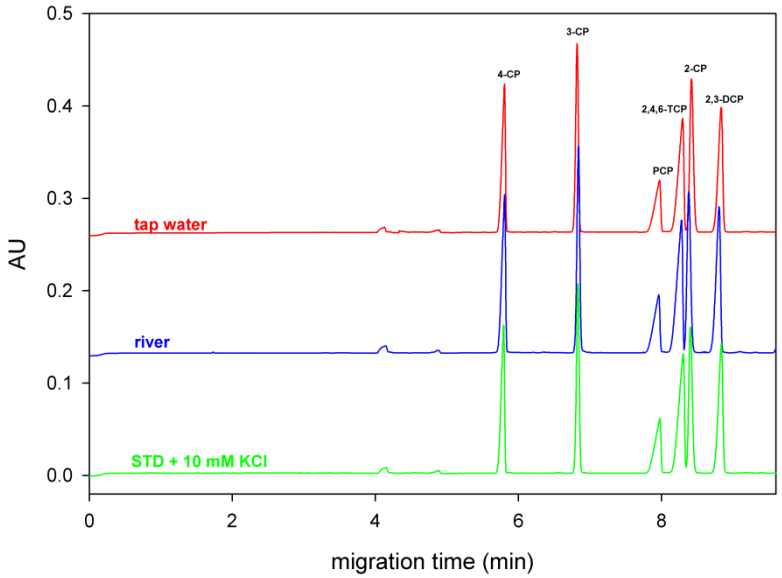

Fig. 1. **Electropherograms of real samples spiked with 10 μg mL^{-1} CPs [4-chlorophenol (4-CP), 3-chlorophenol (3-CP), pentachlorophenol (PCP), 2,4,6-trichlorophenol (2,4,6-TCP), 2-chlorophenol (2-CP), 2,3-dichlorophenol (2,3-DCP)].** EME conditions: extraction voltage, 150 V; donor, KOH (pH 7); acceptor, CsOH (pH 12); SLM, ENB; agitation, 750 rpm. CE conditions: BGE solution, 20 mM $Na_2B_4O_7$. 10 H_2O + 10 mM Na_2HPO_4; pH 9.8; voltage, +15 kV; injection, 0.5 psi for 5 s; 200 nm; 25 °C

Financial support from the Academy of Sciences of the Czech Republic (Institute Research Funding RVO:68081715) and the Grant Agency of the Czech Republic (Grant No. 13-05762S) is gratefully acknowledged.

REFERENCES

1. Kiplagat I. K., Kubáň P., Boček P.: Electrophoresis *32*, 3008 (2011).
2. Strieglerová L., Kubáň P., Boček P.: J. Chromatogr., A *1218*, 6248 (2011).

CHARACTERIZATION OF PREPARED MONILITHIC CAPILLARY COLUMNS

MAGDA STAŇKOVÁ, PAVEL JANDERA, and TOMÁŠ HÁJEK

Department of Analytical Chemistry, Faculty of Chemical Technology, University of Pardubice, Pardubice, Czech Republic
magda.stankova@student.upce.cz

Summary

MEDSA – *N*,*N*-dimethyl-*N*-metacryloxyethyl-*N*-(3-sulfopropyl)ammonium betaine as a zwitterionic polar functional monomer in combination with seven crosslinking monomers were used for preparation of capillary monolithic columns suitable for separation of polar compounds in hydrophilic interaction chromatography (HILIC). Ethylene dimethacrylate, tetramethylene dimethacrylate, hexamethylene dimethacrylate, dioxyethylene dimethacrylate, pentaerythritole triacrylate, bisphenol A dimethacrylate, and bisphenol A glycerolate dimethacrylate were used as crosslinking monomers (Fig. 1). Columns prepared with dioxyethylene dimethacrylate and bisphenol A glycerolate dimethacrylate showed the efficiency up to 70 000 N m^{-1}. Columns provide good repeatability of elution volumes with relative standard deviations lower than 1.3 % on both types of columns. Dual retention mechanism allows the separation in HILIC and RP mode. Capillary monolithic columns, id 0.53 mm, were used in the first dimension of the two-dimensional liquid chromatography for separation of complex mixture of phenolic compounds.

1. Introduction

Currently, reversed-phase chromatography is the most commonly used system in the liquid chromatography, employing a non-polar stationary phase and polar water-organic mobile phases. Hydrophilic interaction chromatography[1], makes use of a polar stationary phase and highly organic mobile phases.

In micro-column liquid chromatography either conventional columns filled with spherical particles or monolithic columns are used. Monolith is formed by a single peace of highly porous material which contains flow through pores and limited populations of mesopores. They may be either inorganic monolithic stationary phase or organic polymers. Organic monoliths can be prepared by *in-situ* radical polymerization in a fused silica capillary filled by homogenous polymerization mixture, comprised of a functional monomer, crosslinking monomer, porogenic solvents, and an initiator of polymerization reaction. Polarity of the resulting stationary phase is controlled by the by functional monomer, the pore structure of the monolith is affected by crosslinking monomers, and by porogenic solvents.

2. Experimental

Ethylene dimethacrylate (EDMA), tetramethylene dimethacrylate (BUDMA), hexamethylene dimethacrylate (HEDMA), dioxyethylene dimethacrylate (DiEDMA), pentaerythritole triacrylate (PETRA), bisphenol A dimethacrylate (BIDMA), and bisphenol A glycerolate

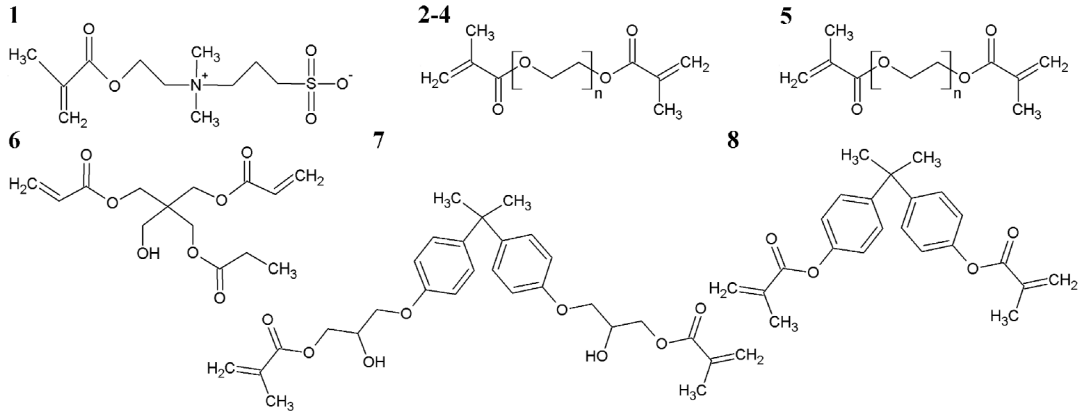

Fig. 1. **Structures of monomers**. 1 – *N*,*N*-dimethyl-*N*-metacryloxyethyl-*N*-(3-sulfopropyl) ammonium betaine, 2– ethylene dimethacrylate, 3 – tetramethylene dimethacrylate, 4 – hexamethylene dimethacrylate, 5 – dioxyethylene dimethacrylate, 6 – pentaerithritol triacrylate, 7 – bisphenol A glycerolate dimethacrylate, 8 – bisphenol A dimethacrylate

dimethacrylate (BIGDMA) were used as crosslinking monomers in generic polymerization mixture. Zwitterionic *N*,*N*-dimethyl-*N*-metacryloxyethyl-*N*-(3-sulfopropyl) ammonium betaine (MEDSA) was used as a functional monomer, 1-propanol and 1,4-butanediol as a porogenic solvents and azobisizobutyronitrile as a thermal initiator of polymerization reaction, all from Sigma-Aldrich, Steinheim, Germany. Distilled water was purified in a DEMIWA 5ROI station, Watek, Ledeč nad Sázavou, Czech republic. Polyimide-coated fused-silica capillaries, 320 and 530 μm id, were purchased from J & W, Folsom, CA, USA.

To improve the adhesion of the monolith to the capillary surface, the inner walls of the capillaries were activated[2]. The capillaries were washed with acetone, water, NaOH, again water until neutral reaction, HCl, and ethanol. Subsequently capillaries were rinsed by solution of 3-(trimethoxysilyl)propyl methacrylate, ethanol, and dried in a stream of nitrogen. After 24 h, the capillaries were filled with polymerization mixture and both ends were sealed by rubber stoppers and the capillary was kept in thermostat for 20 h at 60 °C. When the polymerization reaction was finished, the columns were washed by acetonitrile to remove unreacted part of the polymerization mixture.

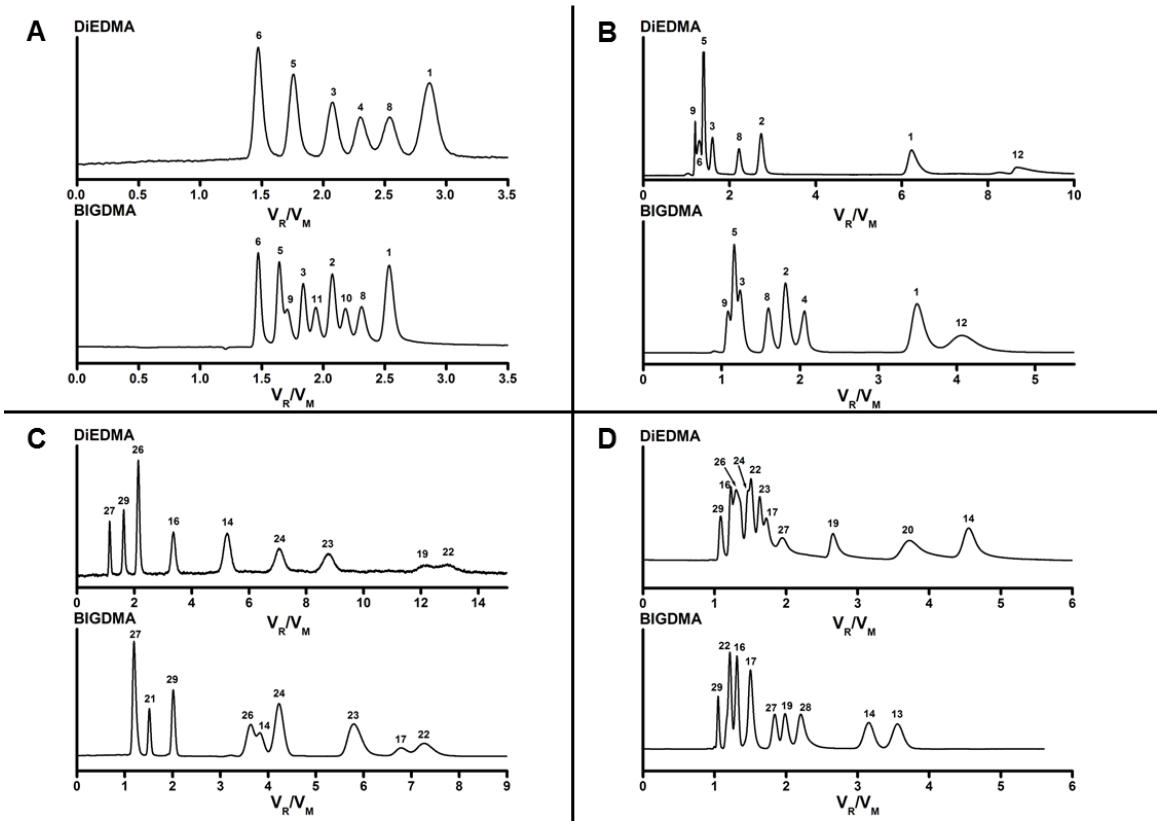

Fig. 2. **Separation of phenolic acids and flavones in HILIC and RP mode, UV detection at 214 nm**
A: Phenolic acids: 40% ACN/60% 10 mM NH_4Ac, DiEDMA: l = 168 mm, F_m = 6.3 μL min^{-1}, p = 19.6 MPa, BIGDMA: l = 183 mm, F_m = 3.3 μL min^{-1}, p = 6.3 MPa.
B: Phenolic acids: 85% ACN/15% 10 mM NH_4Ac, DiEDMA: l = 179 mm, F_m = 2.5 μL min^{-1}, p = 2.8 MPa, BIGDMA: l = 132 mm, F_m = 5.8 μL min^{-1}, p = 3.7 MPa.
C: Flavones: 40% ACN/60% 10 mM NH_4Ac, DiEDMA: l = 168 mm, F_m = 5.5 μL min^{-1}, p = 17.1 MPa, BIGDMA: l = 123 mm, F_m = 3.1 μL min^{-1}, p = 4.4 MPa.
D: Flavones: 80% ACN/20% 10 mM NH_4Ac, DiEDMA: l = 179 mm, F_m = 2.0 μL min^{-1}, p = 3.2 MPa, BIGDMA: l = 123 mm, F_m = 2.1 μL min^{-1}, p = 1.7 MPa.
Analytes: 1 : gallic acid, 2 : protocatechuic acid, 3 : *p*-hydroxybenzoic acid, 4 : salicylic acid, 5 : vanillic acid, 6 : syringic acid, 7 : hydroxyphenylacetic acid, 8 : caffeic acid, 9 : sinapic acid, 10 : *p*-coumaric acid, 11 : ferullic acid, 12 : chlorogenic acid, 13 : (-)epicatechine, 14 : (+) catechine, 15 : flavone, 16 : 7-hydroxyflavone, 17 : apigenine, 18 : lutheoline, 19 : quercetine, 20 : rutine, 21 : naringine, 22 : biochanin A, 23 : naringenine, 24 : hesperetine, 25 : hesperidine, 26 : 4-hydroxycoumarine, 27 : esculine, 28 : morine, 29 : vanillin

3. Results and discussion

The height equivalents of a theoretical plate, HETP (analyte: toluene, 95 % acetonitrile, linear velocity 0.5 mm s^{-1}) were compared for seven different crosslinking monomers. Columns prepared by using polymethylene methacrylate crosslinking monomers provide the HETP between 20 μm and 26 μm. Better efficiency, H = 16.5 μm, in comparison with EDMA, BUDMA, and HEDMA were achieved on the prepared using DiEDMA and BIGDMA crosslinker[3]. The properties of the columns were highly reproducible with the relative standard 0.5–1.3 % for the elution volemes on the columns prepared. The columns show dual retention mechanism, which allows separations both in HILIC and RP mode (Fig. 2). Capillary monolithic columns, prepared in silica capillaries with id 0.53 mm, were used in the first dimension of two-dimensional liquid chromatography, in combination with core-shell non-polar columns in the second, RP dimension, for separation of complex mixture of phenolic compounds[4].

4. Conclusions

The crosslinking monomer in the polymerization mixture significantly affects chromatographic efficiency. Capillary monolithic columns prepared by using dioxyethylene dimethacrylate and bisphenol A glycerolate dimethacrylate provide efficiency up to 70 000 plates per meter. These columns have excellent repeatability of preparation and long stability. Optimized columns were used in the first dimension of two-dimensional chromatography for separation of complex mixture of phenolic compounds[4].

The financial support of GACR project P206/12/0398 is gratefully acknowledged.

REFERENCES

1. Alpert A. J.: J. Chromatogr., A *499*, 177 (1990).
2. Jandera P., Staňková M., Škeříková V., Urban J.: J. Chromatogr., A *1274*, 97 (2013).
3. Staňková M., Jandera P., Škeříková V., Urban J.: J. Chromatogr., A *1289*, 47 (2013).
4. Jandera P., Staňková M., Hájek T.: J. Sep. Sci. *36*, 2430 (2013).

CHANGES IN LIPID METABOLISM AND HORMONES INVOLVED IN ENERGY BALANCE AFTER IMPLEMENTATION OF INTRAGASTRIC BALLOON MEDSIL®

ZDENĚK ŠVAGERA[a,b], MAREK BUŽGA[c], EVŽEN MACHYTKA[d], PAVLÍNA KUŠNIEROVÁ[a,b], and VLADISLAVA ZAVADILOVÁ[c]

[a] Department of Clinical Biochemistry, Institute of Laboratory Diagnostics, University Hospital Ostrava, Ostrava, [b] Department of Biomedical Sciences, Faculty of Medicine, University of Ostrava, Ostrava, [c] Department of Physiology and Pathophysiology, Faculty of Medicine, University of Ostrava, Ostrava, [d] Department of Clinical Studies, Faculty of Medicine, University of Ostrava, Ostrava, Czech Republic
zdenek.svagera@fno.cz

1. Introduction

The prevalence of obesity continues to increase worldwide[1]. Because obesity is associated with a number health-related problems as well as a shortened life span, treating obesity is an important clinical concern[2]. Although various treatments are currently available, many are not efficacious in the long term[3]. Therefore, additional medical treatment options for morbidly obese individuals must be explored. In this study, we examined the effects of the intragastric balloon MedSil® on anthropometric measures and hormones associated with lipid and energy metabolism.

2. Experimental

Twenty-two obese patients (the group comprised 8 male and 14 female subjects, BMI > 30 kg m^{-2}) underwent insertion of the intragastric balloon MedSil® following a clinical exam, body composition scan and collection of blood samples. Three and six months following implantation of the balloon, additional serological measures was taken. Serum concentrations of the following substances were assayed: glucose, triacylglycerols, total cholesterol, and high-density lipoprotein and low-density lipoprotein cholesterol (AU 5420, Beckman Coulter, Inc., Brea, CA, USA). To reduce analytical variation, hormones and cytokines of fat tissue from all patients were analyzed in the same run. Blood samples were kept at −80 °C until the time of analysis. Serum levels of ghrelin, leptin, adiponectin and FGF19 were analyzed by ELISA assay (Biovendor – Laboratorni

Table I
Overview of measured serum parameters

N = 22	Baseline	6 months	*P*-value
Fasting glucose [mmol L^{-1}]	5.7 ± 0.6 (4.9–7.0)	5.5 ± 0.7 (4.6–7.8)	0.075
HbA1c [mmol mol^{-1}]	44 ± 10 (35–71)	39 ± 4,0 (31–50)	0.008
Cholesterol [mmol L^{-1}]	5.7 ± 0.9 (4.6–8,9)	5.6 ± 1.2 (3.8–8.2)	0.481
Triacylglycerols [mmol L^{-1}]	2,0 ± 1,0 (0.9–4,9)	1.9 ± 1.4 (0.8–5.7)	0.267
HDL [mmol L^{-1}]	1.2 ± 0.3 (0.8–1.8)	1.2 ± 0.2 (0.9–1.6)	0.870
LDL [mmol L^{-1}]	4.1 ± 0.8 (3.1–6.4)	3.9 ± 0.9 (2.3–5.9)	0.106
Ghrelin [μg L^{-1}]	240.5 ± 101.5 (21.74–380.1)	335.8 ± 149.2 (145.0–703.2)	< 0.002
Leptin [μg L^{-1}]	30.4 ± 17.2 (6.9–54.5)	14.9 ± 15.5 (4.7–50.3)	< 0.001
Adiponectin [mg L^{-1}]	17.9 ± 9.0 (7.0–33.5)	20.5 ± 10.2 (5.8–36.2)	0.285
FGF 19 [ng L^{-1}]	148.7 ± 132.3 (42.3–621.0)	173.6 ± 73.4 (86.8–340.6)	0.111
FGF 21[ng L^{-1}]	68.2 ± 48.1 (6.0–151.9)	49.9 ± 56.8 (3.0–204.0)	< 0.002

Data are expressed as mean ± SD. *P*-values refer to significantly different values between baseline and 6 months following surgery (F-test)

medicina, Czech Republic). FGF21 was determined by a multiplex assay (Biovendor-Laboratorni Medicina) performed on a Biocode-100A (Applied BioCode Inc., Santa Fe Springs, CA, USA).

All the statistical tests were evaluated at the significance level of 5 %. The Shapiro-Wilk test was used to test normality of the data. The effects of gender and intragastric balloon in the full model were tested using the F-test. The *t*-statistic was used to test if each particular coefficient of explanatory variables was equal to zero. These analyses were performed using R software.

3. Results and discussion

Six months following insertion of the MedSil® balloon, we observed a significant decrease in glycated hemoglobin, but not in fasting glucose, triacylglycerols, cholesterol, LDL and HDL cholesterol. Compared with baseline levels, ghrelin serum levels were increased significantly, while leptin, FGF21 levels significantly decreased, 6 months after balloon insertion. The data of measured serum parameters are summarized in Table I.

There are few available reports on the effect of gastric balloons on hormonal regulation in patients with morbid obesity[4–6]. Two of the hormones that seem to play an important role in the regulation of food intake and body weight are leptin and ghrelin. Ghrelin, which is secreted mainly by the stomach, acts as an orexigenic molecule. The effect of leptin, produced by adipocytes, is opposite to that of ghrelin; in other words, leptin acts as an anorexigenic molecule. Leptin is proportionally released to the amount of fat stored in the white adipose tissue and acts in hypothalamic suppression of food intake and increase in energy expenditure[7]. In the present study, ghrelin serum levels were increased significantly, while leptin levels significantly decreased, 6 months after balloon insertion. These findings are in concordance with the data obtained by other authors[4,5,8]. Six months following the intragastric balloon insertion we found a significant decrease in FGF21 levels, but not in FGF19 levels. FGF21 was considered a metabolic hormone regulated by nutritional status, with beneficial effects on glucose homeostasis and lipid metabolism in animal models[9]. In humans, increased FGF21 levels are associated with obesity in both children[10] and adults[11] indicating a connection between FGF21 and body fat mass. Studies that have analyzed the response of FGF21 to weight loss in humans have shown controversial findings. Mai et al.[12] showed that moderate weight loss (~5 kg) induced no changes in FGF21 levels in 30 obese subjects following a hypocaloric diet and physical activity regimen for six months. The same results were published in 23 non-diabetic, morbidly obese subjects 1 year after laparoscopic Roux-en-Y gastric bypass and laparoscopic sleeve gastrectomy[13]. However, a recently published work describes significant decreases in levels of FGF21 in 17 obese females undergoing laparoscopic sleeve gastrectomy[14], which is in accordance with our results.

4. Conclusion

The MedSil® intragastric balloon is a safe and effective treatment for morbid obesity, with positive effects on glucose homeostasis and the molecules regulating lipid and energy metabolism.

This study was supported by a grant from the Ministry of Education of the Czech Republic, allocated via the University of Ostrava under registration number SGS20/LF/2013.

REFERENCES

1. Obesity and overweight, Factsheet N°311, 2011March - [cited 2013 Jul 30]. Available from: http:// www.who.int /mediacentre/factsheets/fs311/en/ index.html.
2. Ackroyd R., Mouiel J., Chevallier J. M., Daoud F.: Obes Surg *16*, 1488 (2006).
3. Franz M. J., VanWormer J. J., Crain A. L., Boucher J. L., Histon T., Caplan W., Bowman J. D., Pronk N. P.: J. Am. Diet. Assoc. *107*, 1755 (2007).
4. Konopko-Zubrzycka M., Baniukiewicz A., Wróblewski E., Kowalska I., Zarzycki W., Górska M., Dabrowski A.: J. Clin. Endocrinol. Metab. *94*, 1644 (2009).
5. Sekino Y., Imajo K., Sakai E., et al.: Int. Med. *50*, 2449 (2011).
6. Martinez-Brocca M. A., Belda O., Parejo J., Jimenez L., del Valle A., Pereira J. L., Garcia-Pesquera F., et al.: Obes Surg. *17*, 649 (2007).
7. Klok M. D., Jakobsdottir S., Drent M. L.: Obes Rev. *8*, 21 (2007).
8. Mion F., Gincul R., Roman S., Beorchia S., Hedelius F., Claudel N., Bory R. M., Malvoisin E., Trepo F., Napoleon B.: Obes Surg. *17*, 764 (2007).
9. Iglesias P., Selgas R., Romero S., Díez J. J.: Eur. J. Endocrinol. *167*, 301 (2012).
10. Reinehr T., Woelfle J., Wunsch R., Roth C. L.: J. Clin. Endocrinol. Metab. *97*, 2143 (2012).
11. Zhang X., Yeung D. C., Karpisek M., Stejskal D., Zhou Z. G., Liu F., Wong R. L., Chow W. S., Tso A. W., Lam K. S., Xu A.: Diabetes 57, 1246 (2008).
12. Mai K., Schwarz F., Bobbert T., Andres J., Assmann A., Pfeiffer A. F., Spranger J.: Metabolism *60*, 306 (2011).
13. Woelnerhanssen B., Peterli R., Steinert R. E., Peters T., Borbély Y., Beglinger C.: Surg Obes Relat Dis. *7*, 561 (2011).
14. Haluzíková D., Lacinová Z., Kaválková P., Drápalová J., Křížová J., Bártlová M., Mráz M., Petr T., Vítek L., Kasalický M., Haluzík M.: Obesity *21*, 1335 (2013).

STUDY OF THE MOST COMMON ADDITIVES AFFECTING ELECTRO-OSMOTIC FLOW FOR USE IN CAPILLARY ELECTROPHORESIS WITH CONTACTLESS CONDUCTIVITY DETECTION SETUP

KATERINA SVOBODOVA, ALES MADR, and ZDENEK GLATZ

Department of Biochemistry, Faculty of Science and CEITEC, Masaryk University, Brno, Czech Republic
svobodova.k@seznam.cz

Summary

Electrophoretic and electroosmotic phenomena occur in capillary electrophoresis. Both phenomena manifest in dependence on in-capillary conditions. The conditions are changed during method development to get the best separation but it is necessary to respect requirements of a detection technique used as well. Conductivity detection is non-specific detection technique thus signal of the detector can be easily affected by composition of background electrolyte. Electroosmotic flow – manifestation of electroosmotic phenomena – is often modified by an addition of various additives into background electrolyte. The subject of this contribution is a study of effects of additives reversing electroosmotic flow on signal of contactless conductivity detection.

1. Introduction

Capillary electrophoresis with capacitively coupled contactless conductivity detection (CE-C^4D) combines separation efficiency of CE and non-specifity of C^4D. CE-C^4D has been applied for analysis of both inorganic and organic ions, which are not easily detectable by convectional detection techniques[1]. However, some applications demand reduction, suppression or even reversion of electro-osmotic flow (EOF) which can sometimes lead to reduction of signal-to-noise ratio by either presence of additional co-ion with closer electrophoretic mobility to the analyte, or increase of noise and baseline disruption. Subject of this study is to evaluate the effect of the most common additives affecting EOF on the noise of the C^4D signal.

2. Experimental

Agilent G7100A Capillary Electrophoresis System with integrated A/D converter and controlled by Agilent ChemStation software was used. C^4D was in-house-assembled and in-cassette-built. Construction design follows the paper published by Gas et al.[2] with oscillating signal generated by a crystal oscillator working at 1.84 MHz. A capillary made of fused-silica with 50/375 μm inner/outer diameters and 48.0 cm of a total length was used in all experiments. A new capillary was used for every additive tested to avoid any memory effects. Cassette was tempered to constant 25 °C and applied voltage was 24 kV.

Buffer system based on MES (4-Morpholine-ethanesulfonic acid) adjusted by LiOH to pH 6 was used in all experiments at 20 mM concentration and was prepared freshly every day. Among tested additives belong positively charged single- and double-chained surfactants (tetradecyltrimethylammonium bromide, TTAB; hexadecyltrimethylammonium bromide, CTAB; didodecyldimethylammonium bromide, DDAB), positively charged polymers (polyethylenimine, PEI; hexadimethrine bromide, Polybrene), spermine, spermidine and hexamethonium bromide. EOF was measured using UV detection set at 234 nm to detect approx. 2 mm injected plug of 1 mM thiourea dissolved in water.

3. Results and discussion

TTAB, CTAB, spermine, spermidine and hexamethonium bromide reduce and reverse EOF at concentrations affecting C^4D signal. Moreover, TTAB and CTAB show significant memory effect which cannot be solved by intensive rinsing by 1M HCl, 1M NaOH, methanol and acetonitrile in various combinations. This fact hinders utilization of TTAB and CTAB to simple EOF reduction by a low TTAB/CTAB concentration when C^4D signal is not significantly affected yet. Most promising are PEI and Polybrene which reverse EOF at ppm levels by a strong physical attachment. DDAB form vesicular or bi-layer films on the inner capillary wall[3] at μM concentrations, but its low solubility in water-based-solvents is a major hurdle.

Preliminary experiments were done with successive multiple ionic polymer layers (SMIL)[4–5] using Polybrene or PEI layer overlaid with dextran sulphate and then by Polybrene or PEI. SMIL formed by Polybrene layers are much more stable than SMIL formed by PEI. SMIL do not deteriorate C^4D signal and have no effect on C^4D noise. However, there is observed a slight increase (approx. 10 mV) of baseline due to conductive polymers attached to the inner capillary wall.

4. Conclusions

Regulation of EOF by an addition of TTAB and CTAB is not recommended due to a strong memory effect.

They also affect noise of C^4D signal at concentration reversing EOF. Spermine, spermidine and hexamethonium bromide affect noise of C^4D signal at effective concentrations. The most promising are cationic polymers or SMILs which are responsible for stable and reverse EOF. They are also advantageous for possible coupling with mass spectrometry detection.

Financial support granted by the Czech Science Foundation (Project No. P206/11/0009) and the European Social Fund (Project No. CZ.1.07/2.3.00/20.0182 administered by the Ministry of Education, Youth and Sports of the Czech Republic) is highly acknowledged.

REFERENCES

1. Kuban P., Hauser P. C.: Electrophoresis *32*, 30 (2011).
2. Gas B., Zuska J., Coufal P., van de Goor T.: Electrophoresis *23*, 3520 (2002).
3. Melanson J. E., Baryla N. E., Lucy Ch. A.: Anal. Chem. *72*, 4110 (2000).
4. Katayama H., Ishihama Y., Asakawa N.: Anal. Chem. *70*, 2254 (1998).
5. Katayama H., Ishihama Y., Asakawa N.: Anal. Chem. *70*, 5272 (1998).

LOW-COST PAPER-BASED DEVICE FOR SEMI-QUANTITATIVE ECOTOXICOLOGICAL ANALYSIS IN TERRAIN

PAVLÍNA SVOBODOVÁ, LENKA VOJTKOVÁ, ANDREA SUCHOMELOVÁ, DENISA VLČKOVÁ, ZUZANA PETROVÁ, RADIM KNOB, and JAN PETR

Regional Centre of Advanced Technologies and Materials, Department of Analytical Chemistry, Faculty of Science, Palacký University in Olomouc, Olomouc, Czech Republic
palvina@seznam.cz

Summary

In our work, we developed a new paper-based microfluidic chip for the determination of ecotoxicologically important heavy metals Pb(II), Cd(II), Hg(II), and Ni(II). A fast, cheap and portable alternative to common analysis test was developed to detect serious environmental accidents. Our chip needs only 1.0 μL of a sample and allows detection of heavy metals in levels of units of μg L^{-1} with using a mobile phone camera as a processing medium.

1. Introduction

Low-cost paper microfluidic platforms are known as an alternative to common instruments which have high prize and low portability. The concept was introduced by Whitesides group in 2007 (ref.[1]). So far, similar platforms were used for many purposes as basic health tests[2] or for determination of Fe(II), Cu(II), Ni(II) (ref.[3]). Group of Whitesides[4] and Lin[5] pointed out some technical aspects of their preparation using mainly printing by Xerox printers. Our main purpose was to develop a fast, cheap, portable and easy operational alternative to common instruments. Our product is a new paper-based chip for semi-quantitative ecotoxicological purposes. We focused mainly on heavy metals Pb(II), Cd(II), Hg(II) and Ni(II) because of their environmental toxicity, using concentrations of μg L^{-1} while needing only 1.0 μL of sample.

2. Experimental

Paper-microfluidic devices were prepared as follows: a design was drawn using the Corel Draw X5 software; then printed by the Xerox ColorQube 8570 wax printer on filter paper Whatman, Grade 1; the structure (wax melting) was done by ironing using the Tefal Primagliss 2530 iron at highest temperature (205 °C) over a bake paper. Colored spots were processed through Sony Ericsson Xperia mobile phone and reconstructed in the Corel Photo-Paint X5 software. Microscopic observations were done by the optical microscope Motic 102M equipped with a CCD camera. Reagents used for determination of heavy metals were as follows: Pb(II) and Hg(II): potassium iodide, Cd (II): 1,5-diphenylcarbazide, and Ni(II): dimethylglyoxime, all 0.1 mol L^{-1} solutions. Reagent spots on the paper were dried using a common hairdryer.

3. Results and discussion

We designed a ring-size device with 8 spots for analysis creating 8 independent tests on the single chip (Fig. 1). Then we studied the process of channel preparation using one side printing, one side printing with two repetition of printing, and both sides printing. Firstly, we used hot plate in the process of wax melting. Because of low precision and reproducibility of chips prepared, we chose ironing over a bake paper as better suited method. Secondly, we tested different temperatures of the iron from 150 °C to 205 °C and ironing over a bake paper for 5 s to 60 s (with the increase of 5 s) using a wax printed on one side of the paper. Here, we observed that the use of highest temperature (205 °C) applied for 30 s to 45 s formed reproducible channels. Higher times destroyed the paper. We found that the use of both side printing gives more reproducible preparation of channels with reducing time of ironing from 35 s to 10 s.

To evaluate the performance of the chip, those simple analytical reactions for determination of the heavy metals were used: Pb(II) and Hg(II) were determined using potassium iodide, Cd(II) content was evaluated by 1,5-diphenylcarbazide, and dimethylglyoxime was used for determination of Ni(II). The reagents were applied using single channel pipette to the spots for analysis and then dried using a hairdryer to avoid leakage to the central spot. An example of colored spots is displayed in Fig. 2. Different concentrations of Pb(II), Cd(II), Hg(II), and Ni (II), concentrations of 5 μg L^{-1} to 100 μg L^{-1}, were tested.

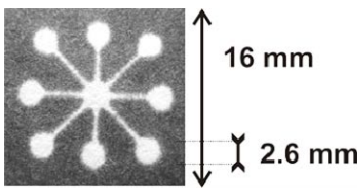

Fig. 1. **Chip design**

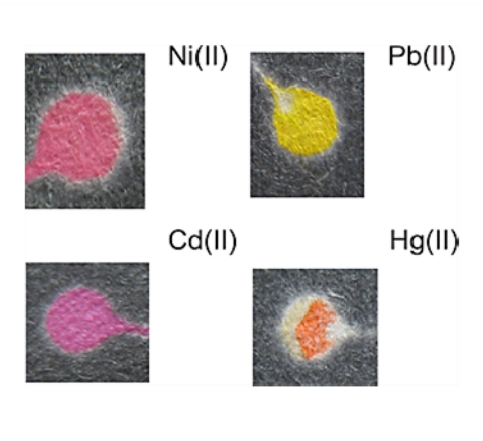

Fig. 2. **An example of colored spots formed on the paper-based microdevice**

Calibrations were linear in the range of 5 μg L^{-1} to 100 μg L^{-1} with correlation coefficients from 0.978 to 0.989.

4. Conclusions

We successfully developed a new low-cost paper-based microfluidic chip for semi-quantitative analysis of ecotoxicologically important heavy metals Pb(II), Cd(II), Hg(II), and Ni(II) that can be used in a terrain to detect environmental accidents. The result is given in less than 5 minutes including data transfer through the mobile phone, reconstruction in the Corel Photo-Paint X5 software, and evaluation.

Authors gratefully acknowledge the financial support by the Operational Program Research and Development for Innovations – European Regional Development Fund (project CZ.1.05/2.1.00/03.0058), and the Operational Program Education for Competitiveness – European Social Fund (projects CZ.1.07/2.3.00/20.0018 and CZ.1.07/2.3.00/35.0023).

REFERENCES

1. Martinez A. W., Phillips S. T., Butte M. J., Whitesides G. M.: Angew. Chem. Int. Ed. *46*, 1318 (2007).
2. Dungchai W., Chailapakul O., Henry C. S.: Anal. Chim. Acta *674*, 227 (2010).
3. Mentele M. M., Cunningham J., Koehler K., Volckens J., Henry C. S.: Anal. Chem. *84*, 4474 (2012).
4. Carrilho E., Martinez A. W., Whitesides G. M.: Anal. Chem. *81*, 7091 (2009).
5. Lu Y., Shi W., Jiang L., Qin J., Lin B.: Electrophoresis *30*, 1497 (2009).

DESIGN AND MODELING OF MICROFLUIDIC CELL CAPTURE DEVICES

MARTON SZIGETI[a], GABOR JARVAS[a,b], and ANDRAS GUTTMAN[a]

[a] *MTA-PE Translational Glycomics Research Group, MUKKI, University of Pannonia, Veszprem, Hungary,*
[b] *CEITEC – Central European Institute of Technology, Brno, Czech Republic*
szigeti@lendulet.uni-pannon.hu

Summary

A novel microfluidic cell capture device design is investigated by means of computational fluid dynamics (CFD) simulation. The device features an array of cylindrically shaped microposts. The physical object is simulated in 2D. The model is based on the laminar form of the Navier-Stokes equation assuming one phase flow with same physical characteristics as water at 293.15 K and constant dynamic viscosity. The velocity field distribution and the formed share stress are calculated by numerical methods. It is concluded that that the cell capture capability of this novel device can be significantly improved by altering the positions of the pillars.

1. Introduction

Microfabricated cell capture devices (MCCDs) are inspired by the electrical circuits of the semiconductor industry. MCCDs usually comprise channels, pillars, junctions and the combinations of those, with a goal of maximizing functionally useable area. They are used for sorting, processing and analyzing minute amount of biological fluids or other biological samples, such as rare cells[1,2]. Cell sorting has particular importance in cancer research since it reduces the complexity of the biological sample (blood) for liquid biopsy[3]. Dealing with such very small number of cells in the target makes MCCDs promising tools for detection, capture and enrichment since the geometrical dimensions of the target cells and the working channels are in the same size range. Due to their small dimensions, experimental analysis with such miniature and complex devices is not only difficult but time and cost intensive. Thus, computational modeling can be used to speed up the development. With regard to MCCDs, computational fluid dynamics (CFD) modeling is widely accepted and probably one of the most frequently used tools today. In this presentation, we focus on the investigation of the shear stress occurring in MCCDs. Furthermore, we demonstrate how CFD simulation can help to detect unexpected dead-volume problems inside the microchip.

2. Numerical experiment

The applied CFD model is based on the laminar form of the Navier-Stokes equation, since the Reynolds number is typically around unity[4] in MBDs:

$$\rho\left(\frac{\partial u}{\partial t}+(u\cdot\nabla)u\right)=\nabla\left(-pI+\eta\left(\nabla u+(\nabla u)^{T}\right)\right) \qquad (1)$$

where u is the linear velocity, ρ is the fluid density, η is the fluid viscosity, t is the time, and p is the pressure. Equtaion 1 shoud be coupled to the so called continuity equation:

$$\nabla \cdot u = 0 \qquad (2)$$

It is assumed, that the flowing fluid fills up the domain of interest (no free surface is taken into account) and has same physical characteristics as water at 293.15 K with constant dynamic viscosity (Newtonian fluid). The sedimentation is neglected, i.e. no vertical flow is expected, and therefore the MBDs are simplified in 2D (see Fig. 1). Equation 1 and 2 were solved with finite element method based numerical solver COMSOL Multiphysics version 4.3.0.151. The meshing was carried out by unmapped Delaunay triangulation method, and the number of elements was 17494. We were interested in the velocity field in the case of fully developed flow; therefore, time independent solutions were used. A typical MBD contains a large number of pillars in order to increase the functionable surface inside the chip[5]. Since the layout of the pillars and their surrounding was isotropic (the geometry was independent from the orientation), just a representative part of the whole chip was modeled to save computational time.

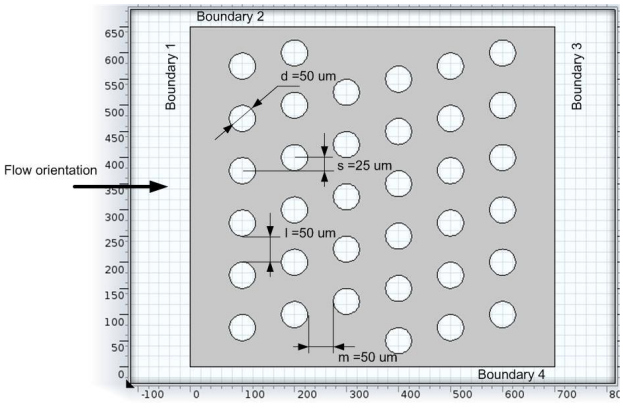

Fig. 1. **The array of micropillars in the modeled domain**

Thirty five pillars were definied, and every second coloumn was shifted with 25 μm in position to the previous one. On the wall of the pillars as well as on Boundary 2 and 4 „no slip“ boundary condition was definied, which meant that the velocity was forced to be zero (u = 0 m s^{-1}). Boundary 1 and 3 were definied as inflow and outflow, respectively.

3. Results and discussion

The obtained velocity field is shown in Fig. 2 (the warmer the color, the higher the velocity). On Boundary 1 (see Fig. 1) the full-length inflow velocity is 0.001 m s^{-1}. As one can see, the wall effect is not significant, since the flow filed distribution between the pillars is homogenous. The three hot points, where the flow velocity is higher are negligible since we are interested in the bulk characteristic only.

Based on the flow channel patterns (indicated with turquoise), which are formed between the pillars, it can be concluded that this micropost arrangement is not efficient enough. Cells, which are transported by laminar flow, can move through the chip without any interaction with the functional surfaces, i.e. the surface of the pillars. If one alters the pillar arrangement (shift the columns of pillars in vertical orientation), the pressure drop could be increased. The higher pressure drop could damage the cells; therefore, the share stress was calculated using the calculated velocity filed. The share stress is the linear function of the velocity filed and can be derived as ref.[6]:

$$\tau_{\omega} = \frac{6\mu Q}{wh^2} \qquad (3)$$

where μ is the dynamic viscosity, Q is the flow velocity, w and h are characteristic geometry sizes of the object. The calculated share stress is around 0.2 Pa, which is much less than the threshold shear stress of 150 Pa, where extensive cell damage could occur[7]. Based on the flow pattern and the calculated share stress, as a first approximation we can consider that the investigated MCCD can be improved by appropriate alteration of the pillar positions.

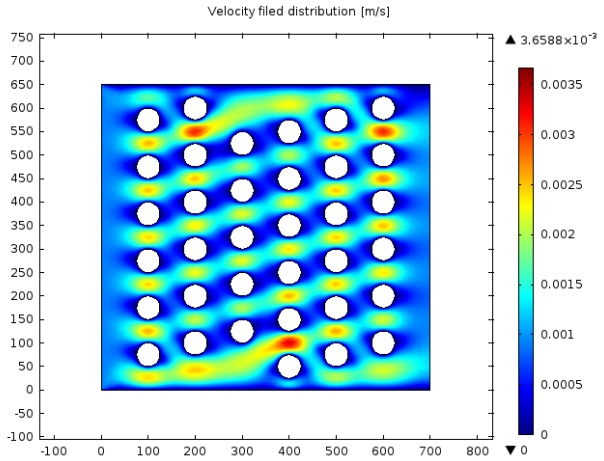

Fig. 2. **The simulated flow velocity distribution**

This project is co-financed by the European Social Fund and the state budget of the Czech Republic under project "Employment of Best Young Scientists for International Cooperation Empowerment, reg. number CZ.1.07/2.3.00/30.0037". The support of the Momentum grant #97101 of the Hungarian Academy of Sciences (MTA-PE Translational Glycomics) and P206/12/G014 of the Grant Agency of the Czech Republic are also gratefully acknowledged.

REFERENCES

1. Autebert J., Coudert B., Bidard F.-C., Pierga J.-Y., Descroix S., Malaquin L., Viovy J.-L.: Methods San Diego Calif. *57*, 297 (2012).
2. Chen J., Li J., SunY.: Lab Chip *12*, 1753 (2012).
3. Wlodkowic D., Cooper J. M.: Anal. Bioanal. Chem. *398*, 193 (2010).
4. Stone H. A., Stroock A. D., Ajdari A.: Annu. Rev. Fluid Mech. *36*, 381 (2004).
5. Nagrath S., Sequist L. V., Maheswaran S., Bell D. W., Irimia D., Ulkus L., Smith M. R., Kwak E. L., Digumarthy S., Muzikansky A., Ryan P., Balis U. J., Tompkins R. G., Haber D. A., Toner M.: Nature *450*, 1235 (2007).
6. Didar T. F., Tabrizian M.: Lab Chip *10*, 3043 (2010).
7. Leverett L. B., Hellums J. D., Alfrey C. P., Lynch E. C.: Biophys. J. *12*, 257 (1972).

SEPARATION OF SOME PHARMACEUTICAL ADDITIVES BY MICROCHIP AND CAPILLARY ELECTROPHORESIS

PETER TROŠKA[a], MARIÁN MASÁR[a], EWA POBOŻY[b], and RÓBERT BODOR[a]

[a] *Department of Analytical Chemistry, Faculty of Natural Science, Comenius University in Bratislava, Bratislava, Slovak Republic,* [b] *Department of Chemistry, University of Warsaw, Warsaw, Poland*
troska@fns.uniba.sk

Summary

Various pharmaceutical additives, erythrosine, methylparaben and propylparaben, were separated by capillary zone electrophoresis (CZE) in pharmaceutical preparations. Separations were carried out on electrophoretic microchip with conductivity detection and on electrophoretic analyzer with UV detection at 254 nm wavelength. Optimal pH of the background electrolyte was 9.75. Microchip with injected volume of a 900 nL has enabled the concentration limit of detection (cLOD) in the range 0.35–6.79 μmol L^{-1} for studied analytes. Using conventional capillary electrophoretic instrument cLOD values were in the range 0.11–0.38 μmol L^{-1}. Both methods allow fast and reproducible determinations of erythrosine, methyl- and propylparabens in various pharmaceutical products (Gastrotuss, Paxeladine and Brufen).

1. Introduction

Different additives are added to the various food, cosmetic and pharmaceutical products. These substances prolong their shelf life and improve the sensory properties such as taste, odor or color. Erythrosine (ER) is synthetic dye with potential carcinogenic, hyperactivity and photosensitivity effect. Preservatives, methylparaben (MP) and propylparaben (PP) are slightly toxic causing allergic and hypersensitive reactions with wide spectrum of antibacterial activity. Due an ionogenic character of these compounds, capillary electrophoresis (CE) or microchip electrophoresis (MCE) are suitable analytical methods for their separation and determination. These work deals with development of electrophoretic separation system for determination of erythrosine, methylparaben and propylparaben in pharmaceuticals by MCE and CE.

2. Experimental

A poly(methylmethacrylate) (PMMA) microchip with on-column conductivity detectors and fused silica (FS) capillary with UV detector working at CZE separations were used. Stock solutions of erythrosine (Sigma-aldrich; Steinheim, Germany) and parabens (Fluka; Buchs, Swiess) were prepared at 200 mg L^{-1} concentrations. A high molecular water-soluble polymer, methylhydroxy-ethylcellulose 30 000 (MHEC; Sigma-Aldrich), was used for elimination of electroosmotic flow (EOF) in both microchip and capillary formats. Pharmaceutical samples (Gastrotuss, Paxeladine and Brufen) were purchased in local pharmacy. Sample pretreatment included only 10 min centrifugation and appropriate dilution.

3. Results and discussion

A high pH (9.75) of the background electrolyte (BGE) enabled separation of fully dissociated parabens and erythrosine according to their ionic mobility with the aid of 1 mmol L^{-1} β-cyclodextrin added to the BGE solution.

Intra-day repeatability of quantitative and qualitative parameters were calculated from three repeated runs with model samples performed on miniaturized and conventional CE platforms with identical BGE during one day. RSD for peak areas were 0.4–3.5 % and 1.2–9.3 % for MCE and CE, respectively and RSD for migration times were 0.8–1.9 % and 0.4–1.7 % for MCE and CE, respectively.

The concentration limits of detection (cLOD) were calculated using method based on 3.3 times of the standard deviation of response and slope of the calibration curve from the peak height of analytes. PMMA microchip working with 900 nL sample volume has allowed to achieve low cLOD values, 0.35 μmol L^{-1}, 0.98 μmol L^{-1} and 6.79 μmol L^{-1} for erythrosine, methylparaben and propylparaben, respectively. The cLOD values obtained from CZE separations on conventional CE analyzer with UV detection were 0.11 μmol L^{-1}, 0.32 μmol L^{-1} and 0.38 μmol L^{-1} for erythrosine, methylparaben and propyl-paraben, respectively.

The three pharmaceutical samples were analyzed for a content of erythrosine, methyl- and propylparabens by proposed method. Only centrifugation and dilution of the analyzed samples were used as sample pretreatment. Determined concentration of erythrosine, methylparaben and propylparaben in pharmaceutical products are summarized in Table I.

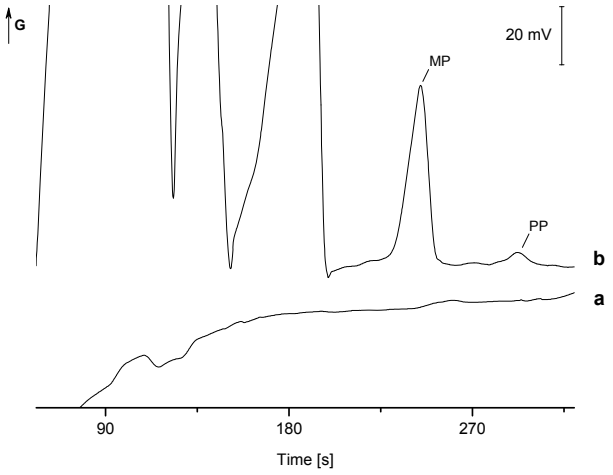

Fig. 1. **Electropherograms from the CZE analyses of pharmaceutical sample Brufen on the PMMA microchip with conductivity detection.** Injected sample: (a) BGE (a blank run), (b) 20-times diluted sample Brufen in 10% BGE and 1 mmol L^{-1} sulfate. G = conductivity

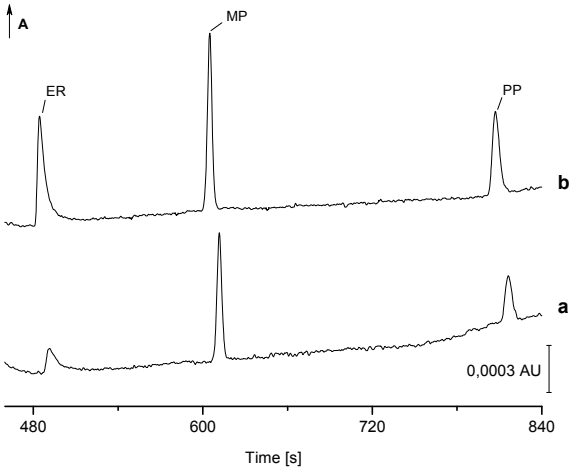

Fig. 2. **Electropherograms from CZE analyses of pharmaceutical sample Paxeladine in the FS capillary with UV detection at 254 nm.** Injected sample: (a) 100-times diluted sample PAXELADINE in 10% BGE and 1 mmol L^{-1} sulfate, (b) the same as in (a) with addition of 10 mg L^{-1} erythrosine, 2.5 mg L^{-1} methylparaben and 2.5 mg L^{-1} propylparaben. A = absorbance

Table I
Concentrations of the studied additives in pharmaceutical samples

Drug	Analyte	Separation platform	$c \pm$ SD [mg L^{-1}]	D_f	n
GASTROTUSS	ER	capillary	80 ± 2	20	3
	MP	capillary	334 ± 10	100	3
	PP	capillary	274 ± 8	100	3
PAXELADINE	ER	capillary	383 ± 67	100	3
	MP	microchip	558 ± 15	100	3
		capillary	582 ± 38	100	3
	PP	microchip	298 ± 16	10	3
		capillary	300 ± 14	100	3
BRUFEN	MP	microchip	838 ± 14	20	3
		capillary	884 ± 12	100	3
	PP	microchip	446 ± 15	20	3
		capillary	470 ± 16	100	3

c – average concentration in the sample, SD – standard deviation, D_f – dilution factor n – number of repeated CZE runs

4. Conclusion

CZE performed on the PMMA microchip with conductivity detection and conventional capillary analyzer with UV detection offered simple, sensitive and reproducible analytical procedure for the determination of erythrosine, methylparaben and propylparaben in the pharmaceuticals.

This work was supported by grants from the Slovak Grant Agency for Science (VEGA 1/1149/12) and the Research & Development Operational Programme funded by the ERDF (Center for Industrial Research of Optimal Method for Synthesis of Highly Effective Drugs, SynAnPharm, ITMS 26240220061).

DERIVATIZATION OF FATTY ALCOHOL ETHOXYLATES FOR LIQUID CHROMATOGRAPHY SEPARATION WITH UV-VIS DETECTION

NIKOLA VAŇKOVÁ, PETR ČESLA, and JAN FISCHER

Department of Analytical Chemistry, Faculty of Chemical Technology, University of Pardubice, Pardubice, Czech Republic
nikola.vankova@student.upce.cz

Summary

The aim of this work was to compare reagents used for derivatization of non-ionic surfactants based on fatty alcohol ethoxylates. In this work, three derivatization reagents were compared: ftalic anhydride, phenyl isocyanate and phenyl isothiocyanate. After selecting the best reagent, the derivatization process was optimized, including composition of the reaction mixture – ratio of the alcohol ethoxylate and the reagent and the derivatization with or without catalyst. Prepared derivatives were analyzed using liquid chromatography with UV-VIS detection.

1. Introduction

Fatty alcohol ethoxylates belong to the group of non-ionic surfactants, which are the most common part of cleaning and laundry agents. Because of massive production and worldwide usage, the impact of fatty alcohol ethoxylates (FAEs) on the environment is monitored. The general formula of FAEs is $CH_3(CH_2)_n(OCH_2CH_2)_yOH$, where *n* used to be in between of 11 and 15, 17 and *y* is usually 0–18. FAEs are prepared by the reaction of fatty alcohol with ethylen oxide. After the reaction, the mixture of different alkyl chain and ethoxy (EO) distribution is obtained and its characterization is important for the setting of the hydrophilic-lipophilic equilibration (HLB). The value of this equilibration determines the size of FAEs solubility, foaming etc.[1,2].

The most frequently used derivatization reagents for UV detection are anhydrides of ftalic and maleinic acids, benzoyl chloride and its analogues, phenyl isocyanate and naphtyl isocyanate. The less common reagent used for derivatization of alcohols is phenyl isothiocyanate, which is usually used for derivatization of amines and amino acids[3–5].

In some cases it is necessary to use catalyst, which accelerates or even enables the reaction. The catalysts suitable for nucleophile reactions are pyridine, triethylamine, diethylamine, dimethylsulfoxide and dimethylformamide[6].

2. Experimental

2.1. Apparatus

The separation of fatty alcohol ethoxylates was realized on the modular liquid chromatograph (Shimadzu, Kyoto, Japan) with UV detection. The liquid chromatograph consisted of degasser DGU 3014, two pumps LC-20AD XR involving binary gradient of mobile phase composition, mixer, six port injection valve with outer loop with the volume 20 μl (Valco – Vici) or 5 μl (Rheodyne, USA), column thermostat LC 120 (ECOM, Czech Republic) and UV detector SPD-20A.

Two columns were selected for the experiments: Zorbax Eclipse XDB-C18 with the length 150 mm and inner diameter 4.6 mm, packed with fully porous 5 μm particle size and Poroshell C18 (150 mm × 3 mm i.d.), packed with porous shell particles of the size 2.7 μm.

2.2. Chemicals

The mobile phase was prepared using acetonitrile (Sigma Aldrich, Steinhein, Germany) and redistilled water filtered by Demiwa 5-ROI (Watek, Ledeč nad Sázavou, Czech Republic) and SG UltraClear apparatus (SG, Hamburg, Germany). The acetic acid was used as an additive for the mobile phase (Penta, Chrudim, Czech Republic).

Three reagents were selected for derivatization process: ftalic anhydride (Sigma Aldrich, Steinhein, Germany), phenyl isocyanate (Merck, Praha, Czech Republic) and phenyl isothiocyanate (Sigma Aldrich, Steinhein, Germany). For preparing esters of ftalic acid, 1,4-dioxane (Lachema, Brno, Czech Republic), urea (Lach-Ner, Neratovice, Czech Republic), 25 % (m/m) water solution of NaOH (Lach-Ner, Neratovice, Czech Republic) and methanol (Sigma Aldrich, Steinhein, Germany) were used. Two catalysts of the reaction between fatty alcohol ethoxylates and phenyl isothiocyanate (PITC) were selected, including pyridine (Lachema, Brno, Czech Republic) and triethylamine (Lach-ner, Neratovice, Czech Republic). For the experiments, five technical samples of fatty alcohol ethoxylates were obtained from Slovasol (Sasol Slovakia, Nováky, Slovakia).

2.3. Conditions of separation

Mobile phase consisted of acetonitrile and redistilled water with the addition of acetic acid at the concentration 0.1 % (v/v). The samples were separated using gradient elution mode. The mobile phase composition programme was 0 min 70 % ACN/water – 30 min 100 % ACN. The mobile phase flow rate used with the column Zorbax

Eclipse XDB-C18 was 1 mL min^{-1} and with the column Poroshell C18 0.4 mL min^{-1}. Column was termostated on the temperature 35 °C. Ftalic acid esters and urethanes were detected at 230 nm, thiourethanes were detected at 280 nm.

3. Results and discussion

The comparison of the separation of FAEs after derivatization with phenyl isocyanate and phenyl isothiocyanate on both C18 columns packed with fully porous particles and packed with porous shell particles is shown on the Fig. 1 and 2. The separation according to the length of alkyl chain and the number of ethoxy units is obtained with both derivative reagents, but the resolution of the oligomers with the different number of ethoxy unit is higher for thiourethane derivatives. The application of porous shell particle stationary phases yielded higher efficiency of the separation of both types of derivatives in comparison to the fully porous particles.

The reaction between phenyl isothiocyanate and alcohol ethoxylate can be catalyzed by pyridine or triethylamine. After the comparison of reaction yileds for derivatization process employing pyridine and triethylamine (Fig. 3), triethylamine was selected as more effective catalyst providing higher reaction yield of the thiourethanes in shorter reaction time.

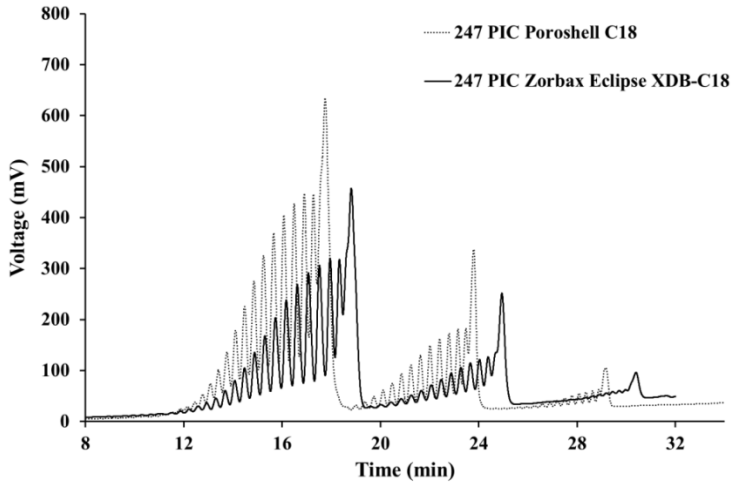

Fig. 1. **Separation of urethanes on the columns Poroshell C18 and Zorbax Eclipse XDB-C18**

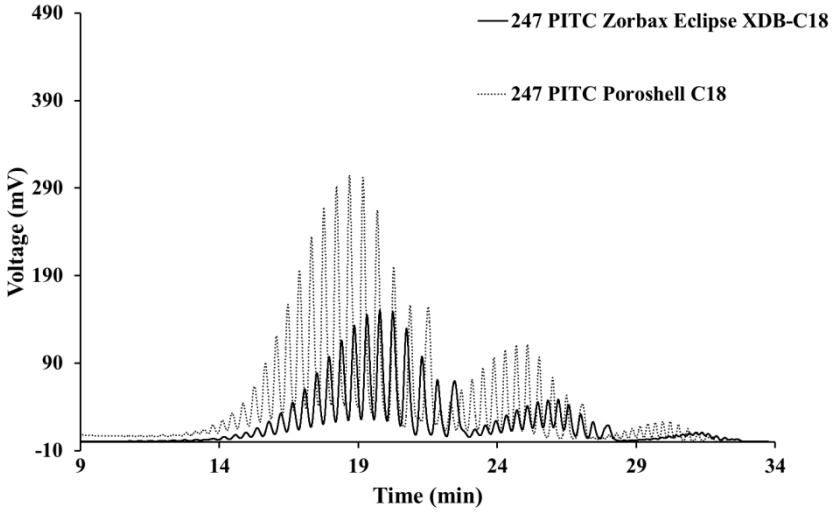

Fig. 2. **Separation of thiourethanes on the columns Poroshell C18 and Zorbax Eclipse XDB-C18**

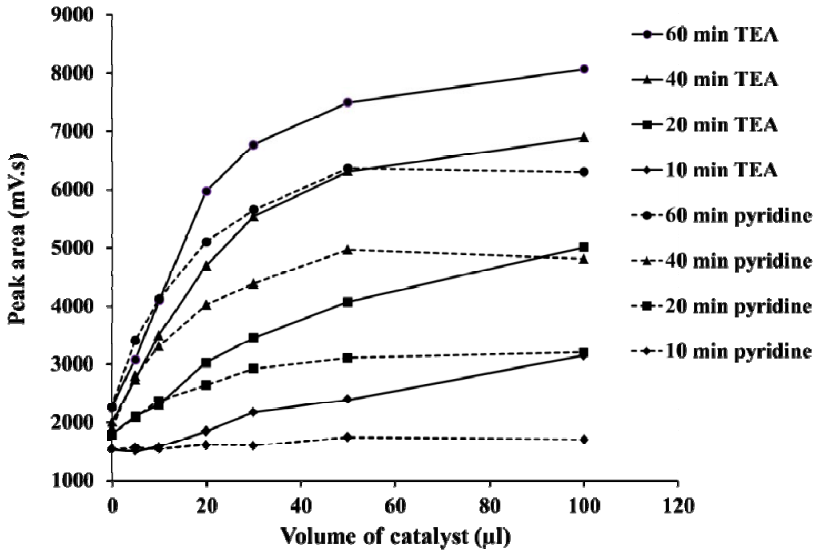

Fig. 3. **Comparison of two catalysts (pyridine and triethylamine) and reaction time**

4. Conclusions

Derivatized fatty alcohol ethoxylates were separated according to the length of alkyl chain and the number of ethoxy units in their molecules. The best results were achieved using derivatization reaction with phenyl isothiocyanate. The optimal mass ratio between alcohol ethoxylate and phenyl isothiocyanate is 2:1. The reaction between phenyl isothiocyanate and alcohol ethoxylates is much faster using catalyst (pyridine, triethylamine). The peak area and thus the reaction yield increases three times with the reaction time 60 min using pyridine or triethylamine in comparison to the derivatization without catalyst. Triethylamine is more efficient as the catalyst of the reaction between alcohol ethoxylates and PITC than pyridine due to the higher reaction yields in shorter time. The optimal ratio between alcohol ethoxylate, phenyl isothiocyanate and triethylamine is 2:1:0.75 (m/m/m). The separation on the C18 column packed with porous shell particles is more efficient than on the column packed with fully porous particles under approximately the same retention times.

This project was supported by University Pardubice internal grant SGFchT06/2013.

REFERENCES

1. Belanger S. E., Dorn P. B., Toy R., Boeije G., Marshall S. J., Wind T., Van Compernolle R., Zeller D.: Ecotoxicol. Environ. Saf. *64*, 85 (2006).
2. Sparham Ch. J.:Determination of alcohol ethoxylates in environmental samples using derivatisation and LC/MS. *Ph.D. Dissertation*, University of Northumbria at Newcastle, 2006.
3. Plata Mária R., Contento Ana M., Ríos A.: Trends Anal. Chem. *30*, 1018 (2011).
4. Micó-Tormos A., Simó-Alfonso E., Ramis-Ramos G.: J. Chromatogr., A *1203*, 47 (2008).
5. Chávez G., Bravo B., Piña N., Arias M., Vivas E., Ysambertt F., Márquez N., Cáceres A.: Talanta *64*, 1323 (2004).
6. Walter W., Bode K.-D.: Angew. Chem. Int. Ed. *6*, 281 (1967).

CZE AND MEKC SEPARATION OF PHENOLIC COMPOUNDS

JANA VÁŇOVÁ, PETR ČESLA, and JAN FISCHER

Department of Analytical Chemistry, Faculty of Chemical Technology, University of Pardubice, Pardubice, Czech Republic
Jana.Vanova@student.upce.cz

Summary

Micellar electrokinetic chromatography was used in this work for separation of selected antioxidants. The critical micellar concentration of homologous series of sodium alkyl sulfates and migration time of their micelles were determined. The effects of pH of background electrolyte, concentration of surfactants and organic modifier on the separation selectivity of flavonoids and phenolic acids were studied.

1. Introduction

Micellar electrokinetic capillary chromatography (MEKC) is a mode of capillary electrophoresis, which combines principles of liquid chromatography and capillary zone electrophoresis. Neutral molecules as well as charged ions can be separated by this technique, including pharmaceuticals, environmental pollutants, cell cultures, biological fluids and substances in food[1–3].

For the process of MEKC, the presence of surfactant micelles in background electrolyte is essential. The micelles are formed if the concentration of surfactant in solution is higher than the critical micelle concentration[4]. The critical micelle concentrations (*cmc*) of the sodium alkyl sulfate surfactants were determined in water, borate buffer (25 mmol L^{-1}, pH 9.30) and buffer with addition of acetonitrile (5–20 %; v/v). Besides of the effect of length of alkyl chain and of the surfactant concentration in background electrolyte on the separation selectivity of natural antioxidants, the effect of organic modifier acetonitrile was investigated, too. In this work, sodium decyl sulfate and sodium dodecyl sulfate were used for the separation of selected flavonoids and phenolic acids. The MEKC separation of antioxidants was compared to the CZE separation in the same buffer without surfactants.

2. Experimental

Sodium decyl sulfate and sodium dodecyl sulfate, selected antioxidants ((–)-epicatechin, (+)-catechin, 4-hydroxyphenylacetic acid, 7-hydroxyflavone, caffeic acid, flavone, gallic acid, hesperetin, hesperidin, chlorogenic acid, naringenin, *p*-hydroxybenzoic acid, quercetin, rutin, salicylic acid) and alkylbenzenes (methylbenzene, ethylbenzene, propylbenzene, butylbenzene, pentylbenzene) were obtained from Sigma-Aldrich (Steinheim, Germany). Sodium tetraborate and boric acid were purchased from Fluka (Buchs, Switzerland), thiourea from LachNer (Brno, Czech Republic) and methanol from J. T. BAKER (Deventer, Netherlands).

All experiments were carried out using capillary electrophoresis Agilent ^{3D}CE (Palo Alto, CA, USA) in fused-silica capillary (non-coated, 48 cm total length, 40 cm effective length, 50 μm i.d.) and voltage 20 kV was applied. Detection wavelength was set at 254 nm. Separation capillary was preconditioned by flushing with electrolyte for 2 min before the analysis. The samples were injected by applying 50 mBar pressure on the inlet sample vial for 5 s.

The stock solutions of antioxidants were prepared in methanol (0.5 g L^{-1}) and for separation the samples were diluted by water to the final concentration of 10 mg L^{-1}.

The critical micelle concentration was determined by the method based on the measurement of the background electrolyte current[5] and by the computational method using the retention model[6], where the migration time of the micelles was obtained using iterative process of migration times of homological series of alkylbenzenes[7].

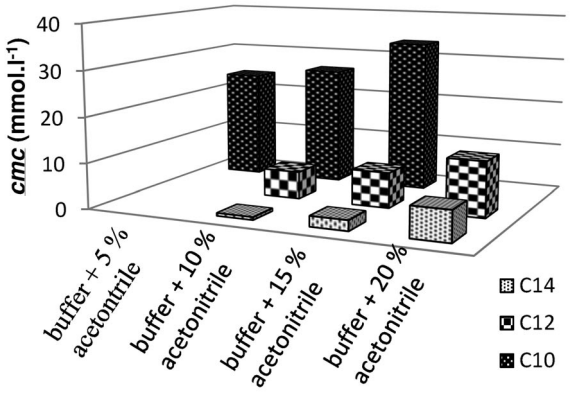

Fig. 1. **The values of critical micelle concentration of sodium decyl-, dodecyl- and tetradecyl sulfate in electrolyte with concentration of acetonitrile 5–20 % (v/v)**

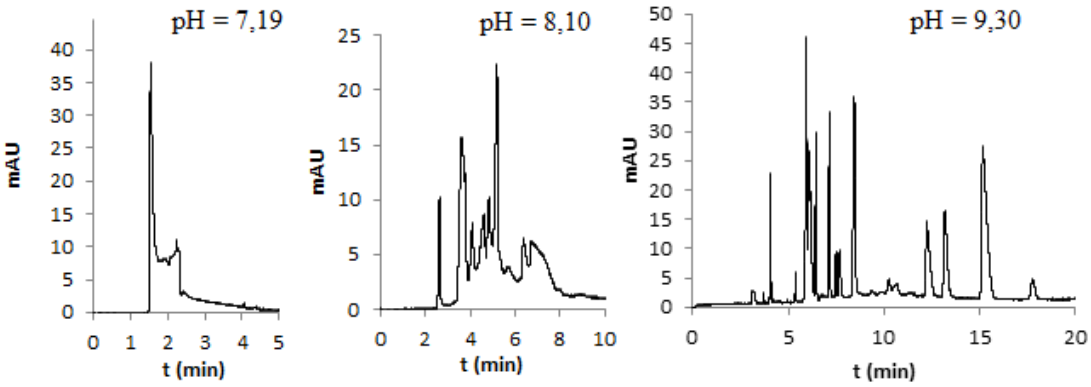

Fig. 2. **Separation of the mixture of antioxidants in 25 mmol L^{-1} borate background electrolyte pH 7.19; 8.10 and 9.30**

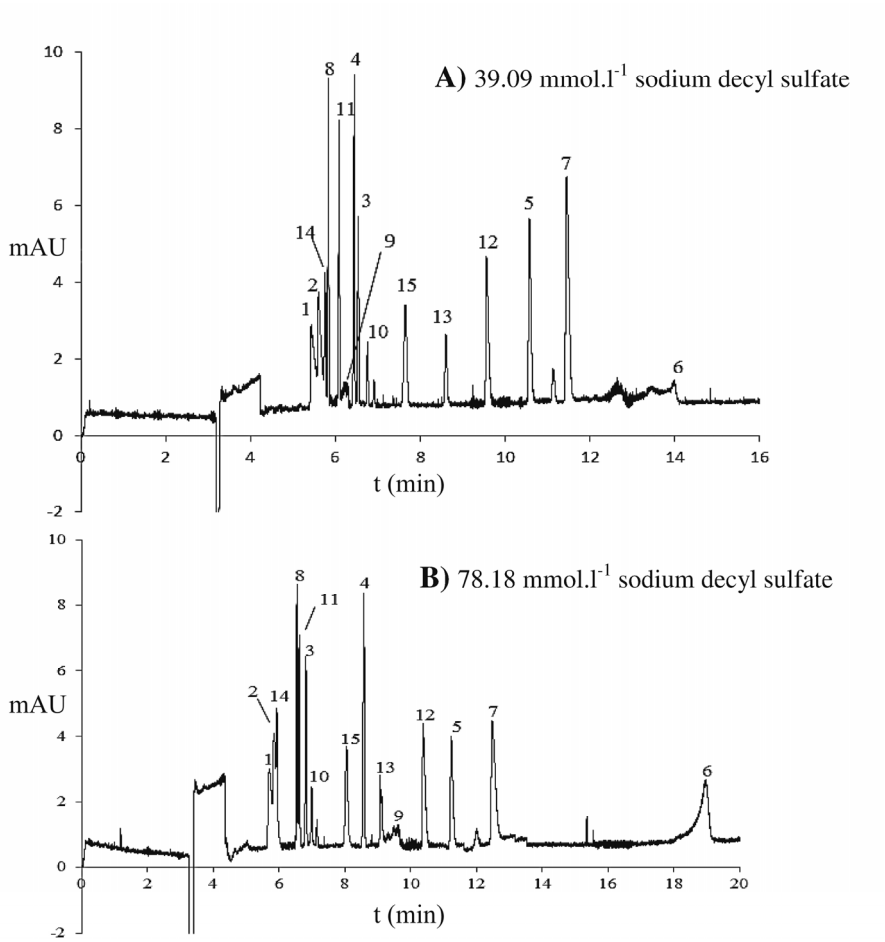

Fig. 3. **Separation of mixture of antioxidants in 25 mmol L^{-1} borate background electrolyte pH 9.30.** Non-coated 48 (40) cm fused silica capillary, 50 μm i.d., applied voltage 20 kV, temperature 25 °C. 1: (–)-epicatechin, 2: (+)-catechin, 3: rutin, 4: hesperetin, 5: naringenin, 6: 4 hydroxyphenylacetic acid, 7: chlorogenic acid, 8: 7-hydroxyflavone, 9: salicylic acid, 10: quercetin, 11: *p*-hydroxybenzoic acid, 12: caffeic acid, 13: gallic acid, 14: flavone, 15: salicylic acid

3. Results and discussion

The values of critical micelle concentrations of sodium alkyl sulfate surfactants were determined by the two methods. The measured values are presented in the Fig. 1. The critical micelle concentration decreases with increasing length of the alkyl chain in the surfactant molecules and increases with increasing concentration of acetonitrile in the background electrolyte.

First, the separation of selected antioxidants was carried out in background electrolyte without the surfactants. The pH of electrolyte was changed in the range of 6.89–9.30.

Separation of the selected antioxidants using different pH of BGE is presented in the Fig. 2. As can be seen from this figure, the increasing value of pH improves the separation selectivity and at pH 9.30, the best separation of flavonoids and phenolic acids was obtained.

The MEKC separation of the mixture of antioxidants in background electrolyte with addition of 0–20 % (v/v) acetonitrile is presented in Fig. 3. The separation time increases both with increasing concentration of sodium alkyl sulfate and with increased concentration of acetonitrile in background electrolyte.

4. Conclusions

Influence of working conditions on the separation of selected antioxidants was studied. The critical micelle concentrations of homologous series of sodium alkyl sulfates were determined by the methods (*i*) based on the measurement of BGE current and (*ii*) based on the retention model. The critical micelle concentration decreases with increasing number of carbons in the alkyl chain and increases with increasing concentration of acetonitrile in BGE.

Separations of the mixture of phenolic acids and flavonoids were carried out in BGE with pH in the range 6.89–9.30 and with different type and concentration of sodium alkyl sulfates and concentration of acetonitrile. Separation time, retention factors of analytes and width of the migration window can be manipulated by using sodium alkyl sulfates with different length of the alkyl chains in their molecules and by varying of the concentration of acetonitrile.

The financial support by the Faculty of Chemical Technology (project No. SGFChT06/2013) is kindly acknowledged.

REFERENCES

1. Nishi H., Terabe S.: J. Chromatogr., A *735*, 3 (1996).
2. Terabe S.: J. Pharm. Biomed. Anal. *10*, 705 (1992).
3. Zhang J., Chakraborty U., Foley J. P.: Electrophoresis *30*, 3971 (2009).
4. Zilin C., Jin-Ming L., Katsumi U., Toshiyuki H.: Anal. Chim. Acta *403*, 173 (2000).
5. Cifuentes A., Bernal J. L., Diez-Masa J. C.: Anal. Chem. *69*, 4271 (1997).
6. Terabe S., Otsuka K., Ichikawa K., Tsuchiya A., Ando T.: Anal. Chem. *56*, 111 (1984).
7. Váňová J., Česla P., Fischer J., in: *XV. Monitorování cizorodých látek v životním prostředí* (Fischer J., Česla P., Vytřas K., ed.), University of Pardubice, 2013.

THIN LAYER CHROMATOGRAPHY AS A SCREENING METHOD FOR HPLC CONDITIONS FOR THE ANALYSIS OF AQUEOUS SOIL EXTRACTS

VERONIKA VOJTKOVÁ and MILAN HUTTA

Department of Analytical Chemistry, Faculty of Natural Sciences, Comenius University, Bratislava, Slovakia
vojtkova@fns.uniba.sk

1. Introduction

In this work we dealt with the study of possibilities of thin layer chromatography analysis of aqueous soil extracts as a screening tool for selection of appropriate chromatographic systems that can be transferred or modified further for high performance liquid chromatography analysis of certain soil constituents.

Many approaches are well known in soil analysis. Numerous authors studied extraction of specific analytes, but our aim is to separate as many substances as possible from organic soil matrix. An efficient extraction technique should be like that it can produce good results within a short time with minimum operator involvement. It should also be cheap, and safe for both the analyst and the environment.

These methods are commonly used in this field of interest: traditional extraction methods including Soxhlet, ultrasonication, mechanical shaking and reflux with methanolic KOH, modern techniques including soxtec (automated soxhlet) supercritical fluid extraction (SFE), microwave-assisted extraction (MAE), pressurised hot water extraction (PHWE), pressurised liquid extraction (PLE) or accelerated solvent extraction (ASE). Authors applied these techniques at polycyclic aromatic hydrocarbons, carbohydrate content, pesticides and herbicides analysis[1,2]. In recent years became popular hot-water extraction because it is green extraction method for different classes of compounds present numerous kinds of matrices such as environmental, food and botanical samples[3].

Soil consists of four main-basic components minerals, organic matter, air and water. Most introductory soil textbooks describe the ideal soil (ideal for the growth of most plants) as being composed of 45 % minerals, 25 % water, 25 % air, and 5 % organic matter[4]. Soil organic matter (SOM) is a complex mixture of substances that can be highly variable in its chemical content. It ranges from freshly deposited plant and animal parts to the residual humus —stable organic compounds that are relatively resistant to further rapid decomposition. Main elements in SOM are carbon, oxygen, hydrogen, nitrogen, phosphorus, and sulfur. Soil is divided into humic substances and non-humic substances. Humic substances are humic acids (HA), fulvic acids (FA) and humins. And non-humic ones are compounds belonging into known classes of biochemistry, such as: carbohydrates, lipids, amino acids[5].

Planar chromatography celebrated its 70th anniversary in 2008, so today it will be 75th (ref.[6]). It comprises all chromatographic techniques that use a planar open stationary phase present as or on a plane (layer), i.e. thin-layer chromatography (TLC), high-performance thin-layer chromatography (HPTLC), ultrathin-layer chromatography (UTLC), and preparative layer chromatography. Today, paper chromatography is hardly used. TLC is a complementary technique to HPLC using an orthogonal selectivity. Mostly, normal phase systems were employed for HPTLC versus reversed phase systems for HPLC.

Humic acids and non-humic compounds are very complex molecules and could cause many problems before HPLC analysis and so it is reasonable to choose thin layer chromatography method with scan possibilities in Origin, which could help us process data.

2. Experimental

2.1. Soil

We used four soil samples: Skalka, Stupava, Šajdíkové Humence, Gbely. The samples of soils were provided with detailed specifications from geology. Soils were diluted in 6 mL of NH_4OH.

2.2. Reagents

Ethanol (Lachema, n.p. Brno), ultrapure water, Simplicity UV, (Millipore S.A.S., France), ammonia solution 28–30 %, (Merck, Darmstadt, Germany), NaCl (Lachema, n.p. Brno).

2.3. Instruments

TLC plates: Fixion 50x8 Na^+, (20 x 20 cm), (Reanal, Budapest, Hungary), Fixion 2 × 8 Anion, (Reanal, Budapest, Hungary), Lucefol (20 × 20 cm)/ (15 × 15 cm), (Kavalier, Czechoslovakia), Silufol (20 × 20 cm) / (15 × 15 cm), (Kavalier, Czechoslovakia), OriginPro 8 Software, OriginLab corporation (USA), Centrifuge Eppendorf AG 22331 (Hamburg, Germany), Containers for developing thin films.

3. Results and discussion

TLC plates were developed in closed chambers, as mobile phase, we used a variety of aqueous solutions (H_2O, NaCl, ethanol). TLC plates were Silufol, Lucefol, Fixion 50 and Fixion 2. To obtain quantitative data from

TLC plates, we used a computer, which was equipped with a conventional scanner. From the obtained images we then received chromatograms (representing graphical dependence of retardation factor and signal strength). These chromatograms were obtained using the program Microcal ORIGIN ® ® Pro 8. The principle of evaluation results using the program Microcal ORIGIN ® ® Pro 8 (Fig. 1).

Samples were plated on four plates: Fixion 50, Fixion 2, Lucefol and Silufol. We studied properties and influence content of mobile phase NaCl, ethanol,water. Figure 2–4 showed influence of NaCl on Fixion 2 plate. Concentration of NaCl was 0.5 M, 0.1 M and 0.01 M. On the figures are shown chromatograms, which we can use as a help before HPLC analysis to consider that method and analytes are suitable for HPLC analysis.

4. Conclusions

This work dealt with the selection of appropriate conditions for analysis soil organic matter by thin layer chromatography as a preparation method before complex HPLC analysis. Program Origin has proved to be helpful in evaluating data.

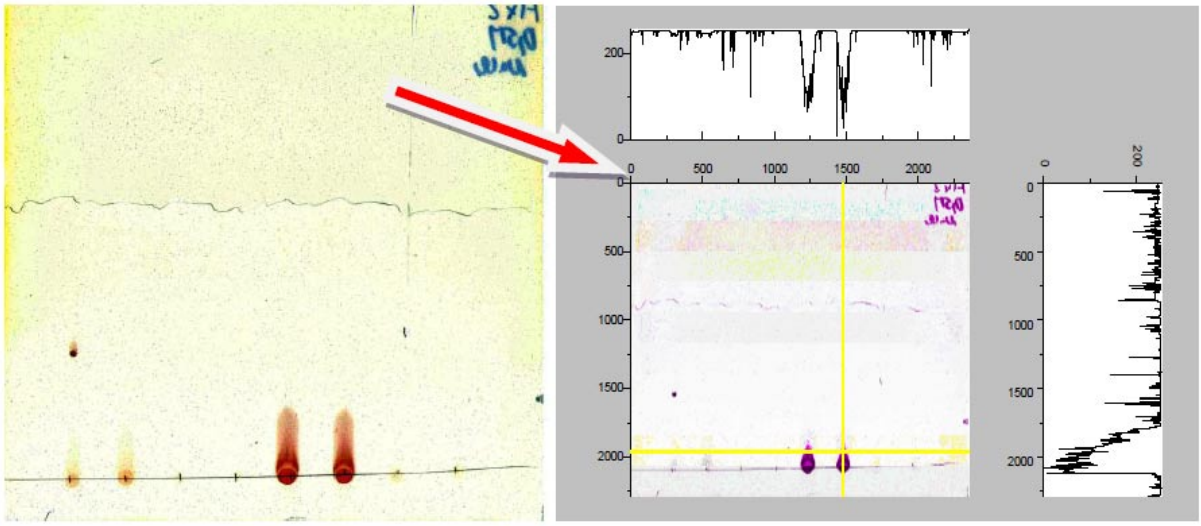

Fig. 1. **Results from Microcal ORIGIN ® ® Pro 8**

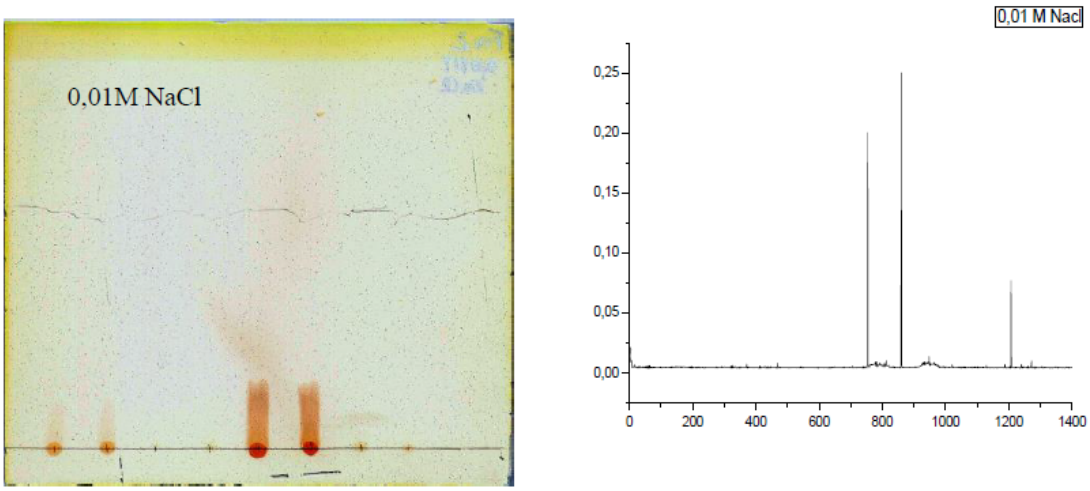

Fig. 2. **0.01 M NaCl**

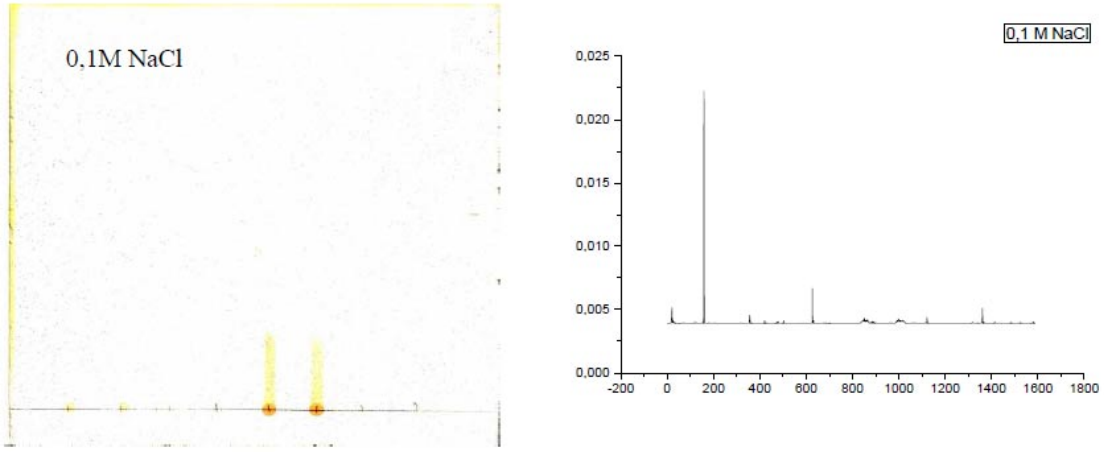

Fig. 3. **0.1 M NaCl**

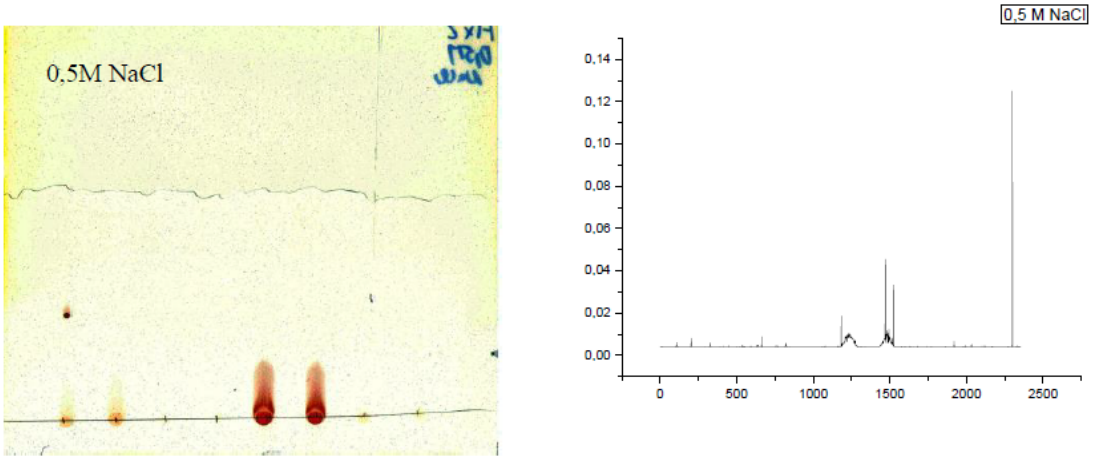

Fig. 4. **0.5 M NaCl**

This work was generously supported by the grant of Scientific Grant Agency of the Ministry of Education of Slovak Republic and the Academy of Sciences – project VEGA 1/1349/12 and the grant of Slovak Research and Development Agency – project APVV-0583-11. This work is partially outcome of the project VVCE-0070-07 of Slovak Research and Development Agency.

REFERENCES

1. Oluseyi T. , et al.: Afr. J. Environ. Sci. Technol. *5*, 482 (2011).
2. Ivo Šafařík, et al.: Plant Soil *143*, 109 (1992).
3. Chin Chye Teo, et al.: J. Chromatogr., A *1217*, 2484 (2010).
4. http://www.nerrs.noaa.gov/doc/siteprofile/acebasin/html/envicond/soil/slform.htm (22.10.2013).
5. http://karnet.up.wroc.pl/~weber/def2.htm (22.10.2013).
6. Morlock G., et al.: J. Chromatogr., A *1217*, 6600 (2010).

UTILIZATION OF MICROPREPARATIVE FAST FOCUSING BY A NEW WIDE pH RANGE ELECTROLYTE SYSTEM BASED ON BIDIRECTIONAL ISOTACHOFORESIS

MARIE VYKYDALOVÁ[a,b], FILIP DUŠA[a,b], MARIE HORKÁ[a], and KAREL ŠLAIS[a]

[a] *Institute of Analytical Chemistry of the ASCR, v. v. i., Brno,* [b] *Department of Biochemistry, Faculty of Science, Masaryk University Brno, Brno, Czech Republic*
vykydalova@iach.cz

Summary

We suggest the possibility of practical utilization of a new electrolyte system for fast preparative focusing in wide pH range based on bidirectional isotachophoresis. The focusing occurs on nonwoven fabric strip positioned in an open horizontal V-shaped trough. It is based on bidirectional ITP with multiple counter ions and spacers created from commercially available simple buffers. Milk spiked with ampicillin was used as a sample and high performance liquid chromatography was as a second dimension for analysis of fast preparative focusing fractions. Speed, easy fraction handling, and possibility of pre-concentration of analytes from a raw sample are the benefits of this technique.

1. Introduction

Biological samples are in most cases very complex. Therefore, their treatment is necessary before each analysis. Pretreatment of sample is crucial step which affect whole experiment. Removal of salts and undesirable substances as well as pre-concentration of sample is required. The micropreparative solution phase isoelectric focusing (sIEF) developed by our group is suitable for this purpose and provides knowledge about a protein p*I*, which helps with protein identification[1]. However, the disadvantage of this technique is time-consuming. Therefore, the fast micropreparative focusing was proposed. This technique combines advantages of bidirectional isotachophoresis (BITP), described in previous works[2–4], with suggested wide pH range electrolyte system.

The performance of the fast focusing based on bidirectional isotachophoresis using our electrolytic system is demonstrated by focusing of ampicillin from milk. The focusing occurs in nonwoven fabric strip separation bed positioned in an open horizontal V-shaped trough and fractions obtained from strip are further analyzed using high performance liquid chromatography (HPLC).

2. Experimental

2.1. Treatment of milk

Milk was spiked with 50 μL mL^{-1} ampicillin. Solution was centrifuged at 14100 × g for 35 min. Milk supernatant was then loaded into a non-woven fabric strip for BITP.

2.2. Fast IEF

The device with a narrow nonwoven strip separation bed placed in a V-shaped trough was described previously[1]. Briefly, a strip with dimensions of 175 mm in length, 2 mm in width and 0.5 mm thick was placed in V-shaped trough made from white polyvinyl chloride sheet. Electrodes were clipped on both ends of trough and connected to the separation bed.

Three different solutions were loaded into a separation bed before each analysis. 50 μL of mixture of substance forming anolyte and catholyte were injected to the anodic end and to the cathodic end of separation bed, respectively and 175 μL of working solution was loaded into the center of the strip. Working solution consisted of 50 μL of p*I* markers solution, 25 μL of spacer's mixture, and 100 μL of sample. Finally, the electrophoretic power supply was switched on and focusing was proceeded for 2 hours.

2.3. HPLC

Agilent 1200 Series (Agilent Technologies, Santa Clara, CA, USA) with 2.7 μm POROSHELL SB120-C18 2.1 × 50 mm reversed phase column (Agilent Technologies, Santa Clara, CA, USA) were used for analysis. 1 μL of fractions obtained from fast focusing and diluted 1:10 with water was injected into the system. 10 mM potassium dihydrogen phosphate pH 3.51 (A) and 10 mM potassium dihydrogen phosphate pH 3.51 with acetonitrile 1:1 (v/v) (B) were chosen as mobile phases. Elution was performed by gradient of B from 5 % (v/v) to 55 % (v/v) over 10 min. Then the mobile phase B was returned to 5 % (v/v) for 5 min, and at the end the column was regenerated by 5 % (v/v) of B for 5 min. The flow of the mobile phase was set to 20 μL min^{-1}. The column was termostated at 40 °C and DAD detector was set to acquire signal at 200 nm.

3. Results and discussion

First, milk spiked with ampicillin was analyzed by fast IEF**.** We have used this technique for two reasons. We were able to desalt and pre-concentrate samples in one step and directly analyze a raw milk sample. After focusing, we cut out the p*I* zone 3.9–5.3 which was defined by colored p*I* markers. Ampicillin was expected here due to its isoelectric point 4.9. Resulting solution obtained by centrifugation of cut out part of the nonwoven fabric strip was analyzed by HPLC.

In obtained chromatogram, the peak of ampicillin was present in 20th minute. Other unidentified peaks which were in chromatograms might come from milk or solutions used in fast focusing. Ampicillin peak in focusing fraction was verified by comparison of tree chromatograms. The first one was obtained by analysis of milk with p*I* markers and without ampicillin, the second one by analysis of p*I* markers only (blank), and the third one by analysis of ampicillin with p*I* markers and without milk (solution of ampicillin).

4. Conclusions

In this paper, the fast focusing in wide pH range based on bidirectional isotachophoresis was described. Fast focusing was allowed by the new electrolyte system. Ampicillin spiked in milk was used from demonstration of this technique. Ampicillin was focused in p*I* zone 3.9–5.3 which was verified by HPLC analysis of the fraction. Advantages of this technique are fast focusing, desalting and pre-concentration of analytes. Moreover, this method is rapid, easy, and cheap and it can separate analytes directly from raw complex mixtures.

This work was supported by the Grant of Ministry of the Interior of the Czech Republic No. VG20112015021, by the Internal Grant Agency of the Ministry of Health of Czech Republic, No. 9678-4, and with institutional support RVO: 68081715.

REFERENCES

1. Dusa F., Slais K.: Electrophoresis *34*, 1519 (2003).
2. Hirokawa T., Watanabe K., Yokota Y., Kiso Y.: J. Chromatogr., A *633*, 251 (1993).
3. Hirokawa T.: J. Chromatogr., A *686*, 158 (1994).
4. Caslavska J., Thormann W.: J. Chromatogr., A *772*, 3 (1997).

INVESTIGATION OF THE INTERCONVERSION BARRIERS OF THE PHTHALIMIDONE DERIVATIVE EM12 AND LENALIDOMIDE BY DEKC

SARAH WALZ and OLIVER TRAPP

Organisch-Chemisches Institut, Ruprecht-Karls-Universität Heidelberg, Heidelberg, Germany

Summary

The phthalimidone derivatives EM12 and Lenalidomide, which are both structurally related to thalidomide, are highly interesting drugs and very recently Lenalidomide attracted great attention as anti-tumor and immune-modulating drug in the therapy for multiple myeloma. EM12 and Lenalidomide are chiral and the stereogenic carbon C-3 in the piperidine-2,6-dione moiety of these phthalimidone derivatives is prone to interconversion due to keto-enol tautomerization. The knowledge of the enantiomerization barrier is mandatory for pharmacokinetic studies and to develop a tailored therapy using the enantiopure or racemic drug. Here we used dynamic electrokinetic chromatography (DEKC) in combination with direct calculation methods to determine the enantiomerization barriers of EM12 and Lenalidomide. The separation of enantiomers of EM12 and Lenalidomide has been performed in an aqueous 50 mM disodium hydrogen phosphat buffer at pH 8 using 20 mg mL^{-1} HDAS-β-cyclodextrin as chiral additive and aqueous 50 mM sodium tetreborate buffer at pH 9.3 using 20 mg mL^{-1} HDAS-β-cyclodextrin as chiral additive, respectively. Enantiomerization of the compounds during the electrokinetic chromatographic separation resulted in pronounced plateau formation between the well separated enantiomers. Peak form analysis yielded the enantiomerization rate constant k_1 as well as the kinetic activation parameters $\Delta G^{\ddagger}$, $\Delta H^{\ddagger}$, and $\Delta S^{\ddagger}$ of enantiomerization by temperature dependent measurements. The enantiomerization barrier $\Delta G^{\ddagger}$ was determined to be 98.3 ± 1.0 kJ mol^{-1}, the activation parameters $\Delta H^{\ddagger}$ = 46.1 ± 2.4 kJ mol^{-1} and $\Delta S^{\ddagger}$ = –170 ± 61 J K^{-1} mol^{-1} for EM12 and $\Delta G^{\ddagger}$ = 91.5 ± 1.0 kJ mol^{-1}, $\Delta H^{\ddagger}$ = 62.41 ± 5.38 kJ mol^{-1} and $\Delta S^{\ddagger}$ = –97.7 ± 6.7 J K^{-1} mol^{-1} for Lenalidomide.

CONTENTS

Oral presentations

Posters

AUTHOR INDEX

CHEMICKÉ LISTY • ročník/volume 107 (S), čís./no. Symposia • LISTY CHEMICKÉ roč./vol. 137, ČASOPIS PRO PRŮMYSL CHEMICKÝ, roč./vol. 123 • ISSN 0009-2770, ISSN 1213-7103 (e-verze), ISSN 1803-2389 (CD verze) • evidenční číslo MK ČR E 321 • Vydává Česká společnost chemická jako časopis Asociace českých chemických společností ve spolupráci s VŠCHT Praha, s ČSPCH a ÚOCHB AV ČR za finanční podpory Nadace Český literární fond a kolektivních členů ČSCH • IČO 444715 • Published by the Czech Chemical Society • VEDOUCÍ REDAKTOR/EDITOR-IN-CHIEF: P. Chuchvalec • REDAKTOŘI/ EDITORS: J. Barek, Z. Bělohlav, P. Drašar, J. Hetflejš, P. Holý, J. Horák, B. Kratochvíl, J. Podešva, P. Rauch; Bulletin: I. Valterová; Webové stránky: R. Liboska, P. Zámostný • ZAHRANIČNÍ A OBLASTNÍ REDAKTOŘI/FOREIGN AND REGIONAL EDITORS: F. Švec (USA), Z. Kolská (Ústí nad Labem) • KONZULTANT/CONSULTANT: J. Kahovec • TECHNICKÁ REDAKTORKA/EDITORIAL ASSISTANT: R. Řápková • REDAKČNÍ RADA/ADVISORY BOARD: K. Bláha, L. Červený, E. Dibuszová, J. Hanika, Z. Havlas, J. Káš, M. Koman, J. Koubek, T. Míšek, K. Melzoch, V. Pačes, O. Paleta, V. Růžička, I. Stibor, V. Šimánek, R. Zahradník • ADRESA PRO ZASÍLÁNÍ PŘÍSPĚVKŮ/MANUSCRIPTS IN CZECH, SLOVAK OR ENGLISH CAN BE SENT TO: Chemické listy, Novotného lávka 5, 116 68 Praha 1; tel./phone +420 221 082 370, +420 222 220 184, e-mail: chem.listy@csvts.cz • INFORMACE O PŘEDPLATNÉM, OBJEDNÁVKY, PRODEJ JEDNOTLIVÝCH ČÍSEL A INZERCE/ INFORMATION ADS: Sekretariát ČSCH, Novotného lávka 5, 116 68 Praha 1; tel. +420 222 220 184, e-mail: chem.spol@csvts.cz, chem.ekonom@csvts.cz • PLNÁ VERZE NA INTERNETU/FULL VERSION ON URL: http://www.chemicke-listy.cz • TISK: Rodomax s.r.o., Rezecká 1164, 549 01 Nové Město nad Metují • Redakce čísla Symposia (ISSUE EDITOR) F. Foret, J. Křenková, A. Guttman, K. Klepárník, P. Boček • SAZBA, ZLOM: ČSCH, Chemické listy • Copyright © 2013 Chemické listy/ Česká společnost chemická • Cena výtisku 177 Kč, roční plné předplatné 2013 (12 čísel) 1793 Kč, individuální členské předplatné pro členy ČSCH 897 Kč. Roční předplatné ve Slovenské republice 96 EUR (doručování via SCHS), individuální členské předplatné pro členy ČSCH 73 EUR (doručování via SCHS), 268 EUR (individuální doručování), ceny jsou uvedeny včetně DPH • DISTRIBUTION ABROAD: KUBON & SAGNER, POB 34 01 08, D-80328 Munich, FRG • This journal has been registered with the Copyright Clearance Center, 2322 Rosewood Drive, Danvers, MA 01923, USA, where the consent and conditions can be obtained for copying the articles for personal or internal use • Pokyny pro autory najdete na http://www.chemicke-listy.cz , zkratky časopisů podle Chemical Abstract Service Source Index (viz http://cassi.cas.org/search.jsp) • Chemické listy obsahující Bulletin jsou zasílány zdarma všem individuálním a kolektivním členům ČSCH a ČSPCH v ČR i zahraničí, do všech relevantních knihoven v ČR a významným představitelům české chemie a chemického průmyslu; v rámci dohod o spolupráci i členům dalších odborných společností • Molekulární námět na obálce: P. Drašar • Dáno do tisku 5.12.2013.